Volume 70A
Number 4
July–Aug. 1966

Physics and Chemistry

U.S. DEPARTMENT OF COMMERCE

SECTION A

JOURNAL OF RESEARCH

NATIONAL BUREAU OF STANDARDS

Journal of Research

of the

National Bureau of Standards

A. Physics and Chemistry

July–Aug. • 1966

VOLUME • 70A

NUMBER • 4

Editor: C. W. Beckett

Associate Editors: D. D. Wagman
J. M. Richardson

Publication dates:
Feb. 1, Apr. 1, June 1, Aug. 1, Oct. 1, Dec. 1, 1966

JOURNAL OF RESEARCH

The National Bureau of Standards Journal of Research reports research and development in the fields of activity shown at right. Also included from time to time are survey articles on topics closely related to the Bureau's scientific and technical program.

The Journal is published in three separate sections as follows:

A. Physics and Chemistry

Contains papers of interest primarily to scientists working in these fields. Issued six times a year. Annual subscription: domestic, $5.00; foreign, $6.00. Single copy, $1.00.

B. Mathematics and Mathematical Physics

Presents studies and compilations designed mainly for the mathematician and the theoretical physicist. Issued quarterly. Annual subscription: domestic, $2.25; foreign, $2.75. Single copy, 75c.

C. Engineering and Instrumentation

Reports research and development results of interest chiefly to the engineer and the applied scientist. Issued quarterly. Annual subscription: domestic, $2.75; foreign, $3.50. Single copy, 75c.

The National Bureau of Standards is a principal focal point in the Federal Government for assuring maximum application of the physical and engineering sciences to the advancement of technology in industry and commerce. Its responsibilities include development and maintenance of the national standards of measurement, and the provision of means for making measurements consistent with those standards; determination of physical constants and properties of materials; development of methods for testing materials, mechanisms, and structures, and making such tests as may be necessary, particularly for government agencies; cooperation in the establishment of standard practices for incorporation in codes and specifications; advisory service to government agencies on scientific and technical problems; invention and development of devices to serve special needs of the Government; assistance to industry, business and consumers in the development and acceptance of commercial standards and simplified trade practice recommendations; administration of programs in cooperation with United States business groups and standards organizations for the development of international standards of practice; and maintenance of a clearinghouse for the collection and dissemination of scientific, technical and engineering information. The scope of the Bureau's activities is suggested in the following listing of its three Institutes and their organizational units.

Institute for Basic Standards. Applied Mathematics. Electricity. Metrology. Mechanics. Heat. Atomic Physics. Physical Chemistry. Laboratory Astrophysics.* Radiation Physics. Radio Standards Laboratory.* Radio Standards Physics & Radio Standards Engineering. Office of Standard Reference Data.

Institute for Materials Research. Analytical Chemistry. Polymers. Metallurgy. Inorganic Materials. Reactor Radiations. Cryogenics.* Materials Evaluation Laboratory. Office of Standard Reference Materials.

Institute for Applied Technology. Building Research. Information Technology. Performance Test Development. Electronic Instrumentation. Textile and Apparel Technology Center. Technical Analysis. Office of Weights and Measures. Office of Engineering Standards. Office of Invention and Innovation. Office of Technical Resources. Clearinghouse for Federal Scientific and Technical Information.**

*Located at Boulder, Colo., 80302.
**Located at 5285 Port Royal Road, Springfield, Va., 22151.

U.S. DEPARTMENT OF COMMERCE
John T. Connor, Secretary

NATIONAL BUREAU OF STANDARDS
A. V. Astin, Director

Order all publications from the Superintendent of Documents
U.S. Government Printing Office, Washington, D.C., 20402

Use of funds for printing this publication approved by the Director of the Bureau of the Budget (June 22, 1966).

JOURNAL OF RESEARCH of the National Bureau of Standards—A. Physics and Chemistry
Vol. 70A, No. 4, July–August 1966

Elastic Constants of Synthetic Single Crystal Corundum

Wayne E. Tefft*

(March 10, 1966)

The elastic constants of synthetic single crystal corundum (aluminum oxide) were calculated from 0 to 900 °K from data obtained by a resonance technique from 80 to 900 °K.

Key Words: Aluminum oxide, corundum, elastic constants, shear modulus, Young's modulus.

1. Introduction

Two previous papers [1, 2][1] have presented respectively, the room temperature values of the elastic constants of synthetic single crystal corundum [1], and the temperature dependence of Young's modulus for certain crystallographic directions. In the present paper we present results of an extension of that work to include measurements of the temperature dependence of the torsional modulus for certain crystallographic directions, and a calculation from all these measurements of the complete set of elastic compliances from 0 to 900 °K. There has been a lapse of several years between the time of performance of this work and its submission for publication, and another paper on the subject [3] has appeared in the meantime. However, the present results cover a wider temperature range and are believed to be more accurate than those previously published.

This work was undertaken for several reasons. First, a knowledge of elastic constants is desirable for an understanding of the interatomic forces in solids, and most useful in this respect are the values of these constants at absolute zero. Second, the variation of elastic constants with temperature is one important test of theories of lattice dynamics.

The availability of different kinds of data on the same material is also of considerable theoretical importance, because of the interrelations between various thermodynamic properties. Since corundum is of technological importance and good single crystal specimens are readily available, very accurate measurements of its specific heat [4] and thermal expansion [5] have already been made. Thus, elastic constant data are desirable to permit a test of thermodynamic relations in which elastic constants appear [5].

Finally, the results presented here may be considered as an example of the precision attainable with the resonance method of elastic constant measurements in its most refined form. It is believed by this author that none of the other techniques in current use is more accurate than the one used here, and these data are presented to support this view.

*Present Address: Xerox Corporation, Solid State Research Department, Rochester, N.Y.

[1] Figures in brackets indicate the literature references at the end of this paper.

2. Experimental Procedure

The determination of the elastic constants of corundum at room temperature, and the temperature dependence of Young's modulus of seven sapphire rods of various orientations, have already been reported [1, 2]. The additional data taken for this experiment consisted of measurements of the temperature dependence of the torsional resonance frequencies of six of the seven rods from 80 to 875 °K. About 40 measurements of torsional frequency were made on each rod. Most of the experimental apparatus was identical in these three studies, and it will be assumed that the reader is familiar with the first two papers.

The torsional resonance frequencies of the original rods were of the order of 20 kHz, which was too high to be excited and detected in the cryostat, and which would have been difficult to measure in the furnace. In order to overcome this problem, the diameter of each rod was reduced by about 50 percent over approximately the middle two-thirds of its length. This was equivalent to attaching loading disks to the ends, in that the resonance frequency was thereby reduced to about one-third of its original value, but this procedure was preferable to that of attaching loading disks because it did not introduce the problem of finding a bonding material suitable for attaching loading disks and unaffected by the wide range of temperatures used. The resultant shape made it impossible to calculate absolute values of the torsional modulus from the resonance frequencies, but since the values at room temperature were already known, only changes with temperature were needed, and the temperature dependence of the modulus frequency relationship was assumed to be the same as for perfect cylinders. This assumption undoubtedly introduced some errors, but these errors are believed to be very small because they would enter through the effect of thermal expansion on small correction factors.

Torsional vibrations were excited and detected in the furnace as previously described [1] for room temperature, except that glass fiber instead of thread was used for the suspension. In order to make measurements at low temperatures, small flats were ground at each end of the specimen, and very small

magnets attached to these. The specimen was then suspended in a horizontal position by two threads in such a way that each magnet was perpendicular to the field of a nearby coil. When an alternating current was passed through one coil, a net torque resulted, and the corresponding vibrations of the rod induced currents in the other coil, which was used to detect resonance. In both high- and low-temperature measurements, the precision of the frequency determinations was of the order of one part in 30,000, although temperature gradients and systematic errors such as changing hardness of bond between magnet and specimen and condensation of ice at low temperature, and gradual crystallization of the glass fibers used for suspension at high temperatures, probably reduced the overall accuracy to about one part in 10^4.

The relation between resonance frequency, f, density, ρ, length, l, and torsional modulus, G, of an isotropic cylinder is [1]

$$G=4\rho l^2 f^2. \tag{1}$$

Thus, if our specimens had been isotropic cylinders, the torsional modulus, G, at any temperature, T, would be related to the torsional modulus at room temperature, G_R, by

$$G=G_R\left(\frac{\rho}{\rho_R}\right)\left(\frac{l}{l_R}\right)^2\left(\frac{f}{f_R}\right)^2.$$

Now if the specimens had been perfect cylinders at room temperature, the anisotropic thermal expansion would have caused their cross sections to become elliptical at any other temperature, because for a crystal of trigonal symmetry, the thermal expansion (fractional change in length) in any direction is given by [5]

$$\epsilon(\theta)=\epsilon_1\cos^2\theta+\epsilon_2\sin^2\theta$$

where ϵ_1 and ϵ_2 are, respectively, the thermal expansions parallel and perpendicular to the crystallographic c-axis, and θ is the angle between the c-axis and the direction under consideration. Thus, the circular cylinder of length l_R and radius r at room temperature becomes an elliptical cylinder of length l and semiaxes a and b at other temperatures. If a is chosen to be perpendicular to both the rod axis and the c-axis, and b is in the plane formed by the rod axis and the c-axis, then these quantities are given by:

$$l=l_R(1+\epsilon_1\cos^2\theta+\epsilon_2\sin^2\theta)$$

$$a=r(1+\epsilon_2)$$

$$b=r(1+\epsilon_1\sin^2\theta+\epsilon_2\cos^2\theta).$$

The density is $\frac{m}{\pi abl}$, so that the equation for G becomes

$$G=G_R\frac{r^2 l_R}{abl}\frac{l^2}{l_R^2}\frac{f^2}{f_R^2}=G_R\frac{r^2 l}{abl_R}\left(\frac{f}{f_R}\right)^2$$

$$=G_R\frac{1+\epsilon_1\cos^2\theta+\epsilon_2\sin^2\theta}{(1+\epsilon_2)(1+\epsilon_1\sin^2\theta+\epsilon_2\cos^2\theta)}\left(\frac{f}{f_R}\right)^2$$

which reduces approximately to

$$G\approx G_R\left(\frac{f}{f_R}\right)^2[1-\epsilon_1+2(\epsilon_1-\epsilon_2)\cos^2\theta+\epsilon_1^2]$$

where the square and higher powers of the difference $(\epsilon_1-\epsilon_2)$, and the cube and higher powers of ϵ_1 and ϵ_2 have been neglected.

Now, it is true that eq (1) is correct only for a circular cylinder, and that it should be modified for the elliptical shape caused by anisotropic thermal expansion. However, it may be shown from the equations of static torsion of elliptical cylinders that the largest correction term is proportional to $\left(\frac{a-b}{r}\right)^2$ which is always very small.

A more serious question is what modification is necessary because of the reduction in diameter over a portion of the length. There seems to be no very rigorous argument here, but one can say qualitatively that since the correction for thermal expansion is quite small, no appreciable error is likely to be introduced because this correction is not made exactly as it should be.

3. Analysis of Data

The systematic errors in the compliances are believed to be smaller than the error introduced by random error in the orientations. In order to achieve a higher degree of accuracy, the amount of data taken was considerably larger than the minimum needed to determine the six independent elastic constants of sapphire. An extensive statistical analysis of these data was made to determine the best values of these constants, and their variation with temperature.

In the original room temperature work, Young's modulus and the torsional modulus were measured on 29 different specimens, and a standard least-squares routine was then used to evaluate the six independent constants from this set of 58 measurements. It was noted, however, that the differences between measured and calculated values of E and G were due primarily to errors in orientation measurements, rather than to errors in the measured values of E and G which is implicitly assumed in the standard least-squares calculation. In order to take this into account, weights were determined by a method described by Deming [6].

After having redetermined the elastic constants at room temperature, and having measured both E and G for several orientations as a function of temperature, the problem arose as to how best to use this information to estimate the temperature dependence of the elastic constants. If measurements on all specimens had been made at identical temperatures, say 50° intervals, then one might simply have carried out the weighted least-squares routine at each of these temperatures, and thereby obtained an adequate representation of the temperature dependence of the elastic constants. This, however, would have involved an enormous amount of experimental work, and would not have significantly improved the accuracy of the results, basically because changes in the constants could be measured with better precision than the absolute values of the constants, and therefore a smaller number of measurements was needed.

It was pointed out in reference 2 that an empirical equation had been found to accurately represent the variation of Young's modulus with temperature. While fitting the experimental data to this equation by means of a least-square routine on an automatic computer, calculations were also made of the values of Young's modulus at 50° intervals from 0 to 900 °K. An attempt was made to fit the torsional modulus variation to the same form of equation. In this case, although the fit was reasonably good, the deviations appeared to be systematic, indicating that the equation did not represent the data within the experimental precision. Therefore, a plot of deviations versus temperature was made for each specimen, and corrections ranging up to about 0.04 percent were made for the calculated values of G at the same 50° temperature intervals.

A further correction was necessitated because the temperature dependence was measured for fewer specimens than were used in the room temperature measurements. It was first thought that an adequate correction would be to adjust the base (room temperature) values of E and G for each specimen so that they agreed with the calculated values in the room temperature curve fit. However, it was noted that the elastic anisotropy increased rather markedly with temperature, and that orientation errors were introducing appreciable scatter at the highest temperature. In order to partially overcome this difficulty, the orientation angles of two of the specimens (those whose calculated modulus values were most sensitive to orientation errors, and which had the largest deviations at room temperature) were adjusted to give the smallest possible deviations of E and G at room temperature (the deviation of either could be made zero in this manner, but not both simultaneously). The remaining deviations in E and G at room temperature for all specimens were then corrected for, and a least-squares solution for the elastic constants made at 50° intervals. The final result was that the errors in temperature dependences of the elastic constants were somewhat smaller even at the highest temperature than were their absolute values at room temperature. Therefore, the values quoted at 900 °K should be in error (in absolute value) by less than twice the errors of absolute value at room temperature. Since measurements were only made down to liquid nitrogen temperature, the errors in the values at absolute zero are somewhat uncertain, but there is reason to believe that they are less in error than the values at 900 °K, although certainly somewhat more in error than the values at room temperature. The reason that these errors are small in spite of the 80° extrapolation is that nearly all the variation takes place at higher temperature; i.e., the modulus temperature curves are very nearly flat up to about 100 °K.

4. Results and Summary

Values of the six elastic compliance constants of corundum in the temperature interval 0 to 900 °K are given in table 1. The base values, at 25 °C and their standard error estimates, are given in the first row.

TABLE 1. *The elastic compliances of corundum in units of* $10^{-12}m^2/N$ (10^{-13} *cm²/dyn*)

The first row lists room temperature values together with their standard deviations. These values were combined with measurements of relative changes with temperature to obtain the values at other temperatures.

Temperature	s_{11}	s_{33}	s_{44}	s_{12}	s_{13}	s_{14}
°K						
273.2	2.353 ±0.002	2.168 ±0.002	6.940 ±0.008	−0.716 ±.007	−0.368 ±.006	0.491 ±.005
0	2.326	2.151	6.765	−.693	−.362	.465
100	2.326	2.152	6.776	−.695	−.363	.467
150	2.330	2.154	6.802	−.698	−.364	.471
200	2.336	2.158	6.841	−.704	−.365	.477
250	2.344	2.163	6.889	−.710	−.366	.483
300	2.353	2.169	6.942	−.716	−.368	.491
350	2.364	2.176	7.000	−.723	−.369	.500
400	2.375	2.183	7.061	−.731	−.370	.509
450	2.386	2.191	7.126	−.740	−.370	.519
500	2.399	2.200	7.193	−.748	−.371	.530
550	2.412	2.209	7.263	−.757	−.372	.541
600	2.425	2.218	7.334	−.766	−.372	.552
650	2.438	2.228	7.407	−.775	−.373	.564
700	2.453	2.237	7.482	−.784	−.373	.576
750	2.467	2.247	7.559	−.796	−.374	.587
800	2.482	2.258	7.638	−.808	−.374	.600
850	2.497	2.268	7.719	−.820	−.374	.613
900	2.512	2.279	7.803	−.832	−.375	.626

These values were determined from measurements on the same set of 29 specimens used in reference 1, but the present results are believed to be slightly more accurate because of improved temperature control and use of a weighted least-squares routine.

The values at other temperatures are based on values at 25 °C, and therefore include in their absolute magnitude the errors of the base values. However, the changes with temperature over any small temperature interval were determined more accurately even though based on only seven specimens, because changes in Young's modulus and the torsional modulus could be measured more accurately than the actual values of these moduli. On the other hand, the anisotropy (as estimated, for example, from the variation in Young's modulus with orientation) increased significantly with increasing temperature. Thus, the

small orientation errors which remained after making the room temperature corrections described earlier would have introduced some error into the temperature dependence of the elastic compliances, even if the moduli had been measured exactly.

The result was that the change in any constant between room temperature and either 0 or 900 °K was determined with an accuracy approximately equal to the accuracy of that constant at room temperature. One cannot make a more precise statement than this because, while systematic errors are believed to be insignificant in the room temperature results, they may be comparable to the random errors at other temperatures. Furthermore, even random errors, such as would result from misorientation, cannot be estimated very well for the temperature dependence measurements because of the small number of specimens used.

5. References

[1] J. B. Wachtman, Jr., W. E. Tefft, D. C. Lam, Jr., and R. P. Stenchfield, Elastic constants of synthetic single crystal corundum at room temperature, J. Res. NBS **64A** (Phys. and Chem.), No. 3, 213–228 (1960).

[2] J. B. Wachtman, Jr., W. E. Tefft, D. C. Lam, Jr., and C. S. Apstein, Exponential temperature dependence of Young's modulus for several oxides, Phys. Rev. **122,** 1754–1759 (1961).

[3] P. Jayarama Reddy, Variation with temperature of the elastic compliances of corundum, Acta. Cryst. **16,** 335 (1963).

[4] G. T. Furukawa, T. B. Douglas, R. E. McCoskey, and D. C. Ginnings, Thermal properties of aluminum oxide from 0 to 1200 °K, J. Res. NBS **57,** 67 (1956) RP2694.

[5] J. B. Wachtman, Jr., T. G. Scuderi, and G. W. Cleek, Linear thermal expansion of aluminum oxide and thorium oxide from 100 to 1100° K, J. Am. Ceram. Soc. **45,** 319–323 (1962).

[6] W. Edwards Deming, Statistical Adjustment of Data, pp. 152–171 (John Wiley & Sons, Inc., New York, N.Y., 1943).

(Paper 70A4–403)

JOURNAL OF RESEARCH of the National Bureau of Standards—A. Physics and Chemistry
Vol. 70A, No. 4, July–August 1966

Phase Equilibria as Related to Crystal Structure in the System Niobium Pentoxide-Tungsten Trioxide

R. S. Roth and J. L. Waring

Institute for Materials Research, National Bureau of Standards, Washington, D.C.

(April 1, 1966)

The phase equilibrium diagram for the binary system niobium pentoxide-tungsten trioxide has been constructed from results of x-ray diffraction studies on both single crystals and powders and from fusion characteristics. Twelve stable compounds have been found in the system. The exact composition of eight of these compounds has been established by single crystal analyses at the $Nb_2O_5 : WO_3$ ratios of 6 : 1, 13 : 4, 7 : 3, 8 : 5, 9 : 8, 1 : 1, 4 :9, and 2 : 7. The approximate compositions of the remaining four other phases are 30 : 1, 6 : 11, 1 : 11, and 1 : 15. The 6 : 1, "6 : 11", 4 : 9, and 2 : 7 phases melt congruently at 1476, 1378, 1380, and 1357 °C, respectively. The "30 : 1", 7 : 3, 8 : 5, 9 : 8, "1 : 11", and "1 : 15" phases melt incongruently at 1470, 1440, 1385, 1375, 1356, and 1358 °C, respectively; and the 13 : 4 and 1 : 1 phases decompose before melting at 1435 and 1115 °C, respectively. The 8 : 5, 9 : 8, "6 : 11", 2 : 7, "1 : 11", and "1 : 15" compounds are shown on the phase diagram as having minimum temperatures of stability. One metastable phase having a narrow range of composition near the 3 : 8 ratio was also encountered. Although Nb_2O_5 apparently exhibits no solid solution, WO_3 was found to accept a maximum of three mole percent niobia in solid solution enabling all the reported polymorphs of WO_3 to be obtained at room temperature.

Key Words: Crystal structure, niobium pentoxide, phase equilibria, system, tungsten trioxide.

1. Introduction

A complete study of the phase relationships in the binary system $Nb_2O_5 - WO_3$ has been conducted as part of a continuing program of fundamental phase equilibria studies of ceramic materials. This particular system was selected for study in order to further the knowledge of the crystal chemistry of niobates in view of the results obtained from previous structural studies of single crystals [1–4].[1]

Due to the complex nature of the x-ray diffraction powder patterns in this system, conflicting interpretations of the data have been reported [5–11]. In a previous study of the Nb_2O_5–WO_3 system, Goldschmidt [5] concluded that Nb_2O_5 could accept more than 50 mole percent WO_3 in solid solution and reported the existence of a compound at approximately $Nb_2O_5 : 3WO_3$. He also found a limited solid solution of Nb_2O_5 in WO_3. Kovba and Trunov [6] reported that the 1 : 3 compound was tetragonal with a structure related to that of a tetragonal tungsten-bronze. Fiegel et al. [7], studied the phase equilibria in the system at 1200 °C and below. They reported only about 33 mole percent solid solution of WO_3 in Nb_2O_5 with a 3 : 2 compound occurring at 1200 °C and a 1 : 1 compound at 1100 °C and below. They found very little, if any, solid solution of Nb_2O_5 in WO_3 and confirmed the existence of a compound at about 1 : 3 with a limited solid solution for both Nb_2O_5 and WO_3. Later [8] they reported that the 1 : 3 composition gave single crystal x-ray diffraction patterns which showed superstructure differing from one crystal to the next. Kovba et al. [9], also attempted to determine the phases formed in this system at about 1200 °C. They concluded that compounds existed at the $Nb_2O_5 : WO_3$ ratios of 4 : 1, 2 : 1, 4 : 7, and 1 : 3. They also reported a phase with variable WO_3 content occurring at high WO_3 concentrations and observed a small amount of solid solution in both Nb_2O_5 and WO_3.

In a description of preliminary phase identification, Roth and Wadsley [1] on the basis of single crystal x-ray diffraction studies reported the existence of five compounds structurally related to Nb_2O_5 occurring at $Nb_2O_5 : WO_3$ ratios of 15 : 1, 6 : 1, 7 : 3, 8 : 5, and 9 : 8. They also confirmed the 1 : 1 phase and noted the existence of at least three phases related to the tetragonal tungsten bronze-type structure. The crystal structures of 6 : 1, 7 : 3, 8 : 5, and 9 : 8, were reported [2, 3] and the "building block" principle was elaborated as the basis of the crystal-chemistry of niobate compounds [4].

Schäfer and Gruehn [10] and Felten [11] have indicated in private communications that their interpretations of x-ray diffraction powder data for the Nb_2O_5–WO_3 system differ in some respects from the previously mentioned published reports.

Because of the conflicting nature of the reported data, it was thought desirable to study completely the phase equilibria of the Nb_2O_5–WO_3 system. With the use of the unit cell dimensions derived from

[1] Figures in brackets indicate the literature references at the end of this paper.

single crystal data the existence of the various phases in the powder patterns can now be established more readily. The exact compositions of phases can often be determined only by a solution of the crystal structure. The approximate composition and even the existence of a phase can sometimes be found only by a rather complete phase equilibria study. The two disciplines, crystal structure analysis and phase equilibria are therefore complimentary and no system can be considered to be well characterized unless both such studies have been made. Therefore, x-ray diffraction data together with the melting points of the compounds and solidus and liquidus temperatures at various compositions across the system have been obtained in order to construct an equilibrium diagram.

2. Sample Preparation and Test Methods

The following starting materials were employed for the preparation of the majority of the specimens:

Nb_2O_5—high purity niobium pentoxide. Spectrographic analysis indicated less than about 0.01 percent Si; 0.001 percent Ca and Mg with As, Cu, and Ta only questionably present.

WO_3 —high purity tungsten anhydride. Spectrographic analysis indicated less than about 0.1 percent Si; 0.001 percent B, Ca, Cr, and Mg; 0.0001 percent Cu with Pb only questionably present.

A few specimens were prepared with less pure starting materials, in order to determine qualitatively the effect of impurities on the equilibrium products. The following is a typical example of the nature of the impurities present in two specimens of Nb_2O_5: WO_3 ratio of 16 : 5. For the less pure specimen the first series transition elements, in general, are present in amounts of an order of magnitude greater than for the more pure specimen.

$Nb_2O_5 : WO_3$ (16 : 5)—higher purity end members. Spectrochemical analyses indicated less than about 0.01 percent Cr, Cu, and Si; 0.001 percent Al, B, Ca, Mg, and Ni; 0.0001 percent Mn with Pb only questionably present.

$Nb_2O_5 : WO_3$ (16 : 5)—less pure end members. Spectrochemical analyses indicated less than about 0.01 percent Al, Ca, Cr, Cu, Fe, Mg, Ni, and Si; 0.001 percent Mn; 0.0001 percent B with Pb only questionably present.

For the preparation of the specimens, the weight percentages were calculated to within ± 0.01 percent, with no corrections made for percentage of purity of the starting materials except for loss on ignition.

For the higher purity specimens, the starting materials were weighed to the nearest ± 0.1 mg, in sufficient quantities to yield 3 g batches. Each batch was mixed in a mechanical shaker for about 15 min and pressed into a disk in a 5/8-in. diam mold at 10,000 lb/in^2. The disks were placed on Pt foil and calcined by heating in air at 700 °C for 19 hrs, with heating and cooling rates of approximately 4 °C/min.

The less pure specimens were weighed out in approximately 1 g batches and mixed with an alumina mortar and pestle. In order to minimize any possible loss of WO_3 these specimens were not calcined after mixing.

Subsolidus, as well as melting point data, were obtained by the quenching technique on samples sealed in platinum tubes. An electrically heated vertical tube furnace wound with 80 percent Pt-20 percent Rh wire was used for the quenching experiments. The furnace was controlled by an a-c Wheatstone bridge controller which was capable of holding the temperature to at least ± 2 °C for an extended period of time. Temperatures were measured with a Pt versus Pt-10 percent Rh thermocouple which had been calibrated against the melting points of Au (1063 °C) and Pd (1552 °C) [12]. The thermocouple was recalibrated several times during the course of the work. Specimens were suspended in the furnace by fine Pt wire. In order to quench the wire was fused allowing the sealed tubes to drop out of the heating chamber into a beaker of water. When the tubes were opened the specimens were examined for physical appearances of melting. The first sign of glazing of the surface of the specimen was interpreted as the first experimental evidence for the solidus temperature. Acceptance of this appearance as evidence of melting was found justified in many specimens by an abrupt difference in the x-ray diffraction powder patterns of the specimens. The formation of a concave meniscus, without the formation of relatively large crystals, indicated the liquidus temperature. The overall reproducibility of the temperature measurements for the experimental data points was within ± 2 °C or better and the overall accuracy of the reported temperatures was within ± 5 °C or better.

Equilibrium was considered to have been obtained when the x-ray diffraction patterns of specimens successively heated for longer times and/or at higher temperatures showed no change. X-ray diffraction powder patterns were made using a high-angle recording Geiger counter diffractometer and nickel-filtered copper radiation, with the Geiger counter traversing the specimen at 1/4°2θ/min and the intensity of the radiation being recorded on the chart at 1°2θ/in. The unit cell dimensions reported can be considered accurate to about ± 2 in the last decimal place listed.

3. Compounds in the Nb_2O_5-WO_3 System

3.1. Nb_2O_5

The stability relations of the various reported polymorphs of Nb_2O_5 have been summarized by several workers [13–17]. It has been concluded that the high-temperature monoclinic form of Nb_2O_5 is the only

stable form at atmospheric pressure [14, 16, 17]. The crystal structure of the high-temperature modification of Nb_2O_5 has been described by Gatehouse and Wadsley [18]. They report this phase to be monoclinic, (space group P2) with 14 formula units in the unit cell and $a = 21.16$ Å, $b = 3.822$ Å, $c = 19.35$ Å, $\beta = 119°50'$. The x-ray diffraction powder pattern previously listed for Nb_2O_5 [19] can be more correctly indexed on the basis of the published single-crystal intensity data and is shown in table 1. This indexing leads to slightly revised values of the unit cell dimensions, as follows: $a = 21.149$ Å, $b = 3.823$ Å, $c = 19.352$ Å, $\beta = 119°48'$, in excellent agreement with the lattice constants given by Gatehouse and Wadsley [18]. The melting point of the pure Nb_2O_5 used for this study was previously determined to be 1485 °C [20].

TABLE 1. *X-ray diffraction powder data for* Nb_2O_5 *(CuK$_\alpha$ radiation)*

d[a]	I[b]	$\frac{1}{d^2}$ obs	$\frac{1}{d^2}$ calc	hkl[c]	d[a]	I[b]	$\frac{1}{d^2}$ obs	$\frac{1}{d^2}$ calc	hkl[c]
16.66	6	0.0036	0.0036	001				0.1526	$80\bar{2}$
10.517	5	.0090	.0090	$20\bar{1}$	2.543	36	0.1546	.1541	$10\bar{7}$
10.063	2	.0099	.0097	101				.1543	$61\bar{4}$
9.615	2	.0108	.0107	$10\bar{2}$	2.523	5	.1571	.1571	$01\bar{5}$
9.148	5	.0120	.0118	200	2.491	26	.1612	.1612	$70\bar{7}$
8.354	4	.0143	.0142	$00\bar{2}$					
6.942	2	.0208	.0206	$30\bar{1}$	2.478	8	.1629	.1623	511
6.486	3	.0238	.0236	$10\bar{2}$				.1625	$21\bar{4}$
6.285	11	.0253	.0252	$10\bar{3}$	2.452	5	.1664	.1662	$41\bar{6}$
5.590	4	.0320	.0319	003				.1672	$61\bar{5}$
								.1865	$41\bar{3}$
5.273	6	.0360	.0359	$40\bar{2}$	2.314	29	.1865	.1869	$61\bar{6}$
5.116	48	.0382	.0382	$40\bar{1}$				.1872	$20\bar{8}$
4.734	4	.0446	.0446	$10\bar{3}$	2.114	4	.2244	.2239	$41\bar{4}$
4.616	36	.0469	.0465	$10\bar{4}$	2.076	38	.2321	.2321	10, 0, $\bar{3}$
3.852	6	.0674	.0670	$30\bar{5}$	2.037	34	.2411	.2410	$20\bar{9}$
					1.912	29	.2736	.2736	020
3.821	6	.0685	.0683	$20\bar{5}$					
			.0684	010				.2846	3, 0, $1\bar{0}$
3.737	100	.0716	.0714	110	1.873	5	.2852	.2847	11, 0, $\bar{7}$
			.0717	$11\bar{1}$				.2847	11, 0, $\bar{3}$
3.636	100	.0756	.0755	$10\bar{5}$				.2855	220
					1.856	3	.2903	.2904	208
3.577	4	.0782	.0782	111					
3.553	4	.0792	.0791	$11\bar{2}$				.3020	2, 0, $1\bar{0}$
					1.819	20	.3020	.3031	11, 0, $\bar{8}$
3.515	4	.0809	.0807	$60\bar{3}$				.3115	$40\bar{7}$
3.483	100	.0824	.0824	602	1.789	16	.3124	.3118	$42\bar{1}$
			.0826	$01\bar{2}$				.3127	902
3.406	4	.0862	.0859	$60\bar{4}$					
3.383	4	.0877	.0877	$30\bar{3}$				.3201	$12\bar{4}$
			.0886	005				.3227	12, 0, $\bar{5}$
3.351	28	.0891	.0890	$31\bar{1}$	1.765	5	.3211	.3230	12, 0, $\bar{6}$
3.316	5	.0909	.0911	$60\bar{1}$				.3231	6, 0, $1\bar{1}$
3.264	4	.0939	.0936	$11\bar{3}$				.3292	$11\bar{9}$
					1.742	23	.3295	.3296	12, 0, $\bar{4}$
3.247	4	.0949	.0951	310	1.727	25	.3353	.3353	8, 0, $1\bar{1}$
3.153	11	.1006	.1003	$01\bar{3}$					
3.078	6	.1055	.1051	$50\bar{6}$				.3422	11, 1, $\bar{4}$
			.1113	$10\bar{6}$	1.709	10	.3424	.3425	11, 1, $\bar{6}$
2.994	7	.1116	.1246	$51\bar{2}$	1.692	20	.3493	.3491	$12\bar{5}$
2.832	36	.1247	.1248	$01\bar{4}$	1.683	51	.3529	.3530	3, 1, $1\bar{0}$
2.826	38	.1252	.1262	$51\bar{3}$				.3531	11, 1, $\bar{3}$
					1.627	8	.3776	.3776	$40\bar{8}$
2.771	31	.1303	.1301	$51\bar{1}$	1.592	27	.3945	.3946	7, 1, $\bar{11}$
2.701	34	.1371	.1367	$21\bar{5}$					
			.1377	$70\bar{6}$				.3982	11, 0, 1
					1.582	20	.3994	.3995	$31\bar{8}$
2.668	3	.1405	.1401	$41\bar{5}$	1.579	18	.4012	.4011	10, 1, $\bar{1}$
			.1405	$20\bar{7}$	1.556	22	.4130	.4133	12, 1, $\bar{8}$
2.644	4	.1431	.1426	510					
			.1433	$80\bar{4}$					
2.628	5	.1448	.1445	$80\bar{3}$					
			.1452	$60\bar{7}$					

[a] Interplaner spacing.
[b] Intensity relative to the strongest peak(s).
[c] Indexed on the basis of a monoclinic unit cell (space group P_2) $a = 21.149$ Å, $b = 3.823$ Å, $c = 19.352$ Å, $\beta = 119°48'$ and the previously reported observed structure factors from the single crystal data [18].

3.2. Compounds Structurally Related to Nb_2O_5

a. Compounds Belonging to the Homologous Series $B_{nm+1}O_{3nm-(n+m)+4}$

Roth and Wadsley [4] have shown that most of the phases formed by the addition to Nb_2O_5 of oxides with cations similar in size to Nb^{+5}, regardless of valence, can be described by the homologous series notation $B_{nmp+1}O_{3nmp-(n+m)p+4}$. Structurally, these phases are made up of blocks of octahedra in a given plane n long and m wide with a variable number (p) of blocks connected by edge sharing of octahedra at the corners of the blocks. Similar block units occur at two levels in the unit cell, zero and one-half, in a

TABLE 2. *X-ray diffraction powder data for the compound* $WNb_{12}O_{33}$ *(CuK$_\alpha$ radiation)*

d[a] obs	I[b] obs	$\frac{1}{d^2}$ obs	$\frac{1}{d^2}$ calc	hkl[c]	d[a] obs	I[b] obs	$\frac{1}{d^2}$ obs	$\frac{1}{d^2}$ calc	hkl[c]
14.77	19	0.0046	0.0046	001	2.167	6	0.2130	0.2135	10. 0, $\bar{6}$
11.08	23	.0081	.0081	$20\bar{1}$	2.128	5	.2209	.2213	801
7.42	16	.0182	.0183	002				.2213	$80\bar{8}$
6.43	8	.0242	.0241	201					
5.54	18	.0326	.0325	$40\bar{2}$	2.116	6	.2233	.2236	007
								.2237	206
5.35	6	.0349	.0348	$40\bar{1}$	2.112	6	.2242	.2244	$51\bar{7}$
5.04	48	.0394	.0394	$40\bar{3}$	2.072	67	.2325	.2328	10, 0, $\bar{7}$
4.937	12	.0410	.0411	003					
4.674	58	.0458	.0458	202	2.042	52	.2398	.2401	405
3.743	76	.0714	.0713	110	2.006	6	.2484	.2487	$91\bar{2}$
								.2669	$80\bar{2}$
3.729	96	.0719	.0718	$11\bar{1}$	1.9375	9	.2664	.2669	$80\bar{9}$
3.702	40	.0730	.0730	004					
3.697	40	.0732	.0732	$60\bar{3}$					
3.670	20	.0742	.0742	$60\bar{2}$	1.9324	8	.2678	.2683	315
3.616	284	.0765	.0766	203	1.9121	60	.2735	.2735	020
					1.8729	4	.2851	.2851	220
3.535	43	.0800	.0798	111	1.8664	5	.2871	.2873	$22\bar{2}$
3.510	300	.0812	.0811	$60\bar{4}$	1.8560	15	.2899	.2903	12, 0, $\bar{5}$
3.437	13	.0847	.0846	$60\bar{1}$				.2910	207
3.415	15	.0857	.0857	$20\bar{5}$	1.8524	29	.2914	.2918	022
3.358	29	.0887	.0887	$31\bar{2}$				.2920	008
					1.8342	8	.2969	.2972	12, 0, $\bar{4}$
3.203	27	.0974	.0975	112					
2.930	16	.1165	.1165	$20\bar{4}$	1.8144	8	.3038	.3040	12, 0, $\bar{7}$
2.901	5	.1189	.1189	$51\bar{2}$	1.8090	20	.3056	.3063	406
2.866	58	.1217	.1218	$51\bar{3}$	1.8007	8	.3084	.3093	$20\bar{9}$
2.836	37	.1243	.1243	113	1.7895	13	.3126	.3123	11, 1, $\bar{5}$
					1.7720	8	.3185	.3185	11, 1, $\bar{6}$
2.799	7	.1277	.1279	$20\bar{6}$					
2.735	41	.1337	.1337	$51\bar{4}$	1.7697	9	.3193	.3193	222
2.706	31	.1365	.1366	312	1.7640	22	.3214	.3217	8, 0, $1\bar{0}$
					1.7567	19	.3240	.3245	12, 0, $\bar{8}$
2.682	17	.1390	.1392	$80\bar{2}$	1.7403	21	.3302	.3305	316
			.1392	$80\bar{5}$	1.7329	19	.3330	.3332	10, 0, 1
2.542	8	.1548	.1548	$51\bar{5}$					
					1.7311	18	.3337	.3339	11, 1, $\bar{7}$
			.1574	$80\bar{1}$	1.6903	20	.3500	.3501	223
2.520	116	.1575	.1580	$40\bar{7}$					
					1.6805	42	.3541	.3545	515
			.1599	$60\bar{7}$				.3547	$62\bar{4}$
2.499	10	.1602	.1603	114	1.6709	26	.3582	.3585	11, 1, $\bar{8}$
					1.6088	21	.3864	.3869	10, 0, 2
2.462	16	.1650	.1651	$51\bar{1}$					
2.410	4	.1722	.1722	$71\bar{2}$	1.6070	23	.3872	.3880	2, 0, $1\bar{0}$
2.339	6	.1828	.1831	404	1.5975	16	.3918	.3924	$91\bar{2}$
					1.5838	21	.3987	.3992	9, 1, $1\bar{0}$
			.1842	$71\bar{5}$					
2.328	15	.1845	.1848	800	1.5801	20	.4005	.4006	14, 0, $\bar{5}$
								.4017	10, 0, $\bar{11}$
			.1865	$71\bar{1}$	1.5734	21	.4039	.4049	119
2.316	29	.1864	.1868	$31\bar{6}$					
					1.5608	19	.4105	.4109	13, 1, $\bar{5}$
2.215	11	.2038	.2043	$60\bar{8}$	1.5527	9	.4148	.4154	14, 0, $\bar{4}$
2.183	7	.2098	.2099	710	1.5405	5	.4214	.4227	4, 0, $\bar{11}$

[a] Interplanar spacing.
[b] Observed intensity.
[c] Indexed on the basis of a monoclinic unit cell (space group C_2) $a = 22.282$ Å, $b = 3.824$ Å, $c = 17.724$ Å, $\beta = 123°22'$ and the previously reported structure factors from the single crystal data [2].

plane perpendicular to one axis which always has a value of approximately 3.8 Å. This axis is the *b*-axis of a monoclinic cell or the *c*-axis of a tetragonal cell. The octahedra occurring at the two different levels are connected to each other by edge sharing except at the junction of four such blocks, two at each level, where they are bonded by a tetrahedrally coordinated cation. Those compounds in the Nb_2O_5–WO_3 system whose structures have been described all have $p=1$ and the formula simplifies to $B_{nm+1}O_{3nm-(n+m)+4}$, where the tetrahedral position is always occupied by W^{+6} ions. In this arrangement when $n=m$, the unit cell is body-centered tetragonal as in PNb_9O_{25} [21]. When $n \neq m$ the cell is C-centered monoclinic.

b. $6Nb_2O_5 \cdot WO_3$, $WNb_{12}O_{33}$)

The unit cell of this compound is C-centered monoclinic (probable space group C_2) having $n=3$, $m=4$ [2]. The indexed x-ray diffraction powder pattern obtained in the present study is listed in table 2. The unit cell dimensions derived from this pattern are $a=22.282$ Å, $b=3.824$ Å, $c=17.724$ Å, $\beta=123°22'$. $WNb_{12}O_{33}$ is apparently stable from room temperature to the congruent melting point at 1476 °C.

c. $7Nb_2O_5 \cdot 3WO_3$ ($W_3Nb_{14}O_{44}$)

The unit cell of this compound is body-centered tetragonal, space group I4/m or $I\bar{4}$($n=4$, $m=4$ [3]). The indexed x-ray diffraction powder pattern is listed in table 3 and the unit cell dimensions derived from this pattern are $a=21.002$ Å, $c=3.820$ Å.

d. $8Nb_2O_5 \cdot 5WO_3$ ($W_5Nb_{16}O_{55}$)

The unit cell of this phase is C-centered monoclinic space group C_2 ($n=4$, $m=5$, [2]). The indexed x-ray diffraction powder pattern is listed in table 4 and the unit cell dimensions derived from this pattern are $a=29.638$ Å, $b=3.820$ Å, $c=23.126$ Å, $\beta=126°27'$.

TABLE 4. *X-ray diffraction powder data for the compound* $W_5Nb_{16}O_{55}$ *(CuKa radiation)*

d^a	I^b	$\frac{1}{d^2}$ obs	$\frac{1}{d^2}$ calc	hkl^c	d^a	I^b	$\frac{1}{d^2}$ obs	$\frac{1}{d^2}$ calc	hkl^c
18.58	7	0.0029	0.0029	001	2.397	4	0.1741	0.1744	91$\bar{2}$
14.84	12	.0045	.0046	20$\bar{1}$	2.382	8	.1763	.1764	711
9.31	13	.0115	.0116	002	2.350	4	.1811	.1811	12,0,$\bar{8}$
7.40	17	.0183	.0183	40$\bar{2}$	2.316	7	.1864	{.1862	207
6.75	4	.0220	.0220	403				{.1873	8,0,$\bar{10}$
6.21	12	.0260	.0260	003	2.294	37	.1900	{.1898	91$\bar{1}$
5.85	6	.0293	.0293	202				{.1903	518
4.935	12	.0411	.0411	60$\bar{3}$	2.254	6	.1969	{.1968	315
4.701	45	.0453	.0453	604				{.1970	10,0,$\bar{10}$
4.652	10	.0462	.0462	004	2.177	6	.2111	.2111	910
4.512	35	.0491	.0491	203	2.104	8	.2260	.2260	51$\bar{9}$
3.771	130	.0703	.0703	110	2.067	8	.2340	.2340	11,1,$\bar{2}$
3.767	142	.0705	.0705	11$\bar{1}$	2.036	52	.2413	.2413	14,0,$\bar{9}$
3.717	26	.0724	.0722	005	2.021	36	.2448	.2448	407
3.705	22	.0729	.0731	80$\bar{4}$	1.9453	4	.2642	.2638	606
3.660	250	.0747	{.0743	80$\bar{3}$	1.9099	37	.2742	.2742	020
			{.0747	204	1.8827	6	.2821	.2823	10,0,$\bar{3}$
3.630	40	.0759	.0759	11$\bar{1}$	1.8783	6	.2835	.2837	12,0,$\bar{12}$
3.587	222	.0777	.0777	80$\bar{5}$	1.8602	17	.2890	.2890	0,0,10
3.539	25	.0798	.0799	31$\bar{2}$	1.8503	7	.2921	.2919	16,0,$\bar{7}$
3.506	8	.0813	.0813	80$\bar{2}$	1.8329	18	.2977	{.2972	16,0,$\bar{6}$
3.406	8	.0862	.0863	403				{.2978	2,0,$\bar{11}$
3.386	10	.0872	.0872	11$\bar{2}$	1.8294	26	.2988	.2988	408
3.252	6	.0946	.0947	40$\bar{7}$	1.8007	12	.3084	.3083	16,0,$\bar{5}$
3.188	16	.0984	.0984	51$\bar{3}$	1.7944	18	.3106	.3107	16,0,$\bar{10}$
3.095	12	.1044	.1044	113	1.7800	4	.3156	{.3153	62$\bar{3}$
3.072	10	.1060	.1061	205				{.3157	4,0,$\bar{12}$
2.980	7	.1126	.1126	800	1.7691	7	.3195	.3195	624
2.897	8	.1192	.1192	10,0,$\bar{6}$	1.7580	25	.3236	{.3233	223
2.832	16	.1246	.1245	71$\bar{3}$				{.3238	12,0,$\bar{13}$
2.817	47	.1260	.1260	71$\bar{4}$	1.7452	8	.3283	.3285	119
2.804	40	.1272	{.1273	11$\bar{4}$	1.7421	14	.3295	.3292	12,0,2
			{.1274	40$\bar{8}$	1.7311	24	.3337	.3336	31$\bar{8}$
2.775	5	.1299	.1300	10,0,$\bar{7}$	1.7229	12	.3369	.3368	15,1,$\bar{9}$
2.740	54	.1332	.1332	71$\bar{5}$	1.6943	28	.3484	{.3479	517
2.732	65	.1340	.1339	10,0,$\bar{2}$				{.3489	22$\bar{4}$
2.727	71	.1345	.1345	313	1.6862	57	.3517	{.3515	15,1,$\bar{10}$
								{.3518	82$\bar{5}$
2.615	8	.1462	.1463	71$\bar{6}$	1.6303	12	.3763	.3762	12,0,3
2.574	16	.1509	.1509	51$\bar{2}$	1.6284	13	.3771	.3772	4,0,$\bar{13}$
2.562	84	.1524	{.1520	10,0,$\bar{1}$	1.6101	10	.3857	.3861	14,0,$\bar{14}$
			{.1528	60$\bar{9}$	1.5888	12	.3962	.3958	11,1,3
2.549	22	.1539	{.1538	80$\bar{9}$	1.5783	14	.4014	{.4015	13,1,$\bar{3}$
			{.1540	405				{.4015	42$\bar{8}$
2.533	8	.1558	.1559	11$\bar{5}$	1.5732	26	.4041	.4041	3,1,$\bar{12}$
2.479	6	.1627	{.1627	91$\bar{5}$				{.4078	17,1,$\bar{6}$
			{.1628	31$\bar{4}$	1.5654	30	.4081	{.4081	10,2,$\bar{2}$
2.425	11	.1701	{.1699	12,0,$\bar{7}$					
			{.1704	91$\bar{6}$					

[a] Interplaner spacing.
[b] Observed intensity.
[c] Indexed on the basis of a monoclinic unit cell (space group C_2) $a=29.638$ Å, $b=3.820$ Å, $c=23.126$ Å, $\beta=126°27'$ and the previously reported observed structure factors from the single crystal data [2].

TABLE 3. *X-ray diffraction powder data for the compound* $W_3Nb_{14}O_{44}$ *(CuK$_\alpha$ radiation)*

d^a obs	I^b obs	$\frac{1}{d^2}$ obs	$\frac{1}{d^2}$ calc	hkl^c	d^a obs	I^b obs	$\frac{1}{d^2}$ obs	$\frac{1}{d^2}$ calc	hkl^c	d^a obs	I^b obs	$\frac{1}{d^2}$ obs	$\frac{1}{d^2}$ calc	hkl^c
14.87	25	0.0045	0.0045	110	2.560	22	0.1526	0.1524	611	1.8620	6	0.2884	0.2884	941
10.52	5	.0090	.0091	200	2.546	122	.1543	.1542	820	1.8564	15	.2902	.2902	880
7.42	33	.0181	.0181	220	2.488	10	.1616	.1615	541	1.8419	28	.2948	.2947	11,3,0/970
6.65	8	.0226	.0227	310	2.441	7	.1679	.1678	750	1.8367	15	.2964	.2967	312
4.951	23	.0408	.0408	330	2.421	16	.1706	.1705	631	1.8007	54	.3084	.3083	10,6,0
4.694	82	.0454	.0453	420	2.358	9	.1799	.1796	701	1.7694	16	.3194	.3194	422
4.118	5	.0590	.0589	510	2.347	8	.1814	.1815	840	1.7546	10	.3248	.3247	871
3.757	142	.0708	.0708	101	2.319	13	.1860	.1859	910	1.7499	40	.3266	.3265	12,0,0
3.712	37	.0726	.0725	440	2.302	41	.1887	.1887	721	1.7305	43	.3339	.3338	961
3.598	480	.0772	.0771	530	2.215	2	.2037	.2040	930	1.6874	65	.3512	.3511	532
3.539	52	.0798	.0799	211	2.152	9	.2159	.2159	811/741	1.6857	85	.3519	.3519	11,2,1/10,5,1
3.321	20	.0907	.0907	620	2.121	3	.2222	.2222	770	1.6612	4	.3624	.3627	12,4,0
3.195	42	.0980	.0980	321	2.100	11	.2268	.2267	10.0.0/860	1.6559	5	.3647	.3647	622
2.968	8	.1135	.1134	710/550	2.067	18	.2341	.2340	831	1.6396	5	.3720	.3718	10,8,0
2.912	22	.1179	.1179	640	2.039	130	.2405	.2403	950	1.6239	4	.3792	.3791	11,4,1
2.826	80	.1252	.1252	501/431	1.9497	3	.2631	.2630	10.4.0	1.6103	35	.3856	.3854	13,1,0/11,7,0
2.756	21	.1317	.1315	730	1.9102	40	.2741	.2743	002	1.5861	40	.3975	.3973	12,1,1/981
2.649	105	.1344	.1343	521	1.9004	10	.2769	.2766	11,1,0	1.5686	62	.4064	.4063	10,7,1
2.623	4	.1453	.1451	800	1.8797	5	.2830	.2831	202					

[a] Interplaner spacings.
[b] Observed intensities.
[c] Indexed on the basis of a tetragonal unit cell (space group I4/m or $I\bar{4}$) $a=21.002$ Å, $c=3.820$ Å.

TABLE 5. *X-ray diffraction powder data for the compound* $W_8Nb_{18}O_{69}$ *(CuK$_\alpha$ radiation)*

d^a	I^b	$\frac{1}{d^2}$ obs	$\frac{1}{d^2}$ calc	hkl^c	d^a	I^b	$\frac{1}{d^2}$ obs	$\frac{1}{d^2}$ calc	hkl^c	d^a	I^b	$\frac{1}{d^2}$ obs	$\frac{1}{d^2}$ calc	hkl^c
18.43	4	0.0029	0.0029	110	2.731	119	0.1341	0.1340	631	1.9340	4	0.2674	0.2673	11,4,1
9.33	8	.0115	.0116	220	2.626	12	.1450	.1449	10,0,0/860	1.9068	40	.2750	.2750	002
6.20	10	.0260	.0261	330	2.622	18	.1455	.1456	721	1.8578	10	.2898	.2898	14,2,0/10,10,0
5.88	10	.0290	.0290	420	2.575	96	.1508	.1507	10,2,0	1.8482	12	.2928	.2927	11,9,0
4.640	8	.0464	.0464	440	2.522	11	.1573	.1572	651	1.8216	48	.3014	.3014	12,8,0
4.563	80	.0493	.0493	530	2.477	15	.1630	.1629	811/741	1.7791	12	.3160	.3159	13,7,0
4.375	5	.0522	.0522	600	2.458	7	.1744	.1745	831	1.7561	15	.3243	.3243	532
3.771	146	.0703	.0702	101	2.378	9	.1769	.1768	11,1,0	1.7474	26	.3275	.3275	15,1,0
3.712	25	.0726	.0725	710/550	2.304	6	.1885	.1884	11,3,0/970	1.7384	7	.3309	.3310	10,9,1
3.642	372	.0753	.0754	640	2.283	38	.1918	.1919	921/761	1.7235	28	.3366	{.3362	14,6,0
3.450	15	.0840	.0840	730	2.253	11	.1970	.1971	10,6,0				{.3368	13,4,1/11,8,1
3.378	17	.0876	.0876	321	2.248	7	.1978	.1977	851	1.6943	57	.3484	.3484	12,7,1
3.185	12	.0986	.0985	820	2.242	6	.2086	.2087	12,0,0	1.6897	65	.3503	.3504	642
3.088	25	.1049	{.1043	660	2.156	9	.2151	{.2145	12,2,0	1.6614	5	.3623	.3624	15,5,0/13,9,0
			{.1050	501/431				{.2151	10,1,1	1.6532	6	.3659	.3658	14,3,1/13,6,1
3.054	15	.1072	.1072	750	2.100	12	.2267	.2267	10,3,1	1.6292	22	.3768	.3768	16,2,0/14,8,0
2.901	5	.1189	.1188	910	2.077	5	.2319	.2319	12,4,0	1.5801	28	.4005	.4006	15,2,1
2.793	82	.1282	.1282	541	2.015	85	.2463	.2463	13,1,0/11,7,0	1.5688	48	.4063	.4064	13,8,1
2.769	26	.1304	.1304	930	1.9584	5	.2607	.2608	12,6,0					

[a] Interplaner spacing.
[b] Observed intensity.
[c] Indexed on the basis of a tetragonal unit cell (space group $I\bar{4}$) $a = 26.270$ Å, $c = 3.814$ Å.

Due to the very large monoclinic cell this powder pattern can only be indexed unambiguously with the aid of single crystal data. By utilizing the published F_{obs} values for $W_5Nb_{16}O_{55}$ [2] it was possible to assign indices to the observed peaks in the powder pattern with reasonable certainty up to about 60°2θ (Cu radiation). $W_5Nb_{16}O_{55}$ is probably not stable below about 1090 °C and melts incongruently at about 1385 °C.

e. $9Nb_2O_5 \cdot 8WO_3$ ($W_8Nb_{18}O_{69}$)

The unit cell of the last compound observed in this structural series has $n = 5$, $m = 5$ [3] and is body-centered tetragonal with the most probable space group $I\bar{4}$. The indexed x-ray diffraction powder pattern is given in table 5 and the unit cell dimensions derived from this pattern are $a = 26.270$ Å, $c = 3.814$ Å. This compound is not stable below about 1265 °C and melts incongruently at about 1375 °C.

It should be noted that the binary equilibrium stability regions of this structural group of compounds tend to decrease with increasing W^{+6} content. This phenomenon is probably due to the increasing size of the basic "building block" unit, and therefore to the greater energy needed to maintain long range ordering.

f. Other Compounds Structurally Related to Nb_2O_5

In addition to the compounds with structures described by the homologous series formula $B_{mnp+1}O_{3nmp-(n+m)p+4}$, the existence of several other phases has been reported, but their structures are, as yet, unknown. Notable among these is the $NbO_{2.482}$ (and $(Ti,Nb)O_{2.482}$) reported by Gruehn and Schäfer [22] which is apparently similar to the 'X' phase reported by Waring and Roth in the system vanadium-oxide-niobium oxide [23]. There are several stable phases in the Nb_2O_5–WO_3 system which fall in this category.

g. $13Nb_2O_5 \cdot 4WO_3$ ($W_4Nb_{26}O_{77}$)

Another phase, previously unreported, was found to occur between the known 6:1 and 7:3 compounds. The composition of this phase was deduced by Schäfer (private communication) to be 13:4 based on oxygen analyses. It was postulated that this compound might have an Nb_2O_5:WO_3 ratio of 16:5 and the structure would then be related to that of Nb_2O_5 by increasing the size of the basic "building blocks" from 3×4 and 3×5 (reported for Nb_2O_5 [18]) to 4×4 and 4×5. However, single crystals obtained from a 16:5 composition were found by A. D. Wadsley (private communication) to have a unit cell which is C-centered monoclinic $a = 29.74$ Å, $b = 3.823$ Å, $c = 26.02$ Å, $\beta = 92°18'$. These values are *not* in agreement with the primitive space group and approximate unit cell dimensions which can be derived for the postulated 16:5 structure. The partially indexed powder pattern is given in table 6. It cannot be fully indexed without the aid of single crystal intensity data due to the very large size of the unit cell. The structure of this phase, is actually a mixture of blocks of 3×4 and 4×4 occurring in alternate sequence to make an "ordered intergrowth" structure [24]. The composition can be arrived at by adding the homologous series twice (as for Nb_2O_5 [4]) $n = 3$, $m = 4$, $p = 1$ ($B_{13}O_{33}$) plus $n = 4$, $m = 4$, $p = 1$ ($B_{17}O_{44}$) = $B_{30}O_{77}$ ($13Nb_2O_5 \cdot 4WO_3$). Although this compound does not form in short-time experiments (about 1 hr) it can be prepared readily by heating for several days at about 1400 °C. This phase was observed to decompose at about 1435 °C into $6Nb_2O_5 \cdot WO_3$ and $7Nb_2O_5 \cdot 3WO_3$.

h. "$30Nb_2O_5$:WO_3"[2]

Another phase was found to occur in the Nb_2O_5-WO_3 system at a ratio of approximately 3.5 mole

[2] Quotation marks are used around a composition whenever the phase referred to has not been completely characterized.

TABLE 6. *X-ray diffraction powder data for the compound* $W_4Nb_{26}O_{77}$ *(CuK$_\alpha$ radiation)*

d^a	I^b	hkl^c	d^a	I^b	hkl^c
14.82	10	200	2.418	10	
12.93	8	002	2.346	7	
7.43	12	400	2.309	22	
6.55	5		2.277	5	
5.19	7		2.113	7	
4.951	14	600	2.067	13	
4.833	15	205	2.055	42	
4.686	60	602	2.042	88	
3.786	18	110	1.912	68	020
3.748	200	111	1.857	12	
		111			
			1.854	15	
3.711	40	007	1.848	25	
		800	1.835	5	
3.657	15	112	1.816	5	
		207	1.805	33	
3.610	250	802			
3.564	190	207	1.781	16	
3.542	50	802	1.763	15	
		311	1.756	19	
3.463	10	113	1.744	13	
3.367	10		1.736	16	
3.264	10	114			
3.199	16		1.731	15	
2.966	5		1.706	5	
			1.689	25	
2.919	15		1.684	68	
2.845	32		1.675	12	
2.832	48				
2.777	10		1.610	25	
2.731	52		1.597	8	
			1.592	20	
2.724	55		1.585	18	
2.529	90				
			1.571	25	
			1.565	38	

[a] Interplaner spacing.
[b] Observed intensity.
[c] Partially indexed on the basis of a C-centered monoclinic unit cell with $a=29.74$ Å, $b=3.823$ Å, $c=26.02$ Å, $\beta=92°18'$ by comparison with the single crystal intensities observed from a film taken with a Weisingberg camera [A. D. Wadsley, private communication].

TABLE 7. *X-ray diffraction powder data for the composition* $30Nb_2O_5:WO_3$ *(CuK$_\alpha$ radiation)*

d^a	I^b	d^a	I^b
16.20	10	2.435	9
13.93	4	2.376	40
10.73	16	2.212	6
8.96	7	2.100	8
8.10	5	2.076	74
6.37	14	2.041	90
5.36	8	1.999	5
5.10	50	1.936	8
4.797	7	1.913	48
4.645	60	1.871	10
3.742	132	1.866	10
3.638	312	1.857	12
3.579	10	1.825	18
3.556	10	1.819	42
3.493	228	1.796	8
3.354	37	1.791	8
3.173	16	1.782	23
3.093	7	1.769	7
2.984	14	1.746	14
2.845	55	1.743	25
2.836	47	1.731	30
2.763	38	1.716	10
2.707	46	1.693	22
2.693	18	1.684	30
2.647	8	1.680	60
2.614	7	1.623	15
2.597	6	1.603	8
2.538	65	1.595	30
2.503	45	1.581	44
2.476	10	1.558	28
2.458	10	1.548	8

[a] Interplaner spacing.
[b] Observed intensity.

percent WO_3. This phase is apparently the same as that previously reported to occur at about 15:1, the structure of which could not be verified [1]. The 30:1 ratio is that deduced by Schäfer (private communication). It is apparently composed of some complex packing of the "building blocks" previously described. One possible structure might be $n=3$, $m=4$, $p=2$ ($B_{25}O_{62}$) plus two blocks of $n=3$, $m=4$, $p=1$ ($B_{25}O_{66}$) $=B_{51}O_{128}$ ($25Nb_2O_5 \cdot WO_3$). Another possibility might be $n=3$, $m=4$, $p=2$ ($B_{25}O_{62}$) $+n=3$, $m=5$, $p=1$ ($B_{16}O_{41}$) $=B_{41}O_{105}$ ($20Nb_2O_5 \cdot WO_3$). The exact structure and composition remain to be proven because no good single crystal data is yet available. The "30:1" phase was found to melt incongruently at about 1470 °C. Its unindexed x-ray diffraction powder pattern is listed in table 7.

3.3. Compounds Containing Pentagonal Bipyramid (Sevenfold) Coordinated Cations

a. $Nb_2O_5 \cdot WO_3$ (WNb_2O_8)

A phase isostructural with Nb_3O_7F [25] might be thought likely to occur in this system, but no such structure has ever been reported in pure oxide systems. Instead a new phase was found with unit cell dimensions related to the tetragonal tungsten bronze-type structures. Single crystals of the 1:1 compound were prepared by decomposing the 9:8 phase (made with the less pure end members) at about 1100 °C. Single crystal precession patterns of this phase made by A. Perloff of the National Bureau of Standards staff showed these crystals to be orthorhombic, probable space groups Pmab or $P2_1ab$. From these data the x-ray diffraction powder pattern given in table 8 was indexed with $a=16.615$ Å, $b=17.616$ Å, $c=3.955$ Å. The compound $Nb_2O_5 \cdot WO_3$ could not be made as a single phase in the quenching experiments. X-ray diffraction powder patterns of these specimens always showed a trace of a metastable bronze-type phase plus some $7Nb_2O_5 \cdot 3WO_3$. However, high temperature x-ray powder patterns showed that the extra phases disappeared quickly above about 900 °C. The 1:1 compound was found to dissociate at about 1115 °C to $8Nb_2O_5 \cdot 5WO_3$ plus a bronze-like phase, probably $4Nb_2O_5 \cdot 9WO_3$.

WNb_2O_8 is related to WTa_2O_8 ($a=16.701$ Å, $b=8.864$ Å, $c=3.877$ Å) by a doubled b-axis. The crystal structure of $LiNb_6O_{15}F$ which is apparently isostructural with WTa_2O_8 was found by S. Andersson and M. Lundberg [26] to be made up of octahedrally coordinated cations. These octahedra are corner shared to form a ring of five octahedra. Within this ring is a cation in sevenfold coordination, in a penta-

TABLE 8. *X-ray diffraction powder data for the compound* WNb_2O_8 *(CuK$_\alpha$ radiation)*

d[a]	I[b]	$\frac{1}{d^2}$ obs	$\frac{1}{d^2}$ calc	hkl[c]	d[a]	I[b]	$\frac{1}{d^2}$ obs	$\frac{1}{d^2}$ calc	hkl[c]	d[a]	I[b]	$\frac{1}{d^2}$ obs	$\frac{1}{d^2}$ calc	hkl[c]
8.83	6	0.0128	0.0129	020	2.250	8	.1976	.1975	611	1.7546	16	.3248	.3246	831
8.30	25	.0145	.0145	200	2.223	8	.2023	.2024	451				.3249	091
4.689	6	.0455	.0455	320	2.203	19	.2061	.2060	541	1.7496	20	.3267	.3266	422
4.403	5	.0516	.0516	040				.2062	080	1.7464	23	.3279	.3281	481
4.259	12	.0551	.0552	140	2.198	19	.2070	.2072	621	1.7247	15	.3362	.3363	052
					2.117	4	.2232	.2233	631				.3366	680
3.952	272	.0640	.0639	001	2.091	8	.2288	.2290	740				.3394	291
3.894	46	.0660	.0660	240						1.7154	16	.3398	.3399	342
3.759	112	.0708	.0708	420	2.078	14	.2316	.2317	800				.3399	152
3.608	4	.0768	.0768	021	2.050	6	.2381	.2379	461					
3.570	9	.0785	.0785	201				.2445	711	1.6969	40	.3473	.3472	841
					2.023	18	.2443	.2446	820				.3477	860
3.449	202	.0841	.0841	340						1.6885	9	.3507	.3508	252
3.279	20	.0930	.0929	031	1.9774	50	.2558	.2557	002	1.6740	7	.3569	.3573	761
3.215	8	.0967	.0966	131	1.9652	7	.2589	.2590	012	1.6684	22	.3593	.3591	522
3.165	22	.0998	.0997	311						1.6662	28	.3602	.3604	911
3.110	98	.1034	.1034	520	1.9473	18	.2637	.2642	480					
								.2702	081	1.6651	27	.3607	.3607	581
					1.9247	13	.2699	.2702	202	1.6625	26	.3618	.3620	10,0,0
3.051	16	.1075	.1074	231				.2703	731	1.6548	5	.3652	.3652	442
2.937	4	.1159	.1160	060				.2831	222	1.6434	4	.3703	.3701	921
2.893	80	.1195	.1196	160	1.8797	16	.2830	.2833	840	1.6396	4	.3720	.3717	062
			.1251	411				.2846	281				.3749	10,2,0
2.825	11	.1253	.1255	331	1.8743	15	.2847	.2847	032	1.6326	12	.3752	.3752	532
			.1303	600	1.8521	18	.2915	.2915	312				.3754	162
2.771	78	.1303	.1305	260										
								.2929	741					
2.725	50	.1347	.1348	421	1.8475	24	.2930	.2934	760	1.6234	14	.3795	.3802	4,10,0
2.654	16	.1420	.1421	540				.2956	801				.3861	602
2.644	18	.1430	.1432	620	1.8373	30	.2962	.2968	580	1.6096	13	.3860	.3861	0.10,1
2.633	12	.1443	.1445	051				.2988	811				.3862	931
					1.8284	15	.2991	.2992	232				.3862	262
			.1481	341									.3893	612
2.599	86	.1481	.1481	151	1.8178	6	.3026	.3027	381	1.6029	9	.3892	.3898	1,10,1
2.573	8	.1511	.1509	431	1.8081	6	.3059	.3061	920	1.5928	6	.3942	.3942	452
2.518	8	.1577	.1577	511						1.5853	8	.3979	.3978	542
2.510	8	.1587	.1590	251				.3073	042					
2.445	44	.1673	.1673	521	1.8017	8	.3081	.3085	821					
								.3109	142	1.5826	8	.3993	.3990	622
					1.7908	7	.3118	.3123	571				.3992	771
2.398	7	.1739	.1739	460	1.7852	6	.3138	.3137	402				.4005	681
2.375	8	.1773	.1771	351	1.7762	9	.3170	.3169	412	1.5808	10	.4002	.4006	2,10,1
			.1834	531				.3218	242				.4087	941
2.334	40	.1835	.1836	161	1.7637	14	.3215	.3219	751	1.5640	14	.4088	.4093	960
2.293	5	.1901	.1903	720				.3223	0,10,0	1.5592	26	.4114	.4116	861
			.1943	601						1.5326	12	.4257	.4260	10,0,1
2.268	23	.1943	.1944	261										

[a] Interplaner spacing.
[b] Observed intensity.
[c] Indexed on the basis of an orthorhombic unit cell (space group Pmab or $P2_1ab$) $a = 16.615$ Å, $b = 17.616$ Å, $c = 3.955$ Å.

gonal bipyramid configuration. These rings are connected by further corner sharing to form double chains. The doubled cell in WNb_2O_8 is probably due to an alternate puckering of the positions occupied by the sevenfold coordinated ions, but the proof of this must await a complete single crystal structure analysis.

b. $4Nb_2O_5 \cdot 9WO_3 (Nb_8W_9O_{47})$

A compound having a general diffraction pattern similar to tetragonal potassium tungsten bronze (K_xWO_3) was reported by Roth and Wadsley [1] to occur at the composition $4Nb_2O_5 \cdot 9WO_3$. Sleight and Magneli [27] described the structure of this phase from a crystal obtained from a 1:3 composition which had been heated to a temperature of 1200–1400 °C. The structure of this crystal was found to be made up of three tetragonal-bronze-like unit cells with four out of the twelve possible five-fold rings being occupied by cations, with oxygens above and below forming pentagonal bipyramid coordination polyhedra. This structure represents the composition $Nb_{16}W_{18}O_{94}$ and has orthorhombic symmetry. The unit cell dimensions found in the present work are $a = 36.692$ Å, $b = 12.191$ Å, $c = 3.945$ Å, and were obtained from the indexed x-ray diffraction powder pattern given in table 9. This compound was found to be stable from at least 1150 °C to the congruent melting point of about 1380 °C.

The presence of cations in the pentagonal holes of the tetragonal tungsten bronze structure suggests a possible homologous series which can be expressed as:

$$nB_{10}O_{30} + mBO \text{ or } B_{10n+m}O_{30n+m}$$

where n is the number of subcells of the tetragonal bronze type in the true unit cell and m is the number of pentagonal bipyramid polyhedra occupied by a cation. Each bronze-type subcell has only four pentagonal holes, therefore the maximum value of m must be equal to or less than $4n$.

c. $2Nb_2O_5 \cdot 7WO_3$ $(Nb_4W_7O_{31})$

One method of reducing the general formula $B_{10n+m}O_{30n+m}$ to include the 4:9 compound and to predict a *minimum* number of other phases is to assume $m = 4$. This results in the formula $B_{10n+4}O_{30n+4}$.

TABLE 9. *X-ray diffraction powder data for the compound* $W_9Nb_8O_{47}$ *(*CuK_α *radiation)*

d^a	I^b	$\frac{1}{d^2}$obs	$\frac{1}{d^2}$calc	hkl^c	d^a	I^b	$\frac{1}{d^2}$obs	$\frac{1}{d^2}$calc	hkl^c	d^a	I^b	$\frac{1}{d^2}$obs	$\frac{1}{d^2}$calc	hkl^c
11.59	4	0.0074	0.0075	110	2.835	5	.1244	0.1244	901	1.8671	15	.2869	.2869	222
10.14	12	.0097	.0097	210				.1248	031				.2905	612
9.16	8	.0119	.0119	400	2.827	9	.1251	.1256	131	1.8553	34	.2905	.2906	322
8.64	9	.0134	.0134	310										
			.0186	500				.1276	721				.2919	15,3,1
7.34	6	.0186	.0186	410	2.799	7	.1277	.1278	231	1.8503	20	.2921	.2926	951
								.1311	911	1.8219	34	.3013	.3012	18,3,0
6.12	6	.0267	.0267	600	2.783	76	.1315	.1315	331	1.8178	53	.3026	.3024	960
6.09	11	.0269	.0269	020						1.8040	6	.3073	.3072	161
5.46	57	.0335	.0335	610	2.732	80	.1340	.1339	12,2,0				.3107	622
5.08	5	.0388	.0388	420	2.727	78	.1344	.1344	640	1.7924	10	.3113	.3116	18,1,1
4.314	22	.0537	.0537	620	2.684	12	.1388	.1387	821					
					2.643	7	.1432	.1434	531	1.7872	5	.3131	.3132	361
4.081	6	.0601	.0602	900				.1514	921				.3172	902
4.064	10	.0605	.0606	030	2.569	77	.1515	.1516	631	1.7749	8	.3174	.3176	032
4.044	10	.0612	.0613	130										
3.945	212	.0643	.0643	001	2.490	6	.1613	.1612	731					
3.867	176	.0669	.0669	910						1.7568	22	.3240	.3239	912
								.1675	12,3,0				.3243	332
3.858	195	.0672	.0672	330	2.442	5	.1677	.1678	940	1.7397	12	.3303	.3304	170
			.0709	301						1.7360	30	.3318	.3319	18,2,1
3.754	6	.0710	.0710	011	2.416	9	.1713	.1712	12,0,1				.3332	661
					2.411	10	.1720	.1719	041	1.7305	60	.3339	.3343	21,1,0
3.732	7	.0718	.0717	111	2.405	6	.1729	.1727	141					
3.678	10	.0739	.0740	211	2.370	52	.1780	.1779	12,1,1	1.7269	80	.3353	.3353	15,5,0
					2.366	64	.1787	.1786	341	1.7238	55	.3365	.3364	370
			0.0743	10,0,0									.3390	15,4,1
3.660	28	.0746	0.0746	820	2.325	22	.1850	.1850	931	1.7172	20	.3391	.3394	12,5,1
3.587	4	.0777	.0777	311										
3.559	14	.0790	.0791	530				.1982	12,2,1				.3441	922
			.0828	501	2.245	33	.1984	.1987	641	1.7045	20	.3442	.3443	632
3.474	6	.0829	.0829	411										
					2.158	4	.2147	.2146	12,4,0	1.6808	6	.3540	.3545	21,2,0
3.388	164	.0871	.0871	920	2.095	10	.2278	.2277	15,3,0					
					2.091	14	.2286	.2284	950	1.6703	7	.3583	.3584	16,5,0
3.384	166	.0873	.0873	630				.2314	15,0,1	1.6540	32	.3655	.3655	18,3,1
3.316	5	.0909	.0910	601	2.078	10	.2316	.2318	12,3,1	1.6513	40	.3667	.3666	961
3.260	13	.0941	.0942	221				.2321	941					
			.0977	611						1.6417	24	.3710	.3707	12,1,2
3.197	60	.0978	.0979	321				.2325	051				.3714	342
					2.072	10	.2330	.2332	151	1.6273	7	.3776	.3777	932
3.145	7	.1011	.1012	10,2,0										
					1.9725	54	.2570	.2570	002				.3909	12,2,2
3.115	4	.1030	.1031	421	1.9681	35	.2582	.2583	15,2,1	1.5991	12	.3911	.3914	642
3.058	20	.1070	.1070	12,0,0	1.9644	12	.2591	.2592	651					
3.048	25	.1076	.1077	040						1.5921	9	.3946	.3947	171
3.019	6	.1097	.1098	521	1.9473	4	.2637	.2637	012	1.5841	40	.3985	.3985	21,1,1
2.964	146	.1138	.1137	12,1,0				.2637	302	1.5818	46	.3997	.3996	15,5,1
										1.5798	42	.4007	.4006	371
2.958	158	.1143	.1143	340	1.9332	45	.2676	.2676	18,2,0					
2.912	17	.1180	.1179	621	1.9278	48	.2691	.2690	660				.4089	18,5,0
2.878	50	.1208	.1207	930				.2748	15,4,0	1.5635	10	.4091	.4094	15,6,0
					1.9072	12	.2749	.2752	12,5,0					

[a] Interplaner spacing.
[b] Observed intensity.
[c] Indexed on the basis of an orthorhombic unit cell with $a=36.692$ Å, $b=12.191$ Å, $c=3.945$ Å.

For the 4:9 compound $n=3$. The composition of $n=2$ is $Nb_2O_5 \cdot WO_3$ and the composition of $n=4$ would be $2Nb_2O_5:7WO_3$. The 1:1 compound does not belong to the general homologous series but has a unique structure only vaguely related to the tetragonal tungsten bronze type, as previously described. The structure predicted for $2Nb_2O_5 \cdot 7WO_3$ would be either orthorhombic with one a-axis multiplied by four or tetragonal with both a-axes doubled. The latter structure, which exhibits a higher symmetry than the former, was found to occur for the 2:7 composition between a minimum temperature of about 1245 °C and the probable congruent melting point of 1357 °C. A crystal structure analysis of this compound is currently being conducted by N. Stephensen [28]. The unit cell dimensions of $Nb_4W_7O_{31}$ are $a=24.264$ Å, $c=3.924$ Å, and were obtained from the indexed x-ray diffraction powder pattern listed in table 10.

d. "$6Nb_2O_5 \cdot 11WO_3$" ($Nb_{12}W_{11}O_{63}$)

Roth and Wadsley [1] reported another compound in this system occurring at a ratio of about $13Nb_2O_5:24WO_3$. Kovba and Trunov [9] described a phase to which they assigned the composition $4Nb_2O_5:7WO_3$. The only logical ratio, near this composition, which could belong to the general formula $B_{10n+m}O_{30n+m}$ is $6Nb_2O_5:11WO_3$. In order to include this composition with the 4:9 and 2:7 compounds in one simplified formula, it is sufficient to postulate a series limited to the case $m=n+1$. The new homologous series formula then becomes $B_{11n+1}O_{31n+1}$. In this case for the 2:7 compound, $n=\infty$ and for $4Nb_2O_5 \cdot 9WO_3$, $n=3$. When $n=2$ the composition is $B_{23}O_{63}$ and the predicted structure has two bronze-like subcells in the unit cell, with three filled pentagonal holes. Such a structure would have a very low symmetry and is apparently not formed

Table 10. *X-ray diffraction powder data for the compound* $W_7Nb_4O_{31}$ *(*CuK_α *radiation)*

d [a]	I [b]	$\frac{1}{d^2}$ obs	$\frac{1}{d^2}$ calc	hkl [c]	d [a]	I [b]	$\frac{1}{d^2}$ obs	$\frac{1}{d^2}$ calc	hkl [c]	d [a]	I [b]	$\frac{1}{d^2}$ obs	$\frac{1}{d^2}$ calc	hkl [c]
10.84	10	0.0085	0.0085	210	2.860	31	0.1223	0.1223	660	1.8664	9	0.2871	0.2869	402
8.56	8	.0136	.0136	220	2.838	8	.1242	.1240	830	1.8606	11	.2887	.2886	412
6.06	8	.0272	.0272	400	2.822	8	.1256	.1257	750	1.8447	24	.2939	.2937	422
5.43	35	.0340	.0340	420	2.816	10	.1261	.1261	601	1.8384	11	.2959	.2960	10,6,1
4.508	8	.0493	.0493	520	2.743	98	.1329	.1329	621	1.8189	12	.3023	.3022	502/432
4.289	18	.0544	.0544	440	2.713	102	.1359	.1359	840	1.8087	36	.3057	.3058	12,6,0
4.046	5	.0611	.0612	600	2.660	10	.1414	.1414	631	1.7878	7	.3129	.3129	11,5,1
3.996	5	.0626	.0628	610	2.851	18	.1500	.1499	711/551				{.3141	442
3.924	194	.0649	.0649	001	2.555	50	.1532	.1533	641	1.7839	8	.3142	{.3142	13,4,0/11,8,0
3.839	256	.0679	.0679	620	2.473	8	.1635	.1635	731					
										1.7468	20	.3277	.3277	622
3.792	25	.0696	.0696	540	2.399	5	.1737	.1737	801	1.7232	50	.3368	.3367	12,4,1
3.735	10	.0717	.0717	201	2.349	50	.1804	.1804	821					
3.617	16	.0764	.0764	630	2.311	10	.1872	.1872	661	1.7160	104	.3396	.3397	14,2,0/10,10,0
3.429	25	.0850	.0849	710/550	2.290	5	.1907	.1906	751	1.6949	15	.3481	.3481	642
3.366	136	.0883	.0883	640	2.232	40	.2008	.2008	841	1.6825	6	.3533	.3533	12,8,0
										1.6480	7	.3682	.3685	802
3.333	8	.0900	.0900	720	2.177	5	.2209	.2208	11,3,0/970	1.6426	30	.3706	.3707	12,6,1
3.265	10	.0938	.0938	411	2.128	12	.2308	.2310	10,6,0					
3.181	52	.0989	.0989	421	2.064	14	.2347	.2348	10,0,1/861	1.6326	15	.3752	.3753	822
3.052	7	.1074	.1074	501/431	1.9620	42	.2598	.2598	002	1.6177	4	.3822	.3821	662
3.034	18	.1086	.1087	800	1.9182	60	.2718	.2718	12,4,0	1.5896	12	.3958	.3957	842
								{.2773	11,2,1/10,5,1	1.5720	63	.4047	.4047	14,2,1/10,10,1
2.942	146	.1155	.1155	820	1.8967	7	.2780	{.2786	10,8,0	1.5535	7	.4144	.4145	12,10,0
2.898	5	.1191	.1193	441										

[a] Interplanar spacing
[b] Observed intensity.
[c] Indexed on the basis of a tetragonal unit cell with $a = 24.264$ Å, $c = 3.924$ Å.

in this system. Experimentally the compound "$6Nb_2O_5 \cdot 11WO_3$" was found to be orthorhombic, probably with the a-axis of the tetragonal bronze subcell tripled. It is stable from about 1210 °C to the apparently congruent melting point of 1378 °C. The x-ray diffraction powder pattern listed in table 11 is indexed with $a = 36.740$ Å, $b = 12.195$ Å, $c = 3.951$ Å. It may be concluded from the size and symmetry of the unit cell, that the homologous series formula $B_{11n+1}O_{31n+1}$ is not correct for this compound. Therefore, "$6Nb_2O_5 \cdot 11WO_3$" either has a defect structure or belongs to some other structural homologous series, as yet unknown. A single crystal structure analysis is currently under study by N. Stephenson [28].

e. Metastable Tetragonal Bronze-Type Solid Solution ("3:8")

In addition to the ordered bronze-like phases which have been found in the Nb_2O_5–WO_3 system, another, apparently disordered, phase has also been reported at about the Nb_2O_5:$3WO_3$ composition [5, 6, 7]. In the present study a tetragonal bronze-type phase without any indication of superstructure in the powder pattern was found to occur from about 72 to 74 mole percent WO_3 in a temperature range from about 1100 to 1250 °C. The unit cell dimensions of this phase were found to vary from about $a = 12.190$ Å, $c = 3.968$ Å for the composition containing 72 mole percent WO_3 to $a = 12.178$ Å, $c = 3.930$ Å for the composition containing 75 mole percent WO_3. It must be concluded that the lower temperature phase is only metastable, because it decomposes at high temperatures into the two ordered compounds, $4Nb_2O_5 \cdot 9WO_3$ and $2Nb_2O_5 \cdot 7WO_3$.

3.4. Compounds Related to the ReO_3 Structure-Type. The Magneli "Shear Phases"

In the temperature interval from about 1270 to 1358 °C, at least two phases have been found to occur with x-ray diffraction powder patterns suggestive of the Magneli "shear phases" [29], which are structurally related to WO_3. These phases have been found to occur between about 91 and 94 mole percent WO_3. Due to the difficulty of obtaining equilibrium and the complex nature of the diffraction patterns, it is very difficult to decipher the exact composition of the phases by powder data alone. Although no single crystals have been examined, the best interpretation of the data suggests that there are two equilibrium phases having the Nb_2O_5:WO_3 ratios of 1:11 and 1:15. These compositions would correspond to the members $n = 13$ and $n = 17$ of the homologous series B_nO_{3n-1}. It is possible that other structurally related phases are formed in this compositional region which have very little or no thermal stability. Unindexed x-ray diffraction powder patterns for the "1:11" and "1:15" phases are given in tables 12 and 13, respectively.

3.5. Polymorphs of WO_3 and WO_3 Solid Solutions

WO_3 has been reported to occur in many different polymorphs [30–32]. None of the various high- or low-temperature polymorphs have been previously reported to be quenchable to room temperature. However, many of these reported phases have been found at room temperature in the Nb_2O_5–WO_3 system.

TABLE 11. *X-ray diffraction powder data for the phase "$6Nb_2O_5 \cdot 11WO_3$" (CuK_α radiation)*

d [a]	I [b]	$\frac{1}{d^2}$ obs	$\frac{1}{d^2}$ calc	hkl [c]	d [a]	I [b]	$\frac{1}{d^2}$ obs	$\frac{1}{d^2}$ calc	hkl [c]
11.62	5	0.0074	0.0075	110	2.328	15	.1846	.1846	931
10.18	14	.0097	.0097	210	2.248	25	.1978	.1977	12,2,1
9.16	8	.0119	.0119	400	2.246	22	.1983	.1983	641
8.62	8	.0135	.0134	310	2.097	7	.2273	.2272	15,3,0
5.47	36	.0334	.0334	610	2.095	8	.2282	.2281	950
4.320	16	.0536	.0536	620	2.072	6	.2330	.2329	151
					1.9754	85	.2563	.2563	002
4.070	8	.0604	.0600	900	1.9355	22	.2669	.2669	18,2,0
			.0605	030	1.9290	26	.2688	.2688	660
3.952	236	.0640	.0641	001				.2743	15,4,0
			.0667	910	1.9087	8	.2745	.2748	12.5.0
3.865	140	.0669	.0672	330					
					1.8696	7	.2861	.2861	222
			.0707	301				.2897	612
3.742	7	.0714	.0708	011	1.8585	13	.2895	.2898	322
			.0715	111					
					1.8528	15	.2913	.2913	15,3,1
3.682	8	.0738	.0738	211	1.8496	11	.2923	.2922	951
3.663	19	.0745	.0741	10,0,0					
			.0743	820	1.8239	25	.3006	.3006	18,3,0
					1.8195	32	.3021	.3021	960
3.596	6	.0774	.0775	311				.3230	912
3.562	10	.0788	.0790	530	1.7593	23	.3231	.3235	332
			.0869	920					
3.388	156	.0871	.0872	630				.3302	170
					1.7384	22	.3309	.3310	18,2,1
3.223	12	.0962	.0964	11,1,0	1.7332	33	.3329	.3328	661
			.0975	611					
3.201	24	.0976	.0976	321	1.7317	35	.3335	.3334	21,1,0
					1.7284	52	.3348	.3348	15,5,0
3.061	14	.1067	.1067	12,0,0	1.7244	51	.3363	.3362	370
3.049	22	.1076	.1076	040				.3384	15,4,1
2.968	100	.1135	.1134	12,1 0	1.7184	8	.3386	.3389	12,5,1
2.959	106	0.1142	0.1143	340					
2.917	10	.1175	.1176	621				.3432	922
2.880	33	.1205	.1205	930	1.7072	22	.3431	.3435	631
2.803	5	.1273	.1273	721					
			.1308	911	1.6559	15	.3647	.3646	18,3,1
2.763	76	.1310	.1313	331	1.6524	25	.3663	.3662	961
								.3697	12,1,2
					1.6442	22	.3699	.3705	342
2.735	45	.1337	.1336	12,2,0					
2.730	49	.1342	.1343	640	1.6294	8	.3766	.3768	932
2.687	12	.1385	.1384	821					
2.644	5	.1431	.1431	531				.3899	12.2.2
			.1510	921	1.6012	12	.3901	.3905	642
2.573	62	.1511	.1513	631					
					1.5926	5	.3943	.3943	171
					1.5858	25	.3977	.3975	21,1,1
2.492	5	.1610	.1609	731	1.5833	32	.3989	.3989	15,5,1
2.421	6	.1706	.1708	12,0,1	1.5801	24	.4005	.4002	371
2.414	7	.1716	.1717	041					
2.373	49	.1776	.1775	12,1,1	1.5654	5	.4081	.4081	18,5,0
2.368	59	.1783	.1783	341	1.5640	7	.4089	.4088	15,6,0

[a] Interplanar spacing.
[b] Observed intensity.
[c] Indexed on the basis of an orthorhombic unit cell with $a = 36.740$ Å, $b = 12.195$ Å, $c = 3.951$ Å.

a. Room Temperature Monoclinic Polymorph

A monoclinic polymorph of WO_3 was reported by Tanisaki [32] to have a monoclinic unit cell with $a = 7.30$ Å, $b = 7.53$ Å, $c = 7.68$ Å, $\beta = 90°54'$ at room temperature. However, the x-ray diffraction powder pattern can be completely indexed with the c-axis equal to one-half that of the true unit cell. The presence of superstructure requiring the doubled cell can apparently only be found with single crystal data. For this reason, the x-ray diffraction powder pattern listed in table 14 has been indexed on the basis of one-half the real c-axis value. The unit cell dimensions obtained from this pattern were found to be $a = 7.299$ Å, $b = 7.535$ Å, $c = 7.688$ (3.844) Å, $\beta = 90°54'$. With 1 mole percent solid solution of Nb_2O_5 in WO_3, the parameters are changed to $a = 7.317$ Å, $b = 7.532$ Å, $c = 7.684$ (3.842) Å, $\beta = 90°55'$. For pure WO_3 this monoclinic polymorph is apparently stable from about 17 °C [32] to about 310 °C.

TABLE 12. *X-ray diffraction powder data for the composition Nb_2O_5:11WO_3 (CuK_α radiation)*

d [a]	I [b]	d [a]	I [b]
4.638	5	1.927	90
4.308	7	1.910	30
3.966	25	1.865	58
3.850	350	1.845	90
3.726	230	1.812B	18
3.690	350	1.712	32
3.116B	15	1.700	14
2.764B	10	1.677	100
2.677	178	1.664	50
2.670	190	1.569	8
2.579	28	1.541	18
2.202	25	1.530	25
2.190	25	1.493B	10
2.139	12		
1.998B	10		

B = broad.
[a] Interplaner spacing.
[b] Observed intensity.

TABLE 13. *X-ray diffraction powder data for the composition Nb_2O_5:15WO_3 (CuK_α radiation)*

d [a]	I [b]	d [a]	I [b]
3.931	25	1.898	27
3.839	284	1.869	65
3.760	116	1.855	20
3.682	336	1.841	40
3.134	10	1.812B	15
3.089	23	1.799	25
2.763	7	1.711	23
2.676	140	1.695	20
2.647	96	1.671B	65
2.584	18	1.652	15
2.214	14	1.573	8
2.181	30	1.555	10
2.152	12	1.546	15
2.006B	10	1.529	34
1.922	58	1.525	30

B = broad.
[a] Interplaner spacing.
[b] Observed intensity.

b. Low-Temperature Triclinic Polymorph

According to Tanisaki [32] the room temperature polymorph of WO_3 transforms to a triclinic form at about 17 °C, on cooling. However, on reheating there is still some of the triclinic form remaining at room temperature, indicating some hysteresis in the phase transition. It was found in the present study, that the room temperature monoclinic polymorph could be partially transformed to the triclinic modification by grinding the specimen in a mortar and pestle, without lowering the temperature. The unit cell dimensions of the triclinic form were reported [32] as $a = 7.30$ Å, $b = 7.52$ Å, $c = 7.69$ Å, $\alpha = 88°50'$, $\beta = 90°55'$, $\gamma = 90°56'$. The indexed x-ray diffraction

TABLE 14. *X-ray diffraction powder data for the room temperature (monoclinic) form of* WO_3 *(CuK$_\alpha$ radiation)*

d [a]	I [b]	$\frac{1}{d^2}$ obs	$\frac{1}{d^2}$ calc	hkl [c]	d [a]	I [b]	$\frac{1}{d^2}$ obs	$\frac{1}{d^2}$ calc	hkl [c]
3.840	154	0.0678	0.0677	001	1.8111	45	0.3049	0.3050	$11\bar{2}$
3.761	160	.0707	.0705	020	1.7977	42	.3094	.3094	112
3.646	268	.0752	.0751	200				.3413	022
3.419	5	.0856	.0853	011	1.7116	48	.3414	.3414	$20\bar{2}$
3.344	65	.0894	.0892	120					
3.114	70	.1031	.1030	$11\bar{1}$	1.6914	40	.3495	.3495	041
3.083	50	.1052	.1052	111	1.6894	32	.3504	.3504	202
2.689	132	.1383	.1382	021					
2.667	72	.1407	.1406	210	1.6740	35	.3569	.3569	240
2.629	54	.1447	.1450	$\bar{2}01$	1.6581	34	.3637	.3636	$40\bar{1}$
					1.6504	24	.3671	.3672	141
					1.6455	42	.3693	.3694	141
2.620	152	.1457	.1455	220	1.6423	80	.3708	.3708	420
2.533	22	.1559	.1558	$12\bar{1}$					
2.514	27	.1582	.1580	121	1.6385	50	.3725	.3725	401
2.176	38	.2112	.2110	$22\bar{1}$	1.6231	5	.3919	.3918	$33\bar{1}$
2.154	36	.2156	.2155	221	1.5843	5	.3984	.3985	331
					1.5584	30	.4117	.4119	$22\bar{2}$
2.103	6	.2262	.2262	031	1.5419	32	.4206	.4208	222
2.043	17	.2395	.2394	320					
2.025	12	.2438	.2439	$13\bar{1}$	1.5384	27	.4225	.4224	$24\bar{1}$
2.016	14	.2461	.2461	131	1.5312	10	.4265	.4268	241
1.9955	20	.2511	.2509	$31\bar{1}$	1.5179	15	.4341	.4341	$42\bar{1}$
					1.5029	20	.4427	.4430	421
1.9709	12	.2574	.2576	311	1.4981	22	.4456	.4459	$13\bar{2}$
1.9216	44	.2708	.2708	002					
1.8838	60	.2818	.2818	040				.4503	132
		.3004		400	1.4899	42	.4505	.4507	$31\bar{2}$
1.8246	133	.3004	.3006	140				.4508	340
					1.4679	14	.4641	.4641	312

[a] Interplaner spacing.
[b] Observed intensity.
[c] Indexed on the basis of a monoclinic unit cell with $a = 7.299$ Å, $b = 7.535$ Å, $c = 3.844$ Å ($\frac{1}{2} \times 7.688$ Å), $\beta = 90°54'$.

powder pattern of the triclinic polymorph obtained at room temperature from a specimen which had been removed from liquid nitrogen, is listed in table 15. The value of the *c*-axis was again halved, as the larger value is not necessary to index the powder pattern. According to Tanisaki, this phase is stable from about −40 °C to about 17 °C. The triclinic polymorph was never observed in any of the Nb_2O_5–WO_3 solid solutions.

c. Lowest Temperature Polymorph (Monoclinic)

From about −40 °C to below liquid nitrogen temperature, another monoclinic polymorph occurs in pure WO_3 which was reported by Tanisaki [32] to have $a = 5.27$ Å, $b = 5.16$ Å, $c = 7.67$ Å, $\beta = 91°43'$. This polymorph can be obtained essentially single phase at room temperature by *quenching* a solid solution of $2Nb_2O_5 : 98WO_3$ from the temperature interval 1230 °C to about 1385 °C, the solidus temperature. This polymorph also occurs as a mixture with other polymorphs in specimens containing 1 and 3 mole percent Nb_2O_5. The unit cell dimensions obtained from the powder pattern for the 2 mole percent Nb_2O_5 specimen are $a = 5.305$ Å, $b = 5.192$ Å, $c = 7.671$ Å, $\beta = 91°33'$. The indexed x-ray diffraction powder pattern is given in table 16, utilizing the 7.671 Å value for c as several peaks necessitating this doubled value are observed in the powder pattern. High-temperature x-ray patterns show this phase to be apparently stable in the 2 mole percent Nb_2O_5 composition up to a temperature of about 735 °C, at which temperature it transforms to a tetragonal polymorph. If the temperature is not raised above about 750 °C, this transition is reversible. However, if the temperature is raised to 900 °C the low-temperature monoclinic polymorph is not recovered and the tetragonal phase transforms to the orthorhombic polymorph.

Tungsten trioxide has been reported to be ferroelectric below about −40 °C [33]. Specimens of sintered WO_3 containing 2 to 4 mole percent Ta_2O_5 were reported to exhibit ferroelectric behavior at room temperature [34]. The low-temperature monoclinic polymorph formed by quenching a specimen containing 2 mole percent Nb_2O_5 was examined for evidence of ferroelectricity [35]. However, no conclusive ferroelectric properties could be found.

TABLE 15. *X-ray diffraction powder data for the triclinic form of* WO_3 *(CuK$_\alpha$ radiation)*

d [a]	I [b]	$\frac{1}{d^2}$ obs	$\frac{1}{d^2}$ calc	hkl [c]	d [a]	I [b]	$\frac{1}{d^2}$ obs	$\frac{1}{d^2}$ calc	hkl [c]	d [a]	I [b]	$\frac{1}{d^2}$ obs	$\frac{1}{d^2}$ calc	hkl [c]
3.840	284	0.0678	0.0677	001	2.159	20	0.2145	0.2145	$\bar{2}21$	1.8040	26	0.3073	0.3068	$\bar{1}12$
3.760	224	.0707	.0707	020	2.154	53	.2155	.2158	$22\bar{1}$	1.8007	43	.3084	.3086	$11\bar{2}$
3.652	350	.0750	.0749	200	2.150	51	.2163	.2163	$2\bar{2}1$	1.7931	26	.3110	.3113	$11\bar{2}$
3.362	20	.0885	.0885	$\bar{1}20$	2.120	3	.2224	.2227	$03\bar{1}$	1.7244	17	.3363	.3360	$02\bar{2}$
3.322	25	.0906	.0906	120	2.082	5	.2306	.2310	031	1.7113	24	.3415	.3420	$20\bar{2}$
3.143	42	.1012	.1013	$\bar{1}\bar{1}1$	2.059	4	.2358	.2360	$\bar{3}20$	1.7013	23	.3455	.3451	$04\bar{1}$
3.099	20	.1041	.1042	$\bar{1}11$	2.046	8	.2388	.2389	$\bar{1}31$				.3457	202
3.085	65	.1051	.1051	$1\bar{1}1$	2.032	5	.2422	.2423	320	1.6975	22	.3470	.3470	022
3.070	42	.1061	.1059	$11\bar{1}$	2.025	10	.2439	.2439	$\bar{1}3\bar{1}$	1.6897	17	.3503	.3506	041
2.714	55	.1359	.1358	$02\bar{1}$	2.011	9	.2474	.2481	$3\bar{1}1$	1.6825	13	.3533	.3536	$\bar{2}40$
										1.6653	16	.3606	.3608	$\bar{1}41$
2.667	108	.1407	.1407	$20\bar{1}$	2.005	12	.2487	.2490	$13\bar{1}$					
2.660	102	.1413	.1413	021	1.9985	10	.2504	.2503	$\bar{1}3\bar{1}$	1.6612	52	.3624	.3620	240
2.640	80	.1435	.1435	$\bar{2}20$	1.9844	9	.2540	.2540	$31\bar{1}$	1.6570	31	.3642	.3635	$40\bar{1}$
2.632	93	.1443	.1443	201	1.9746	12	.2565	.2564	$3\bar{1}1$	1.6537	28	.3657	.3660	$\bar{4}20$
2.600	58	.1480	.1477	220	1.9713	14	.2573	.2568	$\bar{3}11$	1.6502	33	.3672	.3669	$\bar{1}41$
													.3672	401
2.562	13	.1524	.1524	$\bar{1}2\bar{1}$	1.9216	48	.2708	.2708	002	1.6358	30	.3738	.3736	$14\bar{1}$
2.527	11	.1567	.1564	$\bar{1}21$	1.8801	52	.2829	.2829	040					
2.501	15	.1598	.1598	$12\bar{1}$	1.8273	148	.2995	.2995	400					
2.500	17	.1600	.1600	$\bar{1}2\bar{1}$					$\bar{1}40$	1.6337	35	.3747	.3744	$\bar{4}20$
2.202	20	.2063	.2066	$\bar{2}21$	1.8198	44	.3020	.3021	$\bar{1}12$	1.6303	18	.3763	.3760	$\bar{1}41$

[a] Interplaner spacing.
[b] Observed intensity.
[c] Indexed on the basis of a triclinic unit cell with $a = 7.30$ Å, $b = 7.52$ Å, $c = 3.845$ Å ($\frac{1}{2} \times 7.69$ Å), $\alpha = 88°50'$, $\beta = 90°55'$, $\gamma = 90°56'$.

TABLE 16. *X-ray diffraction powder data for the low-temperature monoclinic form of* WO_3 *taken from* $2Nb_2O_5 : 98WO_3$ *solid solution* (CuK_α *radiation*)

d [a]	I [b]	$\frac{1}{d^2}$ obs	$\frac{1}{d^2}$ calc	hkl [c]	d [a]	I [b]	$\frac{1}{d^2}$ obs	$\frac{1}{d^2}$ calc	hkl [c]
3.834	400	0.0680	0.0680	002	1.7990	54	0.3090	0.3090	014
3.703	380	.0729	.0729	110	1.7875	28	.3130	.3130	104
3.145	25	.1011	.1011	102	1.7163	37	.3395	.3394	114
3.083	50	.1052	.1051	012	1.6900	25	.3501	.3501	114
3.067	32	.1063	.1064	102	1.6805	37	.3541	.3542	222
2.691	138	.1381	.1382	112	1.6692	41	.3589	.3592	310
2.641	144	.1433	.1432	200	1.6557	28	.3648	.3648	222
			.1435	112	1.6448	26	.3697	.3696	130
2.594	40	.1486	.1484	020	1.6179	4	.3820	.3821	302
2.458	6	.1655	.1654	021	1.5851	4	.3980	.3981	302
2.294	10	.1900	.1900	013					
					1.5776	5	.4018	.4018	032
2.236	5	.2000	.1998	121	1.5729	10	.4042	.4044	204
			.1999	211	1.5464	18	.4195	.4192	312
2.206	22	.2056	.2058	202	1.5422	21	.4205	.4202	024
2.148	70	.2167	.2163	022	1.5326	6	.4257	.4257	204
			.2165	202					
2.120	12	.2429	.2429	212					
2.002	14	.2496	.2495	122	1.5161	28	.4351	.4349	132
								.4352	312
1.9860	17	.2535	.2536	212	1.5056	26	.4412	.4402	132
1.9815	18	.2547	.2548	122				.4415	214
1.9178	68	.2719	.2719	004	1.4895	13	.4508	.4507	124
1.8521	100	.2915	.2915	220	1.4700	24	.4621	.4614	124
1.8192	27	.3022	.3023	104				.4628	214

[a] Interplaner spacing.
[b] Observed intensity.
[c] Indexed on the basis of a monoclinic unit cell with $a = 5.305$ Å, $b = 5.192$ Å, $c = 7.671$ Å, $\beta = 91°33'$.

d. High-Temperature Orthorhombic Polymorph

Although no thermal effect was indicated with DTA, the room-temperature monoclinic polymorph of pure WO_3 is observed in the high temperature x-ray furnace to transform reversibly at 310 °C to an orthorhombic phase in agreement with Wyart and Foex [31]. This orthorhombic form is observed at room temperature in the solid solutions whenever the low-temperature monoclinic polymorph is heated to about 900 °C and cooled by removing from the furnace. The indexed x-ray diffraction powder pattern of a specimen of this polymorph containing 2 mole percent Nb_2O_5 is listed in table 17. It shows no indication of a doubled c-axis and is indexed on the basis of the smaller orthorhombic cell. The unit cell dimensions obtained for this composition, at room temperature, are $a = 7.384$ Å, $b = 7.512$ Å, $c = 7.692$ (3.846) Å. The orthorhombic phase is observed in this composition to transform to tetragonal in the high temperature x-ray furnace at 510 °C and the reverse transition was observed to take place at 440 °C.

e. Tetragonal High-Temperature Polymorph(s)

In pure WO_3 the orthorhombic polymorph was found to undergo a transition to the tetragonal form at about 750 °C in the high-temperature x-ray furnace. The DTA data indicated that the phase transition occurred at a temperature of 740 °C on heating and 730 °C on cooling. These results are in reasonable agreement with those of previous workers [7, 31]. The tetragonal polymorph is found as a single phase as low as 440 °C in the specimen containing 2 mole percent Nb_2O_5. However, in the 3 mole percent Nb_2O_5 specimen, the low-temperature monoclinic polymorph transforms after heating at about 900 °C into a mixture consisting predominantly of a tetragonal modification with only a trace of the orthorhombic form. The unit cell dimensions[4] obtained at room temperature from this composition are $a = 5.265$ Å, $c = 3.846$ Å, and the x-ray diffraction powder pattern from which the data were obtained, indexed on the basis of the smaller cell, is listed in table 18.

In addition to the transformation at 730–740 °C, another transition is observed at about 900 °C in pure WO_3, as indicated by a very small peak in the DTA pattern. High-temperature x-ray diffraction powder patterns indicate that WO_3 is tetragonal both above and below this minor thermal discontinuity. It is possible that the unit cell has a doubled c-axes below 900 °C and only above this temperature does the powder pattern yield the correct unit cell. However, this hypothesis cannot be verified without single crystal data.

Although WO_3 might be expected to have a cubic polymorph of the ReO_3-type, there is no evidence in either the present work or previously reported studies that such a polymorph exists.

TABLE 17. *X-ray diffraction powder data for the orthorhombic form of* WO_3 *taken from* $2Nb_2O_5{:}98WO_3$ *solid solution* (CuK_α *radiation*)

d [a]	I [b]	$\frac{1}{d^2}$ obs	$\frac{1}{d^2}$ calc	hkl [c]
3.845	248	0.0676	0.0676	001
3.754	156	.0710	.0709	020
3.691	232	.0734	.0734	200
3.427	5	.0852	.0853	011
3.346	18	.0893	.0892	120
3.104	60	.1038	.1037	111
2.686	85	.1386	.1385	021
2.662	80	.1411	.1409	201
2.633	126	.1443	.1442	220
2.525	10	.1568	.1568	121
2.173	42	.2119	.2118	221
2.09[c]	5	.2270	.2271	031
2.056	5	.2365	.2359	320
2.018	20	.2455	.2454	131
1.9976	14	.2506	.2504	311
1.9232	48	.2704	.2704	002
1.8779	33	.2836	.2836	040
1.8461	46	.2934	.2934	400
1.8198	21	.3020	.3019	140
1.8064	37	.3065	.3064	112
1.7119	24	.3412	.3413	022
1.7057	25	.3437	.3437	202
1.6879	35	.3510	.3512	041
1.6740	26	.3569	.3569	240
1.6645	32	.3609	.3610	401
1.6568	34	.3643	.3643	420
1.6453	14	.3694	.3695	141
1.5968	5	.3922	.3922	331
1.5530	10	.4147	.4146	222
1.5349	17	.4244	.4245	241
1.5217	20	.4319	.4319	421
1.4933	16	.4484	.4482	132
			.4486	340
1.4858	13	.4530	.4531	312

[a] Interplaner spacing.
[b] Observed intensity.
[c] Indexed on the basis of an orthorhombic unit cell with $a = 7.384$ Å, $b = 7.512$ Å, $c = 3.846$ Å ($\frac{1}{2} \times 7.692$ Å).

TABLE 18. *X-ray diffraction powder data for the tetragonal form of WO_3 taken from $3Nb_2O_5 : 97WO_3$ solid solution (CuK_α radiation)*

d [a]	I [b]	$\frac{1}{d^2}$ obs	$\frac{1}{d^2}$ calc	hkl [c]
3.847	280	0.0676	0.0676	001
3.725	252	.0721	.0722	110
3.106	58	.1037	.1037	101
2.674	116	.1398	.1398	111
2.638	96	.1438	.1443	200
2.173	40	.2118	.2119	201
2.008	25	.2481	.2480	211
1.923	45	.2705	.2705	002
1.861	48	.2886	.2886	220
1.806	42	.3067	.3066	102
1.707	26	.3430	.3426	112
1.675	40	.3566	.3563	201
1.665	48	.3606	.3608	310
1.597	5	.3922	.3923	301
1.552	8	.4150	.4148	202
1.528	28	.4284	.4284	311
1.489	15	.4510	.4509	212

[a] Interplanar spacing.
[b] Observed intensity.
[c] Indexed on the basis of a tetragonal unit cell with $a = 5.265$ Å, $c = 3.846$ Å.

4. Discussion of Phase Equilibria

The postulated phase equilibrium diagram of the binary system Nb_2O_5–WO_3 is shown in figure 1. The experimental data from which this diagram was constructed are given in table 19. The system contains four compounds which are shown as melting congruently, $6Nb_2O_5 \cdot WO_3$, "$6Nb_2O_5 \cdot 11WO_3$," $4Nb_2O_5 \cdot 9WO_3$, and $2Nb_2O_5 \cdot 7WO_3$. Six compounds melt incongruently "$30Nb_2O_5 \cdot WO_3$," $7Nb_2O_5 \cdot 3WO_3$, $8Nb_2O_5 \cdot 5WO_3$, $9Nb_2O_5 \cdot 8WO_3$, and the two Magneli phases estimated to be "$Nb_2O_5 \cdot 11WO_3$" and "$Nb_2O_5 \cdot 15WO_3$." In addition, two stable phases, $13Nb_2O_5 \cdot 4WO_3$ and $Nb_2O_5 \cdot WO_3$ dissociate before melting as does the apparently metastable disordered bronze type solid solution labeled "3 : 8" in the phase diagram. Six of the compounds (8 : 5, 9 : 8, "6 : 11", 2 : 7, "1 : 11," and "1 : 15") are shown on the phase diagram as having minimum stability temperatures. In many of these cases, it is impossible to determine whether or not the minimum temperature represents a stable transition. The existence of solid solution could neither be definitely established in any of the compounds nor in Nb_2O_5. However, WO_3 accepts a maximum of about 3 mole percent Nb_2O_5 in solid solution.

The solidus temperature between the "30:1" phase and $6Nb_2O_5 \cdot WO_3$ has been found to be about 1464 °C. The exact eutectic composition has not been determined but probably exists between about 7 and 10 mole percent WO_3. The peritectic corresponding to the incongruent melting point of $7Nb_2O_5 \cdot 3WO_3$ occurs at 1440 °C and about 40 mole percent WO_3. However, the composition of the two peritectics at 1385 and 1375 °C and of the eutectic at 1364 °C, were not determined exactly. They probably occur between about 60 and 63 mole percent WO_3.

Both the 8:5 and 9:8 compounds apparently have minimum temperatures of stability. However, all efforts to locate accurately the temperature of these minimums proved inconclusive (table 19). For both compounds, the experimental temperature at which the phase begins to form on heating and the temperature at which it begins to dissociate on cooling had a wide range of overlap. Furthermore, the actual temperature of the minimum stability seemed to be strongly dependent on the purity content (table 19, parts I and II). For these reasons the minimum stability temperatures of the 8:5 and 9:8 are indicated on the phase diagram by dashed lines and the temperatures assigned to each, ~ 1090 and ~ 1265 °C, respectively, represent the best compromise between the inconsistencies in the experimental data.

None of the ordered bronze-type phases can be prepared in reasonable laboratory time at 1100 °C. The "6:11" phase was not found to be well crystallized below about 1210 °C. The minimum line at this temperature is dashed to indicate uncertainty in both the temperature value and the stability relation. The same discussion also is relative for the minimum value of the 2:7. In this case, however, the superstructure lines characteristic of this phase do not begin to appear below about 1245 °C. The three ordered bronze-type phases, "6:11", 4:9, and 2:7, all appear to melt congruently at 1378, 1380 and 1357 °C, respectively. The solidus temperatures between these phases at 1365 and 1335°C appear to be measurably lower than the observed melting temperature of the compounds. However, no eutectic compositions could be experimentally determined, possibly due to reduction and, therefore, the liquidus curves are necessarily dashed (see discussion on reduction in sec. 5).

The ability to distinguish a two-phase region between the two bronze-type phases $4Nb_2O_5 \cdot 9WO_3$ and $2Nb_2O_5 \cdot 7WO_3$ was greatly increased by a separation of those phases in the experiments of long-time duration. The top of the specimens within the two-phase region showed only 4:9 in the x-ray diffraction pattern while the bottom of the specimen showed mostly 2:7. This apparent gravity separation is probably enhanced by an appreciable vapor phase in the sealed Pt tube and is considered to be due mainly to vapor transport. A similar gravity separation takes place throughout most of the system and adds more evidence to the probability of a two-phase region between "$6Nb_2O_5 \cdot 11WO_3$" and $4Nb_2O_5 \cdot 9WO_3$. This two-phase region is based mostly on the different morphology and color of these phases, as well as the slight differences in the superstructure exhibited by single crystal patterns. Almost all of the high-temperature phases in the Nb_2O_5-WO_3 system are needle formers. Most of those which contain appreciable WO_3 are yellow-green or blue-green in color. However, the "6:11" phase is white and forms tabular crystals rather than needles.

A eutectic exists between the 2:7 compound and the Magneli "shear" phases at about 1340 °C and 83 mole percent WO_3. However, the exact compositions of the peritectics at 1356 and 1358 °C, corresponding to the decomposition temperatures have not been determined.

216-375 O - 66 - 2

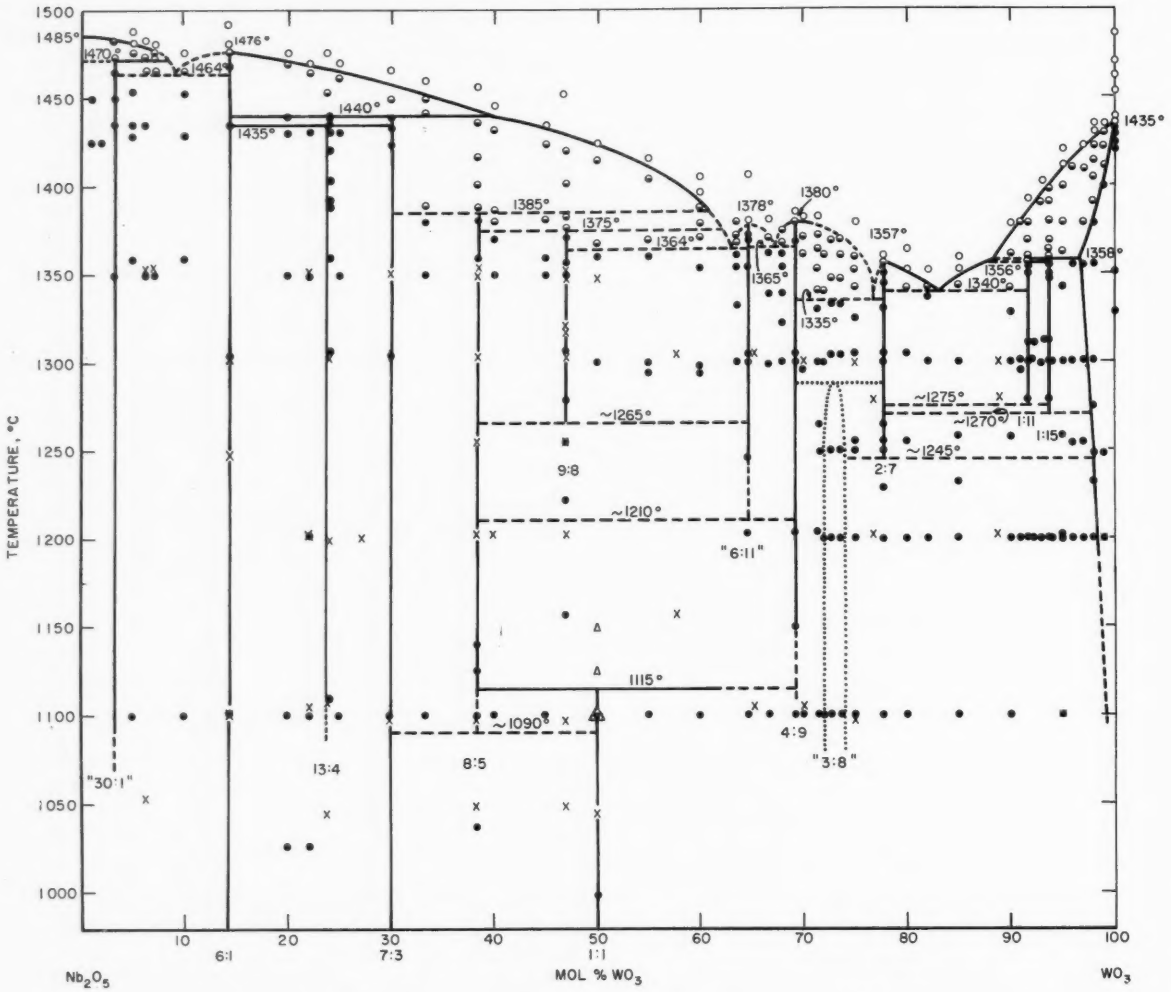

FIGURE 1. *Postulated phase equilibrium diagram of the binary system* Nb_2O_5-WO_3.

Heavy lines represent well-established portions of the system and dashed lines represent not as well-established portions. Dotted lines represent persistent metastable equilibrium.
●—not melted.
◒—partially melted.
○—completely melted.
×—experimental data obtained from "less-pure" materials.
△—high-temperature x-ray data.

Tungsten trioxide has been found to accept a maximum of about 3 mole percent Nb_2O_5 in solid solution at the solidus temperature of 1358 °C. The amount of solid solution decreases with decreasing temperature to about 2 mole percent at 1230 °C and less than 1 mole percent at 1100 °C. The melting point of WO_3 was found, in the present study, to be 1435 °C. This value was independently confirmed by E. M. Levin [36] and is in disagreement with the previously published value of 1472 °C (Jaeger and Germs) [37]. In a discussion of the 1472 °C value for the melting point of WO_3, Phillips and Chang [38] concluded that this temperature was probably too low and might actually represent the eutectic between WO_3 and $W_{20}O_{58}$. However, they did not attempt to experimentally determine the melting points of the compounds WO_3 and $W_{20}O_{58}$ or the solidus temperature between them. The 1435 °C value for the melting point of WO_3 is internally consistent with the experimental phase diagram of both the Nb_2O_5-WO_3 and WO_3-B_2O_3 systems [36]. This value apparently represents the practical melting point for the experimental conditions utilized: sealed Pt tube, heated for very short intervals of time ($\leqq 5$ min). This method is preferable to that of Jaeger and Germs [37] who utilized an open Pt crucible and much longer heating time. However, the true melting point of WO_3 can probably only be established by utilizing an oxygen pressure furnace and extrapolating to one atmosphere pressure.

TABLE 19. *Experimental data for compositions in the binary system* Nb_2O_5–WO_3. *Part I*

Composition		Heat treatments				Results	
		Initial [a]		Final [b]		Physical observation	X-ray diffraction analyses [c]
Nb_2O_5	WO_3	Temp.	Time	Temp.	Time		
Mole %	*Mole %*	*°C*	*Hour*	*°C*	*Hour*		
99	1			1425	65	No melting	Nb_2O_5.
				1450	66	do	Nb_2O_5.
98	2			1425	65	No melting	Nb_2O_5 + "30:1".
96.77	3.23	1350	2			No melting	
(30:1)				1435	46	do	"30:1".
				1450	66	do	"30:1".
				1465	1	No melting (?)	"30:1".
				1474	0.5	Partially melted	"30:1".
				1483	.5	do	
95	5			1100 [d]	60	No melting	"30:1" + Nb_2O_5 (?) + 6:1 (?) [e].
		1359	2			do	"30:1" + 6:1 (?).
				1429	88	do	"30:1" + 6:1 (?).
				1435	46	do	"30:1" + 6:1 (?)
				1454	1	do	"30:1" + 6:1 (?)
				1476	1	Partially melted	"30:1" + 6:1.
				1481	1	Completely melted	
				1488	0.833	do	Low Nb_2O_5.
93.75	6.25	1350	2				
(15:1)				1435	46	No melting	"30:1" + 6:1.
				1468	0.5	Partially melted	"30:1" + 6:1.
				1474	.5	do	"30:1" + 6:1.
				1483	.5	Completely melted	
92.86	7.14	1350	2				
(13:1)				1466	0.5	Partially melted	6:1 + "30:1" (?)
				1473	.117	do	
				1476	.5	do	6:1 (+ unknown).
				1478	16.5	do	6:1.
				1481	0.5	Completely melted	
90	10			1100 [d]	60	No melting	6:1 + "30:1".
		1359	2			do	6:1 + "30:1" (?).
				1429	88	do	6:1 + "30:1" (?).
				1453	1	do	6:1 + "30:1" (?).
				1466	1	Partially melted	
				1476	1	Completely melted	6:1 + low Nb_2O_5.
85.71	14.29			1100 [d]	60	No melting	6:1.
(6:1)		1304	2			do	6:1.
				1435	0.25	do	
				1467	.25	do	6:1.
				1476	.5	Partially melted	
				1481	.5	Completely melted	6:1 + low Nb_2O_5.
				1492	.25	do	Low Nb_2O_5.
80	20			1026	136	No melting	6:1 + 7:3 (+ unknown tr) [e].
				1100 [d]	60	do	6:1 + 7:3.
				1102	65	do	6:1 + 7:3 + 13:4 (+ unknown) [e].
		1350	2			do	6:1 + 7:3 + 13:4 (tr) [e].
				1430	1	do	6:1 + 13:4 + 7:3 (tr) [e].
				1431	17	do	6:1 + 13:4 + 7:3 (tr) [e].
				1440	1	do	6:1 + 7:3.
				1470	0.5	Partially melted	
				1476	.5	Completely melted	
77.78	22.22			1026	136	No melting	6:1 + 7:3 (+ unknown tr) [e].
(7:2)				1100 [d]	60	do	6:1 + 7:3 + 13:4 (+ unknown tr) [e].
				1102	65	do	6:1 + 7:3 + unknown + 13:4 (tr) [e].
				1202	20	do	6:1 + 7:3 (+ unknown tr) [e].
		1350	2			do	
7:2				1431	0.5	do	13:4 + 6:1 + 7:3 [e].
(con)				1465	.5	Partially melted	
				1470	.5	Completely melted	
76.19	23.81			1109	2	No melting	6:1 + 7:3 + unknown [e].
(16:5)				1110	18	do	7:3 + unknown + 6:1 (?) [e].
				1307	1	do	6:1 + 7:3 [e].
		1360	2			do	
				1389	119	do	
				1393	88	do	13:4.
				1404	0.25	do	
				1421	.25	do	
				1431	17	do	13:4 + 6:1 + 7:3 (?) [e].
				1452	0.5	Partially melted	
				1476	.25	Completely melted	
		1360	2				
		1389	119				
		900	0.33			No melting	13:4.
				1435	1.25	do	13:4.
				1439	17	do	13:4 + 7:3 + 6:1 (?) [e].
				1440	1	do	13:4 + 7:3 + 6:1 (?) [e].
				1454	1	Partially melted	13:4 + 6:1 + 7:3 (?) [e].
75	25			1100 [d]	60	No melting	7:3 + 6:1 + 13:4 [e].
				1102	65	do	7:3 + 6:1 + 13:4 + unknown [e].
		1350	2			do	
				1431	17	do	13:4 + 7:3 (?).
				1462	0.5	Partially melted	
				1470	.5	Completely melted	
70	30			1100 [d]	60	No melting	7:3 + "bronze" (tr) [e].
(7:3)		1304	2			do	7:3.
				1423	1	do	

TABLE 19. *Experimental data for compositions in the binary system* Nb_2O_5–WO_3. *Part 1*—Continued.

Composition		Heat treatments				Results	
		Initial [a]		Final [b]		Physical observation	X-ray diffraction analyses [c]
Nb_2O_5	WO_3	Temp.	Time	Temp.	Time		
Mole %	*Mole %*	*°C*	*Hour*	*°C*	*Hour*		
				1434	1	do	7:3.
				1439	17	do	7:3.
				1449	0.583	Partially melted	
				1466	.33	Completely melted	
66.67	33.33			1100 [d]	60	No melting	7:3+1:1+"bronze" (tr) [e].
		1350	2			do	
				1381	1	do	7:3+8:5.
				1389	1	Partially melted (?)	
				1442	0.5	Partially melted	
				1450	.5	do	
				1461	.5	Completely melted	
61.54	38.46			1037	236	No melting	7:3+1:1.
(8:5)				1100 [d]	60	do	7:3+1:1+"bronze" (tr) [e].
				1100	167	do	7:3+1:1+8:5 [e].
				1125	160	do	8:5+1:1+7:3 [e].
				1140	65	do	8:5+1:1+7:3 [e].
		1357	3.5			do	
				1037	236	do	8:5+1:1 (tr) [e].
				1100	167	do	8:5+1:1 (tr) [e].
				1125	160	do	
				1140	65	do	
		1359	2			do	8:5.
				1381	2	do	8:5+7:3 [f].
				1388	2	Partially melted (?)	7:3+8:5 (tr).
				1402	2	do	7:3.
				1417	1	do	
				1437	1	do	
				1457	0.5	Completely melted	
60	40			1100 [d]	60	No melting	7:3+1:1+"bronze" (tr) [e].
		1350	2			do	
				1371	1	do	8:5+9:8 (tr).
				1381	1	Partially melted (?)	8:5.
				1387	1	Partially melted	
				1433	1	do	
				1446	0.5	Completely melted	
55	45			1100 [d]	60	No melting	1:1+7:3+"bronze" (tr) [e].
		1350	2			do	
				1360	0.67	do	9:8+8:5.
				1381	.5	Partially melted (?)	
				1424	.5	Partially melted	
				1435	.5	Completely melted	
52.94	47.06			1157	89	No melting	8:5+1:1+"bronze" [e].
(9:8)				1222	168	do	9:8+8:5+"6:11" [e].
				1255	89	do	9:8+8:5+"6:11" [e].
				1279	64	do	9:8+8:5+"6:11" [e].
				1307	1	do	9:8+8:5+"6:11" [e].
				1350	1	do	9:8+8:5 (tr).
				1351	2	do	9:8+8:5 (tr).
				1351	18	do	9:8+8:5 (tr).
		1357	2			No melting	
				1222	168	do	9:8+8:5+"6:11".
				1255	89	do	9:8+8:5+"6:11".
				1279	64	do	9:8+8:5 [f].
				1371	1	do	9:8+8:5 (tr).
				1377	1	Partially melted (?)	9:8+8:5.
				1383	1	Partially melted	9:8+8:5.
				1402	0.25	do	8:5+Q−liq [f].
				1422	.25	do	
				1452	.25	Completely melted	Poorly crystalline 8:5 [f].
50	50			998	144	No melting	1:1+7:3+"bronze" [e].
				1100 [d]	60	do	1:1+7:3+"bronze" [e].
		1300	2			do	
				1361	0.5	do	9:8+"6:11".
				1368	.67	Partially melted (?)	
				1414	.5	Partially melted	
				1424	.5	Completely melted	
45	55			1100 [d]	60	No melting	1:1+"bronze".
				1294	65	do	9:8+"6:11".
				1404	0.5	Partially melted	
				1415	.583	Completely melted	9:8+Q−liq [f].
		1300	2			No melting	
				1360	0.5	do	9:8+"6:11".
				1370	.5	Partially melted (?)	
40	60			1100 [d]	60	No melting	1:1+"bronze".
				1294	65	do	"6:11"+9:8.
				1405	0.5	Completely melted	Q−liq+"bronze".
		1298	2			No melting	"6:11"+9:8 (?)+8:5 (tr) [e].
				1353	1	do	"6:11"+9:8.
				1371	1	Partially melted	"6:11+9:8.
				1379	1	do	9:8+"6:11"+8:5 tr+Q−liq [e].
				1388	1	do	Q−liq+9:8 (?) [f].
				1396	0.833	Completely melted	"bronze"+Q−liq.
36.36	63.64	1300	2			No melting	
(4:7)				1332	17	do	"6:11"+9:8 (?).
				1354	64	do	"6:11"+9:8 (?).
				1361	0.5	do	"6:11"+9:8 (?).
				1368	.5	Partially melted	"6:11"+9:8 (?).

TABLE 19. *Experimental data for compositions in the binary system* Nb_2O_5–WO_3. *Part I*—Continued.

Composition		Heat treatments				Results	
		Initial [a]		Final [b]		Physical observation	X-ray diffraction analyses [c]
Nb_2O_5	WO_3	Temp.	Time	Temp.	Time		
Mole %	*Mole %*	*°C*	*Hour*	*°C*	*Hour*		
				1372	.5	do	"6:11" + 9:8 (?).
				1380	.5	do [f]	"6:11" + 9:8 (?).
35.29	64.71			1100 [d]	60	No melting	"bronze" + 1:1.
(6:11)				1100	64	do	"bronze" + 1:1.
				1203	19	do	4:9 + 8:5 tr.
				1246	165	do	"6:11".
				1305	48	do	"6:11".
		1298	2			No melting	
				1246	165	do	"6:11".
				1353	1	do	"6:11".
				1369	93	do	"6:11".
				1371	1	do	"6:11".
				1380	1	Completely melted	"bronze" + Q − liq.
				1406	0.5	do	"bronze" + Q − liq.
33.33	66.67			1100 [d]	60	No melting	"bronze" + 1:1.
		1296	2			do	"6:11" + 4:9 (?).
				1339	166	do	"6:11" + 4:9 (?).
				1362	1	do	
				1371	1.5	Partially melted	"6:11" + Q − liq.
				1381	1	Completely melted	"bronze" + Q − liq (tr).
32	68	1300	2			No melting	
				1322	17	do	4:9 + "6:11" (?).
				1339	166	do	4:9 + "6:11" (?).
				1354	64	do	
				1361	0.5	do	
				1368	.5	Partially melted	
				1375	.5	do	
30.77	69.23			1100 [d]	60	No melting	"bronze" + 1:1 (tr).
(4:9)				1100	64	do	"bronze" + 1:1 (tr).
				1150	160	do	Poorly crystalline 4:9.
				1203	19	do	4:9 + "bronze" + 8:5 (?) [e].
				1300 [d]	48	do	4:9.
				1305	48	do	4:9.
		1299	2			do	
				1150	160		4:9.
				1368	1	do	
				1379	0.75	Partially melted	4:9.
				1405	1	Completely melted	"bronze" + Q − liq (tr).
30	70			1100 [d]	60	No melting	"bronze" + 1:1 (tr).
		1296	2			do	
				1361	1	Partially melted	
				1371	1	do	4:9 + Q − liq.
				1382	1	Completely melted	"bronze + Q − liq.
28.57	71.43			1100 [d]	60	No melting	"bronze" + 1:1 (tr).
(2:5)				1203	19	do	"bronze" + 4:9 (?).
				1300 [d]	48	do	4:9 + 2:7 (?).
				1305	48	do	4:9 + 2:7 (?).
		1249	70			do	
				1331	64	do	4:9 + 2:7 (?).
		1265	1			do	"bronze" + 4:9 (?).
				1330	0.5	do	4:9 + 2:7 (?).
		1296	2			do	
				1329	16.5	do	4:9 + 2:7 (?).
				1341	1	Partially melted	4:9 + Q − liq.
				1353	1	do	4:9 + Q − liq.
				1364	1	do	
				1372	1.5	do	
				1382	1	Completely melted	"bronze" + Q − liq.
28	72			1100 [d]	60	No melting	"bronze" + 1:1 (tr) + WO_3 (tr) [e].
		1200	70			do	
		1300	2			do	
				1340	0.5	Partially melted	4:9 + Q − liq.
				1361	.5	do	
27:27	72.73			1100 [d]	60	No melting	"bronze" + WO_3 + 1:1 (tr) [e].
(3:8)				1200	70	do	"bronze".
				1347	64	Partially melted	4:9 + "bronze".
		1200	2			No melting	
		1250	65			do	
				1333	67	do	4:9 + 2:7.
		1200	2				
		1304	16			No melting	
				1369	0.5	Partially melted	
26.42	73.58			1100 [d]	60	No melting	"bronze" + WO_3 + 1:1 (tr) [e].
(14:39)				1200	70	do	"bronze".
		1200	2			do	
		1250	65			do	
				1333	67	do	4:9 + 2:7.
				1347	64	Partially melted	
				1361	0.5	do	
		1200	2				
		1304	16				
				1370	0.5	Partially melted	
25	75			1100 [d]	60	No melting	"bronze" + WO_3 + 1:1 (tr) [e].
(1:3)				1250	2	do	"bronze + L-MonWO_{3m} + "1:1" + WO_{3m} [e].
				1250	260	Partially melted [g]	

TABLE 19. *Experimental data for compositions in the binary system* Nb_2O_5–WO_3. *Part I*—Continued.

Composition		Heat treatments				Results	
		Initial [a]		Final [b]		Physical observation	X-ray diffraction analyses [c]
Nb_2O_5	WO_3	Temp.	Time	Temp.	Time		
Mole %	*Mole %*	*°C*	*Hour*	*°C*	*Hour*		
		1200	2			No melting	
				1255	65	do	"bronze" + 2:7.
				1305	16	do	4:9 + 2:7 (?).
				1343	0.75	Partially melted	4:9 + Q − liq.
				1353	.5	do	4:9 + Q − liq.
				1360	.5	do	
				1379	.5	Completely melted	
		1200	68			No melting	"bronze" + L-MonWO_{3ss} (tr).
				1325	97	do	4:9 + 2:7 (?).
22.22	77.78			1100 [d]	60	No melting	"bronze" + WO_3 + 1:1 (tr) [e].
(2:7)				1100	64	do	"bronze" + WO_3.
				1202	20	do	"bronze" + L-MonWO_{3ss} + WO_3 (?).
				1250	260	Partially melted [g]	
				1265	1	do	"bronze" + L-MonWO_{3ss} [e].
				1300 [d]	48	do	
				1343	0.5	do	
				1360	1	Completely melted	
		1200	2			No melting	
				1229	67	do	"bronze" + Tet WO_{3ss}.
				1255	65	do	2:7.
				1305	16	do	"bronze" + "1:11" [e].
				1342	0.5	Partially melted [g]	
				1351	.583	Completely melted [g]	
		1200	2				
		1249	70			No melting	2:7.
				1229	67	do	2:7.
				1331	64	do	2:7.
				1344	0.75	do	2:7.
				1350	.5	do	
				1357	.5	Partially melted	
20	80			1100 [d]	60	No melting	"bronze" + WO_3 + 1:1 (tr) [e].
				1200	2	do	
				1343	0.5	Partially melted	
		1200	2			No melting	
				1255	65	do	"bronze" + 2:7 + L-MonWO_{3ss} [e].
				1305	16	do	"bronze" + 2:7 + "1:11" + "1:15" (?) [e].
				1342	0.5	Partially melted	
				1352	.5	Completely melted (?)	
				1363	.5	Completely melted	
18	82	1200	2			No melting	
		1300	2			do	2:7 + "1:11".
				1337	0.5	do	2:7 + "1:11".
				1343	.5	Partially melted	2:7 + Q − liq.
				1352	.5	Completely melted	
15	85			1100 [d]	60	No melting	WO_3 + "bronze".
		1200	2			do	
				1232	17	do	"bronze" + L-MonWO_{3ss} + WO_{3ss} (tr).
				1258	16	do	"bronze" + L-MonWO_{3ss} + 2:7 (?) [e].
				1300	16	do	2:7 + "1:11".
				1343	0.5	Partially melted	
				1352	.5	Completely melted	
				1359	.5	do	
10	90			1100 [d]	60	No melting	WO_3 + "bronze".
				1100	20	do	WO_3 + "bronze".
				1200	90	do	L-MonWO_{3ss} + "bronze" + WO_{3ss} (?).
				1250	17	Partially melted [g]	
				1275	144	do	L-MonWO_{3ss} + "bronze".
		1200	2			No melting	
				1258	16	do	L-MonWO_{3ss} + "bronze" + 2:7 (?) [e].
				1300	16	do	"1:11" + "1:15" + 2:7 [e].
				1301	69	do	"1:11" + 2:7.
				1328	0.5	do	
				1342	.5	Partially melted (?)	"1:11" + Q − liq.
				1343	17	Partially melted	"1:11" + Q − liq.
				1361	0.67	do	
				1378	.5	Completely melted	
9	91	1200	2			No melting	
				1295	67	do	"1:11" + 2:7 (tr).
				1301	69	do	"1:11" + 2:7 (tr).
		1200	2				
		1300	2			No melting	
				1379	0.083	Partially melted	
8.33	91.67	1200	2			No melting	
(1:11)				1279	65	do	"1:11" + 2:7 + "1:15" (?) [e].
				1311	70	do	"1:11" + 2:7 (tr) [e].
				1350	17	do	"1:11".
		1200	2				
		1300	2			No melting	"1:11".
				1354	0.33	do	"1:11".
				1355	.5	do	"1:11".
				1357	.5	Partially melted	"1:15" + L-MonWO_{3ss} + Q − liq.
				1359	.5	do	L-MonWO_{3ss} + Q − liq.
				1369	.5	do	L-MonWO_{3ss} + Q − liq.
				1379	.083	do	
				1392	.083	Completely melted	Q − liq.

TABLE 19. *Experimental data for compositions in the binary system* Nb_2O_5–WO_3. *Part I*—Continued.

Composition		Heat treatments				Results	
		Initial [a]		Final [b]		Physical observation	X-ray diffraction analyses [c]
Nb_2O_5	WO_3	Temp.	Time	Temp.	Time		
Mole %	*Mole %*	*°C*	*Hour*	*°C*	*Hour*		
8	92	1200	2			No melting	
				1301	69	do	"1:11" + "1:15" (?).
7.69 (1:12)	92.31	1200	2			No melting	
				1311	70	do	
7.14 (1:13)	92.86	1200	2			No melting	
				1311	70	do	
7	93	1200	2			No melting	
				1299	67	do	"1:15" + "1:11".
		1200	2				
		1300	2				
						No melting	
				1391	0.083	Partially melted	
				1402	.083	Completely melted	
6.66 (1:14)	93.33	1200	2			No melting	
				1312	68	do	"1:15" + "1:11".
6.25 (1:15)	92.75	1200	16			No melting	Tet WO_{3ss} + "bronze" + tr WO_{3ss}.
				1279	65	do	"1:15" + L-MonWO_{3ss} + "1:11" + 2:7 (tr) [e].
				1312	68	do	"1:15" + L-MonWO_{3ss} (?).
				1350	17	do	"1:15" + L-MonWO_{3ss} (?).
		1200	2				
		1300	2				
						No melting	"1:15" + L-MonWO_{3ss} (?) + "1:11" (?) [e].
				1355	0.5	do	"1:15" + L-MonWO_{3ss} (?) + "1:11" (?) [e].
				1369	.5	Partially melted	L-MonWO_{3ss} + Q − liq.
				1380	.083	do	
				1391	.083	do	
				1398	.083	do	
		1200	2				
		1300	2				
		1347	4.5			No melting	"1:15" + L-MonWO_{3ss} (tr).
				1357	0.5	do	"1:15".
				1359	.5	Partially melted	L-MonWO_{3ss} + Q − liq.
				1364	.5	do	L-MonWO_{3ss} + Q − liq.
6	94	1200	2			No melting	
				1299	67	do	"1:15" + L-MonWO_{3ss}.
5	95			1100 [d]	60	No melting	WO_3 + "bronze".
				1100	20	do	WO_3 + "bronze".
				1200	90	do	L-MonWO_{3ss} + "bronze" + WO_3 (tr).
				1202	20	do	L-MonWO_{3ss} + "bronze" + WO_3(tr).
				1250	16	Partially melted (?) [e]	L-MonWO_{3ss} + Q − liq.
				1275	144	Partially melted [e]	L-MonWO_{3ss} + "1:15" + WO_3 (tr).
		1200	2			No melting	L-MonWO_{3ss} + WO_{3ss} + "bronze".
				1200	70	do	L-MonWO_{3ss} + WO_{3ss} + "bronze".
				1258	16	do	L-MonWO_{3ss} + "bronze".
				1299	67	do	"1:15" + L-MonWO_{3ss}.
				1300	16	do	L-MonWO_{3ss} + "1:15" + WO_{3ss} + "1:11" (?) [e].
				1343	0.5	do	
				1343	17	do	"1:15" + L-MonWO_{3ss} + "1:11" (?) [e].
				1362	0.75	Partially melted	L-MonWO_{3ss}.
				1379	.75	do	L-MonWO_{3ss} + Q − liq (?).
				1400	.5	do	
				1411	.083	Completely melted	
				1420	.25	do	L-MonWO_{3ss} (?).
4	96	1200	2			No melting	
				1254	66	do	
				1355	19	do	L-MonWO_{3ss} + "1:15".
				1410	0.083	Partially melted	
		1200	2				
		1301	68			No melting	L-MonWO_{3ss} + "1:15".
				900 [h]	0.25	do	Tet WO_{3ss} + "1:15".
3	97	1200	2			No melting	
				1254	66	do	L-MonWO_{3ss} + 2:7.
				1355	19	do	L-MonWO_{3ss} + Orth WO_{3ss} (?).
				1379	0.083	Partially melted	
				1409	.083	do	
				1422	.083	Completely melted	
		1200	2				
		1301	68			No melting	L-MonWO_{3ss} + "1:15".
				900 [h]	.025	do	Tet WO_{3ss} + "1:15".
2	98	1200	2			No melting	
				1200	90	do	L-MonWO_{3ss} + WO_{3ss} + "bronze".
				1232	17	do	L-MonWO_{3ss}.
				1275	19	do	L-MonWO_{3ss} + WO_{3ss} + "bronze".
				1355	19	do	
				1379	0.083	do	
				1391	.083	Partially melted	
				1405	.083	do	
				1414	.083	do	
				1422	.083	do	
				1430	.083	Completely melted	
				1435	.083	do	L-MonWO_{3ss}.
		1200	2				
		1248	67			No melting	L-MonWO_{3ss}.
				900 [h]	0.25	do	Orth WO_{3ss} + Tet WO_{3ss} (tr).
				900	.25	do	Orth WO_{3ss}.
		1200	2				
		1301	68			No melting	L-MonWO_{3ss}.
				900 [h]	0.25	do	Orth WO_{3ss} + Tet WO_{3ss}.

TABLE 19. *Experimental data for compositions in the binary system* Nb_2O_5–WO_3. *Part I*—Continued.

Composition		Heat treatments				Results	
		Initial [a]		Final [b]		Physical observation	X-ray diffraction analyses [c]
Nb_2O_5	WO_3	Temp.	Time	Temp.	Time		
Mole %	*Mole %*	*°C*	*Hour*	*°C*	*Hour*		
1	99	1200	2			No melting	WO_{3ss} + L-MonWO_{3ss}.
				1200	90	do	WO_{3ss} + L-MonWO_{3ss}.
				1400	0.083	do	
				1411	.083	Partially melted	
				1422	.083	do	
				1430	.083	do	
				1435	.083	Completely melted	
		1200	2				
		1248	67			No melting	WO_{3ss} + L-MonWO_{3ss}.
				900 [b]		do	WO_{3ss}.
0	100			1000	10	No melting	WO_3.
				1329	2	do	WO_3 + TriWO_3.
				1351	48	do	WO_{3ss} + TriWO_3.
				1420	0.083	do	
				1424	.083	do	
				1430	.083	do	
				1433	.083	do	
				1435	.05	Completely melted	
				1435	.083	do	
				1436	.166	do	
				1437	.083	do	
				1439	.083	do	
				1453	.083	do	
				1462	.083	do	
				1470	.083	do	
				1485	.083	do	WO_3 + TriWO_3.

Experimental data for compositions in the binary system Nb_2O_5–WO_3. *Part II (less pure end members)*

Composition		Heat treatments				Results	
		Initial [i]		Final		Physical observation	X-ray diffraction analyses [c]
93.75	6.25			1053	336	No melting	6:1 + Nb_2O_5.
(15:1)		1354	48			do	"30:1" + 6:1 (?).
				1053	336	do	"30:1" + 6:1 (?).
92.86	7.14			1354	40	No melting	"30:1" + 6:1.
(13:1)							
85.71	14.29			1100	66	No melting	6:1.
(6:1)				1248	64	do	6:1.
				1352	66	do	6:1.
77.78	22.22			1104	68	No melting	6:1 + 7:3 + 13:4.
(7:2)				1203	89	do	6:1 + 13:4 + 7:3 (?).
				1352	21	do	6:1 + 7:3 + 13:4 (tr).
76.19	23.81			1044	336	No melting	13:4 + 6:1 (?) + 7:3 (?).
(16:5)				1109	65	do	13:4 + 6:1 (?) + 7:3 (?).
				1200	138	do	13:4 + 6:1 + 7:3.
				1303	71	do	6:1 + 7:3 + 13:4 (tr).
72.73	27.27			1201	89	No melting	13:4 + 7:3.
(8:3)							
70	30			1097	94	No melting	7:3 + 13:4 (tr).
(7:3)				1349	23.5	do	7:3 + 6:1 (tr).
61.54	38.46			1097	94	No melting	7:3 + 1:1.
(8:5)				1201	113	do	8:5 + 7:3 (tr).
				1202	42	do	8:5 + 7:3 + "bronze".
				1255	65	do	8:5 + 7:3 (tr).
				1255	92	do	8:5 + 7:3 (tr).
				1303	16	do	8:5 + 7:3 (tr).
				1350	19	do	8:5 + 7:3 (tr).
		1354	16			No melting	8:5 + 7:3 (tr).
				1048	336	do	8:5 + 7:3 + "bronze" + 1:1.
60	40			1203	89	No melting	8:5 + "bronze" (tr).
(3:2)							
52.94	47.06			1097	70	No melting	7:3 + 1:1 + "bronze" (tr).
(9:8)				1201	113	do	8:5 + "bronze".
				1255	65	do	8:5 + "bronze" + 9:8 (?).
				1303	16	do	9:8 + 8:5 (tr).
				1318	67	do	9:8 + 8:5 (tr).
				1321	19	do	9:8 + 8:5 (tr).
				1348	20	do	9:8 + 8:5 (tr).
				1350	19	do	9:8 + 8:5 (tr).
				1352	21	do	9:8 + 8:5 (tr).
				1352	68	do	9:8 + 8:5 (tr).
		1354	16			do	9:8 + 8:5 (tr).
				1048	336	do	1:1 + 7:3 + "bronze" + 9:8 (tr) + 8:5 (tr).
50	50			1098	336	No melting	1:1 + "bronze" + 7:3.
				1101	66	do	1:1 + "bronze" + 7:3.

Experimental data for compositions in the binary system Nb_2O_5–WO_3. *Part II (less pure end members)*—Continued.

Composition		Heat treatments				Results	
		Initial [1]		Final		Physical observation	X-ray diffraction analyses [c]
		1348	20			do	9:8 + "6:11"[tr].
				1044	336		8:5 + "6:11" + 1:1.
42.31	57.69			1157	89	No melting	"bronze" + 1:1 + 8:5.
(11:15)				1305	22	do	"6:11" + 9:8.
35.14	64.86			1105	67	No melting	"6:11".
(13:24)				1305	22	do	"6:11".
30	70			1105	67	No melting	4:9 + "bronze" (?).
(3:7)				1301	70	do	4:9 + "bronze" (?).
25	75			1097	70	No melting	"bronze" + WO_3 (tr).
(1:3)				1300	44	Partially melted (?)[g]	"bronze".
				1300	70	do	"bronze".
23.17	76.83			1202	24	No melting	"bronze" + WO_{3ss} (?).
(19:63)				1279	46	Partially melted (?)[g]	
11.11	88.89			1202	24	No melting	"bronze" + L-MonWO_{3ss} + WO_{3ss}.
(1:8)				1279	46	Partially melted (?)[g]	"1:11" + "bronze".
				1300	44	do	"1:11" + 2:7.

[a] All specimens were initially calcined at 700 °C for 19 hr with heating and cooling rates of approximately 4 °C/min. Small portions of this calcine were then reheated for the designated time at one or more designated higher temperatures and generally quenched in sealed Pt tubes.

[b] After the initial heat treatment(s) all specimens were reheated at the indicated temperature and quenched in sealed Pt tubes, unless otherwise specified.

[c] The phases identified are given in the order of amount present at room temperature. The phases are not necessarily those present at the temperature to which the specimen was heated.

(?) = interpretation is not certain.

ss = solid solution.

(tr) = trace just barely discernible in x-ray pattern.

"30:1" = a phase of unknown structure occurring at a mole ratio of approximately 30:1 Nb_2O_5:WO_3.

(unknown) = extra peaks in the x-ray pattern which cannot be assigned to any recognized phase.

6:1 = $6Nb_2O_5 \cdot WO_3$ ($WNb_{12}O_{33}$).

low Nb_2O_5 = nonequilibrium phase (similar to the low temperature form of Nb_2O_5), when quenched from above the liquidus and examined at room temperature.

7:3 = $7Nb_2O_5 \cdot 3WO_3$ ($W_3Nb_{14}O_{44}$).

13:4 = $13Nb_2O_5 \cdot 4WO_3$ ($W_4Nb_{26}O_{77}$).

"bronze" = a metastable disordered phase having a variable composition and an undistorted tetragonal-tungsten-bronze type x-ray pattern (designated as "3:8" on the phase diagram).

8:5 = $8Nb_2O_5 \cdot 5WO_3$ ($W_5Nb_{16}O_{55}$).

9:8 = $9Nb_2O_5 \cdot 8WO_3$ ($W_8Nb_{18}O_{69}$).

1:1 = $Nb_2O_5 \cdot WO_3$ (WNb_2O_8).

"6:11" = a tungsten bronze type phase of orthorhombic symmetry and with superstructure lines indicative of the unit cell being tripled in the *a* and *b* directions.

Q − liq = metastable phase or phases which form only from the quenched liquid and give very poorly defined x-ray powder patterns, having the general appearance of the ReO_3 subcell characteristic of most of the compounds in this system.

4:9 = $4Nb_2O_5 \cdot 9WO_3$ ($Nb_8W_9O_{47}$).

L-MonWO_{3ss} = the monoclinic polymorph of WO_3 reported [30] to occur below −40 °C "stabilized" by a small amount of solid solution of Nb_2O_5 in WO_3.

2:7 = $2Nb_2O_5 \cdot 7WO_3$ ($W_7Nb_4O_{31}$).

"1:11" = Magneli "shear" phase having the approximate composition $1Nb_2O_5$:$11WO_3$.

"1:15" = Magneli "shear" phase having the approximate composition $1Nb_2O_5$:$15WO_3$.

Tet WO_{3ss} = the high temperature polymorph of WO_3 stabilized by solid solution of Nb_2O_5 in WO_3.

Orth WO_{3ss} = the orthorhombic polymorph of WO_3 ordinarily stable between about 320 °C and ~ 745 °C, "stabilized" by addition of Nb_2O_5 in solid solution.

Tri WO_3 = the polymorph of WO_3 which is stable just below room temperature and occurs at room temperature when pure WO_3 is ground in a mortar and pestle for a short time.

[d] Specimen heated and cooled at about 4 °C/min rather than quenched.

[e] Nonequilibrium, probably due to incomplete reaction.

[f] Nonbinary equilibrium, postulated as being due to reduction.

[g] Metastable melting.

[h] Pt tube not sealed.

[i] Did not receive preliminary 700° heat treatment.

5. Reduction

As has been previously mentioned there is some tendency for WO_3 to reduce on heating to high temperatures, even in the sealed Pt tubes. This tendency is greatly enhanced by subjecting the specimens to high temperatures for extended periods of time. The problem of reduction of WO_3 is apparently carried into the Nb_2O_5-WO_3 system to such an extent that the system may not be completely binary at high temperatures.

The experimental data indicate that the system probably remains essentially binary as long as no melting occurs. However, above the solidus, reduction very likely takes place and the measured liquidus values may not represent binary equilibrium. The melting relations around the ordered bronze-type phases, from about 60 to 80 mole percent WO_3, were particularly difficult to obtain experimentally. The three compounds at "6:11", 4:9 and 2:7 all appeared to melt congruently with binary solidus relations between them. However, the liquidus values appear to form smooth curves between these congruent melting points without any indication of a change in slope toward a eutectic composition. The phenomena is characteristic of a nonbinary system. For the sake of simplicity, the phase diagram has been drawn to indicate the most likely binary relationships and liquidus curves have been dashed to illustrate the uncertainty in values.

Another indication of reduction occurs in the melting relations of the $B_{nm+1}O_{3nm-(n+m)+4}$ homologous series compounds. The phases $W_3Nb_{14}O_{44}$, $W_5Nb_{16}O_{55}$, and $W_8Nb_{18}O_{69}$ were all observed to melt incongruently. Experimentally these compound compositions were observed to begin to form a second phase at about 1440°, 1385°, and 1375°, respectively. However, compositions in two-phase regions between these compounds did not begin to form the new phase until considerably higher temperatures, even though the specimen may have shown an appearance of partial melting. This apparent increase in the stability temperature of the phases is dependent on the amount of time the specimen is held at temperature, and binary melting relationships can be approximated by only holding the experimental specimens for relatively short periods of time. It may therefore be concluded that reduction takes place in these specimens, when held above the solidus temperatures. However, it has previously been concluded [1–4] that the crystal structure of these compounds precludes any appreciable nonstoichiometry. Therefore, it appears likely that, as the W^{+6} ion is reduced, the Nb/W ratio of these phases shifts towards higher tungsten content, maintaining an essentially constant cation: anion ratio.

In addition to the relatively large amount of reduction which apparently takes place above melting, there is possibly some tendency towards reduction at lower temperatures. The amount of reduction which can take place experimentally below melting is probably several orders of magnitude less than that which occurs above melting because it seems in no way to affect the equilibrium relationships. The only indication of this minor reduction is in a tendency for discoloration of the specimens. Almost any composition in the system, held for long periods of time in a sealed Pt tube will show a much darker green or blue color than does the same composition either held for shorter periods or not sealed. This darker color can always be lightened by annealing the specimen in an open Pt tube, at about 1000 °C.

It is intriguing to postulate that the Nb_2O_5-WO_3 system might more closely approach binary conditions if the experiments were performed under conditions of high oxygen pressure, such as that utilized by Van Hook [39]. Such studies will probably become more common in the near future.

6. Metastable Phases and Nonequilibrium

6.1. Metastable Melting

It can be seen from table 19, that all compositions containing more than about 72 mole percent WO_3 were calcined for about 2 hr at 1200 °C prior to attempting to obtain equilibrium data. This was because the few preliminary heat treatments, performed at temperatures above 1250 °C, without the 1200 °C calcine, exhibited some indication of melting, whereas those with a prior 1200 °C calcine did not show melting until much higher temperatures.

The metastable melting apparently is due to a eutectic type reaction between the metastable bronze-type solid solution (labeled "3:8" on fig. 1) and pure WO_3. It must be emphasized that in order to obtain equilibrium products in the region 72 to 100 mole percent WO_3, this preliminary calcine at 1200 °C is imperative. Without such preliminary heat treatment, neither the 2:7 compound nor the "Magneli-shear" structures can be prepared as single phases.

6.2. Metastable Phases

The bronze-type solid solution previously mentioned ("3:8" of fig. 1) has been interpreted as a metastable phase for several reasons. It appears to be responsible for very low temperature metastable melting which takes place between about 72 and 100 mole percent WO_3. The x-ray powder pattern of the bronze-type solid solution shows no superstructure and the phase must contain disordered pentagonal bypyramid polyhedra. It must be concluded that the disordered phase is metastable because it dissociates on heating to two ordered phases. All compositions between about the 6:11 and 2:7 ratios, when quenched from above the liquidus exhibit the tetragonal bronze-type "disordered" phase with no indication of any superstructure peaks in the x-ray diffraction powder pattern. In addition, many specimens also show a small amount of a quenched liquid phase which exhibits a poorly defined x-ray pattern characteristic of a disordered ReO_3 structure, the basic building unit of all the compounds in the system.

From about 5 mole percent WO_3 to at least 15 mole percent WO_3 another metastable phase is formed from the quenched liquid. This phase has an x-ray pattern, characteristic of the orthorhombic low-temperature form of Nb_2O_5. The diffraction pattern shows diffuse peaks and little or no superstructure lines. This phase never appears below the melting point and only forms as a single phase if the quenching temperature is considerably above the liquidus. The ability of a specimen to be quenched as a phase with a powder pattern similar to the low-temperature form of Nb_2O_5 seems to be dependent on cooling rate and composition. This phenomena has been previously reported for other niobate systems [23, 40].

As shown in table 19, another unknown phase has been found occasionally in nonequilibrium mixtures between about 7 and 25 mole percent Nb_2O_5. All efforts to establish an equilibrium region for this phase have proved negative. It is possible that the unknown compound may represent a complex structure involving a mixture of 3×3 blocks along with the 3×4 and/or 4×4 blocks normally found in other compounds occurring in this composition range. Such a structure would contain a considerable number of Nb^{+5} ions in tetrahedral coordination and would not be expected to form a stable assemblage.

It has been previously mentioned [1] that $WNb_{12}O_{33}$ *appears* to have a small region of homogeneity, in that the 8:1 composition showed only a single phase. However, no change in lattice parameters could be detected. This apparent region of solid solution is most likely due to the very similar powder patterns of the 6:1 compound and the "30:1" phase. A solid solution structure containing either a considerable number of oxygen vacancies or cation interstitials (in either the tetrahedral or octahedral position) would be expected to cause some measurable change in the lattice parameters. One other possible mechanism which has been suggested for solid solution [41] is again raised by the appearance of the "ordered intergrowth" structure of the 13:4 compound, and the suggested possible structure of a 25:1 or 20:1 compound. It is possible that a "disordered intergrowth" of double 3×4 blocks might occur in association with the isolated 3×4 blocks of the $WNb_{12}O_{33}$ compound [24]. Such a disordered structure or "compositional stacking fault" would cause only a slight broadening of some of the lines of an x-ray diffraction powder pattern, as would a mixture of a small amount of the ordered second phase. It is problematical as to whether such a picture of solid solution would represent a stable or only a metastable condition. Nevertheless, proof of such a postulated disorder would necessarily depend upon other data, outside the scope of this project. A careful electron diffraction and/or electron microscope study might prove of value in deciphering the nature of any possible disorder of this type.

7. References

[1] R. S. Roth and A. D. Wadsley, Acta Cryst. **19,** 26 (1965).
[2] R. S. Roth and A. D. Wadsley, Acta Cryst. **19,** 32 (1965).
[3] R. S. Roth and A. D. Wadsley, Acta Cryst. **19,** 38 (1965).
[4] R. S. Roth and A. D. Wadsley, Acta Cryst. **19,** 42 (1965).
[5] H. J. Goldschmidt, Metallurgia **62,** 241 (1960).
[6] L. M. Kovba and V. K. Trunov, Dokl. Adad. Nauk. SSR **147,** 622 (1962).
[7] L. J. Fiegel, G. P. Mohanty, and J. H. Healy, J. Chem. and Eng. Data **9,** 365 (1964).
[8] G. P. Mohanty and L. J. Fiegel, Acta Cryst. **17,** 454 (1964).
[9] L. M. Kovba, V. K. Trunov, and Y. P. Simanov, Zh. Neorgan. Khim. **9,** 1930 (1964).
[10] H. Schäfer and R. Gruehn, private communication to A. D. Wadsley, 4/14/65.
[11] E. J. Felten, private communication to R. S. Roth, 12/2/64.
[12] H. F. Stimson, J. Res. NBS **65A** (Phys. and Chem.) No. 3, 139 (1961).
[13] G. Brauer, Z. anorg. u. allgem. Chem. **248,** 1 (1941).
[14] F. Holzberg, A. Reisman, M. Berry, and M. Berkenblit, J. Am. Chem. Soc. **79,** 2039 (1957).
[15] M. W. Shafer and R. Roy, Z. Krist. **110,** 241 (1958).
[16] H. J. Goldschmidt, J. Inst. Metals **87,** 235 (1958–59).
[17] A. Reisman and F. Holzberg, J. Am. Chem. Soc. **81,** 3182 (1959).
[18] B. M. Gatehouse and A. D. Wadsley, Acta Cryst. **17,** 1545 (1964).
[19] R. S. Roth, J. Res. NBS **62,** 27 (1959) RP2925.
[20] R. S. Roth and J. L. Waring, J. Res. NBS **66A** (Phys. and Chem.) No. 6, 451 (1962).
[21] R. S. Roth, A. D. Wadsley, and S. Andersson, Acta Cryst. **18,** 643 (1965).
[22] R. Gruehn and H. Schäfer, Naturwissenschaften **50,** 642 (1963).
[23] J. L. Waring and R. S. Roth, J. Res. NBS **69A** (Phys. and Chem.) No. 2, 119 (1965).
[24] A. D. Wadsley, S. Andersson, and W. G. Mumme, Acta Cryst. (to be published).
[25] S. Andersson, Acta Chem. Scand. **18,** 2339 (1964).
[26] M. Lundberg and S. Andersson, to be published.
[27] A. Sleight and A. Magneli, Acta Chem. Scand. **18,** 2007 (1964).
[28] N. Stephensen, private communication.
[29] A. Magneli, Arkiv Kemii **1,** 513 (1950).
[30] R. Veda and T. Ichinokawa, Phys. Rev. **82,** 563 (1951).
[31] J. Wyart and M. Föex, Compt. Rend. 2459 (1951).
[32] S. Tanisaki, J. Phys. Soc. Japan **15,** 566 (1960).
[33] B. T. Mathias and E. A. Wood, Phys. Rev. **84,** 1255 (1951).
[34] S. Levine, R. Corwin, and H. L. Blood, Bull. Am. Phys. Soc. Series II, **1,** [5], 255 (1956).
[35] P. H. Fang, private communication.
[36] E. M. Levin, J. Am. Ceram. Soc. **48,** 491 (1965).
[37] F. M. Jaeger and H. C. Germs, Z. anorg. u. allgem. Chem. **190,** 145 (1921).
[38] B. Phillips and L. Chang, Trans. Met. Soc. AIME **230,** 1203 (1964).
[39] H. J. Van Hook, Rev. Sci. Instr. **36,** 1119 (1965).
[40] E. M. Levin, J. Research NBS **70A** (Phys. and Chem.), No. 1, 5 (1966).
[41] A. D. Wadsley, in Non-stoichiometric Compounds, ed. L. Mandelcorn ch. 3, (Academic Press, N.Y., 1964).

(Paper 70A4–404)

JOURNAL OF RESEARCH of the National Bureau of Standards—A. Physics and Chemistry
Vol. 70A, No. 4, July–August 1966

Properties of Aqueous Mixtures of Pure Salts. Thermodynamics of the Ternary System: Water-Calcium Chloride-Magnesium Chloride at 25 °C

R. A. Robinson and V. E. Bower

Institute for Materials Research, National Bureau of Standards, Washington, D.C.

(March 8, 1966)

Isopiestic vapor pressure measurements have been made on the system water-calcium chloride-magnesium chloride at 25 °C. Activity coefficients have been evaluated for each salt in the presence of the other in systems of constant total ionic strength. The excess free energy of mixing has been calculated and compared with the values for analogous systems.

Key Words: Isopiestic measurements, vapor pressure, calcium chloride, mixed solutions, activity coefficients.

1. Introduction

The chemical potentials of each solute in an aqueous mixture of two electrolytes have been determined for many systems. For example, the activity coefficients of both hydrochloric acid and sodium chloride in mixed aqueous solution have been derived from emf measurements [1].[1] The isopiestic vapor pressure method has been used [2] to determine the activity coefficients of each solute in aqueous mixtures of sodium chloride and potassium chloride. These are two examples of mixtures of uniunivalent electrolytes but considerable work has been done with mixtures of 1:1 and 1:2 electrolytes. For example, the systems water-hydrochloric acid-barium chloride and water-hydrochloric acid-strontium chloride have been studied by the emf method [3] as have the systems water-hydrochloric acid-calcium chloride and water-hydrochloric acid-manganous chloride [4], while the isopiestic method has been applied to the systems water-sodium chloride-barium chloride [5] and water-potassium chloride-barium chloride [6]. The emf method has been adapted [7] to give trace activity coefficients for the system water-hydrochloric acid-calcium perchlorate, a 'trace' activity coefficient being the limiting value of the activity coefficient of one salt in a solution where its concentration is vanishingly small and the solution contains virtually only the other salt.

The sodium-sensitive glass electrode has been used [8] to study the systems water-sodium chloride-alkaline earth metal chloride. However, there appears to be no case cited in the literature in which solutions of two biunivalent electrolytes have been studied. We now present data for one system of this type, water-calcium chloride-magnesium chloride.

[1] Figures in brackets indicate the literature references at the end of this paper.

2. Definitions

M_B is the molality (moles per kilogram of solvent) of a solution containing only calcium chloride; it is the molality of the 'reference' solution from which isopiestic data are calculated.

M_C is the molality of a solution containing only magnesium chloride, in isopiestic (vapor-phase) equilibrium with the calcium chloride solution of molality M_B.

m_B, m_C are the molalities of calcium chloride and magnesium chloride, respectively, in a solution containing both these salts and in isopiestic equilibrium with the calcium chloride solution of molality M_B and the magnesium chloride solution of molality M_C.

$R \equiv$ $M_B/(m_B+m_C)$ is the isopiestic ratio.

$y_C \equiv$ $m_C/(m_B+m_C)$, the ionic fraction, is the fraction of magnesium chloride in the mixture of calcium chloride and magnesium chloride.

$m =$ m_B+m_C.

Γ_B is the (molal) activity coefficient of calcium chloride in the reference solution of molality M_B in equilibrium with the solution containing both calcium chloride and magnesium chloride.

Γ_C is the activity coefficient of magnesium chloride at molality M_C in equilibrium with the reference solution of calcium chloride of molality M_B.

γ_B, γ_C are the activity coefficients of calcium chloride and magnesium chloride, respectively, in the mixed solution, at molalities m_B and m_C.

γ_B° is the activity coefficient of calcium chloride in a solution containing calcium chloride only at the same total ionic strength $I=3m_B+3m_C$ as the mixed solution. γ_C° is the activity

coefficient of magnesium chloride in its own solution at this total ionic strength.

φ is the osmotic coefficient of calcium chloride in its own solution.

3. Method

The result of an isopiestic vapor pressure experiment is the knowledge that a set of solutions of known composition have the same water activity, a_W. What is needed are the activity coefficients of the two salts in the mixed solution. This is accomplished by means of the McKay-Perring equation [9]:

$$\ln \gamma_B = \ln \Gamma_B + \ln R + \int_0^{M_B\varphi} f(m, M_B, \gamma_C)\, d(M_B\varphi) \qquad (1)$$

where

$$f(m, M_B, \gamma_C) = \frac{1}{m^2}\left(\frac{\partial m}{\partial \ln \gamma_C}\right)_{a_W} + \frac{1}{m} - \frac{1}{M_B}. \qquad (2)$$

If the isopiestic ratio, $R = M_B/m$, can be expressed as:

$$R = 1 - a\gamma_C - b\gamma_C^2, \qquad (3)$$

the integral reduces to

$$\gamma_C^2 \int_0^{M_B\varphi} (b/M_B)\, d(M_B\varphi).$$

4. Materials

Calcium chloride was prepared from calcium carbonate and hydrochloric acid and recrystallized three times from water slightly acidified with hydrochloric acid. Magnesium chloride was a commercial material, also recrystallized three times from slightly acidified water.

Each salt was dissolved to make a stock solution whose composition was determined by coulometric titration [10].[2] The stock solutions were mixed in suitable proportions to give a series of mixed solutions of known concentrations of calcium chloride and magnesium chloride. The solutions were equilibrated in an isopiestic apparatus in a thermostat at 25 ± 0.01 °C. The time of equilibration varied from three days for the more concentrated solutions to seven days for the more dilute. The concentrations of the solutions at equilibrium were calculated from the loss or gain of water in each solution.

5. Results

The isopiestic data are given in table 1. The second column gives the molality (M_B) of the reference calcium

[2] The analyses were made by George Marinenko of the Analysis and Purification Section.

TABLE 1. *Isopiestic data for the system* H_2O-$CaCl_2$-$MgCl_2$ at 25 °C[a]

Set	M_B	m_B	m_C	γ_C	R(obs)	R(calc)
1	0.3121$_1$	0.2213$_9$	0.0886$_9$	0.2860	1.0065	1.0064
		.0873$_2$	.2204$_0$	.7162	1.0143	1.0147
		.0311$_7$	.2753$_5$	.8983	1.0182	1.0178
			.3060$_9$	1.0	1.0197	1.0194
	0.3166$_2$	0.2717$_5$	0.0435$_2$	0.1380	1.0030	1.0032
		.1811$_9$	.1321$_0$	.4217	1.0094	1.0092
		.1270$_0$	.1853$_1$	.5934	1.0125	1.0126
			.3102$_9$	1.0	1.0191	1.0194
2	0.5606$_1$	0.5053$_1$	0.0538$_1$	0.0962	1.0026	1.0031
		.2986$_3$	.2545$_5$	.4602	1.0134	1.0144
		.0808$_8$	.4658$_8$	.8521	1.0253	1.0225
			.5446$_2$	1.0	1.0294	1.0294
	0.5610$_9$	0.4967$_0$	0.0621$_8$	0.1112	1.0040	1.0036
		.2805$_9$	.2719$_0$	.4921	1.0156	1.0154
		.1108$_9$	.4373$_2$	.7977	1.0235	1.0240
			.5450$_9$	1.0	1.0294	1.0294
	0.5625$_0$	0.3862$_1$	0.1705$_2$	0.3063	1.0104	1.0098
		.1734$_0$	.3772$_7$	.6851	1.0215	1.0209
		.0519$_1$	.4957$_2$	.9052	1.0272	1.0269
			.5463$_2$	1.0	1.0296	1.0294
3	1.0135	0.8706	0.1367	0.1357	1.0062	1.0066
		.6079	.3875	.3893	1.0182	1.0185
		.2680	.7126	.7267	1.0336	1.0333
			.9700	1.0	1.0448	1.0444
	1.0198	0.7503	0.2561	0.2545	1.0133	1.0123
		.3767	.6146	.6200	1.0288	1.0288
		.1597	.8231	.8375	1.0376	1.0379
			.9767	1.0	1.0441	1.0444
4	1.5003	1.3154	0.1720	0.1156	1.0087	1.0072
		0.9250	.5426	.3697	1.0223	1.0226
		.3715	1.0665	.7417	1.0443	1.0438
			1.4191	1.0	1.0572	1.0575
	1.5109	1.1952	0.2975	0.1993	1.0122	1.0124
		0.6434	.8190	.5600	1.0332	1.0337
		.2367	1.2045	.8358	**1.0484**	1.0490
			1.4291	1.0	**1.0572**	1.0575
5	1.8445	1.3317	0.4793	0.2647	1.0185	1.0180
		0.7829	.9961	.5599	1.0368	1.0370
		.2943	1.4582	.8321	1.0525	1.0537
			1.7347	1.0	1.0633	1.0635
	1.8588	1.5716	**0.2671**	0.1453	1.0109	1.0100
		0.9977	**.8067**	.4471	1.0301	1.0299
		.6212	1.1618	.6516	1.0425	1.0427
			1.7475	1.0	1.0637	1.0635
6	2.1878	1.7890	0.3724	0.1723	1.0122	1.0123
		1.2674	.8604	.4044	1.0282	1.0285
		0.6155	1.4722	.7052	1.0479	1.0487
			2.0500	1.0	1.0672	1.0675
	2.2088	1.5047	0.6568	**0.3039**	1.0219	1.0216
		0.8663	1.2539	**.5914**	1.0418	1.0411
		.3369	1.7515	.8387	1.0576	1.0573
			2.0686	1.0	1.0678	1.0675
7	2.4524	1.7806	0.6237	0.2594	1.0200	1.0194
		1.0056	1.3486	.5728	1.0417	1.0418
		0.3413	1.9706	.8524	1.0608	1.0609
			2.2908	1.0	1.0705	1.0706
	2.4732	2.0969	0.3488	0.1426	1.0112	1.0108
		1.4318	.9697	.4038	1.0299	1.0299
		0.6916	1.6634	.7063	1.0502	1.0511
			2.3101	1.0	1.0706	1.0706
8	2.6919	1.8448	0.7859	0.2987	1.0233	1.0235
		1.2071	1.3810	.5336	1.0401	1.0411
		0.4020	2.1294	.8412	1.0634	1.0631
			2.5076	1.0	1.0735	1.0739
	2.6952	2.2653	0.3962	0.1489	1.0127	1.0119
		1.4165	1.1869	.4559	1.0353	1.0354
		0.7960	1.7646	.6891	1.0526	1.0524
			2.5091	1.0	1.0742	1.0739
9	3.2040	2.7101	0.4556	0.1439	1.0121	1.0116
		1.9225	1.1860	.3815	1.0307	1.0305
		0.8894	2.1444	.7068	1.0561	1.0559
			2.9707	1.0	1.0785	1.0783
	3.2061	2.3272	0.8130	0.2589	1.0210	1.0208
		1.2844	1.7808	.5810	1.0460	1.0462
		0.5007	2.5079	.8336	1.0656	1.0657
			2.9736	1.0	1.0782	1.0783

TABLE 1. *Isopiestic data for the system* H_2O-$CaCl_2$-$MgCl_2$ at 25 °C[a]—Continued

Set	M_B	m_B	m_C	y_C	R(obs)	R(calc)
	3.2213	2.2712	0.8798	0.2792	1.0223	1.0224
		1.4070	1.6816	.5445	1.0430	1.0433
		0.4583	2.5623	.8483	1.0664	1.0668
			2.9878	1.0	1.0782	1.0783
10	3.5689	3.0616	0.4646	0.1318	1.0121	1.0111
		2.0524	1.4035	.4061	1.0327	1.0337
		1.0121	2.3665	.7005	1.0563	1.0573
			3.3044	1.0	1.0804	1.0806
	3.5888	2.5711	0.9401	0.2677	1.0221	1.0224
		1.4668	1.9622	.5722	1.0466	1.0471
		0.5128	2.8425	.8472	1.0696	1.0688
			3.3214	1.0	1.0815	1.0806
11	3.8882	2.7993	1.0036	0.2639	1.0224	1.0221
		1.0923	2.5829	.7028	1.0580	1.0583
		0.5415	3.0903	.8509	1.0706	1.0703
			3.5925	1.0	1.0823	1.0825
	3.8898	3.3050	0.5388	0.1402	1.0120	1.0118
		2.2317	1.5309	.4069	1.0338	1.0340
		1.6526	2.0654	.5555	1.0462	1.0463
			3.5924	1.0	1.0828	1.0825
12	4.1086	2.9954	1.0244	0.2548	1.0221	1.0219
		1.7642	2.1606	.5505	1.0468	1.0472
		0.6953	3.1471	.8190	1.0693	1.0700
			3.7860	1.0	1.0852	1.0854
	4.1220	3.5742	0.5018	0.1231	1.0113	1.0106
		2.3894	1.5948	.4003	1.0346	1.0343
		1.1896	2.7009	.6942	1.0595	1.0594
			3.7967	1.0	1.0857	1.0854

[a] $B = CaCl_2$, $C = MgCl_2$. $y_C = m_C/(m_B + m_C)$. $R = M_B/(m_B + m_C)$. R(calc) is calculated by means of eq (3) with the values of the parameters given in table 2.

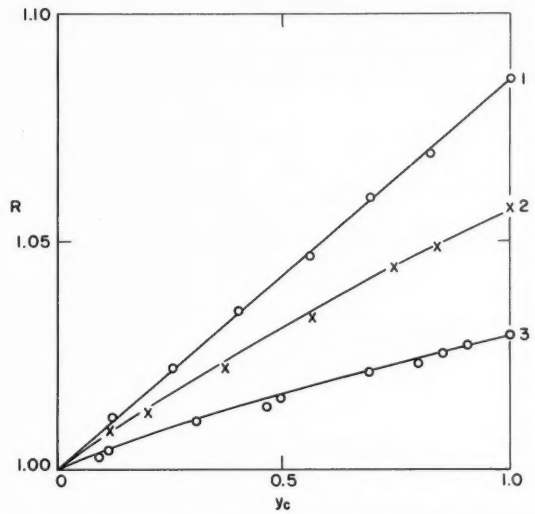

FIGURE 1. *Isopiestic ratio,* $R = M_B/(m_B + m_C)$ *of calcium chloride-magnesium chloride solutions versus ionic fraction.* $y_C = m_C/(m_B + m_C)$. 1. $M_B = 4.1183$. 2. $M_B = 2.1983$. 3. $M_B = 0.5614$.

TABLE 2. *Values of the parameters of eq (3)*

$R = 1 - ay_C - by_C^2$

Set	M_B	$M_B\varphi$	a	b	b/M_B
1	0.3142	0.276	−0.0234	0.0040	0.0127
2	.5614	.523	−.0330	.0036	.0064
3	1.0167	1.069	−.0497	.0053	.0052
4	1.5056	1.816	−.0634	.0059	.0039
5	1.8517	2.451	−.0695	.0060	.0026
6	2.1983	3.192	−.0725	.0050	.0023
7	2.4628	3.827	−.0763	.0057	.0023
8	2.6936	4.444	−.0808	.0069	.0026
9	3.2105	5.989	−.0811	.0028	.0009
10	3.5789	7.203	−.0847	.0041	.0011
11	3.8890	8.312	−.0842	.0017	.0005
12	4.1183	9.177	−.0861	.0007	.0002

chloride solution, the third and fourth column give values of the molalities of calcium chloride (m_B) and magnesium chloride (m_C) in the mixed solutions isopiestic with the reference solution. The next column gives the fraction of magnesium chloride, $y_C = m_C/m$, in the mixture and the next the observed isopiestic ratio, $R = M_B/m$. Plots of these isopiestic ratios, some of which are shown in figure 1, exhibit a slight curvature, more marked in the more dilute solutions. The data were therefore fitted to eq (3) by the method of least squares. The last column of table 1 gives values of the isopiestic ratio calculated by eq (3) with the parameters given in table 2.

6. Calculations of Activity Coefficients

The application of eq (1) requires a knowledge of three quantities. Γ_B (or Γ_C in the corresponding equation for γ_C) can be obtained directly from tables of the activity coefficient of calcium chloride (or magnesium chloride) in its own solution [11]. The isopiestic ratio, R, has already been recorded in table 1. It is in the evaluation of the integral in eq (1) that some difficulty is encountered. Figure 2 is a plot of b/M_B against ($M_B\varphi$), omitting the point at $M_B = 0.3142$ which

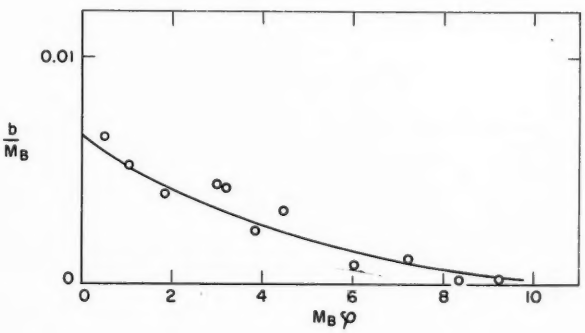

FIGURE 2. b/M_B *versus* $M_B\varphi$.

is badly off the curve. This is not surprising for accurate isopiestic results are difficult to obtain at low concentrations. The curve drawn in figure 2 is that of the equation:

$$b/M_B = 0.0066 - 0.00144\,(M_B\varphi) + 0.000084\,(M_B\varphi)^2 \quad (4)$$

so that the integral in eq (1) is given by:

$$y_C^2(M_B\varphi)[0.0066 - 0.00072\,(M_B\varphi) + 0.000028\,(M_B\varphi)^2] \quad (5)$$

or, multiplying by 0.4343 if eq (1) is to be used with decadic logarithms:

$$y_C^2(M_B\varphi)[0.0029 - 0.00031\,(M_B\varphi) + 0.000012\,(M_B\varphi)^2]. \quad (6)$$

The maximum value of this integral which will be used is at $y_C = 1$, $M_B = 4.1183$, $(M_B\varphi) = 9.177$. The integral then has the value 0.0096, which is much smaller than the other term, $\log R = 0.0356$.

The calculation of activity coefficients in mixed salt solutions may be illustrated as follows. One result from set 8 in table 1 concerns a reference solution of calcium chloride of molality $M_B = 2.6919$. The value of $\log \Gamma_B$ for calcium chloride in its own solution at this concentration is 0.0820. This solution was in isopiestic equilibrium with a mixed solution containing calcium chloride at molality $m_B = 0.4020$ and magnesium chloride at molality $m_C = 2.1294$; the total molality of the solution was $m = 2.5314$ with $y_C = 0.8412$. The isopiestic ratio for this solution was found to be $R = 1.0631$ or $\log R = 0.0266$. Substitution gives 0.0076 $y_C^2 = 0.0054$ as the contribution of the integral term in eq (1). Hence we find $\log \gamma_B = 0.1140$. We have now found the activity coefficient of calcium chloride in a mixed solution of total molality $m = 2.5314$. But $\log \gamma_B^\circ$ for calcium chloride alone in its own solution at this concentration is 0.0355 and therefore $\log \gamma_B/\gamma_B^\circ$ is 0.0785. Making similar calculations for all the solutions in this set of data, we get the results shown in table 3. Figure 3 is a plot of $\log \gamma_B/\gamma_B^\circ$ against m_c from which it can be seen that a straight line represents the variation of $\log \gamma_B/\gamma_B^\circ$ very well. The last column of table 3 gives values obtained by means of the equation

$$\log \gamma_B = \log \gamma_B^\circ + 0.0366\, m_C. \quad (7)$$

The agreement is good and it follows that Harned's rule:

$$\log \gamma_B = \log \gamma_B^\circ - \alpha_B m_C \quad (8)$$

holds with $\alpha_B = -0.0366$. An equally good straight line plot is obtained for the variation of $\log \gamma_C$ with m_B,

$$\log \gamma_C = \log \gamma_C^\circ - \alpha_C m_B \quad (9)$$

with $\alpha_C = 0.0331$.

TABLE 3. *Variation of log γ_B with magnesium chloride concentration at a total molality of about 2.5*

m_B	m_C	m	$\log \gamma_B/\gamma_B^\circ$	$\log \gamma_B/\gamma_B^\circ$(calc)[a]
2.2652	0.3962	2.6614	0.0151	0.0145
1.8448	.7859	2.6307	.0284	.0288
1.4165	1.1869	2.6034	.0433	.0435
1.2071	1.3810	2.5881	.0498	.0506
0.7960	1.7646	2.5606	.0646	.0647
.4020	2.1294	2.5314	.0785	.0780
0	2.5091	2.5091	.0924	.0919
0	2.5076	2.5076	.0918	.0919

[a] Calculated using the equation $\log \gamma_B = \log \gamma_B^\circ + 0.0366\, m_c$.

Harned's rule, however, is usually applied to systems at constant total ionic strength, $I = 3m_B + 3m_c = 3m$, and inspection of table 3 shows that m is not quite constant, varying from 2.5076 to 2.6614. It will be shown later that α_B varies only slowly with m, and the slight departure from exact constancy of the total ionic strength is without appreciable effect on the value of α_B.

Similar calculations of the values of α_B and α_C have been made for the other sets of results in table 1. These values are given in table 4 along with values of $(\alpha_B + \alpha_C)$. These values are also plotted in figure 4. If the behavior of this system were more complicated than that represented by eq (8) and eq (9), for example, if

$$\log \gamma_B = \log \gamma_B^\circ - \alpha_B m_C - \beta_B m_C^2 \quad (10)$$

$$\log \gamma_C = \log \gamma_C^\circ - \alpha_C m_B - \beta_C m_B^2 \quad (11)$$

there is a relation between these α and β coefficients. We developed a general form of this relation in the appendix to a previous paper [5]; for a system of the calcium chloride-magnesium chloride type this takes the form

$$(\alpha_B + \alpha_C) = \text{constant} - 2(\beta_B + \beta_C)m.$$

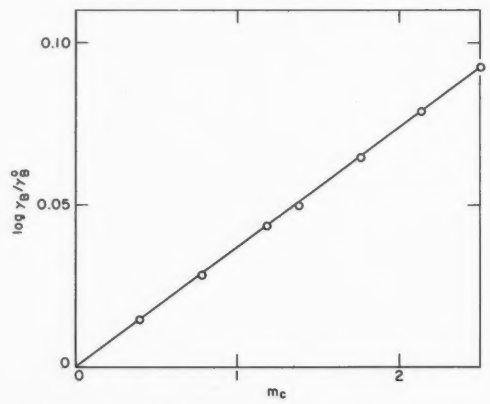

FIGURE 3. *Variation of the activity coefficient of calcium chloride on addition of magnesium chloride $M_B = 2.2636$.*

TABLE 4. *Values of the parameters α_B and α_C of eq (8) and eq (9)*

M_B	α_B	α_C	$(\alpha_B+\alpha_C)$
0.3142	−0.0277	0.0225	−0.0052
.5614	−.0270	.0225	−.0045
1.0167	−.0288	.0250	−.0038
1.5056	−.0314	.0279	−.0035
1.8517	−.0326	.0288	−.0038
2.1983	−.0338	.0314	−.0024
2.4628	−.0336	.0310	−.0026
2.6936	−.0366	.0331	−.0035
3.2105	−.0366	.0346	−.0020
3.5789	−.0363	.0348	−.0015
3.8870	−.0364	.0363	−.0001
4.1183	−.0370	.0373	+.0003

Thus the sum $(\alpha_B+\alpha_C)$ is independent of the total molality only if either both β_B and β_C are zero or else β_B and β_C are equal and opposite in sign. Inspection of figure 4 shows that $(\alpha_B+\alpha_C)$ does vary slightly with the total molality; this variation could be accounted for by ascribing a value of -0.0006 to $(\beta_B+\beta_C)$ or -0.0003 to both β_B and β_C. This would mean a slight curvature in figure 3 but it is so small that it would be difficult to detect experimentally.

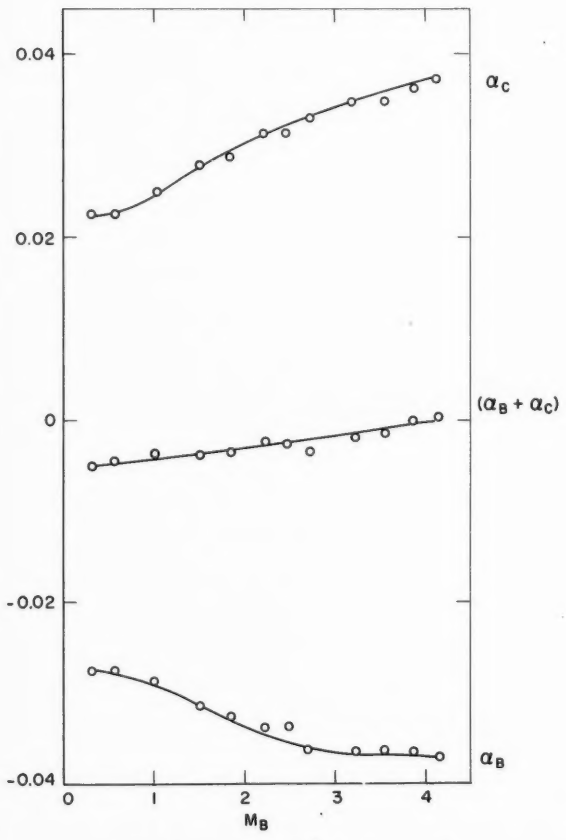

FIGURE 4. *α_B, α_C and $(\alpha_B+\alpha_C)$ versus* M_B.

The fact that α_C is numerically positive means that log γ_C decreases on the replacement of magnesium chloride by calcium chloride at constant total molality. Conversely, log γ_B increases when calcium chloride is replaced by magnesium chloride at constant total molality. For example, the activity coefficient of magnesium chloride in its own solution at 4 *m* is 5.53; in a solution containing 2 *m* magnesium chloride and 2 *m* calcium chloride it is 4.67 and in the limiting case where magnesium chloride is present in vanishingly small amount in 4 *m* calcium chloride solution it is 3.93. The activity coefficient of calcium chloride in its own solution at 4 *m* is 2.93; in a solution containing 2 *m* magnesium chloride and 2 *m* calcium chloride it is 3.48 and the 'trace' activity coefficient in 4 *m* magnesium chloride solution is 4.13 (fig. 5). Thus the trace activity coefficients, the activity coefficient of one salt when the other preponderates in concentration, are almost the same, 3.93 for magnesium chloride and 4.13 for calcium chloride. The same is true at other concentrations. At a total molality of $m=2$, the activity coefficient of magnesium chloride, 1.051, is lowered to 0.915, the 'trace' activity coefficient in 2 *m* calcium chloride solution. On the contrary, the activity coefficient of calcium chloride, which is 0.792 in its own solution, is raised to 0.924 in 2 *m* magnesium chloride solution. The corresponding changes at 0.3 *m* are from 0.476 to 0.469 for magnesium chloride and from 0.455 to 0.464 for calcium chloride.

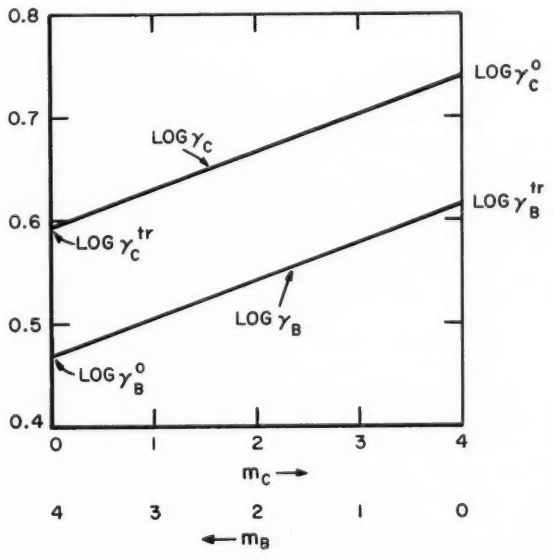

FIGURE 5. *Activity coefficients of calcium chloride and magnesium chloride in mixed aqueous solution at constant total ionic concentration of* 4*m*(I=12).

γ^o = Activity coefficient of a salt in its own solution.
γ^{tr} = "Trace" activity coefficient of one salt in a solution of the other salt.

216-375 O - 66 - 3

7. Excess Free Energy of Mixing

If a solution of $y_B m$ moles of calcium chloride in y_B kg of water is mixed with a solution of $y_C m$ moles of magnesium chloride in y_C kg of water, the resulting solution will consist of $y_B m$ moles of calcium chloride and $y_C m$ moles of magnesium chloride in a kilogram of water. There will be no change in total molality, m, during the process of mixing. The change in free energy during the mixing process will contain an entropy term of the form $3\ RTm[y_B \ln \nu_B + y_C \ln y_C]$, an expression which appears even if all three solutions are ideal. It is therefore ignored in calculating the *excess* free energy of mixing; the excess free energy is that due to departures from ideality of both solvent and solutes. A general equation for this excess free energy of mixing has been developed in the appendix to an earlier paper [6] which, for the calcium chloride-magnesium chloride system, takes the form

$$\frac{\Delta G^E}{2.3026\ RT} = -\frac{3}{2} \cdot m_B m_C (\alpha_B + \alpha_C). \qquad (12)$$

The maximum excess free energy is found when $m_B = m_C = 0.5\ m$, $y_B = y_C = 0.5$,

$$\frac{\Delta G^E(max)}{RT} = -0.8635\ m^2(\alpha_B + \alpha_C). \qquad (13)$$

Some values of the excess free energy of mixing (in calories per kilogram of water, 1 cal = 4.1840J are as follows:

m	0.5	1.0	1.5	2.0	2.5	3.0	3.5	4.0
ΔG^E(max)	1	2	4	6	8	7	6	0

These are remarkably small values. The value at $I = 3$, $m = 1$, 2 cal per kg of water, can be compared with -73, -35, and -17 cal per kg of water for the systems water-hydrochloric acid-barium chloride, water-potassium chloride-barium chloride, and water-sodium chloride-barium chloride, respectively [6]. It also compares with 79 cal per kg of water for the system water-hydrochloric acid-sodium chloride [1] and -54 cal per kg of water for the system water-hydrochloric acid-potassium chloride [12].

8. Vapor Pressure of Mixed Solutions

It has been shown [13] that in many instances the vapor pressure lowering of a mixed solution can be compounded additively from the vapor pressure lowerings of the single salt solutions. For a system of the calcium chloride-magnesium chloride type, the variation in a_w with change in composition at constant total ionic strength is given by [6]:

$$127.82 \log a_w = 127.82 \log a_{w(B)} + 3\alpha_B m^2 y_C - \frac{3}{2}(\alpha_B + \alpha_C) m^2 y_C^2 - 3(\beta_C - \beta_B) m^3 \left(y_C^2 - \frac{2y_C^3}{3}\right) \qquad (14)$$

where a_w $(= p/p^\circ)$ is the water activity of the mixed solution and $a_{w(B)}$ that of a solution containing calcium chloride only at the same total molality m.
If $\beta_B = \beta_C = 0$,

$$127.82 \log a_w = 127.82 \log a_{w(B)} + 3\alpha_B m^2 y_C - \frac{3}{2}(\alpha_B + \alpha_C) m^2 y_C^2 \qquad (15)$$

and if $\alpha_B = -\alpha_C$,

$$127.82 \log a_w = 127.82 \log a_{w(B)} + 3\alpha_B m^2 y_C. \qquad (16)$$

Thus, $\log a_w$ will be a linear function of y_C and a_w $(= p/p^\circ)$ will be very nearly a linear function of y_C. The additivity of vapor pressure lowerings is, therefore, to be sought in systems in which $\alpha_B \approx -\alpha_C$. Inspection of table 4 shows that this is very nearly true for the system calcium chloride-magnesium chloride. One example will illustrate this. From the known osmotic coefficients of calcium chloride solutions [11], it can be calculated that for a solution of concentration 4.1220 m, $a_w = 0.60836$. From set 12 of table 1 we see that this solution had the same water activity as a mixed solution of $m_B = 2.3894$, $m_C = 1.5948$, $m = 3.9842$, $y_C = 0.4003$. For this mixed solution, therefore, $(p^\circ - p)/p^\circ = 0.39164$ and $(p^\circ - p) = 9.303$ mm Hg. In the same way we calculate that for a solution of calcium chloride only at this total molality, 3.9842 m, $a_w = 0.62598$ and the vapor pressure lowering per mole is $(p^\circ - p)/m = 2.230$ mm Hg. We might then expect calcium chloride at molality $m_B = 2.3894$ to contribute 5.328 mm Hg to the vapor pressure lowering of the mixed solution. For a solution of magnesium chloride only at molality 3.9842 m, we calculate $a_w = 0.58212$ and $(p^0 - p)/m = 2.491$ mm Hg so that we would expect magnesium chloride at molality $m_C = 1.5948$ to contribute 3.973 mm Hg to the vapor pressure lowering of the mixed solution. The sum of the two contributions, 9.301 mm Hg, is in very good agreement with the observed value of 9.303 mm Hg.

9. Summary

The behavior of the system calcium chloride-magnesium chloride is comparatively simple. At constant total ionic strength, the logarithm of the activity coefficient of either salt is, to a close approximation, a linear function of the concentration of the other salt. This is also true for the chemical potential of each salt. The activity coefficient of magnesium chloride is decreased by the addition of calcium chloride and, conversely, the activity coefficient of calcium chloride is increased by the addition of magnesium chloride. The "trace" activity coefficient of each salt is almost the same. This behavior is illustrated in figure 5 for a system at a constant total ionic strength of $I = 12$.

The Harned α_B and α_C coefficients, which express the relation between log γ for one salt and the concentration of the other salt, are almost equal in magnitude but opposite in sign. Consequently, the excess free energy of mixing of the system is very small and, moreover, the vapor pressure lowering of the mixed solution can be compounded almost additively from the vapor pressure lowerings of the separate salt solutions.

Grateful acknowledgment is made to the Office of Saline Water for a grant in partial support of this work.

(Paper 70A4–405)

10. References

[1] H. S. Harned, J. Phys. Chem. **63,** 1299 (1959).
[2] R. A. Robinson, J. Phys. Chem. **65,** 662 (1961).
[3] H. S. Harned and R. Gary, J. Am. Chem. Soc. **76,** 5924 (1954).
[4] A. K. Covington, J. Chem. Soc. (London) 4906 (1965).
[5] R. A. Robinson and V. E. Bower, J. Res. NBS **69A** (Phys. and Chem.) No. 1, 19 (1965).
[6] R. A. Robinson and V. E. Bower, J. Res. NBS **69A** (Phys. and Chem.) No. 5, 439 (1965).
[7] J. M. Stokes and R. H. Stokes, J. Phys. Chem. **67,** 2446 (1963).
[8] R. D. Lanier, J. Phys. Chem. **69,** 3992 (1965).
[9] H. A. C. McKay and J. K. Perring, Trans. Faraday Soc. **49,** 163 (1953).
[10] G. Marinenko and J. K. Taylor, J. Res. NBS **67A** (Phys. and Chem.) No. 1, 31 (1963).
[11] R. A. Robinson and R. H. Stokes, Electrolyte Solutions, pp. 478–497, 2d ed., (Butterworths Scientific Publications, London, 1959).
[12] H. S. Harned, J. Phys. Chem. **64,** 112 (1960).
[13] R. A. Robinson and V. E. Bower, J. Res. NBS **69A** (Phys. and Chem.) No. 4, 365 (1965).

JOURNAL OF RESEARCH of the National Bureau of Standards—A. Physics and Chemistry
Vol. 70A, No. 4, July–August 1966

Properties of Aqueous Mixtures of Pure Salts. Thermodynamics of the Ternary System: Water-Sodium Chloride-Calcium Chloride at 25 °C

R. A. Robinson and V. E. Bower

Institute for Materials Research, National Bureau of Standards, Washington, D.C.

(April 20, 1966)

Isopiestic vapor pressure measurements have been made to determine some thermodynamic properties of the system: water-sodium chloride-calcium chloride at 25 °C. Equations are derived for the activity coefficient of each salt in the presence of the other when the total ionic strength is kept constant. The limiting conditions in very dilute solutions are considered and "trace" activity coefficients calculated. A comparison with previous work is made. The excess free energy of mixing is calculated.

Key Words: Calcium chloride, isopiestic measurements, mixed salt solutions, sodium chloride, vapor pressure of aqueous solutions.

1. Introduction

The application of the isopiestic vapor pressure method of determining the activity coefficients of two salts in a mixed salt solution has been described in two previous papers. In one of these [1][1] the system water-sodium chloride-barium chloride was described and in the other [2] the system water-potassium chloride-barium chloride. This paper is concerned with the system water-sodium chloride-calcium chloride.

2. Definitions

The definitions and symbols of the previous paper [1] will be retained except that C now designates calcium chloride.

3. Experimental Procedure

The sodium chloride was a portion of that used in earlier work [1]. Calcium chloride was purified in the manner already described [3]; the following impurities were detected by flame photometry: [2] sodium, 10 ppm; potassium, 10 ppm; strontium, 300 ppm. A stock solution of sodium chloride was made by dissolving a known weight of the salt in a known weight of water. The stock solution of calcium chloride was made by dissolving the salt in water to give a solution approximately $4m$ in concentration; its exact composition was then determined by coulometric titration.[3]

The stock solutions were used to prepare solutions containing both sodium chloride and calcium chloride in known amounts. These solutions were equilibrated in an isopiestic apparatus contained in a thermostat at 25 ± 0.01 °C. The time of equilibration varied from 3 days for the most concentrated solutions ($M_B \sim 5.8$) ($M_C \sim 2.9$) to 7 days for the most dilute solutions ($M_B \sim 0.5$) ($M_C \sim 0.4$). After equilibration, the composition of the solutions at equilibrium was determined from the loss or gain of water by each solution.

4. Isopiestic Data

The experimental results are given in table 1. The second column gives the molality (M_B) of the reference solution of sodium chloride. The next two columns give the molalities of sodium chloride (m_B) and of calcium chloride (m_C), respectively, in the mixed solutions. The fifth column gives values of the ionic fraction, y_C of calcium chloride in the mixed solution, defined as $y_C = 1.5m_C/m$, where $m = m_B + 1.5m_C$. The sixth column gives values of the isopiestic ratio, defined as $R = M_B/m$.

Figure 1 is a plot of isopiestic ratio versus the ionic fraction of calcium chloride for some sets of results in table 1. These isopiestic ratios are much higher than those encountered in the sodium chloride-barium chloride system. For example, in the latter system, a solution of $2.7147m$ sodium chloride was found to be in isopiestic equilibrium with a solution of $1.7610m$ barium chloride, $R = 1.0277$; we now find that a solution $2.7546m$ sodium chloride has the same vapor pressure as a solution of $1.5498m$ calcium chloride,

[1] Figures in brackets indicate the literature references at the end of this paper.
[2] Analysis by R. W. Burke of the Analysis and Purification Section.
[3] Analysis by G. Marinenko of the Analysis and Purification Section.

TABLE 1. *Isopiestic ratios for the system water-sodium chloride-calcium chloride at 25 °C*

Set	M_B	m_B	m_C	y_C	R(obs)	R(calc)	Δ^a
1	0.5339	0.3735	0.1110	0.3083	0.9887	0.9892	+ 0.05
		.2495	.1968	.5419	.9802	.9805	+ .03
		.1268	.2816	.7691	.9721	.9717	− .04
		.....	.3702	1.0	.9615	.9623	+ .08
	0.5408	0.4190	0.0842	0.2316	0.9917	0.9920	+ 0.03
		.3146	.1561	.4267	.9855	.9849	− .06
		.1832	.2470	.6691	.9767	.9757	− .10
		.....	.3746	1.0	.9624	.9623	− .01
2	0.7988	0.6832	0.0769	0.1445	1.0003	1.0000	− 0.03
		.4544	.2297	.4312	0.9999	0.9997	− .02
		.2241	.3842	.7200	.9980	.9988	+ .08
		.....	.5347	1.0	.9980	.9975	− .05
	0.8005	0.5729	0.1519	0.2846	0.9996	0.9999	+ 0.03
		.3405	.3072	.5750	.9990	.9994	+ .04
		.1271	.4497	.8414	.9986	.9983	− .03
3	1.0420	0.6887	0.2294	0.3332	1.0089	1.0092	+ 0.03
		.4375	.3929	.5739	1.0148	1.0152	+ .04
		.2166	.5367	.7880	1.0199	1.0201	+ .02
		.....	.6780	1.0	1.0246	1.0247	+ .01
	1.0524	0.7891	0.1706	0.2449	1.0071	1.0068	− 0.03
		.5393	.3333	.4810	1.0127	1.0129	+ .02
		.3250	.4723	.6855	1.0183	1.0178	− .05
		.....	.6846	1.0	1.0248	1.0247	− .01
4	1.5186	0.9755	0.3348	0.3399	1.0277	1.0279	+ 0.02
		.5078	.6256	.6489	1.0501	1.0517	+ .16
		.2665	.7736	.8132	1.0643	1.0637	− .06
		.....	.9414	1.0	1.0754	1.0770	+ .16
	1.5523	1.2831	0.1656	0.1622	1.0136	1.0135	−0.01
		0.5750	.6029	.6113	1.0494	1.0489	− .05
		.3506	.7412	.7603	1.0615	1.0599	− .16
		.....	.9601	1.0	1.0778	1.0770	− .08
5	1.7785	1.2368	0.3258	0.2832	1.0307	1.0303	− 0.04
		0.7203	.6377	.5709	1.0595	1.0601	+ .06
		.2557	.9204	.8438	1.0869	1.0874	+ .05
		.....	1.0762	1.0	1.1017	1.1027	+ .10
	1.7899	1.5227	0.1600	0.1362	1.0154	1.0147	− 0.07
		1.0256	.4603	.4024	1.0430	1.0428	− .02
		0.5579	.7427	.6666	1.0705	1.0698	− .07
		.....	1.0822	1.0	1.1026	1.1027	+ .01
6	2.7546	1.9144	0.4751	0.2716	1.0497	1.0516	+ 0.19
		1.2728	.8302	.4945	1.0939	1.0935	− .04
		0.6209	1.1974	.7431	1.1397	1.1396	− .01
		.....	1.5498	1.0	1.1849	1.1870	+ .21
	2.7925	1.6266	0.6524	0.3756	1.0719	1.0713	− 0.06
		0.9691	1.0206	.6124	1.1170	1.1153	− .17
		.3633	1.3619	.8490	1.1606	1.1593	− .13
		.....	1.5679	1.0	1.1873	1.1870	− .03
7	3.4285	2.2476	0.6360	0.2980	1.0709	1.0712	+ 0.03
		1.2284	1.1877	.5919	1.1390	1.1404	+ .14
		0.3794	1.6464	.8668	1.2034	1.2042	+ .08
		.....	1.8530	1.0	1.2335	1.2348	+ .13
	3.4631	2.8877	0.3111	0.1392	1.0325	1.0333	+ 0.08
		1.7012	.9474	.4551	1.1091	1.1083	− .08
		0.8440	1.4101	.7148	1.1701	1.1690	− .11
		.....	1.8677	1.0	1.2361	1.2348	− .13
8	4.5821	3.4474	0.5772	0.2007	1.0624	1.0627	+ 0.03
		2.1539	1.2356	.4625	1.1434	1.1433	− .01
		1.3666	1.6382	.6426	1.1983	1.1980	− .03
	4.6196	3.7520	0.4410	0.1499	1.0467	1.0469	+ 0.02
		2.9372	.8548	.3039	1.0948	1.0946	− .02
		.....	2.3610	1.0	1.3044	1.3047	+ .03
9	5.4851	3.8795	0.7894	0.2338	1.0832	1.0835	+ 0.03
		2.8324	1.3051	.4087	1.1451	1.1453	+ .02
		1.4784	1.9724	.6668	1.2362	1.2352	− .10
		.....	2.7106	1.0	1.3490	1.3495	+ .05
10	5.8385	3.5953	1.0884	0.3123	1.1168	1.1169	+0.01
		2.2752	1.7306	.5329	1.1986	1.1981	− .05
		1.0798	2.3162	.7629	1.2820	1.2816	− .04
		.....	2.8500	1.0	1.3657	1.3663	+ .06

[a] $\Delta = R$(calc) − R(obs), where R(calc) is obtained with the aid of eq (1) and the parameters in table 2.

$R = 1.1849$. Moreover, a plot of isopiestic ratio versus ionic fraction of barium chloride gave a straight line, within experimental error; the plot of isopiestic ratio versus ionic fraction of calcium chloride (fig. 1) may appear to be linear but a closer examination, by the method of least squares, reveals a slight curvature.

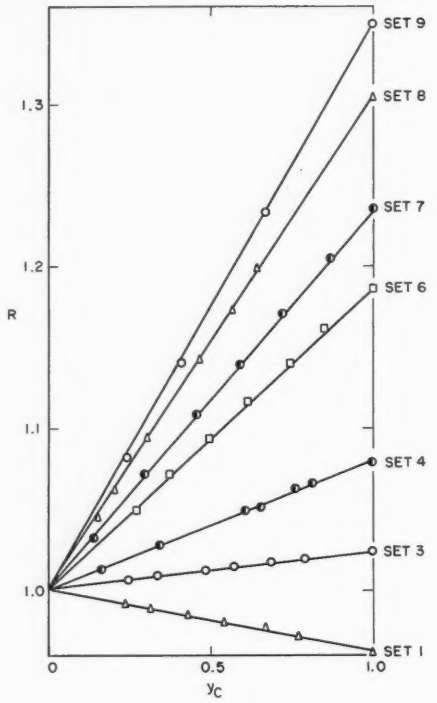

FIGURE 1. *Isopiestic ratio of sodium chloride (B)−calcium chloride (C) solutions versus ionic fraction.*
$R = M_B/m$, $m = m_B + 1.5\ m_C$, $y_C = 1.5\ m_C/m$.

The isopiestic results can be represented by the equation

$$R = M_B/m = 1 - ay_C - by_C^2. \qquad (1)$$

The parameters of this equation were obtained by the method of least squares. The seventh column of table 1 gives values of R calculated by this equation, using the values of a and b given in table 2. The last column of table 1 gives the differences between the observed isopiestic ratios and those calculated using eq (1).

TABLE 2. *Values of the parameters of eq (1) and of the integral in (5)*

Set	M_B (mean)	a	b	b/M_B	φ_B	$M_B\varphi_B$	$\int^a$
1	0.5374	+ 0.0337	0.0040	0.0074	0.9217	0.4953	0.0015
2	.7997	− .0007	.0032	.0040	.9288	.7428	.0022
3	1.0472	− .0287	.0040	.0038	.9372	.9814	.0026
4	1.5355	− .0828	.0078	.0051	.9583	1.4715	.0038
5	1.7842	− .1087	.0060	.0034	.9715	1.7334	.0041
6	2.7736	− .1909	.0039	.0014	1.0304	2.8579	.0059
7	3.4458	− .2406	.0058	.0017	1.0759	3.7073	.0066
8	4.6009	− .3141	.0094	.0020	1.1609	5.3412	.0074
9	5.4851	− .3595	.0100	.0018	1.2298	6.7456	.0082
10	5.8385	− .3781	.0118	.0020	1.2578	7.3437	.0086

[a] This column gives values of the integral $0.4343 \int_0^{M_B\varphi_B} (b/M_B)\ d(M_B\varphi_B)$.

5. Calculation of Activity Coefficients

The immediate result of an isopiestic experiment is the information that a set of solutions, one of which contains only sodium chloride, another contains only calcium chloride, and the remainder contain both sodium chloride and calcium chloride in different proportions, all have the same vapor pressure and the same water activity, a_w. It follows that:

$$2M_B\varphi_B = (2m_B + 3m_C)\varphi = 3M_C\varphi_C, \tag{2}$$

where φ_B is the osmotic coefficient of the solution containing sodium chloride only at molality M_B, φ_C is the osmotic coefficient of the solution containing calcium chloride only at molality M_C, and φ is the osmotic coefficient of the solution containing both sodium chloride at molality m_B and calcium chloride at molality m_C.

It is the activity coefficients of these two salts in the mixed solution that are required. These are obtained by means of the McKay-Perring equation [4]:

$$\ln \gamma_B = \ln \Gamma_B + \ln R + \int_0^{M_B\varphi_B} f(m, M_B, y_C)d(M_B\varphi_B) \tag{3}$$

where γ_B is the activity coefficient of sodium chloride in the mixed solution and Γ_B that of sodium chloride in the reference solution at molality M_B. In eq (3),

$$f(m, M_B, y_C) = \frac{1}{m^2}\left(\frac{\partial m}{\partial \ln y_C}\right)_{a_w} + \frac{1}{m} - \frac{1}{M_B}. \tag{4}$$

There are similar equations for $\ln \gamma_C$. It can be shown that, if the isopiestic ratio can be represented by eq (1), then the integral term in eq (3) reduces to:

$$y_C^2\int_0^{M_B\varphi_B} (b/M_B)d(M_B\varphi_B). \tag{5}$$

Figure 2 is a plot of (b/M_B) against $(M_B\varphi_B)$. The smooth curve is that of the equation

$$b/M_B = 0.0075 - 0.00243(M_B\varphi_B) + 0.000234(M_B\varphi_B)^2. \tag{6}$$

The integral in eq (3) now becomes:

$$y_C^2\{0.0075 - 0.00122(M_B\varphi_B) + 0.000078(M_B\varphi_B)^2\}(M_B\varphi_B) \tag{7}$$

or

$$y_C^2\{0.0033 - 0.00053(M_B\varphi_B) + 0.00034(M_B\varphi_B)^2\}(M_B\varphi_B) \tag{8}$$

if eq (3) is to be used with decadic logarithms.

There is some scatter of the points in figure 2 because it is not easy to get precise values of the b coefficient, especially from measurements on the more dilute solutions. But the maximum value of the integral that will be used in subsequent calculations is only 0.0060; this occurs in the computation of the activity coefficient of calcium chloride in a mixture of total ionic strength $I = 4$. Here the logarithm of the isopiestic ratio is -0.0691 and is therefore more important than the integral term. Consequently, we can tolerate some uncertainty about the exact form of the curve in figure 2. For example, had we considered the data best represented by the dashed straight line shown in figure 2, and carried out the integration of b/M_B with respect to $(M_B\varphi_B)$ accordingly, the value of the integral would still have been 0.0060.

The calculation of an activity coefficient can be illustrated by the following example. The mean of two results in set 6 of table 1 shows that a solution of $2.7736m$ sodium chloride was in isopiestic equilibrium with a solution of $1.5589m$ calcium chloride; the isopiestic ratios of the mixed solutions could be expressed as:

$$R = 1 + 0.1909y_C - 0.0039y_C^2. \tag{9}$$

It has been shown [eq (15) of ref. 2] that the composition of a mixed solution of total ionic strength I in isopiestic equilibrium with a solution of sodium chloride of molality M_B can be obtained by solving the quadratic equation:

$$bIy_C^2 + (aI + M_B)y_C = I - M_B. \tag{10}$$

Putting $a = -0.1909$, $b = 0.0039$, $I = 4.5$, we find that $y_C = 0.8944$ and hence, by eq (9), $R = 1.1676$, $\log R = 0.0673$. But $m = m_B + 1.5m_C = M_B/R = 2.3755$ and therefore $m_B = 0.2509$, $m_C = 1.4164$. At $M_B = 2.7736$, $\log \Gamma_B = -0.1542$ [5]; $\log R$ is 0.0673 and, from eq (8), the integral contributes 0.0052. Hence, by eq (3) $\log \gamma_B = -0.0817$. This is the logarithm of the activity coefficient of sodium chloride in the mixed solution at $I = 4.5$, $y_C = 0.8944$.

The equation

$$\log \gamma_B = \log \gamma_B^0 - \alpha_B I_C \tag{11}$$

is often valid for systems at constant ionic strength.

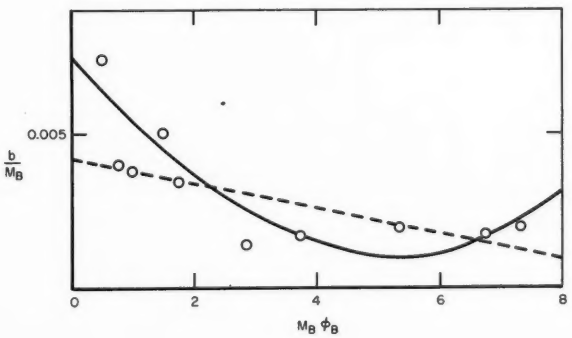

FIGURE 2. b/M_B *versus* $(M_B\varphi_B)$.

Here log $\gamma_B^0(=-0.0830)$ [5] is the logarithm of the activity coefficient of sodium chloride in its own solution at a total ionic strength (or molality) of 4.5 and $I_C=3m_C=4.2492$. Substituting in eq (11), $\alpha_B=-0.0013$.

Similar calculations show that the activity coefficient of calcium chloride in this mixture is given by log $\gamma_C=-0.2065$. But for a solution of calcium chloride only at this total ionic strength ($I=4.5$, $1.5m$), log $\gamma_C^0=-0.1222$ [6]. Substituting in the equation

$$\log \gamma_C = \log \gamma_C^0 - \alpha_C I_B, \tag{12}$$

with $I_B=m_B=0.2509$, gives $\alpha_C=-0.0047$.

In this way, values of α_B and α_C have been calculated at other values of the total ionic strength. They are given in table 3. The figures in parentheses indicate the set number in table 1 corresponding to the data from which the calculations were made. The values of α_B and α_C are plotted in figure 3. They lie on a smooth curve except for the values at $I=0.75$ and 1.0; in these cases log γ_B and log γ_B^0 are very close together and α_B is the result of dividing a small quantity by I_C, so that it is not surprising that there is some scatter. The same holds for the α_C values. "Best" values of α_B and α_C, read from figure 3, are given in the latter part of table 3 (the significance of the values at $I=0$ in fig. 3 is explained in sec. 6). Table 3 also gives values of $(2\alpha_B+\alpha_C)$. It has been shown that for a system of this valence type $(2\alpha_B+\alpha_C)$ is independent of I if eq (11) and eq (12) are valid, that is to say, no terms in higher powers of I_B or I_C are needed. Values of $0.5(2\alpha_B+\alpha_C)$ are plotted in figure 3; there is a small variation of $(2\alpha_B+\alpha_C)$ with I. It could be explained by introducing $\beta_B I_C^2$ and $\beta_C I_B^2$ terms into eq (11) and eq (12), respectively, but β_B and B_C would be so small that their effect on log γ_B and log γ_C would be beyond the experimental error.

TABLE 3. *Values of α_B and α_C calculated from data in table 1*

I	α_B	α_C	"Best" values		$(2\alpha_B+\alpha_C)$
			α_B	α_C	
0.75	−0.0073(1)	0	−0.0106	0.0005	−0.0207
1.0	−.0092(2)	0.0002(2)	−.0092	−.0020	−.0204
1.5	−.0063(3)	−.0098(3)	−.0063	−.0098	−.0224
2.0	−.0052(4)	−.0130(4)	−.0047	−.0126	−.0220
	−.0054(5)	−.0122(5)			
3.0	−.0021(5)	−.0165(5)	−.0018	−.0165	−.0201
	−.0014(6)	−.0165(6)			
4.0	−.0006(6)	−.0186(6)	0	−.0186	−.0186
	.0006(7)	−.0185(7)			
5.0	.0007(7)	−.0190(7)	.0007	−.0192	−.0178
	.0006(8)	−.0186(8)			
6.0	.0016(8)	−.0196(8)	.0016	−.0198	−.0166
	.0024(9)	−.0200(9)			
7.0	.0014(9)	−.0204(9)	.0020	−.0203	−.0163
	.0014(10)	−.0202(10)			

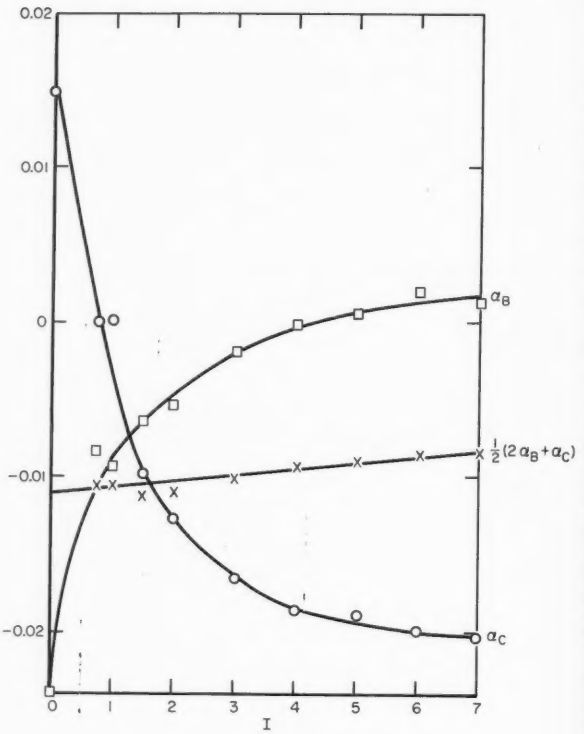

FIGURE 3. α_B, α_C, *and* $0.5(2\alpha_B+\alpha_C)$.

6. Values of α_B and α_C in Dilute Solutions

We now consider what values α_B and α_C might be expected to have when the total ionic strength becomes very small. For this purpose we write for the activity coefficient of the ith ion in a mixed solution [7, 8]:

$$\log \gamma_i = \log \gamma^{st} + \sum_j B_{ij} m_j \tag{13}$$

Here γ^{st} is the activity coefficient calculated on the assumption that the only interionic interaction is of the Debye-Hückel type; it can be expressed as

$$\log \gamma^{st} = \frac{-z_i^2 A I^{1/2}}{1+1.5I^{1/2}} \tag{14}$$

where z_i is the valence of the ith ion. B_{ij} is a coefficient characteristic of the interaction between an ith ion and a jth ion and, in accordance with the Brönsted Principle of Specific Interaction, the summation is to be made over all pairs of *oppositely* charged ions. Thus, in a solution containing both sodium chloride and calcium chloride,

$$\log \gamma_{Cl} = \log \gamma^{st} + B_{Na,Cl} m_{Na} + B_{Ca,Cl} m_{Ca} \tag{15}$$

$$\log \gamma_{Na} = \log \gamma^{st} + B_{Na,Cl} m_{Cl} \tag{16}$$

$$\log \gamma_{Ca} = 4 \log \gamma^{st} + B_{Ca,Cl} m_{Cl}. \tag{17}$$

Writing $B_{Na,Cl} = B_B$ and $B_{Ca,Cl} = B_C$ for brevity, and remembering that $2 \log \gamma_B = \log \gamma_{Na} + \log \gamma_{Cl}$ and $3 \log \gamma_C = \log \gamma_{Ca} + 2 \log \gamma_{Cl}$,

$$\log \gamma_B = \log \gamma^{st} + (m_B + m_C) B_B + \tfrac{1}{2} m_C B_C \tag{18}$$

and

$$\log \gamma_C = 2 \log \gamma^{st} + 2/3.m_B B_B + 1/3.(m_B + 4m_C) B_C. \tag{19}$$

The activity coefficient of either salt in its own solution in the absence of the other salt, at a total ionic strength I, is now given as:

$$\log \gamma_B^\circ = \log \gamma^{st} + I B_B \tag{20}$$

$$\log \gamma_C^\circ = 2 \log \gamma^{st} + 4/9.I B_C \tag{21}$$

where $I_B = m_B$ and $I_C = 3m_C$. These equations enable us to evaluate B_B and B_C from data on dilute single salt solutions; using the values of Janz and Gordon [9] for sodium chloride and of McLeod and Gordon [10] for calcium chloride, we find $B_B = 0.007$ and $B_C = 0.176$.

By γ^{tr} we designate the 'trace' activity coefficient of a salt, that is the activity coefficient of a salt when it is present in vanishingly small amount in a solution which contains virtually only the other salt. Equation (18) gives

$$\log \gamma_B^{tr} = \log \gamma^{st} + 1/3.I(B_B + \tfrac{1}{2} B_C) \tag{22}$$

and eq (19)

$$\log \gamma_C^{tr} = 2 \log \gamma^{st} + 1/3.I(2B_B + B_C). \tag{23}$$

Hence,

$$\alpha_B = 1/I.\ \log \gamma_B^\circ / \gamma_B^{tr} = 2/3.B_B - 1/6.B_C \tag{24}$$

and

$$\alpha_C = 1/I.\ \log \gamma_C^\circ / \gamma_C^{tr} = 1.9.B_C - 2/3 B_B. \tag{25}$$

Substituting numerical values for B_B and B_C, we find $\alpha_B = -0.024$, $\alpha_C = 0.015$. These values are shown in figure 3 at $I = 0$. It will be seen that they are consistent with a reasonable extrapolation of the experimental values at finite concentrations. But $(2\alpha_B + \alpha_C) = -0.0165$, which is in poor agreement with the value of -0.0110 extrapolated from the experimental values. This suggests that the behavior of this system may be more complicated in more dilute solutions.

7. Trace Activity Coefficients

In the case when $I_C \to I(m_B \to 0)$ in eq (11), the trace activity coefficient of sodium chloride is given by

$$\log \gamma_B^{tr} = \log \gamma_B^\circ - \alpha_B I \tag{26}$$

and similarly

$$\log \gamma_C^{tr} = \log \gamma_C^\circ - \alpha_C I. \tag{27}$$

Using the values of α_B and α_C in table 3, values of the trace activity coefficients have been calculated. They are shown in figure 4 along with plots of the activity coefficients of each of the salts in its own solution (γ_B°, γ_C°). This figure is used to emphasize the fact that, at constant total ionic strength, the addition of calcium chloride has only slight effect on the activity coefficient of sodium chloride. On the contrary, addition of sodium chloride has considerable effect on the activity coefficient of calcium chloride.

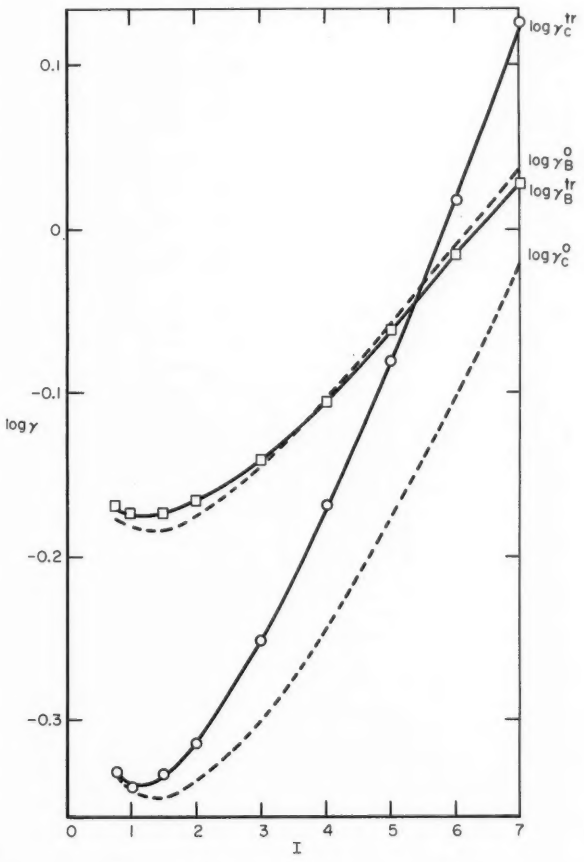

FIGURE 4. *Activity coefficients of sodium chloride and calcium chloride.*

– – – – – – – Activity coefficient of a salt in its own solution.

——— Trace activity coefficient.

8. Comparison With Previous Work

Lanier [11] has used the sodium ion-sensitive glass electrode to measure the activity coefficient of sodium chloride in calcium chloride solutions. In table 4 we compare his values of α_B with those obtained in the present work, and also values of log γ_B^{II} calculated therefrom. The agreement is excellent at $I=3.0$ and $I=6.0$. The agreement between the two values of α_B at $I=1.0$ is not so good, but the values of log γ_B^{II} are in fair agreement.

TABLE 4. *Comparison of α_B and log γ_B^{II} values*

	α_B		$-\log \gamma_B^{\mathrm{II}}$	
I	This work	Lanier [11]	This work	Lanier
1.0	−0.0092	−0.0040	0.173	0.178
3.0	−.0018	−.0020	.142	.140
6.0	.0016	.0013	.016	.014

9. Excess Free Energy of Mixing

It has been shown [2] that the excess free energy of mixing 0.5 kg of water containing 0.5 I moles of a 1:1 salt and 0.5 kg of water containing 0.5(I/3) moles of a 1:2 salt, giving a kilogram of water containing 0.5 I moles of the first salt and 0.5(I/3) moles of the other, the total ionic strength of all three solutions being I, is given by the expression:

$$\frac{\Delta G^E}{2.303RT}=-\frac{I^2}{8}(2\alpha_B+\alpha_C) \qquad (28)$$

provided that eq (11) and eq (12) hold. Using the values of α_B and α_C in table 3, the excess free energy of the sodium chloride-calcium chloride system can be calculated, giving the values shown in table 5.

TABLE 5. *Excess free energy of mixing at 25 °C*

I	0.75	1	1.5	2	3	4	5	6	7
ΔG^E	2	4	9	15	31	51	76	102	136

ΔG^E is expressed in calories per kilogram of water, 1 calorie = 4.1840 J.

These values of the excess free energy of mixing are opposite in sign but comparable in magnitude with those for the sodium chloride-barium chloride and potassium chloride-barium chloride systems.

Grateful acknowledgment is made to the Office of Saline Water for a grant in partial support of this work.

10. References

[1] R. A. Robinson and V. E. Bower, J. Res. NBS **69A** (Phys. and Chem.) No. 1, 19 (1965).
[2] R. A. Robinson and V. E. Bower, J. Res. NBS **69A** (Phys. and Chem.) No. 5, 439 (1965).
[3] R. A. Robinson and V. E. Bower, J. Res. NBS **70A** (Phys. and Chem.) No. 4, 305 (1966).
[4] H. A. C. McKay and J. K. Perring, Trans. Faraday Soc. **49,** 163 (1953).
[5] R. A. Robinson and R. H. Stokes, Electrolyte solutions, Appendix 8.3, 2d. ed., (Butterworths Scientific Publications, London, 1959).
[6] R. H. Stokes, Trans. Faraday Soc. **41,** 637 (1945); see also ref [5], Appendix 8.5.
[7] E. A. Guggenheim, Phil. Mag. [7] **19,** 588 (1935).
[8] G. Scatchard, Chem. Revs. **19,** 309 (1936).
[9] G. J. Janz and A. R. Gordon, J. Am. Chem. Soc. **65,** 218 (1943).
[10] H. G. McLeod and A. R. Gordon, J. Am. Chem. Soc. **68,** 58 (1946).
[11] R. D. Lanier, J. Phys. Chem. **69,** 3992 (1965).

(Paper 70A4–406)

JOURNAL OF RESEARCH of the National Bureau of Standards—A. Physics and Chemistry
Vol. 70A, No. 4, July–August 1966

Use of the Consistency Check in the Vector Verification Method

Alan D. Mighell* and R. A. Jacobson[1]

Institute for Materials Research, National Bureau of Standards, Washington, D.C.

(March 15, 1966)

The consistency check is a type of frequency check in which full use is made of the space group symmetry. It is designed for application to a symmetry map, to a tentative atom map, to the results of superpositions, or to any pseudoelectron-density map. Like the frequency check, its purpose is to aid in the analysis of one of the above maps by assigning a relative weight (relative weight equals the number of other peaks that the given peak is consistent with) to the peaks in these maps. To determine the relative weight, each peak in the map is compared with each of the others to see if it is consistent. Two peaks are considered consistent with each other, if and only if, the set of unique vectors between the two is present in the Patterson map. The method is equivalent to doing a full set of symmetry superpositions at each peak in a symmetry map or a tentative atom map; counting the number of points in the resulting map; and outputting this number at the initial peak position. No assumptions other than that for space group symmetry are required to apply the consistency check to a symmetry map. The resulting map, which has been calculated in a routine fashion directly from the Patterson map, may then be conveniently used as the starting point for the structure analysis of an unknown compound.

Key Words: Crystal, structure, Patterson, vector, symmetry, consistency, frequency, superposition.

1. Introduction

Vector methods based on analysis of the Patterson function are extremely useful in solving crystal structures. Since these methods can be adapted to high speed digital computers, it has been possible to derive both centric and acentric crystal structures from complex Patterson functions.

Vector verification is one type of vector method which has been adapted to the computer. This method has been shown to be a valuable approach to the analysis of the Patterson function [Mighell and Jacobson, 1963, 1964]. The procedures involved in this method are

1. The formation of a map, referred to as a symmetry map, containing only the electron-density space positions consistent with both the Patterson map and the space group of the crystal. The frequency or consistency check is then applied to part or all of the symmetry map.

2. The choice of a trial atomic position, called a tentative atom position, from the symmetry map prepared in step 1.

3. The formation of a new map, referred to as a tentative atom map, containing only the electron-density space positions consistent with the tentative atom position, in addition to the restrictions in step one above. The frequency check or consistency check is then applied to part or all of the tentative atom map.

4. Repetition of steps 2 and 3 until a refinable trial model results.

In the frequency check method [Gorres and Jacobson, 1964], the Patterson map is superimposed on each location in the symmetry, in the tentative atom, or in any similar pseudoelectron-density map. After each superposition, a frequency corresponding to the number of peak coincidences is assigned to the superposition point, resulting in a frequency map indicative of the probable atomic locations.

The consistency check is a type of frequency check in which full use is made of space group symmetry. Closely related methods were reported by Gorres and Gaertner [1965] and Corfield and Rosenstein [1965] at the American Crystallographic Association Meeting in Gatlinburg, Tenn. The consistency check is designed to aid in the analysis of a symmetry map, a tentative atom map, the results of superpositions, or of similar pseudoelectron-density maps. Like the frequency check, the method extends the information present in one of the above maps by assigning a weight to each peak in the map. The procedure may be carried out in a routine fashion as it requires no assumptions about the final structure other than that of space group symmetry.

After the consistency check has been applied to the peaks in a symmetry map or in a tentative atom map, one is in a much better position to distinguish real from

*National Research Council-National Bureau of Standards Postdoctoral Research Associate, 1964–1966.

[1] Present Address: Department of Chemistry, Iowa State University, Ames, Iowa.

spurious peaks. It is then possible to choose in a systematic way the best peaks to use in the tentative atom procedure, the most suitable vectors to use in the superposition procedure, or the most likely peaks to use in the final structure.

2. The Method of the Consistency Check

The consistency check may be run on a symmetry map, on a tentative atom map [Mighell and Jacobson, 1964] or on any pseudoelectron-density map. Before initiating the consistency check, a three-dimensional sharpened Patterson map [Jacobson, Wunderlich, and Lipscomb, 1961] is stored in the memory of the computer. For programming convenience all grid positions having a value above a given value are stored as a 1 and those below as a 0. However, in a later version it is planned to use the actual peak heights. Also all of the peaks in the symmetry or tentative atom map (i.e., grid coordinates that survived the symmetry or tentative atom procedure) are stored in memory as a list.

Each peak in the list is compared against all of the others, one by one, to see if it is consistent. Two points are defined as consistent with each other if, and only if, the set of unique vectors between the two is present in the Patterson map. For example, in the case where there are four equivalent positions in the space group, the unique vectors between atoms located at positions X and Y would be $\mathbf{X}-\mathbf{Y}$, $\mathbf{X}-\mathbf{Y}'$, $\mathbf{X}-\mathbf{Y}''$, $\mathbf{X}-\mathbf{Y}'''$ (the primes indicate atoms related to Y by space group symmetry). For a given peak X (grid coordinates x, y, z) in the list, the total number of peaks in the list that X is consistent with, is recorded and outputted at grid position x, y, z.

Although the entire symmetry map is stored in the computer as a list, it is necessary to execute the consistency check only on the peaks that comprise the asymmetric unit of the symmetry map. The calculations for the entire consistency check are extensive but the method is easy to program and may be successfully carried out in a routine way on a large digital computer. However, if only limited computer time is available or if a small computer is to be used, it is often sufficient to run the consistency check on only a part of the symmetry map or on a part of the tentative atom map.

The symmetry map, or the tentative atom map to which the consistency check has been applied, is outputted in the same format as the input map. In addition, a record is made at every peak of the number of consistencies, that is, the number of other peaks in the map with which it is consistent. Actual peaks tend to be consistent with many more peaks than do spurious peaks.

3. Interpretation of the Results From the Consistency Check

As indicated above, the consistency check may be applied either to a symmetry map or to a tentative atom map. If the check is applied to a symmetry map, the peaks having the highest consistencies are more likely to represent actual atomic positions and are therefore the best possibilities to use as the tentative atom in the tentative atom procedure. Also the peaks, having the highest consistency, may be used to calculate the best vectors to use in the conventional superposition procedure.

The calculation of the symmetry map followed by the applications of the consistency check is based solely on the knowledge of the space group and the Patterson map. No other assumptions as to the arrangement of the atoms in the space group are made. Thus, for a new compound it is possible to calculate in a routine way a Patterson map and a symmetry map to which the consistency check has been applied.

If the consistency check is applied to a tentative atom map or to a similar pseudoelectron-density map, the peaks having the highest consistencies are the best possibilities for final atomic positions, for a second tentative atom, or for a peak on which to base further superpositions.

4. Equivalence of the Consistency Check

The consistency check is exactly equivalent to performing the tentative atom procedure at every peak (grid coordinates that satisfy the symmetry or tentative atom conditions for a given space group) in a symmetry map or in a map resulting from the tentative atom procedure.

For example, take the case in which the consistency check is applied to the results of the symmetry check. Consider a typical peak X in the symmetry map [Mighell and Jacobson, 1963]. Peak X is used as a tentative atom in the tentative atom procedure and the total number of peaks (grid positions that satisfied the conditions of the tentative atom procedure) in the resulting tentative atom map are counted. This number, which tells exactly how many points survive the tentative atom procedure, is placed in the position X in the symmetry map. The same procedure is carried out at all the other peaks in the symmetry map.

The consistency check is also equivalent to doing a series of superpositions (using the set of vectors between the tentative atom and its equivalent positions) at each peak in the symmetry map or in the tentative atom map. If there is only one vector, then the consistency check gives results equivalent to the frequency check [Gorres and Jacobson, 1964]. But in all of the higher space groups, where there is more than one vector, the consistency check is more powerful than the frequency check.

5. Conclusion and Extension

The consistency check, like the frequency check, is a method designed to evaluate the peaks resulting from the symmetry check, the tentative atom procedure, or the standard superposition method. This method can be applied to both centric and acentric

crystals and is especially useful for crystals belonging to space groups of high symmetry. It is useful in distinguishing real peaks form spurious peaks, in ascertaining the centers of peaks, in picking tentative atoms or in selecting vectors for superpositions.

The symmetry map to which the consistency check has been applied can be derived routinely from the Patterson function. This map can then serve as a useful adjunct to other methods of structure solution. For example, it may serve as a starting point for either mathematical or vector phasing methods.

Since the present method has been based entirely on peak positions, a useful extension of the method would be to calculate a symmetry map, a tentative atom map, and a consistency check using the Patterson map with the actual peak heights rather than the bi-valued Patterson. The method would then become considerably more powerful but the computer time and memory requirements would be greatly increased.

6. References

Corfield, P. W. R. and Rosenstein, R. D., paper K6, American Crystallographic Association Meeting (1965), Gatlinburg, Tenn.

Gorres, B. T., and Gaertner, Gregory G., paper N3, American Crystallographic Association Meeting (1965), Gatlinburg, Tenn.

Gorres, B. T. and Jacobson, R. A. (1964), Acta Cryst. **17** 1599.

Jacobson, R. A., Wunderlich, J. A., and Lipscomb, W. N. (1961), Acta Cryst. **14**, 598.

Mighell, A. D. and Jacobson, R. A. (1963), Acta Cryst. **16**, 443.

Mighell, A. D. and Jacobson, R. A. (1964), Acta Cryst. **17**, 1554.

(Paper 70A4–407)

JOURNAL OF RESEARCH of the National Bureau of Standards—A. Physics and Chemistry
Vol. 70A, No. 4, July–August 1966

Self-Reversal in the Spectral Lines of Uranium

Donald D. Laun*

(April 12, 1966)

In 1946, spectrum analysis indicated that the outer-electron configuration of normal uranium atoms was $5f^3\ 6d^1\ 7s^2$, with an energy level designated $^5L_6^\circ$ representing the normal state. Now that conclusion is experimentally verified by the observation of self-reversed lines in uranium spectra emitted by a high-current pulsed arc between metallic electrodes. Fifty-four reversed lines were observed; thirty-eight involve the normal state and sixteen are distributed among four low metastable states of the same configuration.

Key Words: Uranium, spectrum of; spectrum, of uranium; self-reversal, in uranium spectrum.

In 1946, Kiess, Humphreys, and Laun published[1] a "Preliminary description and analysis of the first spectrum of uranium" in which relative intensities and magnetic splitting of strong lines indicated that the outer-electron configuration of normal uranium atoms was $5f^3\ 6d^1\ 7s^2$ with an energy level designated $^5L_6^\circ$ representing the ground state. At that time efforts to confirm this conclusion by observing self-reversal in uranium lines emitted by conventional underwater sparks or d-c arcs failed. However, a high-current pulsed arc (75 A peak current) recently developed by Sugar[2] produced many absorbed or partially reversed lines in uranium spectra, thus providing for the first time a direct experimental verification of the low energy levels of the uranium atom. Those spectrograms were loaned to me for study.

The observations of self-reversed lines in uranium spectra cover the region from 3200 to 4400 Å in the second order of a concave grating with a reciprocal dispersion of 0.86 Å per mm. Spectrograms made in the first order beyond 4100 Å did not show self-reversals, probably because of insufficient resolving power. Between 3413.25 and 4393.60 Å, fifty-four U I lines that show self-reversal were identified; about a dozen of these are indicated in reproductions that appear in Sugar's paper. The distribution of reversed and classified U I lines among low energy levels is shown in table 1. Since 70 percent of these lines involve $^5L_6^\circ$ they prove that this is indeed the ground state of neutral uranium; the remainder verify the reality of four metastable states with low energy.

TABLE 1. *Distribution of reversed lines among low-energy levels of* U I

Electron configuration	Level symbol	Level value	Reversed lines
		cm−1	
$5f^3\ 6d^1\ 7s^2$	$^5L_6^\circ$	0.00	38
$5f^3\ 6d^1\ 7s^2$	$^5K_5^\circ$	620.32	10
$5f^3\ 6d^1\ 7s^2$	$^5L_7^\circ$	3800.81	4
$5f^3\ 6d^1\ 7s^2$	$^5K_8^\circ$	4275.69	1
$5f^3\ 6d^1\ 7s^2$	$^5I_4^\circ$	4453.40	1

This proof is presented in detail in table 2 which is based mainly upon our 1946 publication (see footnote 1) but includes some additional and revised data. The wavelengths and estimated relative intensities represent our original observations of uranium spectra emitted by a d-c (5 A) arc. The corresponding wavenumbers are taken from a *"Table of Wavenumbers"*.[3]

In table 2, the final column displays numerical values of high energy levels (even parity) that combine with the low energy levels (odd parity), symbolized in the preceding column and evaluated in table 1. In both tables the subscripts represent J-values.

In our first paper (see footnote 1), the relative values of energy levels were given to six figures, ending with one decimal. In 1964 Michèle Diringer[4] recalculated the energy levels of U I to seven figures, including two decimals, and reported some new ones. In constructing table 2, I have adopted the energy-level values

*Former member of Spectroscopy Section, NBS; present address: 642 Calumet Avenue, Kiel, Wis. 53402.

[1] C. C. Kiess, C. J. Humphreys, and D. D. Laun, J. Res. NBS., 37, 57; (1946).

[2] J. Sugar, J. Res. NBS., **66A**, (Phys. and Chem.) No. 4, 321; (1962).

[3] C. D. Coleman, W. R. Bozman, and W. F. Meggers, Table of Wavenumbers, NBS Mono. 3, Volume **1**, 1960.

[4] Michèle Diringer, Thèse de Paris, Serie A, No. 4232; 1964.

TABLE 2. *Self-reversed lines of* U I

Wavelength Å (air)	Intensity in arc	Wavenumber K (vac)	Odd level	Even level
4393.60	200	22753.99	$^5L^\circ_6$	22754.05$_6$
4362.05	300	22918.56	$^5L^\circ_6$	22918.54$_7$
4153.97	150	24066.57	$^5L^\circ_6$	24066.57$_7$
3948.45	35	25319.23	$^5L^\circ_6$	25319.25$_5$
3943.82	200	25348.95	$^5L^\circ_6$	25348.96$_6$
3894.12	120	25672.47	$^5L^\circ_6$	25672.44$_7$
3876.13	60	25791.62	$^5L^\circ_6$	25791.58$_6$
3871.04	120	25825.53	$^5L^\circ_6$	25825.54$_6$
3854.22	100	25938.23	$^5L^\circ_6$	25938.20$_6$
3839.62	120	26036.86	$^5L^\circ_7$	29837.61$_7$
3812.00	150	26225.51	$^5L^\circ_6$	26225.54$_6$
3765.35	40	26550.41	$^5L^\circ_6$	26550.40$_6$
3731.45	100	26791.62	$^5L^\circ_6$	26791.63$_6$
3692.75	30	27072.38	$^5L^\circ_6$	27072.36$_6$
3685.78	40	27123.58	$^5K^\circ_5$	27743.91$_6$
3682.46	30	27148.03	$^5L^\circ_6$	27148.06$_7$
3679.38	60	27170.76	$^5K^\circ_5$	27791.12$_5$
3677.39	60	27185.46	$^5L^\circ_7$	30986.26$_8$
3659.58	50	27317.76	$^5K^\circ_5$	27938.06$_5$
3659.16	100	27320.90	$^5K^\circ_5$	27941.22$_6$
3644.24	60	27432.75	$^5K^\circ_5$	28053.03$_6$
3639.49	30	27468.55	$^5K^\circ_6$	31744.23$_5$
3638.20	150	27478.29	$^5L^\circ_7$	31279.09$_8$
3636.31	15	27492.57	$^5I^\circ_4$	31945.94$_5$
3626.36	15	27568.00	$^5K^\circ_5$	28188.34$_6$
3620.08	60	27615.82	$^5L^\circ_6$	27615.76$_6$
3605.28	40	27729.19	$^5L^\circ_6$	27729.20$_5$
3603.36	30	27743.96	$^5L^\circ_6$	27743.91$_6$
3598.94	30	27778.03	$^5L^\circ_6$	27777.97$_7$
3591.74	50	27833.72	$^5K^\circ_5$	28453.97$_4$
3584.88	250	27886.98	$^5L^\circ_6$	27886.96$_7$
3578.33	15	27938.02	$^5L^\circ_6$	27938.06$_5$
3577.92	30	27941.22	$^5L^\circ_6$	27941.22$_6$
3574.76	50	27965.92	$^5L^\circ_6$	27965.89$_7$
3566.60	200	28029.90	$^5K^\circ_5$	28650.26$_5$
3563.66	50	28053.03	$^5L^\circ_6$	28053.03$_6$
3561.41	40	28070.75	$^5L^\circ_7$	31871.52$_6$
3557.84	50	28098.92	$^5L^\circ_6$	28098.92$_6$
3555.32	60	28118.83	$^5L^\circ_6$	28118.81$_7$
3546.55	25	28188.36	$^5L^\circ_6$	28188.34$_6$
3534.33	30	28285.82	$^5L^\circ_6$	28285.75$_7$
3514.61	200	28444.53	$^5I^\circ_6$	28444.53$_5$
3513.68	50	28452.06	$^5L^\circ_6$	28452.12$_7$
3511.44	30	28470.20	$^5L^\circ_6$	28470.14$_6$
3507.34	80	28503.48	$^5L^\circ_6$	28503.42$_5$
3500.07	80	28562.68	$^5L^\circ_6$	28562.66$_5$
3489.37	80	28650.27	$^5I^\circ_6$	28650.26$_5$
3466.30	40	28840.94	$^5I^\circ_6$	28840.90$_5$
3462.22	30	28874.93	$^5I^\circ_6$	28874.90$_6$
3459.92	50	28894.12	$^5L^\circ_6$	28894.11$_5$
3454.61	30	28938.54	$^5K^\circ_5$	29558.81$_6$
3442.95	20	29036.54	$^5I^\circ_6$	29036.60$_5$
3434.28	10	29109.84	$^5I^\circ_6$	29109.80$_6$
3413.25	20	29289.19	$^5K^\circ_5$	29909.50$_4$

reported by Diringer, plus the following new levels: 27148.06$_7$, 27938.06$_5$, 28452.12$_7$, and 29036.60$_5$.

Although the uranium wavelengths reported (see footnote 1) in 1946 were limited to six figures, the corresponding wavenumbers were given to seven figures. The same is true in the present paper. Now the average difference between observed and computed wavenumbers in table 2 is less than ± 0.03 K, which corresponds to an average error in wavelength of about ± 0.005 Å. Up to the present time no lists of uranium wavelengths of higher accuracy have been published.

My thanks go to Jack Sugar of the National Bureau of Standards who made the uranium spectrograms available to me for the above analysis.

(Paper 70A4–408)

JOURNAL OF RESEARCH of the National Bureau of Standards—A. Physics and Chemistry
Vol. 70A, No. 4, July–August 1966

Oscillator Strengths for Ultraviolet Lines of Fe I

Charles H. Corliss and Brian Warner*

(April 1, 1966)

Relative intensities and oscillator strengths for 2000 ultraviolet lines of Fe I from several investigations between 2080 and 4150 Å have been critically discussed and adjusted to a uniform absolute scale. New values for many lines not measured heretofore are reported.

Key words: Atomic spectra, iron, oscillator strengths, transition probability, ultraviolet lines of Fe I.

1. Introduction

During the past 30 years, numerous investigations of intensities and oscillator strengths in the ultraviolet part of the iron spectrum have been carried out. The great variety of forms in which they are reported makes comparisons difficult and obscures systematic errors which could otherwise be discovered and perhaps corrected. Furthermore, the fragmentary nature of these reports often leaves serious gaps in our knowledge of the line strength characteristics of the spectrum. Collection of these published reports into a single compilation not only permits the discovery of errors but discloses the need for certain additional work to be done. In 1964 Corliss and Warner made such a compilation for Fe I in the region 3100 to 9000 Å and supplied many new measurements in the region 4000 to 9900 Å. This provides nearly complete information for Fe I in the regions of interest to astrophysicists who obtain their data through the atmosphere but there remain many lacunae in the ultraviolet part of the spectrum that is of special interest to laboratory spectroscopists and space astrophysicists.

It is the purpose of this paper to extend that work as far as possible into the ultraviolet. To that end we have assembled such published ultraviolet data as were overlooked in our previous compilation or have since appeared, adjusted them to the same absolute scale and supplemented them with new values for many lines not previously measured.

There are in general three different methods which have been used to measure intensities and oscillator strengths in spectra such as Fe I. The three methods find their optimum utility in the measurement of lines of different intensity ranges and of different degrees of excitation. The hook method, which is supposed to provide the most accurate measurements, is limited to the strong lines of the spectrum. Because of the nature of the measurement to be made, the method of total absorption is less precise and consequently may be less accurate than the hook method, but it does permit the measurement of fainter lines. However, both of these methods, because they depend on furnace excitation do not produce lines whose lower levels are far above the ground state of the atom. To observe these lines emission methods are generally used. In emission methods, precise measurements of intensities can usually be made but the population distribution amongst the energy levels of the atoms cannot always be accurately specified. This is in contrast to the first two methods in which thermal equilibrium is assured by furnace excitation.

Work on the ultraviolet spectrum of Fe I which has already been published includes all of the stronger lines. These have been measured by all three of the methods mentioned above. To supplement this work and to complete the description of the intensity structure of Fe I the faint lines in the ultraviolet must be measured. We have done this by means of observations in emission, using arcs and sparks which reveal the faintest lines.

2. Published Data

The previously published data on the ultraviolet part of the first spectrum of iron, Fe I, discussed in this section, is summarized in table 1. A number of measurements made prior to 1962, those of King and King [1938]; Carter [1949]; Mitrofanova [1952]; Aarts, Harting, and Bakker [1954]; Allen and Asaad [1957]; and Hefferlin [1959], have been discussed by Corliss and Warner [1964] and are not further discussed here. The early work of van Milaan [1926] reports measurements of 69 lines in a 1.5 A iron arc and 61 of them in a spark. Comparison with other measurements shows that the lines of the stronger half of the group have been weakened by self-absorption, consequently we have not used van Milaan's data.

*University of London Observatory, London, N.W. 7, England.

216-375 O - 66 - 4

TABLE 1. *Published data on intensities and oscillator strengths in the ultraviolet part of* Fe I *discussed in this paper*

Reference	Date	Wavelength range	No. of lines	Number included	Method	Quantity reported	Temperature	Ref. symbol
		Å					°K	
van Milaan	1926	3680–3800	69	.....	arc	intensity	.....	.....
Sobolev	1943	2585–3648	15	15	arc	P	5300	S3
Sobolev	1943	2912–3723	32	32	arc	*gf*	.....	S5
Gottschalk	1948	3265–4635	122	.....	calc.	S	.....	G
Crosswhite	1958	3200–4148	1060	1000	hollow cathode	intensity	.....	HC
Corliss and Bozman	1962	2084–3100	220	215	arc	log *gf*	5100	CB
Morozova, Startsev, and Frish	1962	2987–4144	117	117	arc	log *gf*	4500	MSF
Margoshes and Scribner	1963	2912–4144	105	105	arc	*gf*	5510	MS
Corliss and Warner	1964	3100–4148	685	680	.....	log *gf*	.....	CW
Penkin	1964	2937–4427	56	55	hook	*f*	2000–2500	PP
Valters, Nikonova, and Startsev	1964	2778–3930	57	57	absorpt.	log *gf*	1750–2020	VNS
Valters and Startsev	1964	2719–3930	89	89	hook	log *gf*	2200	VS
King, Olsen, and Corliss	1965	2502–3201	300	290	absorpt.	log *gf*	1600–3000	KOC

2.1. Calculated Values

Two papers have been published dealing with extensive theoretical calculations of line strengths in Fe I. The first was by Gottschalk [1948] who computed line strengths in intermediate coupling for the $3d^7(^4P)4s - 3d^7(^4P)4p$ and $3d^7(^4F)4s - 3d^7(^4F)4p$ transitions. To test these values we have plotted log S/λ from Gottschalk versus log *gf* from Corliss and Bozman [1962] in figure 1. The figure shows that calculations for the ^4P parent are unreliable but that, except for lines for which log $gf < -1.0$, the calculations for the ^4F parent are in agreement with the measured values. According to Gottschalk, the disagreement in the case of the ^4P parent is caused by the fact that the *L* and the *S* of the ^4P core are not good quantum numbers. The lack of agreement for faint lines (in the case of the ^4F parent) seems to be typical of calculated values. Since only 57 of his lines are of use to us and since these have all been measured many times by others, we have omitted them from our tabulation. It should be noted, however, by those interested in theoretical calculation of line strengths that the method used by Gottschalk has led in certain cases to remarkably accurate values.

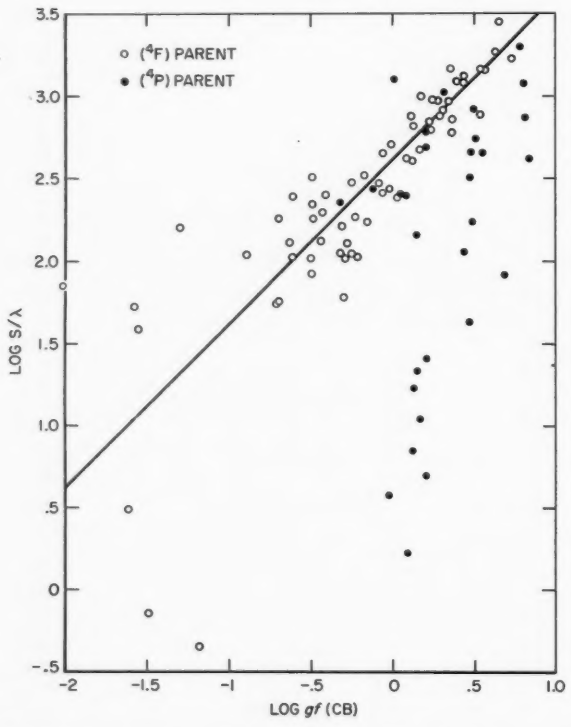

FIGURE 1. *Comparison of log gf-values from Gottschalk [1948] with those from Corliss and Bozman [1962].*

Recently Shore [1965] has investigated simple *LS*-coupling line and multiplet strengths in Fe I and compared them with observed values. He found that the standard deviation within a multiplet was 30 percent or less (i.e., within the experimental error) for about half the multiplets. The fluctuations among multiplets in transition arrays were considerably larger, sometimes amounting to several orders of magnitude. Many of the observed Fe I lines are intersystem transitions which are not predicted in this scheme.

In view of the evident uncertainties in calculated line strengths for Fe I, it seems that at present we are forced to rely almost entirely on measured values. Further investigation by theoreticians of calculations by the method of intermediate coupling would appear to be very much worthwhile, however.

2.2. Russian Measurements

Over the past 50 years, since the introduction of the hook method into the physical laboratories at the University of Leningrad by Rozhdestvenskii, Russian physicists have conducted an outstanding sustained effort in the measurement of oscillator strengths. A number of their papers have been concerned with Fe I. In 1964 Prokofiev, Nikonova, Gruzdev, and Frish published a review of the subject entitled "Oscillator Strengths in the Spectrum Fe I." In

TABLE 2. *Russian measurements of log gf for ultraviolet lines of* Fe I

(1) Wavelength	(2) S3	(3) S5	(4) PP	(5) MSF	(6) VNS	(7) VS	(8) R	(9) N
2584.537	0.10						0.10	
2719.027						0.26	0.26	
2720.904						−0.05	−0.05	
2723.579						−0.49	−0.49	
2735.476	0.10						0.10	
2737.311						−0.39	−0.39	
2742.406						−0.26	−0.26	
2744.069						−0.74	−0.74	
2750.142						−0.35	−0.35	
2756.330						−0.82	−0.82	
2778.221					−0.40		−0.40	
2788.106					0.49	0.20	0.34	2
2795.541					−1.27		−1.27	
2804.521					−0.34		−0.34	
2813.288					0.24		0.24	
2823.277					−0.30		−0.30	
2832.436	−0.10				−0.03		−0.06	2
2838.120					−0.45		−0.45	
2851.798					−0.05		−0.05	
2869.308						−1.68	−1.68	
2874.173						−1.65	−1.65	
2912.159		−1.09				−1.35	−1.22	2
2929.008		−1.00				−1.23	−1.12	2
2936.905		−0.64	−0.76			−0.58	−0.66	3
2941.344		−1.20				−1.43	−1.32	2
2947.877		−0.54	−0.62			−0.56	−0.53	3
2953.941		−0.70	−0.51			−0.67	−0.63	3
2957.366		−0.79	−0.45			−0.91	−0.72	3
2965.256		−0.87				−1.08	−0.98	2
2966.900		−0.21				−0.16	−0.18	2
2969.476					−0.63		−0.63	
2970.106			−0.58				−0.58	
2981.446		−1.16				−1.09	−1.12	2
2983.571		−0.42	−0.33			−0.35	−0.37	3
2987.292				−0.67	−0.53		−0.60	2
2994.428	−0.29	−0.34	−0.51				−0.38	3
2999.512	−0.28	−0.24		0.07	0.11	−0.15	−0.10	5
3000.949		−0.33	−0.47			−0.34	−0.38	3
3003.032				−0.54	−0.56		−0.55	2
3007.283						−1.12	−1.12	
3008.140			−0.42			−0.58	−0.50	2
3009.571				−0.09	−0.08	−0.29	−0.15	3
3016.186				−0.75	−0.68		−0.72	2
3017.629		−1.25				−1.12	−1.18	2
3018.985				−0.31			−0.31	
3024.034		−1.26				−1.07	−1.16	2
3025.844		−0.60	−0.44			−0.58	−0.54	3
3026.464				−0.50	−0.44		−0.47	2
3031.638				−0.54	−0.48		−0.51	2
3037.390	−0.37	−0.42	−0.57			−0.44	−0.45	4
3040.428				−0.68	−0.64		−0.66	2
3041.740					−0.56		−0.56	
3042.022					−0.77		−0.77	
3042.667				−0.60	−0.52		−0.56	2
3047.606	−0.27	−0.31	−0.48			−0.33	−0.35	4
3057.447	0.06	0.02		0.22	0.32	−0.01	0.12	5
3059.087	−0.33	−0.37	−0.62			−0.46	−0.44	4
3067.246	−0.07	−0.20		0.08	0.13	−0.18	−0.05	5
3075.721	−0.37	−0.41		−0.04	−0.06		−0.22	4
3083.743		−0.58		−0.25	−0.16		−0.20	2
3091.579				−0.49	−0.40		−0.44	2
3100.305					−0.19		−0.19	
3100.667					−0.16		−0.16	
3116.634		−0.42			−1.03		−0.73	2
3125.653					−1.00		−1.00	
3139.661				−0.66			−0.66	
3160.658				0.28			0.28	
3165.005				−0.47			−0.47	
3175.447				0.27			0.27	
3178.015				0.16			0.16	
3180.223				0.66			0.66	
3181.922				−0.52			−0.52	
3184.622				−0.49			−0.49	
3184.896						−2.29	−2.29	
3191.660						−2.29	−2.29	
3192.799				0.48			0.48	
3193.227						−1.99	−1.99	
3194.422				−0.29			−0.29	
3196.930				1.01			1.01	

TABLE 2. *Russian measurements of log* gf *for ultraviolet lines of* Fe I—Continued

(1) Wavelength	(2) S3	(3) S5	(4) PP	(5) MSF	(6) VNS	(7) VS	(8) R	(9) N
3199.530				0.57			0.57	
3200.475				0.70			0.70	
3205.400				0.62			0.62	
3210.830				0.53			0.53	
3214.044				1.05			1.05	
3215.940				0.64			0.64	
3219.581				0.74			0.74	
3221.931				−0.98			−0.98	
3222.069				1.09			1.09	
3225.789				1.26			1.26	
3227.063				−0.38			−0.38	
3244.190				0.68			0.68	
3265.618				0.42			0.42	
3271.001				0.46			0.46	
3284.589				−0.27			−0.27	
3286.754				0.90			0.90	
3292.591				0.23			0.23	
3305.972				0.82			0.82	
3306.356				0.87			0.87	
3379.021				−0.20			−0.20	
3383.692				−0.21			−0.21	
3392.654				0.54			0.54	
3394.585				−0.21			−0.21	
3399.336				0.61			0.61	
3406.802				0.21			0.21	
3413.134				0.82			0.82	
3417.843				0.48			0.48	
3418.507				0.40			0.40	
3422.658				0.35			0.35	
3424.286				0.43			0.43	
3426.383				0.05			0.05	
3426.637				0.05			0.05	
3427.121				0.98			0.98	
3428.195				0.34			0.34	
3440.607						−0.49	−0.49	
3440.990						−0.79	−0.79	
3443.878						−1.19	−1.19	
3445.151				0.63			0.63	
3447.280				0.04			0.04	
3450.330				0.14			0.14	
3451.917				0.14			0.14	
3465.862						−1.00	−1.00	
3471.267				−0.21			−0.21	
3475.451						−0.89	−0.89	
3476.704					−1.14	−1.29	−1.22	2
3477.856				−0.78			−0.78	
3490.575						−0.93	−0.93	
3497.842		−1.00	−1.52		−1.38	−1.36	−1.32	4
3521.263			−0.46				−0.46	
3526.042					−1.59		−1.59	
3545.639				0.59			0.59	
3547.203				−0.16			−0.16	
3552.828				0.36			0.36	
3558.517	−0.35	−0.59	−0.22				−0.39	3
3565.381		−0.16	0.02			0.12	−0.01	3
3565.583				0.73			0.73	
3568.423				−0.13			−0.13	
3570.100		0.19	0.34		0.48	0.40	0.35	4
3571.995				0.87			0.87	
3575.118				0.03			0.03	
3575.249				0.18			0.18	
3575.976				0.10			0.10	
3578.380				0.96			0.96	
3581.195			0.51		0.69	0.63	0.61	3
3588.918				0.19			0.19	
3594.632				0.79			0.79	
3595.308				−0.04			−0.04	
3602.08				0.00			0.00	
3608.861	0.24		0.19			0.21	0.21	3
3610.159				1.18			1.18	
3618.769	0.24		0.27			0.28	0.26	3
3631.103				0.10			0.10	
3631.465			0.17			0.27	0.22	2
3637.862				0.09			0.09	
3643.627				0.33			0.33	
3647.844	0.05		0.08			0.12	0.08	3
3649.304						−2.75	−2.75	

TABLE 2. *Russian measurements of log gf for ultraviolet lines of* Fe I—Continued

(1) Wavelength	(2) S3	(3) S5	(4) PP	(5) MSF	(6) VNS	(7) VS	(8) R	(9) N
3651.10				−0.44			−0.44	
3679.915		−1.36	−1.43		−1.36	−1.34	−1.37	4
3683.056					−2.04	−2.17	−2.10	2
3685.998				0.76			0.76	
3687.459			−0.77			−0.45	−0.61	2
3689.457				0.72			0.72	
3701.086				0.88			0.88	
3705.567		−1.19	−1.16		−1.19	−1.06	−1.15	4
3707.048				0.53			0.53	
3707.823					−1.89	−2.01	−1.95	2
3709.248						−0.28	−0.28	
3719.937			−0.47			−0.20	−0.34	2
3722.564		−1.09	−0.98		−1.11	−1.03	−1.05	4
3726.927				0.50			0.50	
3727.621			−0.53			−0.23	−0.38	2
3727.809				0.24			0.24	
3733.319					−1.17	−1.15	−1.16	2
3734.866					0.61	0.52	0.56	2
3737.133			−0.58			−0.35	−0.46	2
3744.105				0.12			0.12	
3745.562					−0.69	−0.53	−0.61	2
3745.901					−1.07	−1.12	−1.10	2
3746.931				0.35			0.35	
3748.264					−0.93	−0.79	−0.86	2
3748.969				0.37			0.37	
3749.488					0.61	0.39	0.50	2
3752.420				−0.52			−0.52	
3754.506				−0.49			−0.49	
3758.235			0.31			0.26	0.28	2
3763.791			0.10			0.11	0.10	2
3766.665				−0.32			−0.32	
3767.194			−0.03			−0.04	−0.04	2
3773.699				−0.60			−0.60	
3787.883			−0.44				−0.44	
3815.843			0.69	0.61			0.65	2
3820.427					0.46	0.36	0.41	2
3824.446					−1.18	−1.11	−1.14	2
3825.883						0.24	0.24	
3827.826				0.56			0.56	
3834.224			0.10			0.03	0.06	2
3840.440						−0.15	−0.15	
3841.050				0.48			0.48	
3849.969			−0.29				−0.29	
3856.373			−1.19		−1.16	−1.05	−1.13	3
3859.913			−0.65			−0.47	−0.56	2
3872.503			−0.05				−0.05	
3878.574					−1.13	−1.13	−1.13	2
3886.284			−0.99			−0.83	−0.91	2
3888.516				0.02			0.02	
3895.658			−1.38		−1.36	−1.39	−1.38	3
3899.709			−1.31		−1.30	−1.27	−1.29	3
3906.481			−2.04		−1.75	−1.86	−1.88	3
3920.260			−1.44		−1.44	−1.45	−1.44	3
3922.913			−1.45		−1.40	−1.37	−1.41	3
3927.922			−1.33		−1.23	−1.27	−1.28	3
3930.298			−1.33		−1.29	−1.24	−1.29	3
3969.260				0.03			0.03	
4005.244				−0.12			−0.12	
4044.612				−0.30			−0.30	
4062.444				0.05			0.05	
4063.596			0.35	0.50			0.42	2
4071.740			0.44	0.49			0.46	2
4079.841				−0.48			−0.48	
4091.557				−1.30			−1.30	
4109.805				−0.11			−0.11	
4114.448				−0.45			−0.45	
4127.611				−0.13			−0.13	
4132.060				−0.16			−0.16	
4132.902				−0.08			−0.08	
4134.680				0.23			0.23	
4143.870				−0.06			−0.06	

it they review critically 18 papers on the subject and tabulate mean values of log *gf* for 1167 lines of Fe I reported in those papers.

There are five Russian papers that report original observations in the ultraviolet region of Fe I; they are discussed individually below. Because none of them report very extensive measurements we have tabulated them separately in table 2. The mean value of log *gf* for each line is given in column 8 of table 2 and entered into table 3, the complete tabulation, in column 10 headed R. The number of observations in table 2 is listed in column 10 of table 3 as a superscript following the R value. All values are normalized to the scale of Corliss and Bozman.

a. Sobolev [1943]

Sobolev published two sets of measurements made using a 3A d-c arc between copper electrodes containing 0.3 percent iron and 0.3 percent tin. From intensity ratios of tin lines he determined a temperature of 5300 °K. Since the two sets overlap, we have listed them in columns 2 and 3 of table 2 under the headings S3 and S5. Sobolev's values compare well with other reliable measurements. In discussing the discrepancies between his own measurements and those of King and King, he states, "It appears that the conditions under which the measurements of King were made were not conditions of thermal equilibrium for the excited levels." Since that time, numerous investigators, e.g., Crosswhite [1958]; Prokofiev, Nikonova, Gruzdev, and Frish [1964]; or Margoshes and Scribner [1963], have shown that the discrepancy is due to scattered light in the short wavelength end of the Kings' spectra, which made their values too small near 3000 Å. The disagreement is shown in figure 3 of Margoshes and Scribner's paper.

b. Parchevsky and Penkin [1954], Penkin [1964]

Parchevsky and Penkin [1954] published relative oscillator strengths for 56 lines of Fe I which they had measured by the hook method at the University of Leningrad. With reference to the accuracy of the hook method, the authors state that the quantity *Nf* can be determined with an error of from 3 to 20 percent, depending on the distance between the peaks of the hooks, and that the error in the quantity *N* depends on the uncertainty in the temperature in the Boltzmann formula and in this case can be as much as 15 percent. This would imply that the maximum error was not greater than 35 percent.

In 1964 Penkin published a review and summary of his past work. In the case of iron, substantial changes were made in many of the *f*-values. Some of the values were changed by factors as large as five. The value for 3872.503 was not changed and is about 3 times as large as the six other values for that line in table 3. For conversion to the CB scale 3.70 was subtracted from the new values. The new values are compared with those of Corliss and Bozman in figure 2 and the converted values are listed in column 4 of table 2.

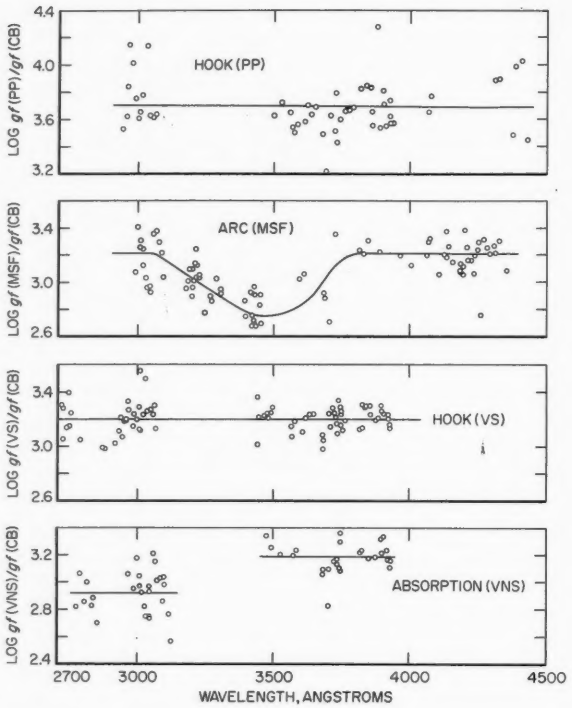

FIGURE 2. *Comparison of some Russian measurements of log* gf-*values with those from Corliss and Bozman [1962] in the wavelength range 2700 to 4500* Å.

c. Morosova, Startsev, and Frish [1962]

Using a free burning arc in air, Morosova, Startsev, and Frish have measured oscillator strengths for Fe I, 117 of which are for lines below 4150 Å. By studying the self-absorption in the arc, they found that they could measure the intensities of lines arising from the low levels that lie above the a^5F level if they used an iron anode, a copper cathode and a current of 1.2 A. By comparison of their intensities with those of Crosswhite [1950], they determined a temperature of 4500 °K for their arc. They carried out their photographic photometry with a tungsten lamp, the crater of a carbon arc, and the calibrated continuum from a krypton lamp. A plot of the ratio of their values to those of Corliss and Bozman, in figure 2, shows that their values are too small in the region from 3100 to 3700 Å. An appropriate correction taken from figure 2 was applied and their values tabulated in table 2 under the heading MSF.

d. Valters, Nikonova, and Startsev [1964]

Measuring the equivalent widths of lines absorbed by iron vapor in a furnace, Valters, Nikonova, and Startsev determined oscillator strengths for 28 lines in the region 2750 to 3150 Å and 28 lines in the region 3450 to 3950 Å. They took special precautions to filter out scattered light from longer wavelengths in their spectrograph. Nevertheless, a plot of the ratio

of their values to those of Corliss and Bozman in figure 2 shows that the values for their short wavelength group are too small, as would be the case if extraneous radiation were superimposed on the absorption lines. From this plot their values have been corrected and adjusted to the CB scale. The corrected values are entered in table 2 under the heading VNS.

e. Valters and Startsev [1964]

Valters and Startsev determined oscillator strengths for 89 lines of Fe I with lower levels a^5F and a^5D from the anomalous dispersion of iron vapor in a furnace. The results cover the same wavelength range as the absorption results of Valters, Nikonova, and Startsev, but a plot of the ratio of their values to those of Corliss and Bozman in figure 2 does not show any dependence on wavelength. This result would be expected because of the nature of the anomalous dispersion method and indeed was also noted in the case of Penkin's results. Valters and Startsev's values have been adjusted to the scale of Corliss and Bozman by subtracting 3.20 and then entered into table 2 under the heading VS.

Figure 2 shows how systematic errors of measurement can seriously override random errors in oscillator strength work.

2.3. Data of Crosswhite

For more than 20 years a program of intensity measurements in atomic and molecular spectra has been conducted at The Johns Hopkins University spectroscopy laboratory by the late Prof. G. H. Dieke. Many of the measurements, particularly those in the spectrum of iron, were made by Dr. H. M. Crosswhite. In 1950 Crosswhite published the results of his intensity measurements in a 2.2 A iron arc. These measurements, which include 1064 lines in the region from 3147 to 5659 Å, have been reduced to oscillator strengths by Corliss and Warner (1964).

In 1958 Crosswhite published a monograph on Fe I which included not only his measurements in the 2.2 A arc but also measurements made in a 1 A arc and in a hollow cathode. Some of these measurements have also been published in the American Institute of Physics Handbook, pp. 7–89 through 7–102. The observations from the 1 A arc are not as numerous as those from the other sources, nor are they any more accurate, so we have not attempted to derive oscillator strengths from them.

With the hollow cathode, however, he has measured more than 1000 lines in the region from 3200 to 4150 Å, about 400 between 2450 and 3200 Å and about 700 lines between 4150 and 8000 Å. Above 3150 Å Crosswhite made his sensitivity calibration with a standard tungsten ribbon-filament lamp calibrated at the National Bureau of Standards; between 2700 and 3100 Å he made an indirect calibration from a study of self-absorption and below 2700 Å he extrapolated. A plot of the ratio of the hollow cathode intensities to those from Meggers, Corliss, and Scribner [1961] shows that, with the exception of a discontinuity at 3730 Å, the ratio is constant from 3200 to 8400 Å. Below 3200 Å the ratio becomes very irregular and the scatter increases. The discontinuity at 3730 Å amounts to 0.35 in the log, which is the same as that found by Corliss and Warner in Crosswhite's 2.2 A arc data. Figure 3 shows the plot in the region 3000 to 4250 Å for lines whose upper levels lie between 46 and 53 kK (kilokaysers). Comparison with the similar plots for the hook method data, which should be free of wavelength dependent errors, indicates that the discontinuity must lie in Crosswhite's intensities. We corrected the discontinuity before further discussion of the data.

Crosswhite's iron hollow cathode tube was filled with neon to a pressure of 3.5 mm Hg and operated at 90 mA. The strong lines were measured photoelectrically. "The much larger group of weaker lines is more conveniently measured photographically. Although the intensity range encountered with the photoelectric measurements was almost 10000:1, the photographic one is much less and can be encompassed by the use of a few neutral screens, with reference being made to the photoelectric values for purposes of plate calibration and standardization." Crosswhite [1958] goes on to say, "In spite of difficulties it appears that, at least within a given multiplet, transition probability determinations are possible. Comparison between different multiplets is more cumbersome than in an equilibrium case, but not impossible. It certainly seems worthwhile to make some effort to utilize the great stability of the intensities which are reproducible to better than 1 percent for a particular experimental arrangement."

It does indeed seem worth an effort to derive oscillator strengths from Crosswhite's measurements of hollow cathode intensities. To carry out this reduction, it is first necessary to determine the relative occupation numbers of the upper energy level of each measured transition. In an equilibrium source these numbers are determined by measuring the temperature of the source and calculating the occupation numbers with Boltzmann's exponential law. At pressures as low as 3.5 mm Hg it is generally thought that a source is no longer in LTE and that the population distribution can no longer be described as simply

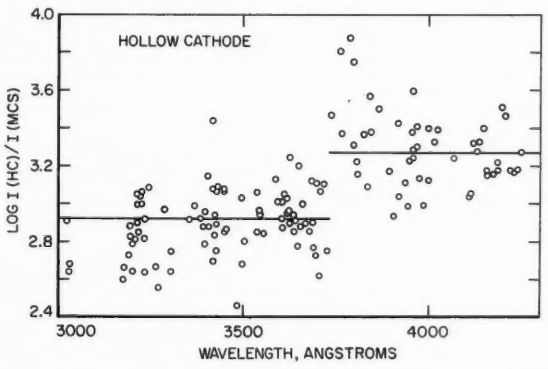

FIGURE 3. *Comparison of the intensity measurements of Crosswhite [1958] in the hollow cathode with those of Meggers, Corliss, and Scribner [1961] in a copper arc for lines of* Fe I *whose upper levels lie between 46 and 53 kK; wavelength range 3000 to 4500 Å.*

exponential. To test this assumption we calculated the relative occupation number of each upper level for a selected group of lines in Crosswhite's hollow cathode list. These are the lines between 3200 and 9000 Å for which transition probabilities are listed in Corliss and Bozman. To calculate the relative occupation numbers of the upper levels of the iron atoms in Crosswhite's hollow cathode we recall that

$$I = h\nu N_n A_{nm}, \text{ so that } I\lambda/A_{nm} \sim N_n$$

or

$$\frac{I\lambda}{g_n A_{nm}} \sim \frac{N_n}{g_n}. \tag{1}$$

Boltzmann's exponential law states that

$$\frac{N_n}{g_n} = \frac{N_0}{g_0} e^{-E/kT}$$

where the subscript 0 refers to the ground state. Now if we plot log $I\lambda/gA$ (or its reciprocal) versus E, the value of the upper energy level, we will see graphically the population distribution amongst the levels of the atom. In figure 4 we have plotted log $gA/I\lambda$ for every line between 3200 and 9000 Å which appears in both Corliss and Bozman (from which the values of gA are taken) and Crosswhite's hollow cathode list (from which the values of I are taken). In most cases each point represents the mean value for 2 to 4 lines. Figure 4 represents the population distribution amongst energy levels of iron atoms in Crosswhite's hollow cathode for every upper level listed in Corliss and Bozman. The dashed line represents an equilibrium distribution at a temperature of 4560 °K. The departures of the individual points from an equilibrium line seem to support an abandonment of the notion of LTE

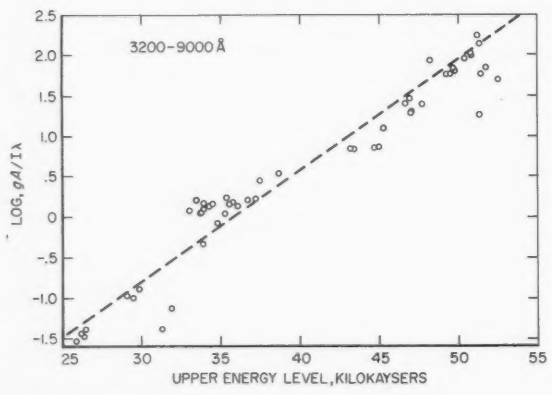

FIGURE 4. *Population distribution (reciprocal) amongst energy levels of iron atoms in Crosswhite's [1958] hollow cathode for every upper level listed in Corliss and Bozman [1962].*

for the most accurate reduction of Crosswhite's hollow cathode intensity measurements to oscillator strengths.

The data shown in figure 4 permit determination of occupation numbers for the iron atoms in the hollow cathode for only about 50 upper energy levels. To obtain a more complete specification of the population distribution, we repeated the process using the oscillator strengths for 2000 lines of Fe I given by Corliss and Warner. This allowed us to find occupation numbers for 323 levels with an average number of determinations per level of about 4. With the value of N/g for each of these levels known, we calculated log gf from each value of hollow cathode intensity using the formula log gf = log I_{hc} + 3 log λ − log N/g − 15.82, where the value of the numerical constant depends on the scale of I. This determination makes no assumption about the population distribution among the upper levels of the iron atoms in the hollow cathode discharge. The values derived are entered in column 9 of the table 3 under the heading HC.

Inspection of table 3 reveals that a number of values of log gf derived from the hollow cathode intensities are in rather wide disagreement with the other tabulated values. We used the values of log I_2 from table XIII of Crosswhite [1958] to derive the values of log gf. Comparison of these log I_2 values with those given in the American Institute of Physics Handbook and with the photoelectric traces of hollow cathode spectra reproduced in both publications indicates that a number of these discrepant values are certainly due to misprints. For this reason, discrepant hollow cathode values have been freely ignored in arriving at the "best" values given in table 3.

2.4. Data of Corliss and Bozman

In 1963 Corliss and Bozman published NBS Monograph 53, "Experimental Transition Probabilities for Spectral Lines of Seventy Elements," which is derived from the intensity measurements of Meggers, Corliss, and Scribner [1961]. They reported 663 oscillator strengths for Fe I of which about 450 lie below 4150 Å. For a number of reasons their scale is suitable to use in a compilation such as ours. The number of values reported is so large that there are numerous lines in common with every published list. This simplifies the problem of putting all measurements onto a common scale. Their absolute scale has been shown by Allen and Corliss [1963] to be reasonably accurate for all the neutral atoms in the iron group. They concluded that the CB scale may be high by 0.05 in log gf, on the average. We discuss the accuracy of the CB absolute scale for Fe I in particular in section 5 of this paper. The temperature of their light source was determined with an accuracy of ±2 percent. The precision of their measurements, while not high, is accurately known and compares well with that of most other published sets of data for Fe I. The comparisons shown in figure 2 indicate that the intensity scale of Meggers, Corliss, and Scribner is correctly calibrated as a function of wavelength from 2700 to 4500 Å.

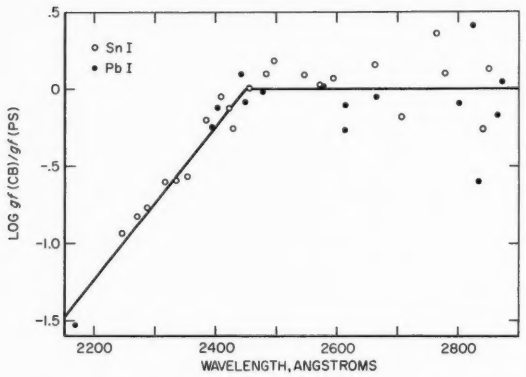

FIGURE 5. *Ratio of the* gf*-values of Corliss and Bozman [1962] to those of Penkin and Slavenas [1963] (normalized to unity above 2450 Å) between 2150 and 3000 Å.*

However, the intensity scale of Meggers, Corliss, and Scribner is subject to a serious systematic error below 2500 Å, where it becomes progressively too small. The origin of this error lies in the notorious lack of any reliable energy calibration procedure for short wavelengths. Soon after the publication of NBS Monograph 53, Penkin and Slavenas [1963] published oscillator strengths for lines of tin and lead which extended down to 2170 Å. They used the hook method, which does not require an intensity calibration of any sort. A plot of the ratio of their values to those of Corliss and Bozman (normalized to unity between 2450 and 3000 Å) is shown in figure 5. The figure shows that the ratio is constant between 2450 and 3000 Å but that the CB scale declines by a factor of 30 between 2450 and 2150 Å. This correction has been applied to the CB values reported in column 8 of table 3.

There are some independent data below 2500 Å that support the correction derived from the work of Penkin and Slavenas. The relative oscillator strengths for Co II calculated by Gruzdev [1962] with the method of intermediate coupling give rise to a correction curve in substantial agreement with that of figure 5. We have, however, preferred to base our calibration on experimental values. Measurement of intensities of Sn I lines in chemiluminescent flames led Gilbert [1963] to the conclusion that the values of Meggers, Corliss, and Scribner [1961] decreased by a factor of 50 between 2500 and 2100 Å. This agrees with our adopted correction.

2.5. Data of Margoshes and Scribner

Margoshes and Scribner [1963] determined relative oscillator strengths for 105 lines of Fe I between 2900 and 4150 Å using a gas stabilized arc (a form of plasma jet) as an emission source. All of these lines had been measured previously, but by other methods. Figure 5 in their paper shows the ratio of their *gf*-values to those of Corliss and Bozman. There appears to be a slight trend of the ratio with wavelength which hardly exceeds the uncertainty of the measurements and we have made no correction. The absolute value of their scale has been altered by adding 0.23 to their values of log *gf*, thereby putting their measurements onto the common scale of table 3. Their values are listed in column 12 under MS.

2.6. Data of Corliss and Warner

In 1964 Corliss and Warner published a compilation of oscillator strengths for Fe I that emphasized the visible and infrared regions of the spectrum. In addition to their own measurements in the visible and infrared, they included all data published prior to 1963, with the exception of Sobolev [1943] and Parchevsky and Penkin [1954] which were not available to them, and the hollow cathode data of Crosswhite [1958] (v. sec. 2.3). These data included King and King [1938], Carter [1949], Crosswhite [1950], Allen and Asaad [1957], and Corliss and Bozman [1962] longward of 3100 Å. The values of Mitrofanova [1952]; Aarts, Harting, and Bakker [1954]; and Hefferlin [1959] were discussed but not incorporated into their "best" value.

The "best" value of Corliss and Warner is entered in column 8 under CW. As in the tabulation of the Russians' measurements, a superscript following the value indicates the number of entries contributing to their "best" value and is used as a weighting factor in arriving at the "best" value in column 13. The CW values include and supersede those of Corliss and Bozman at wavelengths above 3100 Å. Since the CW values end at 3100 Å, the CB values are tabulated in the same column at shorter wavelengths.

2.7. Data of King, Olsen, and Corliss

In 1965 King, Olsen, and Corliss published oscillator strengths for 300 Fe I lines between 2500 and 3200 Å. They were calculated from the equivalent widths of lines absorbed from the continuum of a high pressure Xenon lamp when its radiation was passed through iron vapor in a graphite-tube electric furnace. Scattered light was controlled with a Corex red-purple filter. To avoid the flat portion of the curve-of-growth in the reduction of the data, only the faintest lines in each exposure were measured. Since the lines observed cover a very large range of intensities, a great many spectrograms would be required to put all of the lines on the same scale of intensity. Although 86 separate exposures were made, it was nevertheless necessary to tie some of them together with supplementary data. For this purpose the oscillator strengths of Corliss and Bozman were used. This procedure should not introduce any wavelength dependent error or energy level dependent error, even if such an error were present in the CB data. The only error which could be introduced from the supplementary data would be an

intensity dependent error. Such an error is most unlikely.

In figure 6 is plotted the ratio of oscillator strengths from KOC to those from CB as a function of upper energy level in kilokaysers. With the exception of two points at about 60 kK, there is only a very slight dependence of ratio on upper energy level. Qualitatively, this dependence is in the sense that the KOC temperature scale is slightly smaller than the CB scale which is in accord with results found earlier by Corliss [1962]. The same ratio is plotted as a function of wavelength in figure 7. The ratio seems to be independent of wavelength, with the possible exception of the region from 3100 to 3200 Å. The remarkable departure of the two high level lines at 2542 and 2543 Å from the general trend of the plots is unexplained. The values from this paper are entered in column 11 of table 3 under KOC.

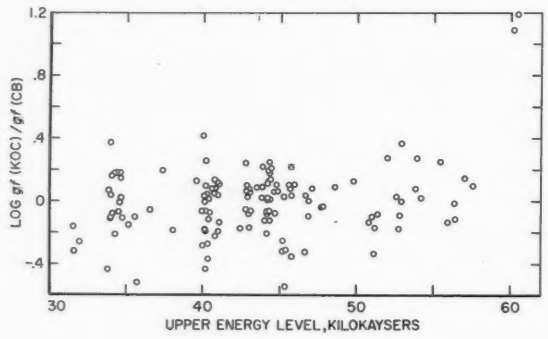

FIGURE 6. *Ratio of gf-values from King, Olsen, and Corliss [1965] to those from Corliss and Bozman [1962] as a function of upper energy level.*

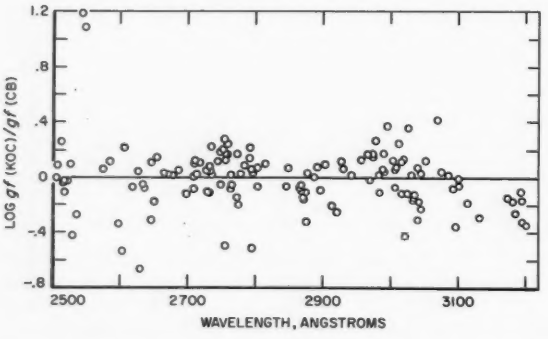

FIGURE 7. *Ratio of gf-values from King, Olsen, and Corliss [1965] to those from Corliss and Bozman [1962] as a function of wavelength; 2500 to 3200 Å.*

3. New Observations

3.1. Data of Warner From ULO

In the region from 2500 to 4150 Å, new observations have been made at the University of London Observatory using both free-burning arcs and sparks. A d-c arc was maintained between two 5 mm diam iron rods. These electrodes were obtained from Messrs. Johnson Matthey and Co. and contain only one or two parts per million of spectroscopically conspicuous impurities. A current of 1 A was drawn from a constant-current source. Such a small current, although necessitating longer exposure times than is usual, has the advantage of considerably reducing the amount of self absorption in strong lines.

The spark source, operated at 10,000 V, was produced between pure iron electrodes in an argon atmosphere at normal pressure. The average current was 1.3 A, which caused the electrodes to glow white hot as in a normal arc. This resulted in a very stable, nonwandering spark. The argon atmosphere removed troublesome O II, N II, O_2^+, and N_2^+ emissions that occur in a spark in air. A few Ar I and Ar II lines are observed. The argon atmosphere also reduced the self-absorption in strong lines to almost negligible amounts. A disadvantage of the spark was that exposure times up to 75 hr were necessary to record the spectral region below 3000 Å. Also, in this region Fe II lines interfered with many neutral lines.

The light from the sources was imaged by means of two quartz lenses onto the grating of the stigmatic Ebert spectrograph in the laboratory of the University of London Observatory. This spectrograph of 3.4 m focal length, has a 15000 lines per inch grating giving a dispersion of 4.75 Å/mm in the first order. A total wavelength region of 2400 Å can be recorded in one exposure. Ilford HP3 plates were used throughout the present investigation. These were brushed continuously during development.

On all plates a spectrum of the iron arc through a calibrated step wedge (placed at the spectrograph slit) was obtained. All arc and spark spectra were traced with the recording microphotometer at the Royal Greenwich Observatory. From the step wedge spectra, photographic calibration curves were drawn for each plate. Line and continuum readings from the charts were converted into intensities with the aid of these characteristic curves. The continuum intensity was subtracted from the apparent line intensity to give the true line intensity.

In general at least three independent intensity measurements were made on each line. Over most of the intensity range the plate-to-plate interagreement of line intensities when placed on a uniform scale, was ~ 0.03 dex. (± 7%). In the arc spectra all strong lines were rejected to avoid effects of self-reversal.

Our intensity measurements in a range of 200 Å near 4100 Å were compared with the Fe I *f*-values given by Corliss and Warner in the manner described by Corliss and Warner and the excitation temperatures

for the two sources derived. For the 1 A d-c arc a value of 4630 ± 70 °K was found. In figure 8 we show the graph from which the excitation temperature of the spark was determined. It can be seen that for upper energy levels where $E < 48$ kK the population of levels in our spark source is closely Boltzmannian. The derived temperature is 6170 ± 30 °K. The departure from linearity in figure 8 for $E > 48$ kK is a reflection of the normalization function applied to the Corliss and Warner f-values, and will be discussed later.

With the above determined excitation temperatures we can calculate from the CB (and CW) Fe I f-values, a theoretical line intensity for all lines in common with the present work (with $E < 48$ kK):

$$\log I_{CB}\lambda^3 = \log gf_{CB} - \frac{625E}{T_{ex}}$$

where E is in kK. We then plot $\log I_{CB}\lambda^3 - \log I_W$ as a function of λ. This gives the wavelength calibration for the plate (i.e., determines the combined effects of plate sensitivity and spectrograph transmission) and at the same time takes care of the λ^3 factor. Using this graph we correct all intensities measured in the present work and obtain values of $\log I_W\lambda^3$ on an arbitrary scale. Relative gf values for all lines were then calculated from

$$\log gf_{rel} = \log I_W\lambda^3 + \frac{625E}{T_{ex}}.$$

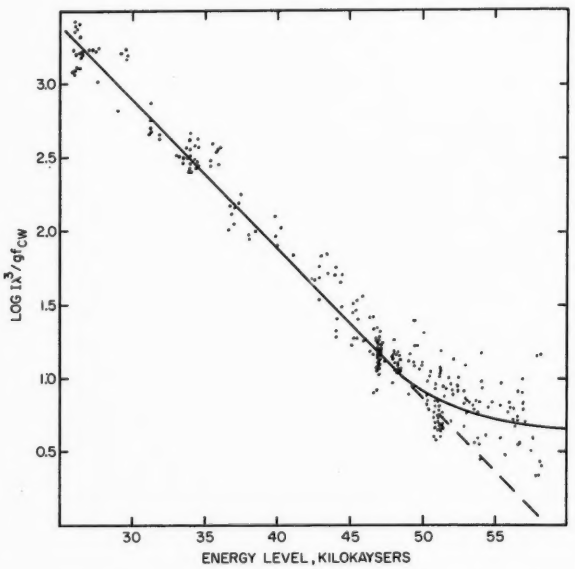

FIGURE 8. *Log ratio of intensity* $\times \lambda^3$ *to gf-value of Corliss and Warner [1964] for* Fe I *lines in the iron spark plotted versus upper energy level.*

These relative values were corrected for departure from a Boltzmann distribution and adjusted to the absolute scale by plotting this $\log gf_{rel} - \log gf_{CB \text{ or } CW}$ versus E for lines in common with CB or CW and applying the indicated correction to every line. The values are listed in columns 6 and 7 of table 3.

3.2. Data of Corliss From NBS

In the region below 2500 Å a new set of observations has been made at the National Bureau of Standards and is reported in column 1 of table 3. Since this region is densely populated with lines of the first and second spectrum of iron, observations were made in the third order of a 30000 lines per inch grating mounted in parallel light. The second order was eliminated with a chlorine filter. A step sector wheel with sector openings in the ratio of two was mounted at the slit and reduced the intensity by that ratio in eight successive steps along the length of the slit image. An achromatic lens at the slit formed an image of the light source on the grating and permitted uniform illumination of the slit (in the absence of the sector wheel).

The light source was a 1 A arc between a 7/32 in. diam rod of commercially pure iron as the lower anode and a pointed 3/8 in. graphite upper cathode. Exposure times were about an hour on Kodak 103a-0 plates. Three sets of plates were measured.

The intensities were estimated by visual interpolation between steps in the sectored spectrograms. With these intensities and gf-values from Corliss and Bozman for the range 2450 to 2540 Å, a plot of log $I\lambda^3/gf$ versus upper energy level was prepared. From this plot preliminary values of log gf for all the measured lines were calculated. Finally, a correction to be applied to all of these values below 2450 Å was prepared by plotting the ratio of these preliminary values to the corrected CB values from column 8 of table 3. After correction, the new values were entered in column 6 of table 3. To make certain that the new values were not affected by self-absorption, the ratio of the new values to those in column 8 were plotted versus the corresponding intensity from Meggers, Corliss, and Scribner for lines between 2450 and 2540 Å. A horizontal plot showed that at 1 A these lines were not self-absorbed.

4. Results

The results of the compilations and measurements discussed in sections 2 and 3 are presented in table 3. The wavelengths are taken in order of preference from Edlén [1955]; from Russell and Moore [1944]; from Kiess, Rubin, and Moore [1961]; or, in a few cases, are calculated from the term combinations. The classifications are taken from the same papers and the numerical values of the energy levels are given to the nearest kayser in columns 2 and 3. The lower excitation potential in electron volts has been calculated by multiplying the lower energy level in column 2 by 0.00012398 and the result, rounded off

to two decimal places, is entered in column 4. The multiplet numbers in column 5 are those assigned by Moore [1945, 1952] in her Multiplet Tables.

The recommended or "best" value of log gf given in column 13 is, in general, the unweighted mean of the individual values of log gf in the previous seven columns. However the CW and R values have been weighted according to the number of contributing values in Corliss and Warner or in table 2 and the weighting number is indicated as a superscript. In a few cases, where there was good reason, individual values were given a weight of zero. If the maximum and minimum values for any line differ by more than 0.4, no best value is recommended unless there is a value obviously discrepant.

Log $gf\lambda$ and log gA/λ have been computed from the best value and are given in the last two columns. Log $gf\lambda$ is useful in dealing with curves of growth in absorption spectra and stellar spectra and log gA/λ in determining temperatures from intensity measurements in emission spectra. It should be noted also that the line strength, S, is equal to $gf\lambda/304$, or $\log S = \log gf\lambda - 2.48$.

5. Discussion of the Absolute Scale

In this section we discuss the various attempts to make absolute determinations of oscillator strengths for lines of Fe I and try to decide if a scale more accurate than that used in this paper can be recommended.

A number of determinations of the oscillator strength of the resonance line of Fe I at 3719.937 Å by various atomic beam experiments have been reported over the past 15 years. They are listed below, with the value of log gf.

Kopfermann and Wessel [1951].....	−0.41
Ziock [1957].....	−0.38
Bell, Davis, King, and Routly [1958]...	−0.54
Ottinger and Ziock [1961].....	−0.50

The mean value here is −0.46, which is 0.14 less than the value reported for that line in our table.

In 1942, R. B. King made absolute determinations of the oscillator strengths of 12 lines of Fe I between 3700 and 3900 Å by measuring the total absorption in a furnace. Bell, Davis, King, and Routly [1958] revised those values on the basis of new vapor pressure data. The revised values for these 12 lines are on a scale of log gf which is 0.25 less than that of our table.

In their work on the abundances of the elements in the solar atmosphere, Goldberg, Müller, and Aller [1960] calculated absolute values of log gf for Fe I lines of the $3d^74s - 3d^74p$ transition array from the f-sum rule, assuming $f_T = 1.0$ The array has 45 lines in the range 3585 to 4150 Å. This f-sum scale is 0.06 less than the scale of our table.

With a somewhat different formulation of the f-sum rule, assuming $f_T = 0.7$, Allen [1960] adjusted a large number of relative oscillator strengths for Fe I to an absolute scale. A comparison of that scale with the scale of Corliss and Bozman made by Allen and Corliss [1963] leads to the conclusion that Allen's f-sum scale is 0.20 less than our present scale.

In an interesting experiment reported to the Aeronautical Systems Division, AFSC in 1965, Karstensen and Richter of the University of Kiel measured the lifetimes of the z^3F_4 and z^3D_1 levels in Fe I. They also calculated them from the oscillator strengths of Corliss and Warner [1964] which are reported on the present scale. The lifetimes in nanoseconds are quoted below from their report.

	z^3F_4	z^3D_1
Karstensen and Richter.....	220 ± 70	100 ± 25
Corliss and Warner.....	240 ± 120	80 ± 40

There does not appear to be any significant difference between the two sets of determinations.

Paul L. Byard [1966] of the Ohio State University Department of Astronomy has been making oscillator strength measurements in Fe I using a luminous shock tube. Preliminary results obtained for a group of lines in the red part of the spectrum show agreement with the values of Corliss and Bozman within the experimental uncertainties.

From a discussion such as this we cannot hope to arrive at an exact correction to be applied to our scale. It is obvious that the absolute scale is still somewhat uncertain. The mean correction obtained from the six determinations mentioned above is −0.11 with a standard deviation of this mean amounting to 0.04. At the present time therefore, it would seem that the scale used in this paper is high by about 0.1 in log gf. In order to keep the scale in this paper uniform with that of our previous work in the visible and infrared parts of the spectrum, we have not applied the correction here. Furthermore, there is little doubt that this figure is subject to some change as more data on the absolute scale of oscillator strengths for Fe I is accumulated.

6. Conclusion

In this paper numerous oscillator strength measurements, both new and old, for 2000 lines of Fe I have been assembled, adjusted to the same scale, and best values for most of the lines suggested. The scale on which they are presented is the same as that used by Corliss and Bozman [1962] for Fe I and by Corliss and Warner [1964]. The values in this paper supersede the values below 4151 Å in Corliss and Warner [1964] and, together with the remaining 1349 lines in that paper, provide a total of 3349 lines of Fe I for which more or less accurate values of oscillator strengths are known. These are more than three-quarters of the classified lines of Fe I which have been observed in the laboratory.

The accuracy of the best values of log gf in table 3, taken as relative values, will vary greatly from line to line, depending on the number and origin of the obser-

vations contributing to it. The standard deviation of the new observations should be about the same as those of Corliss and Warner [1964] which were stated to be about 0.13. Graphical representation of the overall scatter encountered in the construction of curves of growth with those values are given by Bell and Rodgers [1965] for stellar atmospheres and for the solar atmosphere by Goldberg, Kopp, and Dupree [1964]; by Warner [1964]; and by Aller, O'Mara, and Little [1964].

The absolute scale on which these values is reported appears to be about 25 percent higher than the best absolute scale for Fe I that can be established at present. The uncertainty in the best absolute scale, on the basis of the consistency amongst the various sets of determinations considered above seems to be about 11 percent (standard deviation of the mean for six sets). Therefore, for work requiring the best present estimate of the absolute scale, we suggest subtracting 0.10 from our reported values of log *gf*. Improved knowledge of this correction can be expected in the near future.

Warner thanks the Astronomer Royal for the use of the recording microphotometer at the Royal Greenwich Observatory. He is also grateful to E. L. G. Bowell and K. J. H. Phillips for carrying out some of the numerical work. He was supported by a Research Grant from the Department of Scientific and Industrial Research. We also thank Ruth Peterson for her conscientious work in making the tables and putting them on punched cards, and W. R. Bozman who wrote a program for computing several quantities in the tables.

7. References

Aarts, J., Harting, D., and Bakker, C. J. (1954), Physica **20,** 1250.
Allen, C. W. (1960), Monthly Notices Roy. Astron. Soc. **121,** 299.
Allen, C. W. and Asaad, A. S. (1957), Monthly Notices Roy. Astron. Soc. **117,** 36.
Allen, C. W. and Corliss C. H. (1963), Monthly Notices Roy. Astron. Soc. **126,** 37.
Aller, L. H., O'Mara, B. J., and Little, S. J. (1964), Proc. Nat. Acad. Sci. **51,** 1238.
American Institute of Physics Handbook (McGraw-Hill Book Company, Inc., New York, 1957).
Bell, G. D., Davis, M. H., King, R. B., and Routly, P. M. (1958), Ap. J. **127,** 775.
Bell, R. A. and Rodgers, A. W. (1965), Monthly Notices Roy. Astron. Soc. **129,** 127.
Byard, P. L. (1966) (private communication).
Carter, W. W. (1949), Phys. Rev. **76,** 962.
Corliss, C. H. (1962), J. Res. NBS **66A** (Phys. and Chem.) No. 1, 5.
Corliss, C. H. and Bozman, W. R. (1962), Experimental transition probabilities for spectral lines of seventy elements, NBS Mono. No. 53 [Washington: Government Printing Office].
Corliss, C. H. and Warner, B. (1964), Ap. J. Supplement Series **8,** 395, No. 83.
Crosswhite, H. M. (1950), Spectrochimica Acta **4,** 122.
Crosswhite, H. M. (1958), The Spectrum of Iron I, Johns Hopkins Spectroscopic Report No. 13, Baltimore.
Edlén B. (1955), Trans. I. A. U. **9,** 220.
Gilbert, P. T. (1963), Proc. of the Xth Colloq. Spectros. Internat. p. 207.
Goldberg, L., Kopp, R. A., and Dupree, A. K. (1964), Ap. J. **140,** 707.
Goldberg, L., Müller, E. A., and Aller, L. H. (1960), Ap. J. Suppl. Series No. **45,** 87.
Gottschalk, W. M. (1948), Ap. J. **108,** 326.
Gruzdev, P. F. (1962), Opt. Spectry, **13,** 169.
Hefferlin, R. (1959), J. Opt. Soc. Am. **49,** 680, 948.
Kartensen, F. and Richter, J. (1965), New Method of Measuring Transition Probabilities, AF EOAR Grant 63–110.
Kiess, C. C., Rubin, V. C., and Moore, C. E. (1961), J. Res. NBS **65A** (Phys. and Chem.) No. 1, 1.
King, R. B. (1942), Ap. J. **87,** 24.
King, R. B. and King, A. S. (1938), Ap. J. **87,** 24.
King, R. B., Olsen, K. H., and Corliss, C. H. (1965), Ap. J. **141,** 354.
Koperfmann, H. and Wessel, G. (1951), Zeits. f. Physik **130,** 100.
Margoshes, M. and Scribner, B. F. (1963), J. Res. NBS **67A** (Phys. and Chem.) No. 6, 561.
Meggers, W. F., Corliss, C. H., and Scribner, B. J. (1961), Tables of Spectral-line intensities, NBS Mono. No. 32 [Washington: Government Printing Office].
Mitrofanova, L. A. (1952), Izv. Astro. Obs. Pulkovo **19,** 81.
Moore, C. E. (1945), A Multiplet Table of Astrophysical Interest, Contr. Princeton Univ. Obs. No. 20.
Moore, C. E. (1952), An ultraviolet multiplet table, NBS Circ. 488, Sec. 2.
Morzova, N. G., Startsev, G. P., and Frish, M. S. (1960), Physical Problems in Spectroscopy. Proc. of the XIIIth All-Union Conf. on Spectroscopy, Leningrad, 4–12 July 1960. Vol. **1,** p. 45, Moscow, 1962.
Ottinger, C. and Ziock, K. (1961), Zeits, Naturforsch **16a,** 720.
Parchevskii, G. F. and Penkin, N. P. [1954], Vestnik Leningrad State University **11,** 113. Translated by J. Tech. in Astron. Papers Trans. from the Russian, No. II, (1964), Smithsonian Astrophys. Obs., Cambridge, Mass.
Penkin, N. P. (1964), J. Quant. Spectros, Radiative Transfer **4,** 41. Translated by J. Tech. in Astron. Papers Trans. from the Russian, No. II (1964), Smithsonian Astrophys. Obs., Cambridge, Mass.
Penkin, N. P. and Slavenas, I. Y. Y. (1963), Opt. Spectry. **15,** 83.
Prokofiev, V. K., Nikonova, E. I. Gruzdev, F. P., and Frish, M. S. (1964), Bull. Crimean Astrophys. Obs. **31,** 281.
Russell, H. N. and Moore, C. E. (1944), Trans. Am. Phil. Soc. **34,** (Part II) p. 113.
Shore, B. W. (1965), Ap. J. **142,** 94.
Sobolev, N. N. (1943), J. Experimental and Theoretical Physics **13,** 131.
Valters, A. K. Nikonova, E. I., and Startsev, G. P. (1964), Opt. Spectry. **16,** 393 (English transl.).
Valters, A. K., and Startsev, G. P. (1964), Opt. Spectry. **17,** 262 (English transl.).
van Milaan, J. B. (1926), Zeits. f. Physik **38,** 422.
Warner, B. (1964), Monthly Notices Roy. Astron. Soc. **127,** 413.
Warner, B. (1966), Memoirs Roy. Astron. Soc. (in press).
Ziock, K. (1957), Zeits. f. Physik **147,** 99.

TABLE 3.—*Oscillator Strengths for Ultraviolet Lines of Fe* I

Wavelength Å	Energy Levels K	Low e.p. Volts	Mult. No.	Arc	Spk	CB	HC	R(N)	KOC	MS	Best	Log gfλ	Log gA/λ
				Log *gf*									
2084.122	0–47967	0.00	UV 33			1.16					1.16	4.48	7.03
2157.795	416–46745	0.05	UV 24	0.90							0.90	4.23	6.72
2164.550	704–46889	0.09	UV 24	0.56							0.56	3.90	6.38
2166.769	0–46137	0.00	UV 21	1.12		1.18					1.15	4.49	6.97
2171.298	704–46745	0.09	UV 24	0.25							0.25	3.59	6.06
2178.080	416–46314	0.05	UV 21	0.79		0.82					0.80	4.14	6.61
2178.120	704–46601	0.09	UV 22	0.45							0.45	3.79	6.26
2186.483	416–46137	0.05	UV 21	0.56							0.56	3.90	6.36
2186.893	888–46601	0.11	UV 22	−0.02							−0.02	3.32	5.78
2187.195	704–46410	0.09	UV 21	0.56							0.56	3.90	6.36
2191.836	704–46314	0.09	UV 21	0.53		0.45					0.49	3.83	6.29
2196.043	888–46410	0.11	UV 21	0.43		0.45					0.44	3.78	6.24
2200.370	978–46410	0.12	UV 21	0.34							0.34	3.68	6.14
2200.723	888–46314	0.11	UV 21	0.31							0.31	3.65	6.11
2248.858	6928–51381	0.86	UV 70	−0.50							−0.50	2.85	5.27
2250.791	0–44415	0.00	UV 16	−0.79							−0.79	2.56	4.98
2259.511	0–44244	0.00	UV 15	−0.40							−0.40	2.95	5.36
2264.389	6928–51077	0.86	UV 71	−0.11							−0.11	3.24	5.65
2265.055	416–44551	0.05	UV 16	−0.79							−0.79	2.57	4.97
2266.903	7728–51828	0.96	UV 70	−0.61							−0.61	2.75	5.15
2267.085	416–44512	0.05	UV 17	−0.65							−0.65	2.71	5.11
2267.465	6928–51017	0.86	UV 70	−0.08							−0.08	3.28	5.68
2269.099	704–44761	0.09	UV 16	−0.78							−0.78	2.58	4.98
2270.863	0–44023	0.00	UV 15	−1.19							−1.19	2.17	4.57
2271.781	7377–51381	0.91	UV 70	−0.35							−0.35	3.01	5.40
2272.070	416–44415	0.05	UV 16	−0.62							−0.62	2.74	5.13
2272.816	7377–51361	0.91	UV 71	−0.36							−0.36	3.00	5.39
2275.189	888–44827	0.11	UV 16	−1.08							−1.08	2.28	4.67
2276.026	0–43923	0.00	UV 14	−0.31							−0.31	3.05	5.44
2277.098	7728–51630	0.96	UV 71	−0.59							−0.59	2.77	5.16
2277.672	7728–51619	0.96	UV 70	−0.59							−0.59	2.77	5.16
2279.922	704–44551	0.09	UV 16	−0.41							−0.41	2.95	5.34
2280.222	7986–51828	0.99	UV 70	−0.28							−0.28	3.08	5.47
2283.304	978–44761	0.12	UV 16	−0.99							−0.99	2.37	4.76
2283.656	888–44664	0.11	UV 16	−0.97							−0.97	2.39	4.78
2284.086	416–44184	0.05	UV 14	−0.36							−0.36	3.00	5.39
2287.250	704–44411	0.09	UV 14	−0.26							−0.26	3.10	5.49
2289.032	8155–51828	1.01	UV 70	−0.41							−0.41	2.95	5.33
2290.546	7986–51630	0.99	UV 71	−0.35							−0.35	3.01	5.39
2291.122	7728–51361	0.96	UV 71	−0.26							−0.26	3.10	5.48
2292.525	416–44023	0.05	UV 15	−0.71							−0.71	2.65	5.03
2294.406	888–44459	0.11	UV 14	−0.58							−0.58	2.78	5.16
2296.928	888–44411	0.11	UV 14	−1.00							−1.00	2.36	4.74
2297.788	416–43923	0.05	UV 14	−0.26		−0.24					−0.25	3.11	5.49
2298.170	0–43500	0.00	UV 14	−0.16							−0.16	3.20	5.58
2298.657	888–44378	0.11	UV 15	−1.30							−1.30	2.06	4.44
2299.221	704–44184	0.09	UV 14	−0.56							−0.56	2.80	5.18
2300.140	704–44166	0.09	UV 15	−0.58							−0.58	2.78	5.16
2301.685	978–44411	0.12	UV 14	−0.82							−0.82	2.54	4.92
2303.422	978–44378	0.12	UV 15	−0.77							−0.77	2.59	4.97
2303.582	888–44285	0.11	UV 15	−0.68							−0.68	2.68	5.06
2309.000	888–44184	0.11	UV 14	−0.49							−0.49	2.87	5.24
2313.105	704–43923	0.09	UV 14	−0.32							−0.32	3.04	5.41
2320.358	416–43500	0.05	UV 14	−0.31							−0.31	3.06	5.42
2341.575	416–43109	0.05	UV 13	−1.42							−1.42	1.95	4.30
2350.408	0–42533	0.00	UV 11	−1.69							−1.69	1.68	4.02
2355.327	416–42860	0.05	UV 11	−1.33							−1.33	2.04	4.38
2356.196	7377–49805	0.91		−0.20							−0.20	3.17	5.51
2369.457	888–43079	0.11	UV 11	−1.36							−1.36	2.01	4.34
2371.431	704–42860	0.09	UV 11	−0.97							−0.97	2.41	4.73

TABLE 3.—*Oscillator Strengths for Ultraviolet Lines of Fe* I—Continued

Wavelength Å	Energy Levels K	Low e.p. Volts	Mult. No.	Arc	Spk	CB	HC	R(N)	KOC	MS	Best	Log gfλ	Log gA/λ
				Log *gf*									
2373.625	416–42533	0.05	UV 11	−0.63							−0.63	2.75	5.07
2374.519	978–43079	0.12	UV 11	−1.06							−1.06	2.32	4.64
2381.836	888–42860	0.11	UV 11	−0.88							−0.88	2.50	4.81
2389.973	704–42533	0.09	UV 11	−0.86							−0.86	2.52	4.83
2408.045	7728–49243	0.96	UV 68	−1.84							−1.84	1.54	3.84
2411.558	6928–48383	0.86		−1.11							−1.11	2.27	4.57
2429.810	8155–49298	1.01	UV 68	−1.40							−1.40	1.99	4.27
2433.056	8155–49243	1.01	UV 68	−0.78							−0.78	2.61	4.89
2438.183	6928–47930	0.86	UV 62	−0.52							−0.52	2.87	5.14
2439.630	11976–52954	1.48		−0.86							−0.86	2.53	4.80
2439.743	19390–60366	2.40	UV157	0.89		0.50					0.70	4.09	6.36
2440.106	19788–60758	2.45	UV157	0.48		0.37					0.42	3.81	6.08
2442.567	19621–60549	2.43	UV157	0.56		0.66					0.61	4.00	6.27
2443.873	6928–47835	0.86	UV 63	−0.37		−0.33					−0.35	3.04	5.31
2445.213	6928–47812	0.86	UV 63	−1.09							−1.09	2.30	4.57
2447.711	0–40842	0.00	UV 9	−1.08		−1.04					−1.06	2.33	4.60
2450.439	12561–53358	1.56		−0.84							−0.84	2.55	4.82
2451.384	12969–53749	1.61		−1.03							−1.03	2.36	4.63
2453.477	7377–48123	0.91	UV 62	−0.21		−0.24					−0.22	3.17	5.43
2453.568	19621–60366	2.43	UV157	−0.40							−0.40	2.99	5.25
2457.598	6928–47606	0.86	UV 62	0.30							0.30	3.69	5.95
2458.564	6928–47590	0.86	UV 59	−1.38							−1.38	2.01	4.27
2462.182	416–41018	0.05	UV 9	−0.72							−0.72	2.67	4.93
2462.648	0–40594	0.00	UV 9	−0.26							−0.26	3.13	5.39
2463.728	7728–48305	0.96	UV 65	−0.53							−0.53	2.86	5.12
2465.150	7377–47930	0.91	UV 62	0.19							0.19	3.58	5.84
2467.733	7728–48239	0.96	UV 62	−0.48							−0.48	2.91	5.17
2468.880	6928–47420	0.86	UV 59	0.20							0.20	3.59	5.85
2470.961	7377–47834	0.91	UV 63	−0.70							−0.70	2.69	4.95
2472.343	6928–47363	0.86	UV 59	0.00		0.06					0.03	3.42	5.67
2472.896	416–40842	0.05	UV 9	−0.06		0.14					0.04	3.43	5.68
2473.156	0–40422	0.00	UV 8	−0.98							−0.98	2.41	4.66
2474.815	7728–48123	0.96	UV 62	0.23		0.33					0.28	3.67	5.92
2476.654	7986–48351	0.99	UV 62	−0.38							−0.38	3.01	5.26
2476.861	8155–48516	1.01	UV 65	−1.37							−1.37	2.02	4.27
2479.481	7986–48305	0.99	UV 65	−0.27		−0.15					−0.21	3.18	5.43
2479.777	704–41018	0.09	UV 9	0.00		0.14					0.07	3.46	5.71
2483.272	0–40257	0.00	UV 9			0.49					0.49	3.89	6.13
2483.531	7986–48239	0.99	UV 62	−0.18							−0.18	3.22	5.46
2484.186	888–41131	0.11	UV 9	−0.02		0.11					0.05	3.45	5.69
2484.530	11976–52213	1.48		−0.92							−0.92	2.48	4.72
2485.989	7377–47590	0.91	UV 59	−0.74							−0.74	2.66	4.90
2486.372	0–40207	0.00	UV 8			−1.00					−1.00	2.40	4.64
2486.690	7728–47930	0.96	UV 62	−0.15		−0.18					−0.16	3.24	5.48
2487.064	8155–48351	1.01	UV 62	−0.02		−0.03					−0.02	3.38	5.62
2487.370	704–40895	0.09	UV 10	−1.28		−1.33					−1.30	2.10	4.34
2488.144	416–40594	0.05	UV 9			0.51					0.51	3.91	6.15
2488.942	20641–60807	2.56	UV164	0.06							0.06	3.46	5.70
2489.751	978–41131	0.12	UV 9	0.07		0.41					0.24	3.64	5.88
2489.917	8155–48305	1.01	UV 65	−0.25							−0.25	3.15	5.39
2490.645	704–40842	0.09	UV 9			0.38					0.38	3.78	6.01
2491.156	888–41018	0.11	UV 9	0.16		0.29					0.22	3.62	5.85
2491.983	20641–60758	2.56	UV163	−0.02							−0.02	3.38	5.61
2492.640	7728–47834	0.96	UV 63	−1.06							−1.06	2.34	4.57
2493.998	7728–47812	0.96	UV 63	−0.55							−0.55	2.85	5.08
2494.252	6928–47008	0.86	UV 57	−1.06							−1.06	2.34	4.57
2495.869	6928–46982	0.86	UV 57	−0.55							−0.55	2.85	5.08
2496.534	7377–47420	0.91	UV 59	0.17		0.08					0.12	3.52	5.75
2501.133	0–39970	0.00	UV 7	−0.06	−0.11	−0.02					−0.06	3.34	5.57
2501.695	6928–46889	0.86	UV 56	−0.66	−0.57	−0.58			−0.58		−0.60	2.80	5.03

TABLE 3.—*Oscillator Strengths for Ultraviolet Lines of Fe* I—Continued

Wavelength Å	Energy Levels K	Low e.p. Volts	Mult. No.	Arc	Spk	CB	HC	R(N)	KOC	MS	Best	Log gfλ	Log gA/λ
				Log *gf*									
2503.491	20875–60807	2.59	UV164	−0.15							−0.15	3.25	5.48
2504.101	20641–60564	2.56		−1.20							−1.20	2.20	4.43
2504.635	17727–57641	2.20		−2.01							−2.01	1.39	3.62
2505.004	20641–60549	2.56	UV163	−0.54							−0.54	2.86	5.09
2506.569	20875–60758	2.59	UV163	−0.24							−0.24	3.16	5.39
2507.899	7728–47590	0.96	UV 59	0.04	−0.07	−0.05			0.04		−0.01	3.39	5.62
2508.751	7986–47834	0.99	UV 63	−0.98					−1.12		−1.05	2.35	4.58
2508.948	7986–47831	0.99	UV 59	−2.01							−2.01	1.39	3.62
2509.390	17727–57565	2.20		−1.48							−1.48	1.92	4.15
2510.836	416–40231	0.05	UV 7	−0.16	0.04	0.01			0.27		0.04	3.44	5.66
2512.266	6928–46721	0.86	UV 55	−0.68							−0.68	2.72	4.94
2512.361	416–40207	0.05	UV 8	−1.14		−1.10			−1.16		−1.14	2.26	4.48
2515.848	12561–52297	1.56	UV104	−1.15							−1.15	2.25	4.47
2516.249	7377–47107	0.91	UV 57	−1.48					−0.98		−0.98	2.42	4.64
2516.572	7728–47453	0.96	UV 61	−0.96					−1.13		−1.04	2.36	4.58
2517.658	7986–47693	0.99	UV 59	−0.08	−0.23	−0.08			−0.12		−0.12	3.28	5.50
2518.103	704–40405	0.09	UV 7	−0.08	0.02	−0.07			−0.18		−0.08	3.32	5.54
2518.824	20875–60564	2.59		−0.49							−0.49	2.91	5.13
2519.630	8155–47831	1.01	UV 59	−0.31	−0.01	−0.24			−0.27		−0.21	3.19	5.41
2521.920	7377–47017	0.91	UV 58	−0.84							−0.84	2.56	4.78
2522.488	7377–47008	0.91	UV 57	−0.75							−0.75	2.65	4.87
2522.850	0–39626	0.00	UV 7		0.56	0.44					0.50	3.90	6.12
2524.294	888–40491	0.11	UV 7	−0.17	−0.23	−0.20					−0.20	3.20	5.42
2527.436	416–39970	0.05	UV 7	0.15	0.37	0.18					0.23	3.63	5.85
2528.910	20641–60172	2.56	UV162		−0.25						−0.25	3.15	5.37
2529.136	704–40231	0.09	UV 7	−0.06	0.11	−0.23			−0.13		−0.08	3.32	5.54
2529.837	888–40405	0.11	UV 7	−0.47		−0.71					−0.59	2.81	5.02
2530.694	704–40207	0.09	UV 8	−1.28		−1.09			−1.52		−1.30	2.10	4.31
2531.510	20875–60365	2.59	UV162	−0.20					0.32				
2532.876	7728–47197	0.96	UV 56	−1.20					−1.32		−1.26	2.14	4.35
2535.128	7986–47420	0.99	UV 60	−1.20					−1.62				
2535.609	978–40405	0.12	UV 7	−0.18	−0.18	−0.06			−0.33		−0.19	3.21	5.42
2537.460	11976–51374	1.48	UV102	−0.49	−0.42				−0.45		−0.45	2.95	5.16
2539.358	7377–46745	0.91	UV 55	−0.78	−0.75				−0.77		−0.77	2.63	4.84
2539.575	7728–47093	0.96	UV 56	−1.78					−2.00		−1.89	1.51	3.72
2540.973	888–40231	0.11	UV 7		−0.22	−0.02					−0.12	3.29	5.49
2542.101	21039–60365	2.61	UV162	0.91	1.07	0.87			2.05				
2543.920	20875–60172	2.59	UV162	0.91	0.99	0.86			1.94				
2544.706	20641–59927	2.56	UV162	0.76		0.50					0.63	4.04	6.24
2545.980	704–39970	0.09	UV 7		−0.11	−0.05					−0.08	3.33	5.53
2549.614	416–39626	0.05	UV 7		−0.39	−0.18					−0.28	3.13	5.32
2550.812	7986–47177	0.99	UV 55	−1.28							−1.28	2.13	4.32
2552.604	888–40052	0.11	UV 8	−1.58					−1.72		−1.65	1.76	3.95
2552.832	7728–46889	0.96	UV 55	−1.07					−1.16		−1.12	2.29	4.48
2554.518	22947–62081	2.84		−0.93							−0.93	2.48	4.67
2555.648	8155–47272	1.01	UV 58	−1.58					−1.80		−1.69	1.72	3.91
2556.304	12561–51668	1.56	UV102	−0.50	−0.18				−0.28		−0.39	3.02	5.21
2556.862	6928–46027	0.86	UV 53	−1.02					−1.03		−1.02	2.39	4.58
2557.268	11976–51069	1.48	UV101	−1.40					−1.67		−1.54	1.87	4.06
2560.558	8155–47197	1.01	UV 56	−1.11					−1.30		−1.20	2.21	4.40
2561.262	7986–47017	0.99	UV 58	−1.39					−1.63		−1.51	1.90	4.09
2561.856	8155–47177	1.01	UV 55	−1.20					−1.31		−1.26	2.15	4.34
2562.224	8155–47172	1.01	UV 55	−0.88					−1.07		−0.98	2.43	4.62
2563.820	7728–46721	0.96	UV 55	−1.79							−1.79	1.62	3.81
2564.561	8155–47136	1.01	UV 58	−1.19					−1.21		−1.20	2.21	4.40
2567.860	17927–56859	2.22	UV130	−0.72							−0.72	2.69	4.88
2568.862	7986–46902	0.99	UV 54	−1.06					−1.17		−1.12	2.29	4.47
2569.595	6928–45833	0.86	UV 52	−1.03					−1.15		−1.09	2.32	4.50
2569.742	7986–46889	0.99	UV 55	−0.99					−1.11		−1.05	2.36	4.54
2571.570	12561–51436	1.56	UV103						−1.83		−1.83	1.58	3.76

TABLE 3.—*Oscillator Strengths for Ultraviolet Lines of Fe* I—Continued

Wavelength Å	Energy Levels K	Low e.p. Volts	Mult. No.	Arc	Spk	CB	HC	R(N)	KOC	MS	Best	Log gfλ	Log gA/λ
				Log *gf*									
2572.752	12969–51826	1.61	UV102	−0.75					−0.96		−0.85	2.56	4.74
2576.692	6928–45726	0.86	UV 52	−0.27	−0.23	−0.23			−0.15		−0.22	3.19	5.37
2579.266	7986–46745	0.99	UV 55	−1.21					−1.41		−1.31	2.10	4.28
2580.066	8155–46902	1.01	UV 54	−1.51					−1.62		−1.56	1.85	4.03
2580.281	12561–51305	1.56		−0.97							−0.97	2.44	4.62
2580.454	7986–46727	0.99	UV 54	−1.81					−1.69		−1.75	1.66	3.84
2580.561	12969–51708	1.61		−0.97							−0.97	2.44	4.62
2580.939	8155–46889	1.01	UV 55	−1.66							−1.66	1.75	3.93
2584.537	6928–45608	0.86	UV 52		0.08	0.17		0.10[1]	0.28		0.16	3.57	5.75
2586.557	21716–60366	2.69	UV171	−0.65							−0.65	2.76	4.94
2592.285	21999–60564	2.73		−0.63							−0.63	2.78	4.95
2593.510	19351–57897	2.40	UV146	−0.25	−0.23				0.16		−0.11	3.30	5.47
2594.150	7377–45914	0.91	UV 52	−0.84					−1.00		−0.92	2.49	4.66
2595.422	8155–46673	1.01	UV 54	−1.75					−2.11		−2.00	1.41	3.58
2598.855	12969–51436	1.61	UV103	−1.25							−1.25	2.16	4.33
2599.565	7377–45833	0.91	UV 52			0.27			−0.08		0.10	3.51	5.68
2605.658	6928–45295	0.86	UV 51	−0.78	−0.89	−0.37			−0.91		−0.86	2.56	4.72
2606.828	7377–45726	0.91	UV 52			−0.01			0.21		0.10	3.52	5.68
2609.220	22249–60564	2.76		−0.55							−0.55	2.87	5.02
2610.750	704–38996	0.09	UV 6	−1.96					−2.10		−2.03	1.39	3.54
2612.773	416–38678	0.05	UV 6	−1.72					−1.87		−1.80	1.62	3.77
2614.495	7728–45965	0.96	UV 52	−1.06					−1.10		−1.08	2.34	4.49
2618.019	7728–45914	0.96	UV 52	−0.22	−0.36	−0.11			−0.18		−0.22	3.20	5.35
2618.711	0–38175	0.00	UV 6	−1.71					−1.76		−1.74	1.68	3.83
2623.367	888–38996	0.11	UV 6						−1.84		−1.84	1.58	3.73
2623.532	7728–45833	0.96	UV 52	−0.09	−0.22	−0.02			0.02		0.00	3.42	5.57
2627.230	7377–45428	0.91	UV 51	−1.69							−1.69	1.73	3.88
2629.579	978–38996	0.12	UV 6	−1.58		−1.43			−2.09		−2.09	1.33	3.47
2632.238	7986–45965	0.99	UV 52	−0.33		−0.27			−0.36		−0.32	3.10	5.24
2632.595	704–38678	0.09	UV 6	−1.56	−1.63				−1.76		−1.70	1.72	3.86
2635.810	7986–45914	0.99	UV 52		−0.16	0.02			−0.06		−0.07	3.35	5.49
2636.479	7377–45295	0.91	UV 51	−1.01					−1.22		−1.12	2.30	4.44
2641.647	7377–45221	0.91	UV 50	−0.59	−0.63	−0.49			−0.81		−0.63	2.79	4.93
2643.999	8155–45965	1.01	UV 52		−0.19	−0.09			0.02		−0.09	3.33	5.47
2645.423	888–38678	0.11	UV 6	−1.96					−2.14		−2.05	1.37	3.51
2647.559	416–38175	0.05	UV 6	−1.67		−1.65			−1.84		−1.72	1.70	3.84
2648.164	11976–49727	1.48	UV 99	−1.68							−1.68	1.74	3.88
2648.548	24336–62081	3.02		−0.71							−0.71	2.71	4.84
2651.708	7728–45428	0.96	UV 51	−1.08					−1.15		−1.12	2.30	4.43
2655.140	11976–49628	1.48	UV100	−1.64					−2.00		−1.82	1.60	3.73
2656.145	19390–57028	2.40	UV156	0.16	0.23	0.23			0.38		0.25	3.67	5.80
2656.793	11976–49604	1.48	UV 99	−0.74					−0.98		−0.86	2.56	4.69
2660.396	7986–45563	0.99	UV 51	−1.18					−1.41		−1.30	2.12	4.25
2661.196	7986–45552	0.99	UV 50						−1.74		−1.74	1.69	3.81
2662.057	7728–45282	0.96	UV 50	−0.70	−0.66	−0.77			−0.75		−0.72	2.71	4.83
2666.400	7728–45221	0.96	UV 50	−0.87					−1.02		−0.94	2.49	4.61
2666.813	6928–44415	0.86	UV 48	−0.36		−0.35			−0.34		−0.35	3.08	5.20
2666.966	11976–49461	1.48	UV100	−0.10	−0.51				−0.39		−0.39	3.04	5.16
2667.914	704–38175	0.09	UV 6	−2.07					−2.33		−2.20	1.23	3.35
2669.492	19621–57070	2.43	UV156	−0.10					0.09		0.00	3.43	5.54
2673.214	8155–45552	1.01	UV 50	−1.08					−1.23		−1.16	2.27	4.38
2679.063	6928–44244	0.86	UV 47	−0.14	−0.23	−0.11			−0.09		−0.14	3.29	5.40
2680.454	7986–45282	0.99	UV 50	−0.73	−0.79				−0.92		−0.81	2.62	4.73
2680.910	12561–49851	1.56	UV100	−1.75					−1.90		−1.82	1.61	3.72
2681.586	19562–56843	2.42	UV145	−0.15					0.19		0.02	3.45	5.56
2684.857	7986–45221	0.99	UV 50	−1.78					−1.97		−1.97	1.46	3.57
2689.213	7377–44551	0.91	UV 48	−0.29		−0.24			−0.18		−0.24	3.19	5.30
2689.830	12561–49727	1.56	UV 99	−0.36	−0.39				−0.72		−0.49	2.94	5.04
2690.069	0–37163	0.00	UV 4	−1.91					−2.15		−2.03	1.40	3.50
2692.250	11976–49109	1.48	UV 98	−1.14					−1.36		−1.25	2.18	4.28

216-375 O - 66 - 5

TABLE 3.—*Oscillator Strengths for Ultraviolet Lines of Fe* I—Continued

Wavelength Å	Energy Levels K	Low e.p. Volts	Mult. No.	Arc	Spk	CB	HC	R(N)	KOC	MS	Best	Log gfλ	Log gA/λ
				Log *gf*									
2692.658	8155–45282	1.01	UV 50	−0.84					−1.89		−1.89	1.54	3.64
2694.222	416–37521	0.05	UV 4	−2.86					−3.01		−3.01	0.42	2.52
2694.536	19351–56452	2.40	UV144	0.02	0.01				0.29		0.11	3.54	5.64
2695.036	6928–44023	0.86	UV 47	−1.35							−1.35	2.08	4.18
2695.662	19757–56843	2.45	UV145	0.02					0.19		0.10	3.53	5.63
2696.284	19351–56428	2.40	UV143	0.29					0.69		0.49	3.92	6.02
2697.022	12561–49628	1.56	UV100	−0.46					−0.59		−0.52	2.91	5.01
2699.108	7377–44415	0.91	UV 48		−0.49	−0.43			−0.55		−0.49	2.94	5.04
2701.908	20641–57641	2.56	UV161	−0.67	−0.01						−0.67	2.76	4.86
2702.453	19390–56383	2.40	UV154	−0.47	0.08						0.08	3.51	5.61
2706.012	19390–56334	2.40	UV154	0.43	0.30	0.40			0.39		0.38	3.81	5.91
2706.583	7728–44664	0.96	UV 48			−0.04			−0.12		−0.08	3.35	5.45
2707.451	20641–57565	2.56		−0.40							−0.40	3.03	5.13
2708.570	20641–57550	2.56	UV161	0.42	0.37	0.51			0.61		0.48	3.91	6.01
2709.700	23784–60677	2.95	UV180						0.87		0.87	4.30	6.40
2709.989	19562–56452	2.42	UV144	−0.32					−0.18		−0.25	3.18	5.28
2710.543	12969–49851	1.61	UV100	−0.26	−0.12	−0.44			−0.31		−0.34	3.09	5.18
2711.656	7377–44244	0.91	UV 47	−0.44		−0.45			−0.44		−0.44	2.99	5.08
2714.062	20875–57709	2.59	UV161	−0.35	−0.24						−0.30	3.13	5.22
2714.870	7728–44551	0.96	UV 48	−1.10	−1.21				−1.19		−1.20	2.23	4.32
2715.323	704–37521	0.09	UV 4	−2.33					−2.70		−2.70	0.73	2.82
2716.410	19621–56423	2.43	UV154	−0.68							−0.68	2.75	4.84
2717.368	7377–44166	0.91	UV 47	−1.68					−1.73		−1.70	1.73	3.82
2717.787	7728–44512	0.96	UV 49	−0.96					−1.21		−1.08	2.35	4.44
2718.436	7986–44761	0.99	UV 48	−0.24	−0.41	−0.28			−0.17		−0.28	3.15	5.24
2719.027	0–36767	0.00	UV 5		0.04	0.15		0.26[1]			0.15	3.58	5.67
2719.418	19621–56383	2.43	UV154	0.44							0.44	3.87	5.96
2720.194	17550–54301	2.18	UV129	−0.07	0.01				−0.09		−0.05	3.38	5.47
2720.516	416–37163	0.05	UV 4	−2.26					−2.71		−2.71	0.72	2.81
2720.904	416–37158	0.05	UV 5		−0.12	−0.13		−0.05[1]			−0.10	3.33	5.42
2722.032	11976–48703	1.48	UV 97	−0.99					−1.51		−1.51	1.92	4.01
2723.579	704–37410	0.09	UV 5			−0.34		−0.49[1]			−0.42	3.02	5.10
2724.344	19757–56452	2.45	UV144	−0.56	−0.45						−0.50	2.94	5.02
2724.954	7728–44415	0.96	UV 48	−0.33		−0.42					−0.38	3.06	5.14
2725.311	12561–49243	1.56	UV 98	−1.04							−1.04	2.40	4.48
2725.602	7986–44664	0.99	UV 48	−1.49					−1.76		−1.62	1.82	3.90
2725.805	20875–57550	2.59	UV161	−0.52	−0.31						−0.42	3.02	5.10
2726.054	8155–44827	1.01	UV 48			−0.37			−0.32		−0.34	3.10	5.18
2726.237	21039–57709	2.61	UV161	0.24	0.22				0.29		0.25	3.69	5.77
2728.021	7377–44023	0.91	UV 47	−0.63	−0.87	−0.59			−0.72		−0.70	2.74	4.82
2728.819	19788–56423	2.45	UV154			0.34			0.22		0.28	3.72	5.80
2728.970	888–37521	0.11	UV 4						−2.50		−2.50	0.94	3.02
2730.982	8155–44761	1.01	UV 48	−0.74					−0.89		−0.82	2.62	4.69
2731.281	21039–57641	2.61	UV161		−0.32				0.12				
2733.582	6928–43500	0.86	UV 46		0.34	0.42			0.51		0.42	3.86	5.93
2734.006	7986–44551	0.99	UV 48	−0.73	−0.92	−0.82			−0.76		−0.81	2.63	4.70
2734.269	17550–54112	2.18	UV125	0.15		0.02			0.04		0.07	3.51	5.58
2734.616	7728–44285	0.96	UV 47	−1.27					−1.40		−1.34	2.10	4.17
2735.476	7377–43923	0.91	UV 46			0.07		0.10[1]	0.30		0.16	3.60	5.67
2736.960	7986–44512	0.99	UV 49	−0.32							−0.32	3.12	5.19
2737.311	888–37410	0.11	UV 5		−0.35	−0.33		−0.39[1]			−0.36	3.08	5.15
2738.214	8155–44664	1.01	UV 48	−1.52							−1.52	1.92	3.99
2741.100	24336–60807	3.02	UV181	−0.23							−0.23	3.21	5.28
2741.578	12969–49433	1.61	UV 98	−1.09							−1.09	2.35	4.42
2742.016	704–37163	0.09	UV 4	−1.71	−2.12				−1.93		−1.92	1.52	3.59
2742.255	7728–44184	0.96	UV 46		−0.39	−0.44			−0.32		−0.38	3.06	5.13
2742.406	704–37158	0.09	UV 5		−0.23	−0.46		−0.26[1]			−0.32	3.12	5.19
2743.564	7728–44166	0.96	UV 47			−0.64			−0.70		−0.67	2.77	4.84
2744.069	978–37410	0.12	UV 5		−0.69	−0.69		−0.74[1]	−0.49		−0.65	2.79	4.86
2744.529	7986–44411	0.99	UV 46			−0.53			−0.32		−0.42	3.02	5.09

TABLE 3.—*Oscillator Strengths for Ultraviolet Lines of Fe* I—Continued

Wavelength Å	Energy Levels K	Low e.p. Volts	Mult. No.	Arc	Spk	CB	HC	R(N)	KOC	MS	Best	Log gfλ	Log gA/λ
				Log *gf*									
2746.982	6928–43321	0.86	UV 45			0.13			−1.00		0.13	3.57	5.64
2747.556	17727–54112	2.20	UV125	−0.21	−0.11				−0.22		−0.18	3.26	5.33
2749.688	8155–44512	1.01	UV 49	−1.33							−1.33	2.11	4.18
2750.142	416–36767	0.05	UV 5		−0.38	−0.40		−0.35[1]			−0.38	3.06	5.13
2750.708	17927–54271	2.22	UV125	−0.34							−0.34	3.10	5.17
2750.872	17550–53892	2.18	UV128	0.18		0.01			0.30		0.16	3.60	5.67
2751.808	12969–49298	1.61		−1.34							−1.34	2.10	4.17
2753.687	8155–44459	1.01	UV 46	−0.55		−0.70			−0.52		−0.59	2.85	4.91
2754.033	7986–44285	0.99	UV 47	−0.58		−0.72			−0.59		−0.63	2.81	4.87
2754.427	7728–44023	0.96	UV 47	−0.87	−1.20				−0.99		−1.02	2.42	4.48
2755.184	19621–55906	2.43	UV153	−0.53							−0.53	2.91	4.97
2756.268	416–36686	0.05	UV 4	−1.06	−0.84	−0.87			−1.37		−1.04	2.40	4.46
2756.330	888–37158	0.11	UV 5	−2.00				−0.82[1]	−0.38		−0.60	2.84	4.90
2757.317	8155–44411	1.01	UV 46	−0.35	−0.62	−0.40			−0.25		−0.30	3.14	5.20
2759.814	8155–44378	1.01	UV 47	−0.69	−0.84	−1.01			−0.76		−0.83	2.61	4.67
2761.480	19552–55754	2.42	UV140	−0.87							−0.87	2.57	4.63
2761.781	7986–44184	0.99	UV 46			−0.16			−0.24		−0.20	3.24	5.30
2762.028	7728–43923	0.96	UV 46			−0.16			−0.14		−0.15	3.29	5.35
2762.773	17927–54112	2.22	UV125	−0.15	−0.46						−0.30	3.14	5.20
2763.108	7986–44166	0.99	UV 47	−0.65	−0.82	−0.64			−0.70		−0.70	2.74	4.80
2764.323	17727–53892	2.20	UV128	0.14		−0.16					−0.01	3.43	5.49
2765.700	11976–48123	1.48	UV 92	−1.80					−1.99		−1.90	1.54	3.60
2766.910	8155–44285	1.01	UV 47	−0.76	−1.15	−1.02			−0.83		−0.94	2.50	4.56
2767.523	7377–43500	0.91	UV 46						−0.39		−0.39	3.05	5.11
2768.432	17550–53661	2.18	UV126	−0.54					−0.60		−0.57	2.87	4.93
2769.298	19390–55490	2.40	UV151	0.26					0.26		0.26	3.70	5.76
2769.672	6928–43023	0.86	UV 44	−1.31					−1.47		−1.39	2.05	4.11
2770.695	17727–53808	2.20	UV123	−0.73					−0.07				
2772.075	6928–42992	0.86	UV 45	−0.24	−0.44	−0.22			−0.39		−0.32	3.12	5.18
2772.320	17550–53610	2.18		−0.35							−0.35	3.09	5.15
2772.511	17727–53785	2.20		−0.43							−0.43	3.01	5.07
2772.860	24119–60172	2.99	UV179	−0.57	−0.36						−0.46	2.98	5.04
2773.907	19390–55430	2.40	UV151	−1.40							−1.40	2.04	4.09
2774.150	17727–53763	2.20	UV127	−1.50							−1.50	1.94	3.99
2774.730	8155–44184	1.01	UV 46	−0.93		−0.85			−1.05		−0.94	2.50	4.55
2778.221	6928–42912	0.86	UV 44		−0.40	−0.30		−0.40[1]	−0.27		−0.34	3.10	5.15
2780.526	11976–47930	1.48	UV 92	−1.74							−1.74	1.70	3.75
2780.700	20641–56593	2.56	UV160	−0.48					0.96				
2781.837	7986–43923	0.99	UV 46		−0.76	−0.81			−0.90		−0.82	2.62	4.67
2782.055	17727–53661	2.20	UV126	−0.74					−0.98		−0.86	2.58	4.63
2784.017	20875–56783	2.59	UV160	−0.95							−0.95	2.49	4.54
2784.346	19621–55526	2.43	UV152	−0.71					−0.69		−0.70	2.74	4.79
2786.180	17927–53808	2.22	UV123	−1.20							−1.20	2.25	4.29
2787.120	19621–55490	2.43	UV151	−1.20							−1.20	2.25	4.29
2787.933	11976–47835	1.48	UV 93						−0.71		−0.71	2.74	4.78
2788.106	6928–42784	0.86	UV 44		0.54	0.35		0.34[2]	0.58		0.43	3.88	5.92
2789.477	17550–53389	2.18	UV125	−0.43					−0.29		−0.36	3.09	5.13
2789.803	21716–57550	2.69	UV170	−0.06		0.01			0.15		0.03	3.48	5.52
2790.762	17927–53749	2.22		−1.58							−1.58	1.87	3.91
2791.787	19621–55430	2.43	UV151	−0.25	0.08	0.02			0.07		−0.02	3.43	5.47
2792.397	12561–48362	1.56	UV 95	−1.03					−1.11		−1.07	2.38	4.42
2794.157	17550–53329	2.18	UV124	−1.32							−1.32	2.13	4.17
2794.703	7728–43500	0.96	UV 46	−1.24					−1.22		−1.23	2.22	4.25
2795.006	0–35768	0.00	UV 3	−2.29		−2.05			−2.56		−2.30	1.15	3.18
2795.541	7377–43138	0.91	UV 44	−1.10				−1.27[1]	−1.10		−1.16	2.29	4.32
2796.872	12561–48305	1.56	UV 96	−1.51					−1.65		−1.58	1.87	3.90
2797.776	7377–43109	0.91	UV 45		−0.64	−0.54			−0.48		−0.55	2.90	4.93
2802.285	26406–62081	3.27		−1.01							−1.01	2.44	4.47
2803.168	416–36079	0.05	UV 3	−2.74					−2.87		−2.80	0.65	2.68
2803.613	19788–55446	2.45	UV151	−0.43					−1.81				

TABLE 3.—*Oscillator Strengths for Ultraviolet Lines of Fe* I—Continued

Wavelength Å	Energy Levels K	Low e.p. Volts	Mult. No.	Arc	Spk	CB	HC	R(N)	KOC	MS	Best	Log gfλ	Log gA/λ
							Log *gf*						
2804.521	7377–43023	0.91	UV 44		−0.30	−0.28		−0.34[1]	−0.36		−0.32	3.13	5.16
2804.865	21999–57641	2.73	UV170	−0.39							−0.39	3.06	5.09
2805.808	11976–47606	1.48	UV 92	−1.56					−1.66		−1.61	1.84	3.87
2806.072	18378–54005	2.28	UV139	−1.03							−1.03	2.42	4.45
2806.985	7377–42992	0.91	UV 45		−0.20	−0.25			−0.17		−0.21	3.24	5.27
2807.246	0–35612	0.00	UV 2	−2.52					−2.81		−2.68	0.77	2.80
2808.328	7728–43326	0.96	UV 45	−1.55					−1.31		−1.43	2.02	4.05
2810.834	21999–57565	2.73		−1.21							−1.21	2.24	4.27
2811.160	12561–48123	1.56	UV 92	−1.90							−1.90	1.55	3.58
2812.042	21999–57550	2.73	UV170	−0.85							−0.85	2.60	4.63
2813.288	7377–42912	0.91	UV 44		0.27	0.16		0.24[1]	0.26		0.23	3.68	5.71
2815.017	18378–53892	2.28	UV138	−1.14							−1.14	2.31	4.34
2815.506	12969–48476	1.61	UV 95	−1.06					−1.10		−1.08	2.37	4.40
2817.505	7728–43210	0.96	UV 44			−1.12					−1.12	2.33	4.35
2819.286	22249–57709	2.76	UV170	−0.21							−0.21	3.24	5.26
2820.804	416–35856	0.05	UV 2	−2.83							−2.83	0.62	2.64
2821.630	18378–53808	2.28	UV134	−1.73							−1.73	1.72	3.74
2823.277	7728–43138	0.96	UV 44		−0.15	0.27		−0.30[1]			−0.22	3.23	5.25
2824.700	22249–57641	2.76	UV170	−0.95							−0.95	2.50	4.52
2825.557	7728–43109	0.96	UV 45		−0.20	−0.26					−0.23	3.22	5.24
2825.689	0–35379	0.00	UV 3	−2.01		−1.90					−1.96	1.49	3.51
2825.995	704–36079	0.09	UV 3	−2.92							−2.92	0.53	2.55
2827.893	416–35768	0.05	UV 3	−2.29							−2.29	1.16	3.18
2828.809	7986–43326	0.99	UV 45		−0.81	−1.01					−0.91	2.54	4.56
2832.436	7728–43023	0.96	UV 44		0.05	0.06		−0.06[2]			0.00	3.45	5.47
2833.401	18378–53661	2.28	UV137	−0.91							−0.91	2.54	4.56
2834.177	12561–47834	1.56	UV 93	−1.97							−1.97	1.48	3.50
2834.414	12969–48239	1.61	UV 92	−1.95							−1.95	1.50	3.52
2834.755	20641–55907	2.56	UV159	−0.74							−0.74	2.71	4.73
2835.457	0–35257	0.00	UV 2	−2.04		−1.99					−2.02	1.43	3.45
2835.951	12561–47812	1.56	UV 93	−1.11					−1.21		−1.16	2.29	4.31
2836.315	22650–57897	2.81	UV175	−0.78							−0.78	2.67	4.69
2838.120	7986–43210	0.99	UV 44			−0.42		−0.45[1]			−0.44	3.01	5.02
2840.423	416–35612	0.05	UV 2	−2.02		−1.95					−1.98	1.47	3.48
2840.938	17727–52916	2.20	UV123	−1.11							−1.11	2.34	4.35
2843.631	7377–42533	0.91	UV 43		−0.53	−0.54					−0.54	2.91	4.92
2843.978	7986–43138	0.99	UV 44		0.13	−0.01			−0.07		0.02	3.47	5.48
2845.596	7728–42860	0.96	UV 43		−0.80	−0.61					−0.70	2.75	4.76
2845.714	11976–47107	1.48	UV 88		0.09						0.09	3.54	5.55
2846.831	11976–47093	1.48	UV 87	−1.22	−1.20				−1.38		−1.27	2.18	4.19
2848.715	7986–43079	0.99	UV 43			−1.22			−1.15		−1.18	2.27	4.28
2851.798	8155–43210	1.01	UV 44			0.17		−0.05[1]	−0.19		−0.02	3.44	5.44
2852.952	11976–47017	1.48	UV 89	−1.97					−2.01		−1.99	1.47	3.47
2853.685	11976–47008	1.48	UV 88		−0.61				−1.50		−1.50	1.96	3.96
2853.774	20875–55906	2.59	UV159	−0.47	−0.13				−0.24		−0.28	3.18	5.18
2857.996	18378–53358	2.28		−0.95	−0.47						−0.47	2.99	4.99
2858.897	888–35856	0.11	UV 2	−2.20	−2. 5				⅔2.24		−2.23	1.23	3.23
2861.996	17927–52858	2.22		−1.78							−1.78	1.68	3.67
2862.495	8155–43079	1.01	UV 43	−1.33					−1.35		−1.34	2.12	4.11
2863.431	11976–46889	1.48	UV 87	−0.41	−0.56	−0.25			−0.34		−0.39	3.07	5.06
2863.864	704–35612	0.09	UV 2	−1.63	−1.84	−1.73			−1.83		−1.76	1.70	3.69
2866.626	7986–42860	0.99	UV 43	−0.97	−0.99	−1.05			−1.10		−1.03	2.43	4.42
2867.311	12969–47834	1.61	UV 93	−0.99					−1.17		−1.08	2.38	4.37
2867.563	12969–47831	1.61	UV 90	−0.86					−1.12		−0.99	2.47	4.46
2867.880	12561–47420	1.56	UV 91	−1.62					−1.81		−1.72	1.74	3.73
2868.213	19757–54612	2.45	UV142	−0.72							−0.72	2.74	4.73
2868.454	18378–53230	2.28	UV135	−0.45							−0.45	3.01	5.00
2869.308	416–35257	0.05	UV 2	−1.48	−1.57	−1.47		−1.68[1]	−1.62		−1.56	1.90	3.89
2869.833	19913–54748	2.47	UV142	−0.89							−0.89	2.57	4.56
2871.730	19788–54600	2.45	UV149	−1.67							−1.67	1.79	3.78

TABLE 3.—*Oscillator Strengths for Ultraviolet Lines of Fe* I—Continued

Wave-length Å	Energy Levels K	Low e.p. Volts	Mult. No.	Arc	Spk	CB	HC	R(N)	KOC	MS	Best	Log gfλ	Log gA/λ
				Log *gf*									
2872.335	7728–42533	0.96	UV 43	−0.86		−0.78			−0.95		−0.86	2.60	4.59
2873.655	20641–55430	2.56	UV158	−0.83							−0.83	2.63	4.62
2874.173	0–34782	0.00	UV 2		−1.59	−1.43		−1.65[1]	−1.54		−1.55	1.91	3.90
2874.890	19351–54125	2.40	UV142	−0.63	−0.23								
2875.303	11976–46745	1.48	UV 86	−0.84		−0.56			−0.88		−0.76	2.70	4.69
2877.302	11976–46721	1.48	UV 86	−0.36	−0.45	−0.26			−0.22		−0.32	3.14	5.13
2878.762	22838–57565	2.83		−0.53							−0.53	2.93	4.92
2878.962	12969–47693	1.61	UV 90	−1.67							−1.67	1.79	3.78
2879.461	19552–54271	2.42	UV136	−1.38							−1.38	2.08	4.07
2880.581	8155–42860	1.01	UV 43	−1.93					−1.96		−1.94	1.52	3.51
2886.317	12561–47197	1.56	UV 87	−1.17					−1.37		−1.27	2.19	4.17
2887.360	19390–54014	2.40	UV150	−1.65							−1.65	1.81	3.79
2887.806	21716–56334	2.69	UV167	−0.19		−0.29					−0.24	3.22	5.20
2887.961	19621–54237	2.43	UV149	−1.14							−1.14	2.32	4.30
2889.890	19390–53983	2.40	UV149	−0.90							−0.90	2.56	4.54
2889.991	20020–54612	2.48	UV142	−0.80							−0.80	2.66	4.64
2890.414	12969–47556	1.61		−2.24							−2.24	1.22	3.20
2890.868	26225–60807	3.25	UV184	−1.02							−1.02	2.44	4.42
2891.410	12561–47136	1.56	UV 89	−1.99							−1.99	1.47	3.45
2891.705	20875–55446	2.59	UV158		−0.34						−0.34	3.12	5.10
2891.904	19788–54357	2.45		−0.94	−0.38						−0.94	2.52	4.50
2892.479	19562–54125	2.42	UV142	−0.63							−0.63	2.83	4.81
2893.763	7986–42533	0.99	UV 43	−1.80					−1.85		−1.82	1.64	3.62
2893.882	12561–47107	1.56	UV 88	−1.11					−1.02		−1.06	2.40	4.38
2894.506	18378–52916	2.28	UV134	0.19	0.28	0.45			0.45		0.34	3.80	5.78
2895.036	12561–47093	1.56	UV 87	−0.45	−0.42	−0.31			−0.23		−0.35	3.11	5.09
2897.635	19788–54289	2.45			−0.73						−0.73	2.73	4.71
2898.867	17727–52213	2.20		−1.37							−1.37	2.09	4.07
2899.416	18378–52858	2.28	UV133	0.00	0.12	0.15			0.06		0.08	3.54	5.52
2901.382	12561–47017	1.56	UV 89	−0.72	−0.76				−0.47		−0.65	2.81	4.79
2901.910	19351–53801	2.40	UV142	−0.15		−0.10			−0.01		−0.09	3.37	5.35
2905.570	26351–60758	3.27	UV182	−0.66	−0.38						−0.52	2.94	4.91
2907.518	21999–56383	2.73	UV167	−0.07	0.13	0.12					0.06	3.52	5.49
2908.864	19757–54125	2.45	UV142	−0.57							−0.57	2.89	4.86
2909.313	19621–53983	2.43	UV149	−1.40							−1.40	2.06	4.03
2910.930	22249–56593	2.76	UV168	−0.98							−0.98	2.48	4.45
2912.159	0–34329	0.00	UV 1		−1.35	−1.17		−1.22[2]	−1.38	−1.11	−1.24	2.22	4.19
2914.306	12969–47272	1.61	UV 89	−0.76	−0.79				−1.28				
2918.023	26106–60366	3.24	UV182	0.59	0.64	0.75					0.66	4.13	6.09
2918.354	19552–53808	2.42	UV134	−0.41	−0.44						−0.42	3.05	5.01
2919.838	19562–53801	2.42	UV142	−0.69	−0.53						−0.61	2.86	4.82
2920.290	20038–54271	2.48	UV136	−1.50							−1.50	1.97	3.93
2920.691	12969–47197	1.61	UV 87	−0.47	−0.59	−0.19			−0.44		−0.42	3.05	5.01
2922.383	12969–47177	1.61	UV 86	−1.51					−1.61		−1.56	1.91	3.87
2922.620	17550–51756	2.18	UV122	−0.84	−0.89						−0.86	2.61	4.57
2923.288	26351–60549	3.27	UV182	0.25	0.40	0.75					0.47	3.94	5.90
2923.851	21716–55907	2.69	UV166	0.10	0.28	0.41			0.28		0.27	3.74	5.70
2924.002	21716–55906	2.69	UV166	0.30	0.28						0.29	3.76	5.72
2925.359	22249–56423	2.76	UV167	−0.10	0.04						−0.03	3.44	5.40
2925.901	12969–47136	1.61	UV 89	−0.79	−0.79				−0.94		−0.84	2.63	4.59
2928.105	17550–51692	2.18	UV121	−1.07							−1.07	2.40	4.35
2929.008	416–34547	0.05	UV 1		−1.13			−1.12[2]	−1.21	−1.03	−1.12	2.35	4.30
2929.118	26628–60758	3.30	UV182		0.17						0.17	3.64	5.59
2929.620	12969–47093	1.61	UV 87	−1.23		−1.14			−1.35		−1.24	2.23	4.18
2930.590	20020–54132	2.48	UV141	−1.95							−1.95	1.52	3.47
2931.420	19788–53892	2.45	UV148	−1.15							−1.15	2.32	4.27
2931.803	21999–56098	2.73	UV166	−0.94							−0.94	2.53	4.48
2934.370	17550–51619	2.18	UV117	−1.38							−1.38	2.09	4.04
2936.120	12969–47017	1.61	UV 89	−1.21							−1.21	2.26	4.21
2936.905	0–34040	0.00	UV 1		−0.56	−0.59		−0.66[3]		−0.44	−0.60	2.87	4.82

TABLE 3.—*Oscillator Strengths for Ultraviolet Lines of Fe* I—Continued

Wave-length Å	Energy Levels K	Low e.p. Volts	Mult. No.	Arc	Spk	CB	HC	R(N)	KOC	MS	Best	Log gfλ	Log gA/λ
				Log *gf*									
2937.806	17727–51756	2.20	U V122	−0.11	−0.44				−0.48		−0.34	3.13	5.08
2939.072	17927–51942	2.22	U V118	−0.98	−0.57						−0.78	2.69	4.64
2940.586	22846–56843	2.83	U V173	−0.34	−0.47						−0.40	3.07	5.02
2941.344	704–34692	0.09	U V 1		−1.40	−1.30		−1.32[2]	−1.28	−1.25	−1.31	2.16	4.11
2941.770	19562–53546	2.42	U V141		−0.81						−0.81	2.66	4.61
2945.050	19788–53734	2.45		−0.45	−0.52						−0.48	2.99	4.94
2945.870	26628–60564	3.30		−1.39							−1.39	2.08	4.03
2946.095	12969–46902	1.61		−2.25							−2.25	1.22	3.17
2947.116	26628–60549	3.30	U V182	0.24							0.24	3.71	5.66
2947.363	18378–52297	2.28	U V131	−0.42	−0.32						−0.37	3.10	5.05
2947.877	416–34329	0.05	U V 1		−0.45	−0.55		−0.53[3]		−0.42	−0.43	3.04	4.99
2948.433	21999–55906	2.73	U V166	0.25	0.23	0.26					0.25	3.72	5.67
2948.733	17727–51630	2.20	U V118	−0.99							−0.99	2.48	4.43
2949.688	17727–51619	2.20	U V117	−1.54							−1.54	1.93	3.87
2950.240	17550–51436	2.18	U V120	0.08	−0.18				−0.39		−0.28	3.19	5.13
2951.356	19788–53661	2.45		−1.27							−1.27	2.20	4.14
2953.486	22249–56098	2.76	U V166	0.12	0.36						0.24	3.71	5.65
2953.941	704–34547	0.09	10		−0.62	−0.65		−0.63[3]		−0.50	−0.61	2.86	4.80
2954.654	18378–52213	2.28	U V132	−0.13	−0.23				−0.33		−0.23	3.24	5.18
2956.710	17550–51361	2.18	U V118	−1.00							−1.00	2.47	4.41
2956.860	21716–55526	2.69	U V165	−0.72							−0.72	2.75	4.69
2957.366	888–34692	0.11	10		−0.87	−0.90		−0.72[2]	−0.75	−0.69	−0.77	2.70	4.64
2958.462	21999–55791	2.73	317	−1.39							−1.39	2.08	4.02
2959.682	22650–56428	2.81	U V172	−0.01							−0.01	3.46	5.40
2959.993	21716–55490	2.69	316	0.62	0.74	0.61					0.66	4.13	6.07
2960.299	20038–53808	2.48	148	−0.39	−0.28						−0.34	3.13	5.07
2960.666	23784–57550	2.95	U V178	−0.63							−0.63	2.84	4.78
2961.700	17550–51305	2.18	U V119	−2.29							−2.29	1.18	3.12
2962.110	11976–45726	1.48	57	−2.02							−2.02	1.45	3.39
2963.710	23111–56843	2.86	U V173	−1.24							−1.24	2.23	4.17
2964.196	20875–54600	2.59		−1.18							−1.18	2.29	4.23
2965.256	978–34692	0.12	10		−0.96	−1.15		−0.98[2]	−0.97	−0.91	−0.99	2.48	4.42
2965.811	19621–53329	2.43	U V147	−0.49							−0.49	2.98	4.92
2966.260	17927–51630	2.22	104	−0.80	−0.92						−0.86	2.61	4.55
2966.900	0–33695	0.00	10		−0.27	−0.29		−0.18[2]		−0.12	−0.21	3.26	5.20
2968.481	19552–53230	2.42	U V135	−0.67							−0.67	2.80	4.74
2969.361	888–34556	0.11	11	−1.65	−1.61	−1.82			−1.83		−1.73	1.74	3.68
2969.476	6928–40594	0.86	30	−0.79	−0.74	−0.77		−0.63[1]			−0.73	2.74	4.68
2970.106	888–34547	0.11	10		−0.73	−0.89		−0.58[1]		−0.68	−0.72	2.75	4.69
2972.277	17727–51361	2.20	104	−0.50	−0.54				−0.71		−0.58	2.89	4.82
2973.134	704–34329	0.09	10		−0.46	−0.67			−0.49		−0.54	2.93	4.86
2973.237	416–34040	0.05	10		−0.39	−0.40			−0.23		−0.34	3.13	5.06
2974.780	22846–56452	2.83	335	−0.95							−0.95	2.52	4.45
2975.655	20641–54237	2.56			−0.55						−0.55	2.92	4.85
2976.126	18378–51969	2.28	146	−0.20	−0.12	−0.47			−0.19		−0.24	3.23	5.16
2976.550	11976–45563	1.48	56	−1.74							−1.74	1.73	3.66
2976.922	22846–56428	2.83	334	−1.05							−1.05	2.42	4.35
2978.060	19788–53358	2.45		−1.39							−1.39	2.08	4.01
2980.532	22249–55791	2.76	317	−0.04	0.16	−0.27					−0.05	3.42	5.35
2981.446	416–33947	0.05	11		−1.00	−1.04		−1.12[2]	−1.00	−0.91	−1.03	2.44	4.37
2981.852	17550–51077	2.18	104	−0.07	0.06	−0.45			−0.55				
2982.234	24119–57641	2.99	460	−0.98							−0.98	2.49	4.42
2983.571	0–33507	0.00	9		−0.38	−0.39		−0.37[3]		−0.27	−0.36	3.11	5.04
2984.785	6928–40422	0.86	29	−0.89		−0.61					−0.75	2.72	4.65
2986.457	888–34363	0.11	11	−2.12		−2.35			−2.18		−2.22	1.26	3.18
2986.653	19621–53094	2.43	200	−0.89	0.00						−0.89	2.59	4.51
2987.292	7377–40842	0.91	30	−0.44	−0.61	−0.56		−0.60[2]	−0.52		−0.56	2.92	4.84
2988.473	11976–45428	1.48	56	−1.24					−1.56		−1.40	2.08	4.00
2988.942	21999–55446	2.73	316	−1.25							−1.25	2.23	4.15
2990.393	21999–55430	2.73	316	0.44	0.53	0.42			0.46		0.46	3.94	5.86

TABLE 3.—*Oscillator Strengths for Ultraviolet Lines of Fe* I—Continued

Wavelength Å	Energy Levels K	Low e.p. Volts	Mult. No.	Arc	Spk	CB	HC	R(N)	KOC	MS	Best	Log gfλ	Log gA/λ
				Log *gf*									
2994.428	416–33802	0.05	9		−0.34	−0.42		−0.38[3]		−0.22	−0.35	3.13	5.04
2994.503	978–34363	0.12	11	−0.23							−0.23	3.25	5.16
2995.838	24339–57709	3.02	460	−1.30							−1.30	2.18	4.09
2996.386	19552–52916	2.42	148	−0.09	0.01	−0.40			−0.03		−0.13	3.35	5.26
2999.512	6928–40257	0.86	30		0.10	−0.15		−0.10[5]		0.06	−0.06	3.42	5.33
3000.453	11976–45295	1.48	56	−0.23	−0.33	−0.39					−0.32	3.16	5.07
3000.949	704–34017	0.09	9		−0.35	−0.43		−0.38[3]		−0.25	−0.36	3.12	5.03
3001.663	24336–57641	3.02	506	−0.85							−0.85	2.63	4.54
3003.032	7728–41018	0.96	30		−0.50	−0.61		−0.55[2]	−0.49		−0.54	2.94	4.85
3004.119	19621–52899	2.43	199	−0.56							−0.56	2.92	4.83
3004.620	12561–45833	1.56	57	−1.87							−1.87	1.61	3.52
3005.302	19390–52655	2.40	199	−0.38	−0.18						−0.28	3.20	5.11
3006.598	20641–53892	2.56		−1.20							−1.20	2.28	4.19
3007.147	11976–45221	1.48	55	−0.17	−0.32	−0.55					−0.35	3.13	5.04
3007.283	704–33947	0.09	11		−1.26	−1.48		−1.12[1]	−1.41	−1.23	−1.30	2.18	4.09
3008.140	888–34122	0.11	9		−0.50	−0.50		−0.50[2]	−0.58	−0.48	−0.51	2.97	4.88
3009.094	19390–52613	2.40	198	−0.03	0.04				−0.23		−0.07	3.41	5.32
3009.571	7377–40594	0.91	30		−0.09	−0.21		−0.15[3]	−0.13	−0.16	−0.15	3.33	5.24
3011.482	22249–55446	2.76	316	0.50	0.54	0.43			0.68		0.54	4.02	5.93
3011.883	20038–53230	2.48	U V135	−0.92							−0.92	2.56	4.47
3014.175	7728–40895	0.96	31	−1.79	−1.54				−1.73		−1.69	1.79	3.70
3015.913	19621–52769	2.43	198	−0.20	−0.11				−0.24		−0.18	3.30	5.21
3016.186	7986–41131	0.99	30		−0.70	−0.69		−0.72[2]	−0.58		−0.68	2.80	4.71
3017.629	888–34017	0.11	9		−1.13	−1.16		−1.18[2]	−1.26	−1.11	−1.17	2.31	4.21
3018.134	19390–52514	2.40	199	−0.83							−0.83	2.65	4.55
3018.985	7728–40842	0.96	30		−0.25	−0.37		−0.31[1]	−0.23	−0.32	−0.30	3.18	5.08
3019.290	19788–52899	2.45	199	−0.23							−0.23	3.25	5.15
3020.492	704–33802	0.09	9			−0.71			−1.14				
3020.640	0–33096	0.00	9			−0.13					−0.13	3.35	5.25
3021.074	416–33507	0.05	9		−0.19	−0.32				−0.06	−0.19	3.29	5.19
3024.034	888–33947	0.11	11		−1.04	−1.05		−1.16[2]	−1.16	−0.99	−1.09	2.39	4.29
3025.283	7377–40422	0.91	29	−1.67					−1.68		−1.68	1.80	3.70
3025.638	19390–52431	2.40	198	0.63	0.92	0.84					0.80	4.28	6.18
3025.844	978–34017	0.12	9		−0.50	−0.88		−0.54[3]	−0.51	−0.48	−0.57	2.91	4.81
3026.464	7986–41018	0.99	30		−0.42	−0.35		−0.47[2]	−0.54		−0.45	3.03	4.93
3029.235	12561–45563	1.56	56	−1.05	−1.02				−1.28		−1.12	2.36	4.26
3030.149	19621–52613	2.43	198	0.71	0.78	0.87			0.90		0.82	4.30	6.20
3030.605	18378–51365	2.28	145	−1.37							−1.37	2.11	4.01
3031.213	19788–52769	2.45	198	0.57	0.72	0.88			0.71		0.72	4.20	6.10
3031.638	8155–41131	1.01	30		−0.47	−0.31		−0.51[2]	−0.44	−0.51	−0.46	3.02	4.92
3033.101	19552–52512	2.42	146	−0.73	−0.65						−0.69	2.79	4.69
3034.510	12969–45914	1.61	57	−1.30							−1.30	2.18	4.08
3037.390	888–33802	0.11	9		0.32	−0.50		−0.45[4]		−0.30	−0.43	3.05	4.95
3037.781	7986–40895	0.99	31	−1.56					−1.81		−1.68	1.80	3.70
3039.322	19621–52514	2.43	199	−0.77	−0.38						−0.77	2.71	4.61
3040.428	7377–40257	0.91	30	−0.60	−0.64	−0.46		−0.66[2]	−0.64	−0.72	−0.63	2.85	4.75
3041.639	12561–45428	1.56	56		−0.26	−0.21			−0.52		−0.33	3.15	5.04
3041.740	7728–40594	0.96	30		−0.50	−0.57		−0.56[1]	−0.49		−0.53	2.95	4.84
3042.022	8155–41018	1.01	30		−0.69	−0.82		−0.77[1]	−0.78	−0.81	−0.77	2.71	4.60
3042.667	7986–40842	0.99	30	−0.21	−0.53	−0.34		−0.56[2]	−0.56	−0.63	−0.48	3.00	4.89
3045.077	7377–40207	0.91	29	−1.12	−1.29						−1.20	2.28	4.17
3045.594	19788–52613	2.45	198	−0.88	−0.51						−0.70	2.78	4.67
3046.930	19621–52431	2.43	198	−0.76	−0.52						−0.64	2.84	4.73
3047.050	23784–56593	2.95	457	−0.32	−0.17						−0.24	3.24	5.13
3047.606	704–33507	0.09	9		−0.31	−0.40		−0.35[4]		−0.22	−0.33	3.15	5.04
3053.065	19552–52297	2.42	146	0.05	0.06						0.06	3.54	5.43
3053.440	8155–40895	1.01	31	−1.67							−1.67	1.81	3.70
3055.264	12561–45282	1.56	55	−0.13	−0.33	−0.29					−0.25	3.24	5.12
3056.250	21039–53749	2.61		−0.72							−0.72	2.77	4.65
3057.447	6928–39626	0.86	28		0.22	0.05		0.12[5]	0.17	0.24	0.14	3.63	5.51

TABLE 3.—*Oscillator Strengths for Ultraviolet Lines of Fe* I—Continued

Wavelength Å	Energy Levels K	Low e.p. Volts	Mult. No.	Arc	Spk	CB	HC	R(N)	KOC	MS	Best	Log gfλ	Log gA/λ
				Log *gf*									
3057.802	7728–40422	0.96	29	−1.92							−1.92	1.57	3.45
3059.087	416–33096	0.05	9		−0.43	−0.56		−0.44[4]		−0.37	−0.44	3.05	4.93
3060.545	24119–56783	2.99	457	−0.43	−0.38						−0.40	3.09	4.97
3060.985	12561–45221	1.56	55	−0.86	−1.06				−1.23		−1.05	2.44	4.32
3062.872	23784–56423	2.95	456	−0.99							−0.99	2.50	4.38
3063.149	17550–50187	2.18	102	−1.85							−1.85	1.64	3.52
3063.933	19552–52181	2.42	147	−0.49	−0.23						−0.36	3.13	5.01
3066.483	21999–54600	2.73	313	−0.11	−0.13				1.94		−0.12	3.37	5.24
3067.246	7377–39970	0.91	28		0.10	−0.11		−0.05[5]	0.30		0.00	3.49	5.36
3067.952	21716–54301	2.69	315a	−0.38	−0.15						−0.26	3.23	5.10
3068.175	12969–45552	1.61	55	−0.18	−0.48				−0.28		−0.31	3.18	5.05
3073.244	24575–57104	3.05	549	−1.17							−1.17	2.32	4.19
3073.982	21716–54237	2.69	313	−0.48							−0.48	3.01	4.88
3074.157	24339–56859	3.02	457	−0.49							−0.49	3.00	4.87
3075.721	7728–40231	0.96	28	−0.16	0.05	−0.15		−0.22[4]	−0.11	−0.09	−0.15	3.34	5.21
3078.014	7728–40207	0.96	29	−1.25	−1.37				−1.54		−1.39	2.10	3.97
3078.436	20038–52512	2.48	146	−0.12	0.22						0.05	3.54	5.41
3081.278	24339–56783	3.02	457	−1.34							−1.34	2.15	4.02
3081.832	11976–44415	1.48	53	−1.82							−1.82	1.67	3.54
3083.152	19788–52213	2.45	197	−0.90							−0.90	2.59	4.46
3083.743	7986–40405	0.99	28	−0.16	−0.14	−0.27		−0.20[2]	−0.25	−0.29	−0.22	3.27	5.14
3087.420	26140–58520	3.24		−0.49							−0.49	3.00	4.87
3090.209	22249–54600	2.76	313	−0.53							−0.53	2.96	4.82
3091.579	8155–40491	1.01	28	−0.27	−0.38	−0.34		−0.44[2]	−0.41	−0.52	−0.40	3.09	4.95
3092.778	7728–40052	0.96	29	−1.85	−1.96						−1.90	1.59	3.45
3093.806	12969–45282	1.61	55	−0.76	−0.74				−1.21				
3094.870	21999–54301	2.73	315a	−0.65							−0.65	2.84	4.70
3095.270	21716–54014	2.69	314	−0.63							−0.63	2.86	4.72
3096.044	21999–54289	2.73		−1.10							−1.10	2.39	4.25
3098.192	21716–53983	2.69	313	0.19	0.15				0.15		0.16	3.65	5.51
3098.963	17927–50189	2.22	102	−1.37							−1.37	2.12	3.98
3099.897	8155–40405	1.01	28	0.04	−0.02	0.10			−0.29		−0.04	3.45	5.31
3099.970	7377–39626	0.91	28						−0.27		−0.27	3.22	5.08
3100.305	7986–40231	0.99	28	−0.19	−0.16	−0.25		−0.19[1]	−0.25	−0.39	−0.24	3.25	5.11
3100.667	7728–39970	0.96	28	−0.17	−0.13	−0.28		−0.16[1]	−0.22	−0.26	−0.20	3.29	5.15
3100.838	19390–51630	2.40	196a	−0.38							−0.38	3.11	4.97
3101.004	21999–54237	2.73	313	−0.88							−0.88	2.61	4.47
3102.644	7986–40207	0.99	29	−2.10							−2.10	1.39	3.25
3103.760	19552–51762	2.42		−1.32							−1.32	2.17	4.03
3107.978	21716–53882	2.69		−0.73							−0.73	2.76	4.62
3109.050	19913–52067	2.47	165	−1.36							−1.36	2.13	3.99
3111.686	20641–52769	2.56	260	−0.79							−0.79	2.70	4.55
3112.079	23784–55907	2.95	455	−0.03	0.32						0.14	3.63	5.48
3113.592	22249–54357	2.76		−0.41							−0.41	3.08	4.93
3114.054	12561–44664	1.56	53	−2.55							−2.55	0.94	2.79
3115.656	24772–56859	3.07		−1.18							−1.18	2.31	4.16
3115.862	24339–56423	3.02	456	−1.47							−1.47	2.02	3.87
3116.250	19757–51837	2.45	165	−0.96							−0.96	2.53	4.38
3116.634	8155–40231	1.01	28	−0.69		−0.88		−0.73[2]	−1.07		−0.82	2.67	4.52
3116.984	26140–58213	3.24	578a	−1.24							−1.24	2.25	4.10
3117.640	7986–40052	0.99	29	−1.98					−2.39		−2.18	1.31	3.16
3119.496	19621–51668	2.43	194	0.20	0.07				−0.09		0.06	3.55	5.40
3120.220	22249–54289	2.76		−0.83							−0.83	2.66	4.51
3120.436	19788–51826	2.45	194	0.12	0.01				−0.14		0.00	3.49	5.34
3121.760	17927–49951	2.22	102	−1.19							−1.19	2.30	4.15
3123.353	19562–51570	2.42	164	−0.88							−0.88	2.61	4.46
3123.545	21999–54005	2.73		−1.22							−1.22	2.27	4.12
3124.099	20020–52020	2.48	165	−1.28							−1.28	2.21	4.06
3125.653	7986–39970	0.99	28	−0.52	−0.70	−0.65		−1.00[1]	−0.93		−0.76	2.73	4.58
3128.901	12561–44512	1.56	54	−1.47							−1.47	2.03	3.87

TABLE 3.—*Oscillator Strengths for Ultraviolet Lines of Fe* I—Continued

Wavelength Å	Energy Levels K	Low e.p. Volts	Mult. No.	Arc	Spk	CW(N)	HC	R(N)	KOC	MS	Best	Log gfλ	Log gA/λ
				Log *gf*							Log gf		
3129.178	19757–51705	2.45	161	−0.72							−0.72	2.78	4.62
3129.335	11976–43923	1.48	52	−0.76	−1.04				−1.34				
3132.514	25900–57814	3.21	578	0.08	−0.10						−0.01	3.49	5.33
3134.112	7728–39626	0.96	28		−1.05				−1.18		−1.12	2.38	4.22
3135.590	21999–53882	2.73		−0.92							−0.92	2.58	4.41
3135.863	19788–51668	2.45	194	−0.97							−0.97	2.53	4.36
3139.661	19351–51192	2.40	155	−0.90	−0.47			−0.66[1]			−0.78	2.72	4.55
3140.391	26140–57974	3.24	578	0.19	−0.07						0.06	3.56	5.39
3142.453	19757–51570	2.45	164	0.04	−0.25				−0.30		−0.17	3.33	5.16
3142.891	18378–50187	2.28	144	−0.09	−0.20				−0.48		−0.26	3.24	5.07
3143.243	0–31805	0.00	7	−2.67					−3.20		−3.20	0.30	2.13
3143.990	25900–57698	3.21	578	0.47	0.19						0.33	3.83	5.66
3144.488	19913–51705	2.47	161	−0.18	−0.37						−0.28	3.22	5.05
3144.924	19621–51409	2.43	195	−1.46							−1.46	2.04	3.87
3145.057	24119–55906	2.99	455	−0.29	−0.13						−0.21	3.29	5.12
3146.475	19562–51335	2.42	160	−1.50							−1.50	2.00	3.83
3147.793	24339–56098	3.02	455	−0.50	−0.24	−0.30[1]					−0.35	3.15	4.98
3148.178	22249–54005	2.76		−1.22							−1.22	2.28	4.11
3148.408	19621–51374	2.43	194	−0.65	−0.38	−0.63[1]					−0.55	2.95	4.78
3149.492	23784–55526	2.95	453	−1.49							−1.49	2.01	3.84
3150.304	26479–58213	3.28	578a	−0.13	−0.24	0.02[1]					−0.12	3.38	5.21
3151.353	21999–53722	2.73	311	0.41		0.45[1]					0.43	3.93	5.76
3151.867	416–32134	0.05	7	−2.91							−2.91	0.59	2.42
3153.200	19757–51462	2.45	161	0.23	−0.06	0.10[1]			−0.18		0.02	3.52	5.35
3154.505	19913–51604	2.47	161	−0.17		−0.31[1]					−0.24	3.26	5.09
3155.134	20020–51705	2.48	161	−1.26							−1.26	2.24	4.07
3155.293	19621–51305	2.43	193	−0.52	−0.50	−0.63[1]					−0.55	2.95	4.78
3155.796	19390–51069	2.40	192a	−1.35							−1.35	2.15	3.98
3156.275	26140–57814	3.24	578	0.30	0.05	0.40[1]					0.25	3.75	5.58
3156.464	24119–55791	2.99	454	−0.64	−0.32						−0.48	3.02	4.85
3157.040	19562–51229	2.42	160	0.36	0.06	0.35[1]			0.06		0.21	3.71	5.54
3157.880	19913–51570	2.47	164	0.26	−0.10	0.26[1]			−0.17		0.06	3.56	5.39
3158.990	23784–55430	2.95	452	−0.89							−0.89	2.61	4.44
3159.248	21039–52683	2.61	259	−1.43							−1.43	2.07	3.90
3159.437	22249–53892	2.76		−1.38							−1.38	2.12	3.95
3160.200	26340–57974	3.26	578	0.00	−0.08						−0.04	3.46	5.28
3160.344	19390–51023	2.40	192a	−0.37	−0.22						−0.30	3.20	5.02
3160.658	19562–51192	2.42	155	0.46	0.14	0.39[1]		0.28[1]	0.16		0.29	3.79	5.61
3161.373	12561–44184	1.56	52	−0.94	−1.09	−0.96[1]			−1.41				
3161.558	19788–51409	2.45	195	−1.25							−1.25	2.25	4.07
3161.949	19351–50968	2.40	160	0.16	0.13	0.13[1]			−0.13		0.07	3.57	5.39
3162.335	19757–51370	2.45	159	−0.44	−0.63						−0.54	2.96	4.78
3164.308	19757–51351	2.45	163	−0.85	−0.61						−0.73	2.77	4.59
3165.005	19562–51149	2.42	155	−0.24	−0.43	−0.32[1]		−0.47[1]			−0.36	3.14	4.96
3165.860	19757–51335	2.45	160	−0.01	−0.18	−0.06[1]			−0.29		−0.14	3.36	5.18
3166.435	20641–52213	2.56	259	0.28	0.21	0.22[1]			0.15		0.22	3.72	5.54
3166.596	17727–49298	2.20	100	−0.01							−0.01	3.49	5.31
3166.982	24339–55906	3.02	455	−1.51							−1.51	1.99	3.81
3167.907	26140–57698	3.24	578	0.07		0.19[1]					0.13	3.63	5.45
3168.858	19913–51461	2.47	160	−0.42		−0.21[1]					−0.32	3.18	5.00
3171.353	11976–43500	1.48	52	−1.01	−0.66	−0.90[1]					−0.86	2.64	4.46
3171.663	20020–51540	2.48	160	−0.59							−0.59	2.91	4.73
3172.067	17727–49243	2.20	99	−0.61	−0.58	−0.62[1]					−0.60	2.90	4.72
3172.292	22249–53763	2.76	312	−1.27							−1.27	2.23	4.05
3173.400	23245–54748	2.88	333	−0.55							−0.55	2.95	4.77
3173.663	17727–49227	2.20	101	−0.57	−0.59	−0.41[1]					−0.52	2.98	4.80
3174.222	26479–57974	3.28	578	−1.45							−1.45	2.05	3.87
3175.447	19351–50833	2.40	155	0.44	0.13	0.42[2]		0.27[1]	0.25		0.32	3.82	5.64
3175.970	23270–54748	2.88	333	−0.87							−0.87	2.63	4.45
3176.366	21039–52512	2.61	258	−0.45	−0.31	−0.44[1]					−0.40	3.10	4.92

TABLE 3.—*Oscillator Strengths for Ultraviolet Lines of Fe* I—Continued

Wavelength Å	Energy Levels K	Low e.p. Volts	Mult. No.	Arc	Spk	CW(N)	HC	R(N)	KOC	MS	Best	Log gfλ	Log gA/λ
				Log *gf*									
3178.015	19351–50808	2.40	156	0.32	0.01	0.33[1]		0.16[1]	0.06		0.18	3.68	5.50
3178.545	24339–55791	3.02	454	−0.42	−0.24						−0.33	3.17	4.99
3178.967	19621–51069	2.43	192a	−0.48	−0.35	−1.21[1]					−0.42	3.08	4.90
3179.479	12969–44411	1.61	52	−1.14							−1.14	2.36	4.18
3180.223	19757–51192	2.45	155	0.77		0.74[2]		0.66[1]	0.54		0.69	4.19	6.01
3180.756	704–32134	0.09	7	−2.10	−2.19				−2.48		−2.26	1.24	3.06
3181.522	20875–52297	2.59	258	−0.06	0.06						0.00	3.50	5.32
3181.922	24336–55754	3.02	505	−0.13				−0.52[1]			−0.32	3.18	5.00
3182.060	19562–50980	2.42	159	−0.22	−0.42						−0.32	3.18	5.00
3182.980	17727–49135	2.20	100	−0.25		−0.25[1]					−0.25	3.25	5.07
3183.582	19621–51023	2.43	192a	−1.22							−1.22	2.28	4.10
3184.112	26875–58272	3.33	711	−0.72							−0.72	2.78	4.59
3184.622	19757–51149	2.45	155	−0.41	−0.52			−0.49[1]			−0.47	3.03	4.84
3184.896	416–31805	0.05	7	−1.80	−1.99	−1.87[2]		−2.29[1]	−2.15		−2.00	1.50	3.31
3187.171	23245–54612	2.88	333	−0.95							−0.95	2.55	4.36
3188.026	21999–53358	2.73		−0.63							−0.63	2.87	4.68
3188.567	19351–50704	2.40	159	−0.09	−0.19				−0.36		−0.21	3.29	5.10
3188.819	20020–51370	2.48	159	0.29	0.05				0.01		0.12	3.62	5.43
3190.020	20875–52213	2.59	259	−0.74	−0.60	−0.61[1]					−0.65	2.85	4.66
3190.651	24575–55907	3.05	548	−0.23	−0.07						−0.15	3.35	5.16
3190.816	24575–55906	3.05	548	−0.28	0.12						−0.08	3.42	5.23
3191.116	20641–51969	2.56	258	−0.72							−0.72	2.78	4.59
3191.660	0–31323	0.00	8	−1.80	−1.99	−1.86[2]		−2.29[1]	−2.19		−2.00	1.50	3.31
3192.417	17927–49243	2.22	100	−0.96							−0.96	2.54	4.35
3192.799	20020–51331	2.48	155	0.58		0.43[1]		0.48[1]	0.35		0.46	3.96	5.77
3193.227	0–31307	0.00	7		−1.41	−1.68[1]		−1.99[1]	−1.85	−1.74	−1.73	1.77	3.58
3193.303	19913–51219	2.47	159		0.47						0.47	3.97	5.78
3194.422	19913–51208	2.47	155	−0.21	−0.28	−0.07[1]		−0.29[1]			−0.21	3.29	5.10
3196.147	22846–54125	2.83	333	0.13		0.24[1]					0.18	3.68	5.49
3196.930	19562–50833	2.42	155	1.04	0.77	1.00[2]		1.01[1]		0.74	0.93	4.43	6.24
3197.521	27560–58825	3.42	711	−0.43							−0.43	3.07	4.88
3198.266	21039–52297	2.61	258	−1.03							−1.03	2.47	4.28
3199.530	19562–50808	2.42	156	0.64	0.29	0.67[2]		0.57[1]			0.57	4.08	5.88
3200.475	19913–51149	2.47	155	0.73	0.52	0.81[2]		0.70[1]	0.41		0.66	4.17	5.97
3200.785	704–31937	0.09	8	−2.59			−2.89		−2.96		−2.81	0.70	2.50
3202.562	24575–55791	3.05	547	−0.09	−0.01	−0.02[1]	−0.08				−0.05	3.46	5.26
3205.400	20020–51208	2.48	155	0.69	0.42	0.67[2]		0.62[1]			0.60	4.11	5.91
3207.089	19351–50523	2.40	159	−0.50		−0.51[1]	−0.79				−0.60	2.91	4.71
3207.649	22838–54005	2.83	382	−1.45			−1.60				−1.52	1.99	3.79
3208.470	27666–58825	3.43	711	0.32	0.17	0.60[1]	0.84						
3209.297	27560–58710	3.42	711	−0.04	0.27	0.90[1]	1.14						
3210.230	19562–50704	2.42	159	0.30	0.03	0.34[1]	0.25				0.25	3.76	5.55
3210.830	19913–51048	2.47	156	0.59	0.36	0.54[2]	0.48	0.53[1]			0.51	4.02	5.81
3211.487	20020–51149	2.48	162	0.09	0.03		−0.22				−0.03	3.48	5.27
3211.683	26875–58002	3.33	711	0.91	0.77		1.03				0.90	4.41	6.20
3211.872	17927–49053	2.22	98	−0.02							−0.02	3.49	5.28
3211.989	19351–50475	2.40	158	0.73		0.70[1]	−0.17				0.72	4.23	6.02
3214.044	19757–50862	2.45	156	1.02	0.90	1.05[2]	1.13	1.05[1]			1.03	4.54	6.33
3214.396	704–31805	0.09	7	−1.86	−1.77	−1.87[1]	−1.79				−1.82	1.69	3.48
3214.624	18378–49477	2.28	143				−1.38				−1.38	2.13	3.92
3215.940	19913–50999	2.47	156	0.59	0.45	0.57[2]	0.56	0.64[1]			0.56	4.07	5.86
3217.380	19351–50423	2.40	157	0.41	0.22	0.37[2]	0.42				0.36	3.87	5.66
3219.581	19757–50808	2.45	156	0.75	0.59	0.63[1]	0.68	0.74[1]			0.68	4.19	5.98
3219.806	19562–50611	2.42	158	0.57	0.44	0.39[1]	0.45				0.46	3.97	5.76
3221.931	20020–51048	2.48	156					−0.98[1]			−0.98	2.53	4.32
3222.069	19351–50378	2.40	156	1.05	0.92	1.09[2]	1.11	1.09[1]			1.06	4.57	6.36
3223.273	11976–42992	1.48	51	−1.89							−1.89	1.62	3.41
3223.480	26628–57641	3.30		−0.97	−0.38						−0.97	2.54	4.33
3223.844	7986–38996	0.99	27	−1.19							−1.19	2.32	4.11
3225.789	19351–50342	2.40	155	1.29	1.07	1.20[2]	1.27	1.26[1]			1.22	4.73	6.52

TABLE 3.—*Oscillator Strengths for Ultraviolet Lines of Fe* I—Continued

Wavelength Å	Energy Levels K	Low e.p. Volts	Mult. No.	Arc	Spk	CW(N)	HC	R(N)	KOC	MS	Best	Log gfλ	Log gA/λ
				Log *gf*									
3226.714	704–31686	0.09	8	−3.13			−3.44				−3.28	0.23	2.02
3227.063	20020–50999	2.48	156	−0.43		−0.29[1]	−0.76	−0.38[1]			−0.37	3.14	4.93
3227.798	19562–50534	2.42	157	0.80			0.69				0.74	4.25	6.04
3228.003	22838–53808	2.83	379	0.19			−0.26				0.19	3.70	5.49
3228.254	19913–50880	2.47	157	0.23	0.12		−0.03				0.11	3.62	5.41
3228.900	20020–50981	2.48	157	−0.18	−0.32		−0.34				−0.28	3.23	5.02
3229.122	978–31937	0.12	8	−2.26	−2.31		−2.28				−2.28	1.23	3.02
3229.595	22846–53801	2.83	333	−0.63	−0.52						−0.58	2.93	4.72
3229.994	24575–55526	3.05	546	0.28	0.37						0.32	3.83	5.62
3230.210	19913–50861	2.47	158	0.27	0.00		−0.08				0.06	3.57	5.36
3230.963	19757–50699	2.45	157	0.47	0.21	0.47[2]	0.29				0.38	3.89	5.68
3231.576	11976–42912	1.48	50				−1.57				−1.57	1.94	3.73
3232.155	21039–51969	2.61	258	−1.66							−1.66	1.85	3.64
3233.053	26106–57028	3.24	620	0.68	0.91	0.93[1]	0.94				0.86	4.37	6.16
3233.967	19562–50475	2.42	158	0.47	0.27	0.45[2]	0.40				0.41	3.92	5.70
3234.614	416–31323	0.05	8	−2.08	−2.18	−2.12[1]	−2.10				−2.12	1.39	3.17
3235.312	21999–52899	2.73	309	−1.93							−1.93	1.58	3.36
3235.592	21716–52613	2.69	308	−1.11			−1.36				−1.24	2.27	4.05
3235.833	22838–53734	2.83		−1.37							−1.37	2.14	3.92
3236.223	416–31307	0.05	7	−1.88	−1.91	−1.96[1]	−1.77				−1.88	1.63	3.41
3237.234	20875–51756	2.59	256	−1.54							−1.54	1.97	3.75
3238.313	24575–55446	3.05	545	−1.52							−1.52	1.99	3.77
3238.535	24507–55376	3.04	397				−1.36				−1.36	2.15	3.93
3239.029	18378–49243	2.28	142	−1.09			−1.32				−1.20	2.31	4.09
3239.436	19562–50423	2.42	157	0.74	0.53	0.90[2]	0.80				0.77	4.28	6.06
3240.013	24575–55430	3.05	545				−1.33				−1.33	2.18	3.96
3240.122	19757–50611	2.45	158	−1.28							−1.28	2.23	4.01
3241.502	8155–38996	1.01	27	−3.26			−2.03				−3.26	0.25	2.03
3242.268	20875–51708	2.59	255	−1.46			−1.53				−1.50	2.01	3.79
3243.109	19788–50614	2.45	192	−0.94			−1.03				−0.98	2.53	4.31
3243.406	26875–57698	3.33	710	−0.11	0.00		0.05				−0.02	3.49	5.27
3244.190	19562–50378	2.42	156	0.70	0.47	0.80[2]	0.81	0.68[1]			0.71	4.22	6.00
3246.005	888–31686	0.11	8	−2.05	−2.06	−2.06[1]	−2.15				−2.08	1.43	3.21
3246.482	20875–51668	2.59	252	−0.39	−0.23		−0.56				−0.39	3.12	4.90
3246.962	17727–48516	2.20	95	−0.15	−0.07		−0.67				−0.11	3.40	5.18
3247.278	19913–50699	2.47	157	−0.17	−0.08		−0.30				−0.18	3.33	5.11
3248.206	19757–50534	2.45	157	0.33	0.14	0.34[1]	−0.24				0.27	3.78	5.56
3249.037	21999–52769	2.73	308	−1.39							−1.39	2.12	3.90
3249.191	20641–51409	2.56	253	−0.56	−0.34	−0.68[1]	−0.56				−0.54	2.97	4.75
3249.504	12561–43326	1.56	51	−2.52							−2.52	0.99	2.77
3250.394	23052–53808	2.86	379	−0.65			0.21				−0.65	2.86	4.64
3250.625	17550–48305	2.18	95	−0.41	−0.45	−0.39[1]	−0.59				−0.46	3.05	4.83
3251.236	17727–48476	2.20	93	−0.23	−0.15	−0.08[1]	−0.65				−0.15	3.36	5.14
3252.916	20641–51374	2.56	252	−0.31	−0.18	−0.32[1]	−0.37				−0.30	3.21	4.99
3253.610	26225–56951	3.25	681	0.10	0.34	0.14[1]	−0.07				0.13	3.64	5.42
3253.834	20641–51365	2.56	250				−0.85				−0.85	2.66	4.44
3253.949	21039–51762	2.61	257	−0.69	−0.33		−0.82				−0.51	3.00	4.78
3254.363	26351–57070	3.27	620	0.67	0.90	0.82[1]	0.83				0.80	4.31	6.09
3254.734	21716–52431	2.69	308	−0.92			−1.14				−1.03	2.48	4.26
3257.244	24119–54811	2.99	451	−0.35	−0.15						−0.25	3.26	5.04
3257.594	17550–48239	2.18	90	−0.04	−0.08	−1.16[1]	−0.36				−0.16	3.35	5.13
3259.991	19757–50423	2.45	157	−0.22	−0.33	−0.31[1]	−0.34				−0.30	3.21	4.98
3260.261	20641–51305	2.56	250	−0.55	−0.26		−0.64				−0.48	3.03	4.80
3261.332	27560–58213	3.42	712	−0.39		−0.25[1]	−0.15				−0.26	3.25	5.02
3262.009	27167–57814	3.37	710	−0.34		0.05[1]					−0.14	3.37	5.14
3263.370	19552–50187	2.42	144	−0.84	−0.43	−0.83[1]	−0.74				−0.71	2.80	4.57
3264.512	17727–48351	2.20	90	−0.41	−0.31	−0.28[1]	−0.46				−0.36	3.15	4.92
3264.710	19913–50534	2.47	157	−0.96	−0.59		−1.14				−0.78	2.73	4.50
3265.047	704–31323	0.09	8	−2.20	−2.27	−2.12[1]	−2.14				−2.18	1.33	3.10
3265.618	17550–48163	2.18	91	0.47	0.43	0.47[2]	0.51	0.42[1]			0.46	3.97	5.74

TABLE 3.—*Oscillator Strengths for Ultraviolet Lines of Fe* I—Continued

Wavelength Å	Energy Levels K	Low e.p. Volts	Mult. No.	Arc	Spk	CW(N)	HC	R(N)	KOC	MS	Best	Log gfλ	Log gA/λ
				Log *gf*									
3268.234	17927–48516	2.22	95	−0.41	−0.38	−0.38[1]	−0.64				−0.45	3.06	4.83
3269.235	27395–57974	3.40	710	−0.52		−0.29[1]					−0.40	3.11	4.88
3269.416	17727–48305	2.20	95	−1.94							−1.94	1.57	3.34
3269.964	17550–48123	2.18	90	−1.67			−0.57				−1.67	1.84	3.61
3271.001	17727–48290	2.20	91	0.48	0.41	0.51[2]	0.54	0.46[1]			0.48	3.99	5.76
3271.487	26225–56783	3.25	680	−0.51	−0.27		−0.37				−0.38	3.13	4.90
3271.684	11976–42533	1.48	49	−1.57			−1.70				−1.64	1.87	3.64
3272.596	12561–43109	1.56	95	−1.98							−1.98	1.53	3.30
3272.710	27666–58213	3.43	712	−1.04		−0.60[1]	−0.73				−0.79	2.72	4.49
3274.227	17927–48460	2.22	95	−1.84							−1.84	1.68	3.44
3274.453	27167–57698	3.37	710	−0.11	−0.12	−0.01[1]	−0.09				−0.08	3.44	5.20
3275.685	22249–52769	2.76	308	−1.34			−1.30				−1.32	2.20	3.96
3275.848	23784–54301	2.95	450a	−1.53			−1.58				−1.56	1.96	3.72
3276.471	17727–48239	2.20	90	−0.54	−0.54	−0.65[1]	−0.70				−0.61	2.91	4.67
3278.741	19552–50043	2.42	144	−0.45	−0.38	−0.47[1]	−0.56				−0.46	3.06	4.82
3279.739	24119–54600	2.99	449	−0.69			−0.84				−0.76	2.76	4.52
3280.261	26628–57104	3.30	620	0.66	0.81	0.81[1]	0.82				0.78	4.30	6.06
3280.763	24339–54811	3.02	451	−2.17			−1.07				−2.17	1.35	3.11
3281.824	12561–43023	1.56	50	−2.38							−2.38	1.14	2.90
3282.720	23784–54237	2.95	449	−1.35							−1.35	2.17	3.93
3282.891	26406–56859	3.27	680	0.21	0.24	0.12[1]	0.01				0.14	3.66	5.42
3283.430	7728–38175	0.96	27	−2.99			−2.26				−2.99	0.53	2.28
3284.589	17727–48163	2.20	91	−0.27	−0.35	−0.27[1]	−0.46	−0.27[1]			−0.32	3.20	4.95
3285.200	24181–54612	3.00	396	−0.79		−0.05[1]	−0.05						
3286.022	17927–48351	2.22	90	−0.92	−0.41		−1.01				−0.96	2.56	4.31
3286.444	27395–57814	3.40	710	−0.30							−0.30	3.22	4.97
3286.754	17550–47967	2.18	91	0.81	0.77	0.80[2]	1.04	0.90[1]			0.85	4.37	6.12
3287.117	23711–54125	2.94	396	−0.48			−0.66				−0.57	2.95	4.70
3288.651	19552–49951	2.42	144	−1.01							−1.01	2.51	4.26
3288.967	17727–48123	2.20	90	−0.89	−0.75		−0.93				−0.86	2.66	4.41
3289.442	22838–53230	2.83	380	−0.83			−0.90				−0.86	2.66	4.41
3290.714	17550–47930	2.18	90	−1.13			−1.47				−1.30	2.22	3.97
3290.990	17927–48305	2.22	95	−0.19	−0.21	−0.24[1]	−0.29				−0.23	3.29	5.04
3292.022	26225–56593	3.25	680	0.61	0.70	0.71[1]	0.63				0.66	4.18	5.93
3292.591	17927–48290	2.22	91	0.16	0.12	0.21[1]	0.22	0.23[1]			0.19	3.71	5.46
3293.142	12969–43326	1.61	51	−2.06							−2.06	1.46	3.21
3296.467	20875–51201	2.59	250	−1.00	−0.64		−1.07				−0.82	2.70	4.45
3296.806	26628–56951	3.30	619	−1.21			−1.07				−1.14	2.38	4.13
3298.133	17927–48239	2.22	90	−0.10	−0.10	−0.12[1]	−0.18				−0.12	3.40	5.15
3298.537	27666–57974	3.43	710	−1.30							−1.30	2.22	3.97
3299.077	27395–57698	3.40	710				−0.92				−0.92	2.60	4.35
3299.509	12561–42860	1.56	49	−2.56			−1.22				−2.56	0.96	2.71
3301.227	22947–53230	2.84	380	−0.93	−0.54		−0.84				−0.77	2.75	4.50
3301.917	26106–56383	3.24	617				−0.44				−0.44	3.08	4.83
3303.574	24339–54600	3.02	449	−0.52			−0.69				−0.60	2.92	4.67
3304.346	27560–57814	3.42	710	−1.42							−1.42	2.10	3.85
3305.972	17727–47967	2.20	91	0.69	0.61	0.80[1]	0.72	0.82[1]			0.73	4.25	6.00
3306.356	17927–48163	2.22	91	0.74	0.81	0.82[1]	0.94	0.87[1]			0.84	4.36	6.11
3306.490	26624–56859	3.30	680				−0.22				−0.22	3.30	5.05
3307.008	23784–54014	2.95	450	−0.85			−0.76				−0.80	2.72	4.47
3307.234	26106–56334	3.24	617	0.35	0.50	0.45[1]	0.46				0.44	3.96	5.71
3308.761	19390–49604	2.40	190	−1.43							−1.43	2.09	3.83
3310.347	23784–53983	2.95	449	−0.19	−0.05		−0.26				−0.17	3.35	5.09
3310.496	26225–56423	3.25	679	−0.23	−0.08		0.02				−0.10	3.42	5.16
3311.451	7986–38175	0.99	27	−3.52							−3.52	0.00	1.74
3312.224	24119–54301	2.99	450a	−1.22							−1.22	2.30	4.04
3313.723	12969–43138	1.61	50	−2.54							−2.54	0.98	2.72
3314.070	27543–57709	3.41	736	−1.02							−1.02	2.50	4.24
3314.441	21039–51201	2.61	250	−0.87			−0.85				−0.86	2.66	4.40
3314.742	26624–56783	3.30	680	0.56	0.63	0.82[1]	0.82				0.71	4.23	5.97

TABLE 3.—*Oscillator Strengths for Ultraviolet Lines of Fe* I—Continued

Wavelength Å	Energy Levels K	Low e.p. Volts	Mult. No.	Arc	Spk	CW(N)	HC	R(N)	KOC	MS	Best	Log gfλ	Log gA/λ
				Log *gf*									
3315.164	26628–56783	3.30	618	−2.30							−2.30	1.22	2.96
3317.121	18378–48516	2.28	139	−0.54	−0.56	−0.61[1]	−0.67				−0.60	2.92	4.66
3319.258	24119–54237	2.99	449	−0.37	−0.31	−0.43[1]	−0.37				−0.37	3.15	4.89
3320.650	19621–49727	2.43	190	−0.89	−0.61						−0.75	2.77	4.51
3320.779	24507–54612	3.04	396	−0.59	−0.46		0.44				−0.52	3.00	4.74
3322.474	23711–53801	2.94	396	−0.18	−0.37	−0.12[1]	−0.11				−0.20	3.32	5.06
3323.738	22838–52916	2.83	379	0.22	0.35	0.30[1]					0.29	3.81	5.55
3324.372	26351–56423	3.27	617	−0.73			−0.47				−0.60	2.92	4.66
3324.538	19390–49461	2.40	191	−0.41	−0.34	−0.39[1]	−0.41				−0.39	3.13	4.87
3325.468	19788–49851	2.45	191	−0.43	−0.41	−0.46[1]	−0.49				−0.45	3.07	4.81
3327.497	19390–49434	2.40	190	−1.05	−0.76	−1.09[1]	−0.81				−0.93	2.59	4.33
3327.961	17550–47590	2.18	86	−2.29							−2.29	1.23	2.97
3328.867	26351–56383	3.27	617	0.42	0.59	−1.59[1]	0.77				0.59	4.11	5.85
3329.532	24575–54600	3.05	542a	−0.68			−0.41				−0.54	2.98	4.72
3329.970	24336–54357	3.02		−1.31							−1.31	2.21	3.95
3330.316	24339–54357	3.02		−1.03							−1.03	2.49	4.23
3331.613	19621–49628	2.43	191	−0.53	−0.61	−0.61[1]	−0.59				−0.58	2.94	4.68
3331.778	20038–50043	2.48	144	−0.91	−0.53		−0.35				−0.72	2.80	4.54
3334.220	19621–49604	2.43	190	−1.22	−0.64	−0.82[1]	−0.87				−0.78	2.74	4.47
3334.278	26351–56334	3.27	617				−0.45				−0.45	3.07	4.80
3335.513	12561–42533	1.56	49	−2.42	−1.30						−2.42	1.10	2.83
3335.770	22947–52916	2.84	379	−0.07	−0.35	−0.16[1]	−0.07				−0.16	3.36	5.09
3336.254	26628–56593	3.30	618	−0.31	−0.02		−0.30				−0.21	3.31	5.04
3337.666	21716–51668	2.69	304	−0.12	−0.15	−0.09[1]	−0.10				−0.12	3.40	5.13
3338.638	24181–54125	3.00	396	−0.44		−0.53[1]	−0.53				−0.50	3.02	4.75
3339.195	19788–49727	2.45	190	−0.69	−0.62	−0.81[1]	−0.68				−0.70	2.82	4.55
3339.582	24336–54271	3.02	502	−0.70							−0.70	2.82	4.55
3340.567	18378–48305	2.28	139	−0.35	−0.35	−0.38[1]	−0.25				−0.33	3.19	4.92
3341.906	21716–51630	2.69	303	−0.24	−0.21		−0.06				−0.17	3.35	5.08
3342.216	18378–48290	2.28	137	−0.52	−0.41	−0.29[1]	−0.31				−0.38	3.14	4.87
3342.298	22947–52858	2.84	378	−0.15	−0.40		0.32				−0.28	3.24	4.97
3343.240	17550–47453	2.18	88	−1.95			−0.78				−1.95	1.57	3.30
3343.678	24339–54237	3.02	449	−0.79			−0.76				−0.78	2.74	4.47
3345.679	19552–49433	2.42	141	−2.40			−1.02				−2.40	1.12	2.85
3346.936	17550–47420	2.18	87	−1.24	−0.97	−1.38[1]	−1.34				−1.23	2.29	4.02
3347.507	24119–53983	2.99	449	−1.50			−0.83				−1.50	2.02	3.75
3347.927	18378–48239	2.28	138	−0.44	−0.43	−0.45[1]	−0.37				−0.42	3.10	4.83
3349.739	22838–52683	2.83	377	−1.65							−1.65	1.88	3.60
3350.284	19788–49628	2.45	191	−1.36							−1.36	2.17	3.89
3351.524	17727–47556	2.20	89	−0.88	−0.75		−0.79				−0.81	2.72	4.44
3351.746	21999–51826	2.73	304	−0.36	−0.30	−0.39[1]	−0.40				−0.36	3.17	4.89
3352.929	19788–49604	2.45	190	−1.45							−1.45	2.08	3.80
3353.267	19621–49434	2.43	190	−1.19	−1.07						−1.13	2.40	4.12
3354.064	23052–52858	2.86	378	−0.27	−0.34	−0.31[1]	−0.04				−0.30	3.23	4.95
3355.229	26628–56423	3.30	617	0.45	0.53	0.59[2]	0.60				0.55	4.08	5.80
3355.517	7728–37521	0.96	25	−3.14							−3.14	0.39	2.11
3356.403	18378–48163	2.28	137	−0.56	−0.67	−0.56[1]					−0.60	2.93	4.65
3356.695	24575–54357	3.05		−0.78							−0.78	2.75	4.47
3359.488	6928–36686	0.86	25	−2.05	−2.01		−2.19				−2.08	1.45	3.17
3359.814	26628–56383	3.30	617	−0.78	−0.35	−0.35[1]	−0.35				−0.35	3.18	4.89
3360.922	19552–49298	2.42	142	−1.44			−1.17				−1.30	2.23	3.94
3361.959	22947–52683	2.84	377	−0.97							−0.97	2.56	4.27
3363.815	22249–51969	2.76	307	−1.30			−0.74				−1.30	2.23	3.94
3364.639	20875–50587	2.59	245	−1.56							−1.56	1.97	3.68
3366.789	21716–51409	2.69	302				0.19				0.19	3.72	5.43
3366.867	17727–47420	2.20	87	−0.27			−0.52				−0.40	3.13	4.84
3367.159	19552–49243	2.42	142				0.29				0.29	3.82	5.53
3368.248	26225–55906	3.25	678	−0.89							−0.89	2.64	4.35
3368.983	22838–52512	2.83	376	−1.63							−1.63	1.90	3.61
3369.146	19788–49461	2.45	191	−1.31							−1.31	2.22	3.93

TABLE 3.—*Oscillator Strengths for Ultraviolet Lines of Fe* I—Continued

Wavelength Å	Energy Levels K	Low e.p. Volts	Mult. No.	Arc	Spk	CW(N)	HC	R(N)	KOC	MS	Best	Log gfλ	Log gA/λ
				Log *gf*									
3369.549	21999–51668	2.73	304	0.62	0.53	0.51[2]	0.48				0.53	4.06	5.77
3370.785	21716–51374	2.69	304	0.72	0.71	0.69[2]	0.93				0.75	4.28	5.99
3372.074	17550–47197	2.18	83	−0.66	−0.74	−0.82[1]	−0.74				−0.74	2.79	4.50
3372.352	24119–53763	2.99	447	−1.73							−1.73	1.80	3.51
3373.874	21999–51630	2.73	303	−1.14	−0.74		−0.66				−0.85	2.68	4.39
3374.176	17927–47556	2.22	89		−1.07						−1.07	2.46	4.17
3375.724	24119–53734	2.99		−1.93							−1.93	1.60	3.31
3378.676	21716–51305	2.69	301	0.17	0.13		0.24				0.18	3.71	5.42
3379.021	17550–47136	2.18	85	−0.15	−0.27		−0.10	−0.20[1]			−0.18	3.35	5.06
3380.112	22249–51826	2.76	304	0.36	0.41	0.33[1]	0.36				0.36	3.89	5.60
3381.340	22947–52512	2.84	376	−0.75	−0.50	0.40[1]	0.37				−0.62	2.91	4.62
3381.990	24507–54067	3.04		−1.44							−1.44	2.09	3.80
3382.404	17550–47107	2.18	84	−0.75	−0.77	−0.74[1]	−0.74				−0.75	2.78	4.49
3383.387	21039–50587	2.61	245	−1.84							−1.84	1.69	3.40
3383.692	17727–47272	2.20	85	−0.25	−0.35		−0.27	−0.21[1]			−0.27	3.26	4.97
3383.981	17550–47093	2.18	83	0.10	0.01	0.17[2]	0.14				0.12	3.65	5.36
3384.765	7986–37521	0.99	25	−3.20							−3.20	0.33	2.04
3387.410	22249–51762	2.76	306	−0.16	−0.28	−0.43[1]	−0.25				−0.28	3.25	4.95
3388.966	24772–54271	3.07	502	−0.92							−0.92	2.61	4.31
3389.748	17927–47420	2.22	87	−0.77	−0.69	−1.01[1]	−0.83				−0.82	2.71	4.41
3392.014	24336–53808	3.02	499	−0.13	−0.19		−0.07				−0.13	3.40	5.10
3392.306	17727–47197	2.20	83	0.01	−0.07	0.15[1]	0.06				0.04	3.57	5.27
3392.654	17550–47017	2.18	85	0.42	0.37	0.46[2]	0.34	0.54[1]			0.43	3.96	5.66
3393.382	23052–52512	2.86	376	−0.75	−0.63		−0.55				−0.64	2.89	4.59
3393.623	22838–52297	2.83	376	−1.28							−1.28	2.25	3.95
3393.915	18378–47834	2.28	136	−1.18			−1.10				−1.14	2.39	4.09
3394.085	19788–49243	2.45	188	−0.93			−1.06				−1.00	2.53	4.23
3394.585	17727–47177	2.20	81	−0.10	−0.26	−0.19[1]	−0.05	−0.21[1]			−0.16	3.37	5.07
3395.080	24339–53785	3.02		−1.70							−1.70	1.83	3.53
3396.386	7728–37163	0.96	25	−2.99							−2.99	0.54	2.24
3396.977	7728–37158	0.96	26		−1.70	−1.63[1]	−1.62				−1.65	1.88	3.58
3397.221	24336–53763	3.02	503	−0.83							−0.83	2.70	4.40
3397.560	24339–53763	3.02	447				−0.90				−0.90	2.63	4.33
3397.640	7986–37410	0.99	26	−1.92	−1.93	−1.90[1]	−1.87				−1.90	1.63	3.33
3398.220	22249–51668	2.76	304	−0.96	−0.60		−1.00				−0.85	2.68	4.38
3399.230	21999–51409	2.73	302				−0.30				−0.30	3.23	4.93
3399.336	17727–47136	2.20	85	0.51	0.42	0.55[2]	0.66	0.61[1]			0.55	4.08	5.78
3400.662	24336–53734	3.02		−1.06							−1.06	2.47	4.17
3401.007	24339–53734	3.02		−1.32							−1.32	2.21	3.91
3401.520	7377–36767	0.91	26	−1.30	−1.45	−1.35[1]	−1.24				−1.34	2.19	3.89
3402.256	26106–55490	3.24	614	0.63	0.63	0.43[1]	0.44				0.53	4.06	5.76
3403.299	21999–51374	2.73	304	−0.52	−0.46		−0.44				−0.47	3.06	4.76
3404.356	17727–47093	2.20	83	0.45	0.32	0.46[2]	0.39				0.42	3.95	5.65
3404.755	21999–51361	2.73	300	−0.98			−0.45				−0.98	2.55	4.25
3404.923	21716–51077	2.69	300	−1.23							−1.23	2.30	4.00
3405.830	21716–51069	2.69	299	−0.64	−0.58						−0.61	2.92	4.62
3406.442	26406–55754	3.27	676	0.23	0.23		0.19				0.22	3.75	5.45
3406.802	17927–47272	2.22	85	0.09	0.03	0.09[1]	0.24	0.21[1]			0.13	3.66	5.36
3407.461	17550–46889	2.18	83	0.79	0.85	0.77[2]	1.10				0.86	4.39	6.09
3409.218	26106–55430	3.24	614	−0.62	−0.38		−0.19				−0.40	3.13	4.83
3409.605	19788–49109	2.45	188	−1.87							−1.87	1.66	3.36
3410.031	24575–53892	3.05	542	−0.57							−0.57	2.96	4.66
3410.171	27543–56859	3.41	735	0.39	0.36	0.27[1]	0.40				0.36	3.89	5.59
3410.905	7377–36686	0.91	25	−2.18	−2.11		−1.52				−2.14	1.39	3.09
3411.134	21716–51023	2.69	299	−1.00			−0.93				−0.96	2.57	4.27
3411.353	21999–51305	2.73	301	0.07	−0.05	−0.14[1]	0.17				0.01	3.54	5.24
3413.134	17727–47017	2.20	85		0.58	0.64[2]	0.74	0.82[1]			0.68	4.21	5.90
3414.564	26628–55906	3.30		−1.00							−1.00	2.53	4.22
3415.532	17927–47197	2.22	83	−0.19	−0.38	−0.37[1]	−0.23				−0.29	3.24	4.93
3416.679	20038–49298	2.48	142	−1.82			−1.07				−1.82	1.71	3.40

TABLE 3.—*Oscillator Strengths for Ultraviolet Lines of Fe* I—Continued

Wavelength Å	Energy Levels K	Low e.p. Volts	Mult. No.	Arc	Spk	CW(N)	HC	R(N)	KOC	MS	Best	Log gfλ	Log gAλ
				Log *gf*									
3417.273	8155–37410	1.01	26	−2.14							−2.14	1.39	3.08
3417.843	17927–47177	2.22	81	0.44	0.39	0.45[2]	1.17	0.48[1]			0.44	3.97	5.66
3418.176	26479–55727	3.28	577	−0.51							−0.51	3.02	4.71
3418.507	17927–47172	2.22	81	0.37	0.29	0.40[2]	0.62	0.40[1]			0.41	3.94	5.63
3418.905	24507–53748	3.04		−0.94							−0.94	2.59	4.28
3419.154	26140–55379	3.24	576	−0.65			−0.46				−0.56	2.97	4.66
3419.706	22947–52181	2.84	377	−0.46	−0.43	−0.67[1]	−0.54				−0.52	3.01	4.70
3422.499	24119–53329	2.99	444	0.30	0.06						0.18	3.71	5.40
3422.658	17927–47136	2.22	85	0.23	0.16	0.25[2]	0.38	0.35[1]			0.27	3.80	5.49
3424.286	17550–46745	2.18	81	0.41	0.29	0.41[2]	0.54	0.43[1]			0.42	3.95	5.64
3425.009	24575–53763	3.05	541	0.45	0.34	0.39[1]	0.49				0.42	3.95	5.64
3426.337	18378–47556	2.28	135				−0.19				−0.19	3.34	5.03
3426.383	17550–46727	2.18	82	0.12		0.18[2]	−0.09	0.05[1]			0.09	3.62	5.31
3426.637	17727–46902	2.20	82	0.14	0.07	0.13[1]	0.24	0.05[1]			0.13	3.66	5.35
3427.121	17550–46721	2.18	81	0.86	0.80	0.75[2]	1.07	0.98[1]			0.87	4.40	6.09
3428.195	17727–46889	2.20	81	0.33	0.24	0.23[2]	0.46	0.34[1]			0.30	3.84	5.52
3428.746	29056–58213	3.60	836	−0.02	−0.27		1.13				−0.14	3.40	5.08
3431.815	22838–51969	2.83	376	−0.03	−0.17	−0.22[1]	−0.16				−0.14	3.40	5.08
3432.023	23052–52181	2.86	377	−1.10							−1.10	2.44	4.12
3434.029	22249–51361	2.76	300	−1.08	−0.83		−1.82				−0.96	2.58	4.26
3436.045	26351–55446	3.27	614	−0.88							−0.88	2.66	4.34
3437.046	24575–53661	3.05	539	0.13		−0.04[1]	0.12				0.07	3.61	5.29
3437.631	19621–48703	2.43	187	−1.63			−1.26				−1.44	2.10	3.78
3437.952	26351–55430	3.27	614	−0.09	−0.03	−0.08[1]	0.13				−0.02	3.52	5.20
3439.039	21999–51069	2.73	299	−0.73	−0.63						−0.68	2.86	4.53
3440.607	0–29056	0.00	6		−0.52	−0.30[1]	−0.11	−0.49[1]			−0.44	3.10	4.77
3440.990	416–29469	0.05	6		−0.69	−0.93[2]	−0.75	−0.79[1]			−0.82	2.72	4.39
3442.364	18378–47420	2.28	134	−0.19	−0.23	−0.13[1]	−0.60				−0.18	3.36	5.03
3442.671	7728–36767	0.96	26	−1.64	−1.89		−1.64				−1.72	1.82	3.49
3442.979	24772–53808	3.07	499				−0.50				−0.50	3.04	4.71
3443.878	704–29733	0.09	6		−0.96	−1.21[1]	−0.99	−1.19[1]			−1.09	2.45	4.12
3445.151	17727–46745	2.20	81	0.52	0.45	0.48[1]	0.79	0.63[1]			0.57	4.11	5.78
3446.791	21039–50043	2.61	244	−1.08			−0.44				−1.08	2.46	4.13
3446.947	8155–37158	1.01	26	−2.53			−0.97				−2.53	1.01	2.68
3447.280	17727–46727	2.20	82	0.06	−0.05	−0.02[2]	0.10	0.04[1]			0.02	3.56	5.23
3448.786	22838–51826	2.83	372	−1.36			−1.02				−1.19	2.35	4.02
3448.869	20641–49628	2.56	242	−1.25							−1.25	2.29	3.96
3450.330	17927–46902	2.22	82	0.14	0.02	0.14[2]	0.27	0.14[1]			0.14	3.68	5.35
3451.628	19552–48516	2.42	139	−0.45	−0.54		−0.54				−0.51	3.03	4.70
3451.917	17927–46889	2.22	81	0.16	0.01	0.20[1]	0.25	0.14[1]			0.15	3.69	5.36
3452.276	7728–36686	0.96	25	−1.08	−1.34	−1.06[1]	−1.07				−1.14	2.40	4.07
3453.022	22249–51201	2.76	301	−0.05	−0.22	−0.29[1]	−0.06				−0.16	3.38	5.05
3457.090	29056–57974	3.60	835	−0.20		−0.32[1]					−0.26	3.28	4.95
3457.512	19788–48703	2.45	187	−1.58							−1.58	1.96	3.63
3458.304	19552–48460	2.42	139	−0.17	−0.29	−0.31[1]	−0.23				−0.25	3.29	4.96
3459.429	21716–50614	2.69	297	−0.41	−0.53		0.19				−0.47	3.07	4.74
3459.911	24336–53230	3.02	501	0.28	0.17	0.18[1]	0.22				0.21	3.75	5.42
3462.354	17727–46601	2.20	79		−0.95	−1.18[1]	−0.88				−1.00	2.54	4.21
3462.808	22838–51708	2.83	373	−1.34							−1.34	2.20	3.87
3463.304	11976–40842	1.48	48	−1.65	−1.66						−1.66	1.88	3.55
3464.914	20875–49727	2.59	241	−1.00	−0.92		−0.98				−0.97	2.57	4.23
3465.862	888–29733	0.11	6		−0.84	−1.03[1]	−0.87	−1.00[1]			−0.94	2.60	4.26
3466.279	19390–48231	2.40	185				−1.36				−1.36	2.18	3.84
3466.500	6928–35768	0.86	24	−1.86	−1.94						−1.90	1.64	3.30
3468.847	20641–49461	2.56	242	−0.12	−0.11	−0.15[1]	−0.16				−0.14	3.40	5.06
3469.012	26628–55446	3.30	614	0.08	0.13						0.10	3.64	5.30
3469.390	22947–51762	2.84	375	−1.32			−0.01				−1.32	2.22	3.88
3469.834	21039–49851	2.61	242	−0.32	−0.44	−0.50[1]	−0.26				−0.38	3.16	4.82
3471.267	17927–46727	2.22	82				−0.28	−0.21[1]			−0.24	3.30	4.96
3471.346	18378–47177	2.28	130				−0.09				−0.09	3.45	5.11

TABLE 3.—*Oscillator Strengths for Ultraviolet Lines of Fe* I—Continued

Wavelength Å	Energy Levels K	Low e.p. Volts	Mult. No.	Arc	Spk	CW(N)	HC	R(N)	KOC	MS	Best	Log gfλ	Log gA/λ
				Log *gf*									
3473.303	24575–53358	3.05		−0.31							−0.31	3.23	4.89
3473.497	7986–36767	0.99	26	−2.49			−1.10				−2.49	1.05	2.71
3475.451	704–29469	0.09	6		−0.74	−0.93[1]	−0.80	−0.89[1]			−0.84	2.70	4.36
3475.651	17550–46314	2.18	78	0.28	−0.09		0.39				0.10	3.64	5.30
3475.867	19621–48383	2.43	186	−0.57			−0.20				−0.38	3.16	4.82
3476.336	18378–47136	2.28	133	−0.86	−0.78		−0.50				−0.71	2.83	4.49
3476.704	978–29733	0.12	6		−1.07	−1.36[2]	−1.19	−1.22[2]		−1.24	−1.24	2.30	3.96
3476.853	20875–49628	2.59	242		−0.08		−0.13				−0.10	3.44	5.10
3477.007	19552–48305	2.42	139		−0.29		−0.54				−0.42	3.12	4.78
3477.856	17927–46673	2.22	82	−0.68	−0.83	−0.97[1]	−0.84	−0.78[1]			−0.82	2.72	4.38
3478.374	19621–48362	2.43	185	−1.45			−1.30				−1.38	2.16	3.82
3478.788	19552–48290	2.42	137	−1.24			−0.70				−1.24	2.30	3.96
3479.683	23784–52514	2.95	443	−1.04			0.86				−1.04	2.50	4.16
3481.558	18378–47093	2.28	132	−1.60			−1.13				−1.60	1.94	3.60
3483.009	7377–36079	0.91	24	−1.72	−2.01	−2.12[1]	−2.02				−1.97	1.57	3.23
3484.858	19788–48476	2.45	185	−1.19			−0.17				−1.19	2.35	4.01
3484.972	19552–48239	2.42	138	−0.78	−0.79		−0.76				−0.78	2.76	4.42
3485.342	17727–46410	2.20	78	−0.02	−0.15	−0.01[2]	−0.05				−0.05	3.49	5.15
3486.556	17927–46601	2.22	79	−1.15	−1.08		−1.13				−1.12	2.42	4.08
3489.670	23784–52431	2.95	442	0.26	0.18	0.12[1]	0.15				0.18	3.72	5.38
3490.575	416–29056	0.05	6			−1.04[2]	−0.47	−0.93[1]			−1.00	2.54	4.20
3493.290	11976–40594	1.48	48	−1.72			−1.37				−1.54	2.00	3.65
3493.698	21999–50614	2.73	297				−0.40				−0.40	3.14	4.79
3494.170	19552–48163	2.42	137	−1.10	−0.86		−0.46				−0.98	2.56	4.21
3495.288	20641–49243	2.56	238	0.27	0.20	0.24[2]	0.29				0.25	3.79	5.44
3496.190	19788–48383	2.45	186				−1.03				−1.03	2.51	4.16
3497.110	17550–46137	2.18	78	0.27	0.12	0.20[2]	0.12				0.18	3.72	5.37
3497.842	888–29469	0.11	6	−0.94	−1.23	−1.45[1]	−1.29	−1.32[4]		−1.27	−1.27	2.27	3.92
3500.164	23193–51755	2.87	327	−1.45							−1.45	2.09	3.74
3500.568	20875–49433	2.59	238	−0.16	−0.33	−0.81[1]	−0.66						
3504.455	22838–51365	2.83	371	−1.09			−0.47				−1.09	2.45	4.10
3504.864	18378–46902	2.28	131	−0.57	−0.73		−0.58				−0.63	2.91	4.56
3505.065	24336–52858	3.02	498	0.03	−0.11		0.07				0.00	3.54	5.19
3506.500	18378–46889	2.28	130	−0.04	−0.13	0.09[1]	0.08				0.00	3.54	5.19
3507.139	29469–57974	3.65	835	−0.38	−0.51						−0.44	3.10	4.75
3507.390	24772–53275	3.07	500				−0.38				−0.38	3.16	4.81
3508.494	24119–52613	2.99	442	0.32	0.18	−0.21[1]	0.00						
3509.120	22846–51335	2.83	326	−0.77			−0.74				−0.76	2.79	4.43
3509.736	23270–51755	2.88	327	−0.78							−0.78	2.77	4.41
3509.870	17927–46410	2.22	78	−0.56	−0.63	−1.29[1]	−0.80						
3510.446	20038–48516	2.48	139		−0.39	−0.85[1]	−0.40						
3511.748	20641–49109	2.56	238	−0.86	−0.95		−0.92				−0.91	2.64	4.28
3512.080	22997–51462	2.85	327				−0.92				−0.92	2.63	4.27
3512.239	22997–51461	2.85	326	−0.49			−0.29				−0.39	3.16	4.80
3512.970	24772–53230	3.07	501	−0.63							−0.63	2.92	4.56
3513.065	12561–41018	1.56	48	−1.41	−1.41						−1.41	2.14	3.78
3513.820	6928–35379	0.86	24		−0.48	−0.50[1]	−0.30			−0.72	−0.50	3.05	4.69
3514.626	19390–47835	2.40	183	−0.77							−0.77	2.78	4.42
3516.403	24339–52769	3.02	442	0.08	−0.01	−0.40[1]	−0.18						
3516.550	23111–51540	2.86	326	−0.20			−0.23				−0.22	3.33	4.97
3518.680	23193–51604	2.87	327	−0.39	−0.65		−0.31				−0.45	3.10	4.73
3518.860	17727–46137	2.20	78	−0.68	−0.93	−1.48[1]	−0.87						
3520.855	21039–49433	2.61	238	−0.52	−0.64		−0.76				−0.64	2.91	4.54
3521.263	7377–35768	0.91	24		−0.32	−0.49[1]	−0.34	−0.46[1]		−0.55	−0.43	3.12	4.75
3521.833	17927–46314	2.22	78	−0.35	−0.58		−0.10				−0.46	3.09	4.72
3522.268	22846–51229	2.83	326	0.04	−0.30		0.00				−0.09	3.46	5.09
3522.896	23193–51570	2.87	330	−0.57	−0.71		−0.99				−0.76	2.79	4.42
3523.300	23193–51567	2.87	326	−0.22	−0.55		−0.39				−0.39	3.16	4.79
3524.075	20875–49243	2.59	239	0.05	−0.01						0.02	3.57	5.20
3524.242	18378–46745	2.28	130	0.01	−0.21		0.08				−0.04	3.51	5.14

TABLE 3.—*Oscillator Strengths for Ultraviolet Lines of Fe* I—Continued

Wavelength Å	Energy Levels K	Low e.p. Volts	Mult. No.	Arc	Spk	CW(N)	HC	R(N)	KOC	MS	Best	Log gfλ	Log gA/λ
				Log *gf*									
3525.856	22997–51351	2.85	329	−0.33			−0.14				−0.24	3.31	4.94
3526.042	704–29056	0.09	6	−1.36		−1.61[1]	−1.19	−1.59[1]			−1.52	2.03	3.66
3526.168	7728–36079	0.96	24			−0.89[1]	−0.67				−0.78	2.77	4.40
3526.230	23111–51462	2.86	327				0.67				0.67	4.22	5.85
3526.377	23111–51461	2.86	326	0.72	0.60						0.66	4.21	5.84
3526.470	18378–46727	2.28	131	0.25							0.25	3.80	5.43
3526.673	23193–51540	2.87	326	0.70	0.38		0.74				0.61	4.16	5.79
3527.792	22997–51335	2.85	326	0.48	0.13	0.46[1]	0.59				0.36	3.91	5.54
3528.316	12561–40895	1.56		−2.25							−2.25	1.30	2.93
3528.942	6928–35257	0.86	23	−3.73							−3.73	−0.18	1.45
3529.531	24575–52899	3.05	537	−0.69			−0.55				−0.62	2.93	4.56
3529.818	23245–51567	2.88	326	0.56	0.24	0.44[1]	0.44				0.42	3.97	5.60
3530.385	22650–50968	2.81	326	0.12		0.10[1]	0.17				0.13	3.68	5.31
3531.446	19621–47930	2.43	182	−0.99	−0.92		−1.12				−1.01	2.54	4.17
3533.008	23270–51567	2.88	326	0.60	0.42		0.50				0.51	4.06	5.69
3533.201	23245–51540	2.88	326	0.90	0.58	0.63[1]	0.93				0.76	4.31	5.94
3534.530	28820–57104	3.57	811	−0.44	−0.36		−0.18				−0.33	3.22	4.85
3534.914	12561–40842	1.56	48	−1.69	−1.67						−1.68	1.87	3.50
3536.556	23193–51461	2.87	326	0.99	0.73	1.00[2]	1.21				0.99	4.54	6.17
3537.491	20875–49135	2.59	239	−0.44	−0.46		−0.40				−0.43	3.12	4.75
3537.729	21039–49298	2.61	239	−0.04	−0.03		0.11				0.01	3.56	5.19
3537.896	22846–51103	2.83	327	0.25	−0.11		0.39				0.07	3.62	5.25
3538.310	28605–56859	3.55	775	−0.60	−0.52		−0.30				−0.47	3.08	4.71
3538.550	20038–48290	2.48	137	−1.14	−0.91						−1.02	2.53	4.16
3538.790	28820–57070	3.57	811	−0.89			−0.03				−0.89	2.66	4.29
3540.121	23111–51351	2.86	329	0.25	−0.06	0.19[1]	0.45				0.13	3.68	5.31
3540.711	7377–35612	0.91	23	−1.71	−1.68		−1.47				−1.62	1.93	3.56
3541.083	22997–51229	2.85	326	1.15	0.79	1.08[2]	1.10				1.04	4.59	6.22
3542.076	23111–51335	2.86	326	1.15	0.75	1.01[2]	1.16				1.01	4.56	6.19
3542.243	18378–46601	2.28	128				−0.33				−0.33	3.22	4.85
3543.392	19621–47835	2.43	183	−0.93	−0.82		−0.85				−0.87	2.68	4.31
3543.669	27543–55754	3.41	734	0.21	0.21	0.12[1]	0.28				0.20	3.75	5.38
3544.631	21039–49243	2.61	239	−0.49	−0.59	−0.68[1]	−0.45				−0.55	3.00	4.63
3545.639	22997–51192	2.85	321	0.35	0.24	0.33[1]	0,50	0.59[1]			0.40	3.95	5.57
3545.832	24575–52769	3.05	536	−0.27	0.08		−0.56				−0.10	3.45	5.07
3546.210	19621–47812	2.43	183	−1.39			−0.99				−1.19	2.36	3.98
3547.203	22650–50833	2.81	321	−0.29	−0.24	−0.37[1]	−0.31	−0.16[1]			−0.27	3.28	4.90
3548.037	24336–52512	3.02	496	−0.31	−0.27	−0.40[1]	−0.19				−0.29	3.26	4.88
3549.868	12969–41131	1.61	48	−1.30	−1.44	−1.43[1]	−1.43				−1.40	2.15	3.77
3551.114	22997–51149	2.85	321	−1.16							−1.16	2.39	4.01
3552.112	24772–52916	3.07	499	−0.30	−0.17		−0.12				−0.20	3.35	4.97
3552.420	19788–47930	2.45	182	−1.45			−0.97				−1.45	2.10	3.72
3552.828	23193–51331	2.87	321	0.20	−0.08	0.10[1]	0.17	0.36[1]			0.15	3.70	5.32
3553.741	28820–56951	3.57	810	0.97	1.06	0.78[1]	1.00				0.95	4.50	6.12
3554.120	7728–35856	0.96	23	−1.40	−1.60		−1.82				−1.50	2.05	3.67
3554.500	23245–51370	2.88	325	−0.10	0.04		0.11				0.02	3.57	5.19
3554.922	22846–50968	2.83	326	1.47	1.13	1.19[2]	1.11				1.22	4.77	6.39
3556.680	23111–51219	2.86	325	−0.24			−0.38				−0.31	3.24	4.86
3556.877	22997–51103	2.85	327	0.92	0.53	0.85[1]	0.99				0.82	4.37	5.99
3558.517	7986–36079	0.99	24	−0.30	−0.04	−0.27[2]	−0.26	−0.39[3]		−0.24	−0.28	3.27	4.89
3559.506	24772–52858	3.07	498	0.12	0.30	−0.48[1]	0.21				0.21	3.76	5.38
3560.076	23111–51192	2.86	321	−1.09							−1.09	2.46	4.08
3560.705	26225–54301	3.25	675	0.04	0.03	−0.65[1]	−0.07				0.00	3.55	5.17
3562.269	26225–54289	3.25		−1.07							−1.07	2.48	4.10
3564.110	12969–41018	1.61	48	−1.66	−1.65						−1.66	1.89	3.51
3564.533	19788–47834	2.45	183	−0.67	−0.40						−0.54	3.01	4.63
3565.381	7728–35768	0.96	24			0.16[2]	0.21	−0.01[3]		0.26	0.11	3.66	5.28
3565.583	23111–51149	2.86	321	0.75			0.66	0.73[1]			0.71	4.26	5.88
3566.316	18378–46410	2.28	127	−0.86	−0.90						−0.88	2.67	4.29
3566.590	19390–47420	2.40	181				−1.23				−1.23	2.32	3.94

216-375 O - 66 - 6

TABLE 3.—*Oscillator Strengths for Ultraviolet Lines of Fe* I—Continued

Wavelength Å	Energy Levels K	Low e.p. Volts	Mult. No.	Arc	Spk	CW(N)	HC	R(N)	KOC	MS	Best	Log gfλ	Log gA/λ
				Log *gf*									
3567.038	23193–51219	2.87	325	−0.02	−0.33	−0.45[1]	0.14						
3567.360	19788–47812	2.45	183	−0.88	−1.01		−0.72				−0.87	2.68	4.30
3567.748	26140–54161	3.24	571	−0.87							−0.87	2.68	4.30
3568.423	23193–51208	2.87	321	−0.47	−0.70			−0.13[1]					
3568.828	26225–54237	3.25	673	−0.10	−0.10		0.07				−0.04	3.51	5.13
3568.978	21716–49727	2.69	294	−0.06	−0.01	−0.24[1]	0.01				−0.08	3.47	5.09
3570.100	7377–35379	0.91	24			0.43[2]	0.30	0.35[4]		0.55	0.39	3.94	5.56
3570.243	22650–50652	2.81	326	1.47							1.47	5.02	6.64
3571.226	11976–39970	1.48	46	−1.47	−1.41		−0.24				−1.44	2.11	3.73
3571.995	22846–50833	2.83	321	0.66	0.36	0.66[1]	0.70	0.87[1]			0.65	4.20	5.82
3572.600	22997–50980	2.85	325	−0.41	−0.59		−0.24				−0.41	3.14	4.75
3573.400	26624–54600	3.30	673	−0.01	−0.11		0.90				−0.06	3.49	5.10
3573.836	19390–47363	2,40	181				−0.14				−0.14	3.41	5.02
3573.896	26628–54600	3.30	611		0.63		0.72				0.68	4.23	5.84
3574.256	26479–54449	3.28	574	−0.95							−0.95	2.60	4.21
3575.118	23245–51208	2.88	321	−0.22	−0.34			0.03[1]			−0.18	3.37	4.98
3575.249	22846–50808	2.83	322	0.03			0.25	0.18[1]			0.15	3.70	5.31
3575.374	24336–52297	3.02	496	0.53	0.43	0.19[1]	0.43				0.40	3.95	5.56
3575.976	23193–51149	2.87	321	−0.07	−0.39	−0.50[1]	0.07	0.16[1]			0.40	3.95	5.56
3576.760	26351–54301	3.27	613a	0.21	0.45	−0.25[1]	0.04				0.40	3.95	5.56
3578.380	23270–51208	2.88	321	−0.30	−0.66			0.96[1]			−0.48	3.07	4.68
3579.829	26140–54067	3.24	573	−0.71							−0.71	2.84	4.45
3581.195	6928–34844	0.86	23			0.58[2]	0.59	0.61[3]			0.60	4.15	5.76
3581.650	21716–49628	2.69	295	−0.26	0.09		−0.12				−0.10	3.45	5.06
3581.816	24772–52683	3.07	497	−0.01	−0.03		0.03				0.00	3.55	5.16
3582.201	26106–54014	3.24	612	0.57	0.73	0.70[1]	0.78				0.70	4.25	5.86
3582.560	19788–47693	2.45	181		−0.27		−1.35						
3582.690	23245–51149	2.88	328	−0.74			−0.47				−0.60	2.95	4.56
3583.337	26550–54449	3.29	574	0.08	0.05	0.24[1]	0.02				0.10	3.65	5.26
3584.663	21716–49604	2.69	294	0.90	0.79	0.72[1]	0.83				0.81	4.36	5.97
3584.790	23111–50999	2.86	322	−0.08			1.07				−0.08	3.47	5.08
3584.960	26351–54237	3.27	611	0.91	0.79		0.35				0.85	4.40	6.01
3585.193	23784–51668	2.95	438	−0.19			0.83				−0.19	3.36	4.97
3585.321	7728–35612	0.96	23	−0.43	−0.30	−0.49[1]	−0.10			−0.41	−0.41	3.14	4.75
3585.707	7377–35257	0.91	23	−0.61	−0.61	−0.67[2]	−0.57			−0.74	−0.64	2.91	4.52
3586.114	26106–53983	3.24	611	1.10	1.05	1.00[1]	1.12				1.07	4.62	6.23
3586.740	22650–50523	2.81	325	−0.22			0.00				−0.11	3.44	5.05
3586.986	7986–35856	0.99	23	−0.40	−0.22	−0.41[1]	−0.37			−0.39	−0.36	3.19	4.80
3587.240	23111–50980	2.86	325	0.02	−0.24		0.30				−0.11	3.44	5.05
3587.424	19552–47420	2.42	134	−0.35	−0.32		−0.26				−0.29	3.26	4.87
3587.752	26406–54271	3.27		0.59	0.18								
3588.516	23711–51570	2.94	394	−0.28							−0.28	3.27	4.88
3588.615	22846–50704	2.83	325	0.31	0.21		0.60				0.40	3.95	5.56
3588.918	23193–51048	2.87	322	−0.06			0.27	0.19[1]			0.13	3.68	5.29
3589.106	6928–34782	0.86	23	−1.24	−1.09	−1.30[1]	−1.39				−1.26	2.29	3.90
3589.456	21999–49851	2.73	295	−0.48	−0.67		0.27				−0.58	2.98	4.58
3589.586	24119–51969	2.99		−0.66							−0.66	2.90	4.50
3590.086	23784–51630	2.95	440	−0.65	−0.44		−0.17				−0.54	3.02	4.62
3590.990	25900–53739	3.21	573	−0.75			−0.63				−0.69	2.87	4.47
3591.345	22997–50833	2.85	321	−0.51	−0.65		−0.27				−0.48	3.08	4.68
3591.485	26550–54386	3.29	568	−0.50	−0.54						−0.52	3.04	4.64
3592.486	20875–48703	2.59	237	−1.00	−0.88		−1.04				−0.97	2.59	4.19
3592.680	26140–53967	3.24	569	−0.46			−0.36				−0.41	3.15	4.75
3592.881	17727–45552	2.20	77	−1.47			−1.44				−1.46	2.10	3.70
3593.329	26340–54161	3.26	571	−0.34	−0.58		−0.26				−0.39	3.17	4.77
3594.632	22997–50808	2.85	322	0.63	0.33	0.61[2]	0.81	0.79[1]			0.63	4.19	5.79
3595.308	23193–50999	2.87	322	−0.01	−0.47	−0.26[1]	−0.08	−0.04[1]			−0.17	3.39	4.99
3595.857	19788–47590	2.45	181	−1.18	−1.11		−1.15				−1.15	2.41	4.01
3596.198	19621–47420	2.43	181	−0.74	−0.90	−1.00[1]	−0.71				−0.84	2.72	4.32
3597.050	26340–54132	3.26	569	0.00	−0.50	−0.13[1]	−0.20						

TABLE 3.—*Oscillator Strengths for Ultraviolet Lines of Fe* I—Continued

Wavelength Å	Energy Levels K	Low e.p. Volts	Mult. No.	Arc	Spk	CW(N)	HC	R(N)	KOC	MS	Best	Log gfλ	Log gA/λ
				Log *gf*									
3598.721	26225–54005	3.25	674	−0.35			−0.73				−0.54	3.02	4.62
3598.930	26479–54258	3.28	568				−1.02				−1.02	2.54	4.14
3598.980	23270–51048	2.88	322	−0.73			−0.59				−0.66	2.90	4.50
3599.624	28820–56593	3.57	809	0.31	0.35	0.34[1]	0.45				0.36	3.92	5.52
3602.080	23245–50999	2.88	322	−0.54	−0.66		−0.18	0.00[1]					
3602.460	23111–50862	2.86	322				0.13				0.13	3.69	5.28
3602.534	23111–50861	2.86	324	0.26	0.11	0.20[1]	0.20				0.19	3.75	5.34
3602.774	22838–50587	2.83	370	−1.16							−1.16	2.40	3.99
3603.207	21716–49461	2.69	295	0.71	0.73	0.75[2]	0.80				0.75	4.31	5.90
3603.572	19621–47363	2.43	181	−1.53			−1.24				−1.38	2.18	3.77
3603.673	20641–48383	2.56		−1.24							−1.24	2.32	3.91
3603.828	24772–52512	3.07	496	−0.17	0.00		0.22				0.02	3.58	5.17
3604.383	23245–50981	2.88	323	−0.73	−0.76						−0.74	2.82	4.41
3604.701	26624–54357	3.30		−0.46			−0.30				−0.38	3.18	4.77
3605.206	26628–54357	3.30		0.07							0.07	3.63	5.22
3605.450	21999–49727	2.73	294	1.20	0.94	0.99[2]	1.11				1.05	4.61	6.20
3606.682	21716–49434	2.69	294	1.24	1.27	1.05[2]	0.99				1.14	4.70	6.29
3608.146	22997–50704	2.85	325	−0.10	−0.20	−0.99[1]	0.29						
3608.861	8155–35856	1.01	23			0.30[1]	0.27	0.21[3]		0.31	0.25	3.81	5.40
3609.486	23111–50808	2.86	322	−0.77							−0.77	2.79	4.38
3610.159	22650–50342	2.81	321	1.10	0.77	1.13[2]	1.01	1.18[1]			1.05	4.61	6.20
3610.703	23193–50880	2.87	323	−0.23	−0.39		−0.21				−0.28	3.28	4.87
3612.068	22846–50523	2.83	325	0.26	−0.08	0.26[1]	0.56				0.15	3.71	5.30
3612.940	12561–40231	1.56	46	−1.59	−1.66		−1.11				−1.62	1.94	3.53
3613.110	23193–50861	2.87	324	−0.56	−0.78		−0.50				−0.61	2.95	4.54
3613.459	26225–53892	3.25	672	−0.12							−0.12	3.44	5.03
3613.612	26624–54289	3.30		−0.62	−0.59						−0.60	2.96	4.55
3614.109	26628–54289	3.30		−0.29	−0.51						−0.40	3.16	4.75
3614.711	26225–53882	3.25		−0.14							−0.14	3.42	5.01
3615.190	26479–54132	3.28	569	−1.29			−0.83						
3615.665	11976–39626	1.48	46	−1.79	−1.88		−1.43				−1.84	1.72	3.31
3615.959	26624–54271	3.30		−1.12							−1.12	2.44	4.03
3616.162	25900–53546	3.21	569	−0.48	−0.60		−0.64				−0.57	2.99	4.58
3616.326	19552–47197	2.42	132	−1.06	−0.93		−0.93				−0.97	2.59	4.18
3617.090	24575–52213	3.05	535				−0.77				−0.77	2.79	4.38
3617.788	24336–51969	3.02	496	0.87	0.89	0.87[2]	0.97				0.89	4.45	6.04
3618.285	22846–50475	2.83	324	−0.76							−0.76	2.80	4.39
3618.392	21999–49628	2.73	295	0.02	0.24		0.28				0.18	3.74	5.33
3618.769	7986–35612	0.99	23			0.27[1]	0.67	0.26[3]		0.37	0.28	3.84	5.43
3619.772	19390–47008	2.40	180	−1.06			−0.93				−1.00	2.56	4.15
3620.228	22997–50611	2.85	324	−0.85			−0.72				−0.78	2.78	4.37
3620.880	23270–50880	2.88	323	−0.96							−0.96	2.60	4.19
3621.464	21999–49604	2.73	294	0.94	0.95	0.97[2]	1.03				0.97	4.53	6.12
3621.718	28820–56423	3.57	808	−0.09	0.17		0.48				0.04	3.60	5.19
3622.001	22249–49851	2.76	295	0.82	0.81	0.80[2]	0.87				0.82	4.38	5.97
3623.188	19390–46982	2.40	180	0.27	0.17	0.25[2]	0.26				0.24	3.80	5.39
3623.440	20641–48231	2.56	233	−0.55	−0.55		−0.23				−0.44	3.12	4.71
3623.772	23111–50699	2.86	323	−0.17	−0.59		−0.01						
3624.056	26340–53925	3.26	570	−0.63							−0.63	2.93	4.52
3624.310	19552–47136	2.42	133	−0.83	−0.88		−0.54				−0.75	2.81	4.40
3625.140	22846–50423	2.83	323	0.17	−0.07	0.29[2]	0.43				0.17	3.73	5.32
3627.060	28820–56383	3.57	808	−0.53	−0.41		−0.03				−0.47	3.09	4.68
3628.094	17727–45282	2.20	77	−1.04	−1.18						−1.11	2.45	4.03
3628.806	24119–51668	2.99	438	−1.15	−0.95						−1.05	2.51	4.09
3630.353	22997–50534	2.85	323	0.02	−0.20	0.04[1]	0.26				−0.05	3.51	5.09
3631.103	22846–50378	2.83	322	0.61			0.83	0.10[1]					
3631.465	7728–35257	0.96	23			0.23[1]	0.53	0.22[2]			0.22	3.78	5.36
3632.042	24772–52297	3.07	496	0.79	0.75	0.71[1]	0.78				0.76	4.32	5.90
3632.558	23784–51305	2.95	437	−0.02	−0.01		−0.28				−0.08	3.48	5.06
3632.980	20038–47556	2.48	135	−0.40	−0.41	−0.19[1]	−0.25				−0.31	3.25	4.83

TABLE 3.—*Oscillator Strengths for Ultraviolet Lines of Fe* I—Continued

Wavelength Å	Energy Levels K	Low e.p. Volts	Mult. No.	Arc	Spk	CW(N)	HC	R(N)	KOC	MS	Best	Log gfλ	Log gA/λ
				Log *gf*									
3633.087	23711–51229	2.94	390	−0.04			−0.18				−0.11	3.45	5.03
3633.833	24119–51630	2.99	440	−0.36	−0.49		−0.14				−0.33	3.23	4.81
3634.326	23711–51219	2.94	389	0.12	−0.02	0.35[1]	0.38				0.21	3.77	5.35
3635.190	24336–51837	3.02	490	−0.17	−0.45		0.09				−0.31	3.25	4.83
3636.186	17727–45221	2.20	77		−0.46	−0.40[1]	−0.55				−0.47	3.09	4.67
3636.496	26340–53831	3.26	568	−0.49							−0.49	3.07	4.65
3636.650	24336–51826	3.02	493		−0.32		−0.30				−0.31	3.25	4.83
3636.995	20875–48362	2.59	233	−0.39	−0.49		−0.08				−0.32	3.24	4.82
3637.251	19621–47107	2.43	180	−0.66	−0.90		−0.65				−0.74	2.82	4.40
3637.730	20641–48123	2.56	229	−1.29	−0.75		−0.72						
3637.862	23711–51192	2.94	385	−0.10	−0.38		0.13	0.09[1]			0.04	3.60	5.18
3638.300	22249–49727	2.76	294	0.66	0.58	0.64[2]	0.69				0.64	4.20	5.78
3640.392	21999–49461	2.73	295	0.86	0.86	0.89[2]	0.95				0.89	4.45	6.03
3641.454	23245–50699	2.88	323	−1.25	−0.83						−1.25	2.31	3.89
3643.627	23711–51149	2.94	385	0.08	0.00	0.24[1]	0.28	0.33[1]			0.19	3.75	5.33
3643.716	21039–48476	2.61	233	−0.21			−0.22				−0.22	3.34	4.92
3643.812	12969–40405	1.61	46	−1.46			0.17						
3644.798	26140–53569	3.24	570	−0.22	−0.59						−0.40	3.16	4.74
3645.090	22997–50423	2.85	323	−0.26		−0.15[1]	−0.05				−0.15	3.41	4.99
3645.494	23111–50534	2.86	323	−0.42	−0.40		0.04				−0.41	3.15	4.73
3645.822	25092–52512	3.11	496	0.50	0.48	0.59[2]	0.67				0.57	4.13	5.71
3647.427	12561–39970	1.56	46	−1.17	−0.87						−1.02	2.54	4.12
3647.844	7377–34782	0.91	23			0.09[2]	0.38	0.08[3]		0.19	0.14	3.70	5.28
3649.304	0–27395	0.00	5	−2.34	−2.45		−2.59	−2.75[1]			−2.53	1.03	2.61
3649.509	21716–49109	2.69	291	0.88	0.87	0.78[2]	1.04			0.75	0.85	4.41	5.99
3649.699	23711–51103	2.94	391	−0.60							−0.60	2.96	4.54
3650.031	24181–51570	3.00	394	0.32	0.58		0.61				0.50	4.06	5.64
3650.281	19621–47008	2.43	180	0.21	0.08		0.39				0.23	3.79	5.37
3650.554	26225–53610	3.25		−0.42							−0.42	3.14	4.72
3651.100	22997–50378	2.85	322	−0.76			0.52	−0.44[1]			−0.60	2.96	4.54
3651.470	22249–49628	2.76	295	1.00	0.98	0.94[1]	1.06				1.00	4.56	6.14
3652.256	24336–51708	3.02	494		−0.85						−0.85	2.71	4.29
3653.352	20875–48239	2.59	229	−1.48							−1.48	2.08	3.66
3653.763	19621–46982	2.43	180	−0.72	−0.83		−0.77				−0.77	2.79	4.37
3654.660	17927–45282	2.22	77	−1.61	−1.53		−1.29				−1.48	2.08	3.66
3655.467	22838–50187	2.83	369	0.10	0.12	0.21[1]	0.18				0.15	3.71	5.29
3656.227	26406–53749	3.27		0.01	−0.28						−0.14	3.42	4.99
3656.358	23193–50534	2.87	323	−1.05							−1.05	2.51	4.08
3657.139	19552–46889	2.42	130	−0.71	−0.81	−0.46[1]	−0.57				−0.64	2.92	4.49
3657.890	24507–51837	3.04	395	−0.18	−0.58	−0.12[1]	−0.13				−0.14	3.42	4.99
3658.025	24339–51668	3.02	438	0.55							0.55	4.11	5.68
3658.550	20641–47967	2.56	231	−1.27	−1.21		−0.86				−1.11	2.45	4.02
3659.519	19788–47107	2.45	180	0.10	0.02	0.20[2]	0.19				0.14	3.70	5.27
3660.330	23111–50423	2.86	323	−1.03							−1.03	2.53	4.10
3661.360	19788–47093	2.45	179	−1.23	−1.06		−0.92				−1.07	2.49	4.06
3663.250	24119–51409	2.99	439	−0.51	−0.63		−0.34				−0.49	3.07	4.64
3663.458	20875–48163	2.59	231	−0.60	−0.83		−0.28				−0.72	2.84	4.41
3663.950	23784–51069	2.95	435	−0.90	−0.83						−0.86	2.70	4.27
3664.537	24181–51462	3.00	391	−0.08		−0.19[1]	0.00				−0.09	3.47	5.04
3664.694	24181–51461	3.00	390	−0.45	−0.54		−0.26				−0.42	3.14	4.71
3666.240	19621–46889	2.43	179	−0.76		−0.84[1]	−0.56				−0.72	2.84	4.41
3666.944	12969–40231	1.61	46	−2.25			−1.01				−2.25	1.31	2.88
3667.252	25900–53161	3.21	570	0.21	−0.29	0.17[1]	0.00						
3667.999	25900–53155	3.21	569	−0.03	−0.49		−0.09						
3668.214	26140–53394	3.24	568	−0.29	−0.57		−0.33				−0.40	3.16	4.73
3668.893	20875–48123	2.59	229	−1.30			−1.10				−1.20	2.36	3.93
3669.151	24119–51365	2.99	437	0.09	−0.02		0.10				0.06	3.62	5.19
3669.523	21999–49243	2.73	291	0.65	0.57	0.69[2]	0.64				0.65	4.21	5.78
3670.071	23784–51023	2.95	435		0.26						0.26	3.82	5.39
3670.810	20038–47272	2.48	133	−0.73	−0.83		−0.69				−0.75	2.81	4.38

TABLE 3.—*Oscillator Strengths for Ultraviolet Lines of Fe* I—Continued

Wavelength Å	Energy Levels K	Low e.p. Volts	Mult. No.	Arc	Spk	CW(N)	HC	R(N)	KOC	MS	Best	Log gfλ	Log gA/λ
				Log *gf*									
3671.510	26340–53569	3.26	570	−0.97							−0.97	2.59	4.16
3671.689	22249–49477	2.76		−1.18	−1.02						−1.10	2.46	4.03
3672.722	19788–47008	2.45	180	−0.88	−1.03		−0.89				−0.93	2.63	4.20
3674.766	22838–50043	2.83	369	−0.17	−0.33	−0.03[1]	−0.20				−0.18	3.39	4.95
3675.434	21039–48239	2.61	229	−1.89							−1.89	1.68	3.24
3675.694	24507–51705	3.04	391	−1.29	−1.14						−1.22	2.35	3.91
3676.314	20641–47835	2.56	228	0.13	0.04	0.15[1]	0.14				0.12	3.69	5.25
3676.879	24181–51370	3.00	389	−0.75	−0.74		−0.42				−0.64	2.93	4.49
3677.309	28605–55791	3.55	773	0.35	0.45		0.97				0.40	3.97	5.53
3677.477	18378–45563	2.28	125	−0.80	−0.84		−0.85				−0.83	2.74	4.30
3677.631	22249–49433	2.76	291	0.89	0.78	0.85[2]	0.65				0.80	4.37	5.93
3678.862	19552–46727	2.42	131	−0.30	−0.41	−0.28[1]	−0.15				−0.28	3.29	4.85
3678.980	18378–45552	2.28	124	−1.21			−0.95				−1.08	2.49	4.05
3679.330	20641–47812	2.56	228				−1.13				−1.13	2.44	4.00
3679.530	24181–51351	3.00	393				−0.45				−0.45	3.12	4.68
3679.915	0–27167	0.00	5		−1.22	−1.27[2]	−1.05	−1.37[4]		−1.33	−1.30	2.27	3.83
3680.675	25900–53061	3.21	568	0.14		0.35[1]	0.14				0.21	3.78	5.34
3681.227	26628–53785	3.30		−0.36	−0.47						−0.42	3.15	4.71
3681.651	24181–51335	3.00	390	−0.58			−0.47				−0.52	3.05	4.61
3681.880	29799–56951	3.69	951				−0.26				−0.26	3.31	4.87
3682.226	28605–55754	3.55	772	1.16	0.97	1.24[2]	1.29				1.18	4.75	6.31
3683.056	416–27560	0.05	5	−2.03	−2.12	−1.94[2]	−2.14	−2.10[2]			−2.05	1.52	3.08
3683.616	20038–47177	2.48	130	−1.32	−1.19						−1.26	2.31	3.87
3684.110	21999–49135	2.73	292	0.63	0.62	0.63[2]	0.72				0.65	4.22	5.77
3685.998	23711–50833	2.94	385	0.74		0.78[2]	0.81	0.76[1]			0.77	4.34	5.89
3686.260	19552–46673	2.42	131	−0.53	−0.48		−0.49				−0.50	3.07	4.62
3687.098	17550–44664	2.18	75	−0.70	−0.80						−0.75	2.82	4.37
3687.459	6928–34040	0.86	21	−0.43	−0.31	−0.42[2]	−0.11	−0.61[2]		−0.47	−0.47	3.10	4.65
3687.656	21999–49109	2.73	291	0.58	0.31		0.35				0.41	3.98	5.53
3688.198	26628–53734	3.30		−1.04							−1.04	2.53	4.08
3688.476	26225–53329	3.25	669	−0.11	−0.49						−0.30	3.27	4.82
3689.010	19621–46721	2.43	178	−1.72							−1.72	1.85	3.40
3689.457	23711–50808	2.94	386	0.75	0.42	0.81[2]	0.81	0.72[1]			0.72	4.29	5.84
3689.897	24575–51668	3.05	533	−0.96			−0.70				−0.83	2.74	4.29
3690.450	25092–52181	3.11	497	−0.18	−0.43		−0.30				−0.30	3.27	4.82
3690.730	28820–55907	3.57	807	0.51	0.58	0.54[1]	0.54				0.54	4.11	5.66
3693.008	24339–51409	3.02	439	−0.25	−0.39		−0.08				−0.24	3.33	4.88
3694.005	24507–51570	3.04	394	1.04		1.09[2]	1.19				1.10	4.67	6.22
3695.054	20875–47930	2.59	229	0.32	0.35	0.37[2]	0.37				0.36	3.93	5.48
3695.507	20641–47693	2.56	225	−1.43	−1.06		−1.11				−1.20	2.37	3.92
3696.030	19552–46601	2.42	128	−2.05							−2.05	1.52	3.07
3697.426	24181–51219	3.00	389		0.06	0.43[1]	0.36				0.28	3.85	5.40
3697.536	26624–53661	3.30	670				−0.04				−0.04	3.53	5.08
3698.611	24336–51365	3.02	491	−0.11	−0.23	−0.17[1]	−0.16				−0.17	3.40	4.95
3699.147	24336–51361	3.02	490	−0.56	−0.73		−1.04				−0.62	2.95	4.50
3701.086	24181–51192	3.00	385	0.94		1.09[2]	1.05	0.88[1]			1.01	4.58	6.13
3702.033	22947–49951	2.84	369	−0.12	−0.17	−0.12[1]	0.02				−0.10	3.47	5.02
3702.500	12969–39970	1.61	46	−1.64	−1.65	−1.60[1]					−1.63	1.94	3.49
3703.556	22249–49243	2.76	291	−0.04	−0.04	0.32[1]	0.03				0.07	3.64	5.19
3703.697	23711–50704	2.94	389	0.04	−0.29		0.33				0.18	3.75	5.30
3703.824	23052–50043	2.86	369	−0.07	−0.06		−0.04				−0.06	3.51	5.06
3704.021	24772–51762	3.07	495	−0.98	−0.69		−0.62				−0.76	2.81	4.36
3704.464	21716–48703	2.69	290	0.42	0.32	0.42[2]	0.49				0.41	3.98	5.53
3705.567	416–27395	0.05	5		−1.04	−1.12[3]	−0.90	−1.15[4]		−1.09	−1.10	2.47	4.02
3707.048	24181–51149	3.00	385	0.53		0.63[1]	0.76	0.53[1]			0.61	4.18	5.73
3707.458	20641–47606	2.56	229	−1.02							−1.02	2.55	4.10
3707.578	31307–58272	3.88	978	0.14							0.14	3.71	5.26
3707.823	704–27666	0.09	5			−1.53[1]	−1.75	−1.95[2]		−1.71	−1.78	1.79	3.34
3707.922	17550–44512	2.18	76	0.64			0.79				0.72	4.29	5.84
3708.602	19788–46745	2.45	178	−1.19			−0.70						

TABLE 3.—*Oscillator Strengths for Ultraviolet Lines of Fe* I—Continued

Wavelength Å	Energy Levels K	Low e.p. Volts	Mult. No.	Arc	Spk	CW(N)	HC	R(N)	KOC	MS	Best	Log gfλ	Log gA/λ
							Log *gf*						
3709.248	7377–34329	0.91	21		−0.20	−0.26[3]	0.05	−0.28[1]		−0.29	−0.30	3.27	4.82
3709.535	24119–51069	2.99	435	−0.17	0.02						−0.08	3.49	5.04
3709.665	20641–47590	2.56	225	−0.63							−0.63	2.94	4.49
3711.224	20875–47812	2.59	228	−0.19	−0.22	0.03[1]	0.19				−0.13	3.44	4.99
3711.411	24772–51708	3.07	494	−0.07	−0.18		0.03				−0.07	3.50	5.05
3715.914	18378–45282	2.28	124	−0.49	−0.59	−0.39[1]	−0.38				−0.46	3.11	4.65
3716.442	23711–50611	2.94	388	0.58	0.30	0.58[2]	0.65				0.54	4.11	5.65
3717.837	17550–54449	2.18	706	−1.64							−1.64	1.93	3.47
3718.409	22249–49135	2.76	292	−0.13	−0.14	0.02[1]	0.20				−0.01	3.56	5.10
3719.937	0–26875	0.00	5			−0.36[3]	−0.21	−0.34[2]		−0.31	−0.32	3.25	4.79
3721.189	24336–51201	3.02	491				−0.48				−0.48	3.09	4.63
3721.278	26875–53739	3.33	705	0.03			0.13				0.08	3.65	5.19
3721.396	20038–46902	2.48	131	−0.72	−0.68		−0.40				−0.60	2.97	4.51
3721.510	24507–51370	3.04	389	−0.03			0.40						
3721.606	24339–51201	3.02	437	−0.17	−0.06		−0.04				−0.09	3.48	5.02
3722.026	22249–49109	2.76	291	−0.46			0.00						
3722.564	704–27560	0.09	5		−0.96	−1.08[3]	−0.78	−1.05[4]		−1.05	−1.02	2.55	4.09
3724.380	18378–45221	2.28	124	0.27	0.05	0.21[2]	0.35				0.22	3.79	5.33
3725.498	24575–51409	3.05	534	−0.56	−0.56	−0.55[1]	0.56				−0.56	3.01	4.55
3726.927	24507–51331	3.04	385	0.53	0.29	0.26[1]	0.06	0.50[1]			0.40	3.97	5.51
3727.096	23711–50534	2.94	387	0.36	0.14		0.59				0.25	3.82	5.36
3727.621	7728–34547	0.96	21			−0.25[3]	0.16	−0.38[2]		−0.28	−0.30	3.27	4.81
3727.809	24181–50999	3.00	386				0.41	0.24[1]			0.32	3.89	5.43
3728.670	20641–47453	2.56	227	−0.68	−0.73	−0.60[1]	−0.44				−0.61	2.96	4.50
3730.388	24575–51374	3.05	533	0.31	0.29	0.43[1]	0.34				0.34	3.91	5.45
3730.945	21039–47834	2.61	228	−0.36	−0.34	−0.22[1]	−0.24				−0.29	3.28	4.82
3731.376	21039–47831	2.61	225	−0.47	−0.38	−0.33[1]	0.20				−0.39	3.18	4.72
3732.399	17727–44512	2.20	76	0.31	0.28	0.30[2]	0.42				0.32	3.89	5.43
3733.319	888–27666	0.11	5		−1.08	−1.22[3]	−1.18	−1.16[2]		−1.16	−1.18	2.39	3.93
3734.866	6928–33695	0.86	21			0.55[3]	0.65	0.56[2]		0.58	0.57	4.14	5.68
3735.325	23711–50475	2.94	388	0.79			0.43				0.61	4.18	5.72
3737.133	416–27167	0.05	5			−0.49[3]	−0.67	−0.46[2]		−0.43	−0.50	3.07	4.61
3738.308	26351–53094	3.27	609	0.79	0.83	0.82[2]	0.83				0.82	4.39	5.93
3739.120	17927–44664	2.22	75	−1.36	−1.41						−1.38	2.19	3.73
3739.317	17550–44285	2.18	74	−1.48			−1.36				−1.42	2.15	3.69
3740.061	27395–54125	3.40	707	−0.45	−0.50		−0.70				−0.55	3.02	4.56
3740.247	26225–52954	3.25	667	0.08		0.26[1]	0.27				0.20	3.77	5.31
3741.486	27666–54386	3.43	701	−1.13	−0.97						−1.05	2.52	4.05
3742.151	31805–58520	3.94	978	−0.53							−0.53	3.04	4.57
3742.621	23711–50423	2.94	387	0.37		0.27[1]	0.07				0.24	3.81	5.34
3742.937	27666–54376	3.43	704	−0.76			−1.41						
3743.364	7986–34692	0.99	21	−0.35	−0.27	−0.36[3]	−0.24			−0.43	−0.34	3.23	4.76
3743.781	21999–48703	2.73	290				−1.16				−1.16	2.41	3.94
3744.105	24507–51208	3.04	385	0.19		0.31[1]		0.12[1]			0.21	3.78	5.31
3745.562	704–27395	0.09	5			−0.62[2]	−0.72	−0.61[2]		−0.59	−0.63	2.94	4.47
3745.901	978–27666	0.12	5		−1.09	−1.15[2]	−1.17	−1.10[2]		−1.09	−1.12	2.45	3.98
3746.486	17727–44411	2.20	73	−1.28	−1.15		−1.06				−1.16	2.41	3.94
3746.931	24181–50862	3.00	386	0.29	0.15	0.41[1]	−0.38	0.35[1]			0.30	3.87	5.40
3748.264	888–27560	0.11	5		−0.87	−0.87[3]	−0.93	−0.86[2]		−0.81	−0.87	2.70	4.23
3748.492	28820–55490	3.57	805				−0.65				−0.65	2.92	4.45
3748.969	23711–50378	2.94	386	0.47	0.02		0.45	0.37[1]			0.43	4.00	5.53
3749.488	7377–34040	0.91	21			0.43[3]	0.41	0.50[2]		0.43	0.44	4.01	5.54
3750.677	21039–47693	2.61	225	−1.26	−0.82						−0.82	2.75	4.28
3751.059	26624–53275	3.30	667				−0.62				−0.62	2.95	4.48
3751.820	21716–48362	2.69	287	−1.03	−0.98		−0.30				−1.00	2.57	4.10
3752.420	24507–51149	3.04	385	−0.62	−0.70		−0.52	−0.52[1]			−0.59	2.98	4.51
3753.154	19390–46027	2.40	177	−1.45	−1.39		−1.60				−1.48	2.09	3.62
3753.613	17550–44184	2.18	73	−0.09	−0.20	0.02[2]	−0.11				−0.07	3.50	5.03
3754.506	24181–50808	3.00	386	−0.41		−0.30[1]	−0.49	−0.49[1]			−0.42	3.15	4.68
3756.069	17550–44166	2.18	74	−1.17	−1.28	−1.03[1]	−0.90				−1.10	2.47	4.00

TABLE 3.—*Oscillator Strengths for Ultraviolet Lines of Fe* I—Continued

Wavelength Å	Energy Levels K	Low e.p. Volts	Mult. No.	Arc	Spk	CW(N)	HC	R(N)	KOC	MS	Best	Log gfλ	Log gA/λ
				Log *gf*									
3756.939	28820–55430	3.57	805	0.37	0.56	0.63[1]	0.42				0.50	4.07	5.60
3757.459	26624–53230	3.30	668	−0.18	−0.20		−0.36				−0.25	3.32	4.85
3758.235	7728–34329	0.96	21			0.36[3]	0.27	0.28[2]		0.26	0.31	3.88	5.41
3759.155	29313–55907	3.63	855	−0.43	−0.31		−0.82				−0.37	3.21	4.73
3759.597	27666–54258	3.43	701	−2.22							−2.22	1.36	2.88
3760.052	19390–45978	2.40	177	0.14	0.08	0.18[2]	0.19				0.15	3.73	5.25
3760.533	17927–44512	2.22	76	−0.36	−0.42	−0.61[2]	−0.34				−0.47	3.11	4.63
3761.069	27167–53748	3.37	706	−1.40							−1.40	2.18	3.70
3761.410	20875–47453	2.59	227	−0.90	−0.95	−1.06[1]	−0.88				−0.95	2.63	4.15
3762.205	27167–53739	3.37	705	−0.54			−0.84				−0.69	2.89	4.41
3763.791	7986–34547	0.99	21			0.12[3]	0.17	0.10[2]		0.07	0.11	3.69	5.21
3765.541	26106–52655	3.24	608	1.19	1.28	0.98[2]	0.99				1.08	4.66	6.18
3765.700	26351–52899	3.27	608				−0.52				−0.52	3.06	4.58
3766.092	20875–47420	2.59	226	−1.21	−1.02		−1.37				−1.20	2.38	3.90
3766.665	24507–51048	3.04	386	−0.38	−0.65		−0.44	−0.32[1]			−0.45	3.13	4.65
3767.194	8155–34692	1.01	21			−0.01[3]	0.03	−0.04[2]		−0.08	−0.02	3.56	5.08
3768.030	17927–44459	2.22	73	−0.92	−0.94						−0.93	2.65	4.17
3768.230	22947–49477	2.84	368	−1.35							−1.35	2.23	3.75
3769.995	24181–50699	3.00	387		−0.41	−0.46[1]	−0.34				−0.40	3.18	4.69
3770.305	21716–48231	2.69	287		−0.51		−0.53				−0.52	3.06	4.57
3770.405	19621–46136	2.43	177				−1.40				−1.40	2.18	3.69
3771.473	26106–52613	3.24	607	−0.99							−0.99	2.59	4.10
3773.364	24575–51069	3.05	531	−1.14							−1.14	2.44	3.95
3773.699	24507–50999	3.04	386	−0.46		−0.85[1]	−0.57	−0.60[1]			−0.62	2.96	4.47
3774.827	17927–44411	2.22	73	−0.66	−0.60	−0.81[2]	−0.73				−0.72	2.86	4.37
3775.860	21999–48476	2.73	287	−1.26	−1.10		−1.54				−1.18	2.40	3.91
3776.455	17550–44023	2.18	74	−0.66	−0.68	−0.83[2]	−0.80				−0.76	2.82	4.33
3777.061	24119–50587	2.99	432	−0.78	−0.64						−0.71	2.87	4.38
3777.452	20641–47107	2.56	223	−0.71	−0.75	−0.87[1]	−0.90				−0.81	2.77	4.28
3778.320	22838–49298	2.83	367	−0.85	−0.76		−0.91				−0.84	2.74	4.25
3778.509	26225–52683	3.25	664	−0.09	−0.09	−0.17[1]	−0.14				−0.12	3.46	4.97
3778.699	17727–44184	2.20	73	−1.21	−1.14		−1.30				−1.22	2.36	3.87
3779.213	22249–48703	2.76	290	−1.52							−1.52	2.06	3.57
3779.444	26406–52858	3.27	665			−0.28[1]					−0.28	3.30	4.81
3781.188	17727–44166	2.20	74			−1.49[1]	−1.31				−1.40	2.18	3.69
3781.938	29357–55791	3.64	917	−0.59	−0.25		−0.23				−0.36	3.22	4.73
3782.450	24181–50611	3.00	388	−0.70			−0.61				−0.66	2.92	4.43
3782.608	24772–51201	3.07	491	−0.92	−0.66		−1.01				−0.86	2.72	4.23
3785.706	26106–52514	3.24	608	−0.64	−0.49		−0.68				−0.60	2.98	4.49
3785.950	19621–46027	2.43	177	−0.08	−0.07	−0.15[2]	−0.15				−0.12	3.46	4.97
3786.176	22838–49243	2.83	367	−0.06	0.03		−0.22				−0.08	3.50	5.01
3786.678	8155–34556	1.01	22	−1.53	−1.65	−1.61[3]	−1.61				−1.60	1.98	3.49
3787.164	29357–55754	3.64	916	−0.33	−0.14		−0.39				−0.29	3.29	4.80
3787.883	8155–34547	1.01	21		−0.36	−0.49[3]	−0.44	−0.44[1]		−0.56	−0.47	3.11	4.62
3789.178	21999–48383	2.73	289	−0.43	−0.39	−0.56[1]	−0.59				−0.49	3.09	4.60
3789.570	21039–47420	2.61	226	−1.80			−0.82						
3789.808	27167–53546	3.37	702	−0.54	−0.63						−0.58	3.00	4.51
3790.094	7986–34363	0.99	22	−1.13	−1.21	−1.17[4]	−1.16			−1.29	−1.18	2.40	3.91
3790.656	24507–50880	3.04	387	−0.99			−0.82				−0.90	2.68	4.19
3790.756	17550–43923	2.18	73	−1.10	−1.11		−1.16				−1.12	2.46	3.97
3791.504	20641–47008	2.56	223	−1.16	−1.02		−0.89				−1.02	2.56	4.07
3791.730	27560–53925	3.42	703	−0.89							−0.89	2.69	4.20
3792.156	21999–48362	2.73	287	−0.55	−0.48	−0.67[1]	−0.47				−0.54	3.04	4.55
3792.833	17927–44285	2.22	74	−1.55	−1.39		−1.46				−1.47	2.11	3.62
3793.360	24507–50861	3.04	388	−0.89			−0.86				−0.88	2.70	4.21
3793.478	24181–50534	3.00	387	−0.36	−0.42		−0.37				−0.38	3.20	4.71
3793.872	22947–49298	2.84	367	−0.58	−0.46		−0.55				−0.53	3.05	4.56
3794.340	19788–46136	2.45	177	−0.24	−0.18	−0.17[2]	−0.16				−0.18	3.40	4.91
3795.004	7986–34329	0.99	21		−0.39	−0.34[3]	−0.45			−0.43	−0.38	3.20	4.71
3796.000	19390–45726	2.40	176	−2.17							−2.17	1.41	2.92

TABLE 3.—*Oscillator Strengths for Ultraviolet Lines of Fe* I—Continued

Wavelength Å	Energy Levels K	Low e.p. Volts	Mult. No.	Arc	Spk	CW(N)	HC	R(N)	KOC	MS	Best	Log gfλ	Log gA/λ
				Log *gf*									
3797.517	26106–52431	3.24	607	0.82	0.94	0.65[2]	0.63				0.74	4.32	5.83
3797.950	20875–47197	2.59	222	−1.10	−1.01		−1.03				−1.05	2.53	4.04
3798.513	7377–33695	0.91	21		−0.72	−0.70[3]	−0.59			−0.76	−0.70	2.88	4.39
3799.550	7728–34040	0.96	21		−0.47	−0.43[3]	−0.50			−0.57	−0.47	3.11	4.61
3801.682	22838–49135	2.83	367	−0.20	−0.08	−0.11[1]	−0.27				−0.16	3.42	4.92
3801.804	22947–49243	2.84	367	−0.51			−0.60				−0.56	3.02	4.52
3801.975	26875–53169	3.33	704	−0.35	−0.65		−0.34				−0.45	3.13	4.63
3802.283	26624–52916	3.30	666	−0.50	−0.34		−0.56				−0.47	3.11	4.61
3803.220	18378–44664	2.28	122	−2.62	−1.60						−2.62	0.96	2.46
3804.013	26875–53155	3.33	702	−0.38	−0.58	−0.50[1]	−0.53				−0.50	3.08	4.58
3805.345	26628–52899	3.30	608	0.99	1.10	0.91[2]	0.91				0.96	4.54	6.04
3806.203	27543–53808	3.41	731	−0.14			−0.10				−0.12	3.46	4.96
3806.699	26351–52613	3.27	607	0.77	0.83	0.61[2]	0.41				0.65	4.23	5.73
3807.539	17927–44184	2.22	73	−0.23	−0.25	−0.47[2]	−0.22				−0.33	3.25	4.75
3808.286	24336–50587	3.02	489	−1.07	−0.76		−1.19				−0.92	2.66	4.16
3808.731	20641–46889	2.56	222	−0.31	−0.26	−0.29[1]	−0.30				−0.29	3.29	4.79
3809.043	23052–49298	2.86	367		−0.85		−1.13				−0.99	2.59	4.09
3810.759	26624–52858	3.30	665	−0.14	−0.06	−0.20[1]	−0.15				−0.14	3.44	4.94
3811.050	20875–47107	2.59	223	−1.72			−1.13						
3811.892	22249–48476	2.76	287	−0.54	−0.38	−0.62[1]	−0.58				−0.53	3.05	4.55
3812.966	7728–33947	0.96	22		−0.61	−0.61[3]	−0.57			−0.59	−0.60	2.98	4.48
3813.059	20875–47093	2.59	222				−0.07				−0.07	3.51	5.01
3813.638	21716–47930	2.69	283	−0.76	−0.66		−0.92				−0.78	2.80	4.30
3813.891	29313–55526	3.63	854	−0.22	0.03						−0.10	3.48	4.98
3814.525	8155–34363	1.01	22	−1.74	−1.84	−1.77[2]	−1.75				−1.77	1.81	3.31
3814.785	27543–53749	3.41		−0.48	−0.42						−0.45	3.13	4.63
3815.843	11976–38175	1.48	45			0.60[3]	0.60	0.65[2]		0.49	0.60	4.18	5.68
3816.342	17727–43923	2.20	73	−0.47	−0.53		−0.58				−0.53	3.05	4.55
3816.908	24507–50699	3.04	387	−0.22	−0.66								
3817.650	26875–53061	3.33	701	−0.24	−0.41	−0.29[1]	0.03				−0.31	3.27	4.77
3819.497	27395–53569	3.40	703	−0.45	−0.41						−0.43	3.15	4.65
3820.427	6928–33096	0.86	20			0.41[3]	0.41	0.41[2]			0.41	3.99	5.49
3821.181	26351–52514	3.27	608	0.95	0.97	0.73[1]	0.82				0.87	4.45	5.95
3821.836	21039–47197	2.61	222	−0.41	−0.22	−0.21[1]	−0.34				−0.30	3.28	4.78
3824.076	20875–47017	2.59	224	−0.81	−0.60		−0.17				−0.70	2.88	4.38
3824.306	26628–52769	3.30	607	1.52			0.42						
3824.446	0–26140	0.00	4		−1.26	−1.15[3]	−1.19	−1.14[2]			−1.17	2.41	3.91
3825.404	18378–44512	2.28	123	−1.50	−0.86		−1.49						
3825.883	7377–33507	0.91	20			0.24[3]	0.35	0.24[1]			0.26	3.84	5.34
3826.836	21999–48123	2.73	283	−1.00	−0.68		−0.76				−0.81	2.77	4.27
3827.575	21716–47835	2.69	284				−0.70				−0.70	2.88	4.38
3827.826	12561–38678	1.56	45			0.53[3]	0.60	0.56[1]			0.55	4.13	5.63
3828.510	22249–48362	2.76	287	−1.19	−0.79		−1.26						
3829.125	29799–55907	3.69	948	−0.64	−0.58		−0.79				−0.67	2.91	4.40
3829.458	26406–52512	3.27	663	−0.48	−0.29		0.39				−0.38	3.20	4.69
3829.764	20641–46745	2.56	221	−1.31	−1.26		−0.36				−1.28	2.30	3.79
3830.761	21039–47136	2.61	224	−0.97			−0.40						
3830.864	21716–47812	2.69	284	−0.80		−0.59[1]	−0.72				−0.70	2.88	4.37
3833.310	20641–46721	2.56	221	−0.19	−0.14	−0.14[2]	−0.14				−0.15	3.43	4.92
3834.224	7728–33802	0.96	20			−0.02[3]	0.04	0.06[2]		−0.09	0.01	3.59	5.08
3836.332	26624–52683	3.30	664	0.25	0.35	0.28[1]	0.30				0.30	3.88	5.37
3837.137	21039–47093	2.61	222	−0.89	−0.89	−0.90[1]	−0.85				−0.88	2.70	4.19
3839.258	24575–50614	3.05	529	0.40	0.52	0.30[2]	0.57				0.42	4.00	5.49
3839.630	31937–57974	3.96	995	−0.57	0.32								
3840.440	7986–34017	0.99	20			−0.20[3]	−0.15	−0.15[1]		−0.25	−0.19	3.39	4.88
3841.050	12969–38996	1.61	45			0.45[3]	0.68	0.48[1]		0.33	0.47	4.05	5.54
3842.901	20875–46889	2.59	222	−1.30							−1.30	2.28	3.77
3842.975	20875–46889	2.59	221	−1.47			−1.12				−1.30	2.28	3.77
3843.260	24575–50587	3.05	528	0.47	0.67	0.49[2]	0.54				0.53	4.11	5.60
3845.171	19552–45552	2.42	124	−0.63	−0.48	−0.55[1]	−0.58				−0.56	3.02	4.51

TABLE 3.—*Oscillator Strengths for Ultraviolet Lines of Fe* I—Continued

Wavelength Å	Energy Levels K	Low e.p. Volts	Mult. No.	Arc	Spk	CW(N)	HC	R(N)	KOC	MS	Best	Log gfλ	Log gA/λ
							Log *gf*						
3845.692	28605–54600	3.55	771	−0.75	−0.67		−0.63				−0.68	2.90	4.39
3846.001	27167–53161	3.37	703	−0.74			−1.01				−0.88	2.71	4.19
3846.412	28820–54811	3.57	804	0.00	0.30		0.17				0.16	3.75	5.23
3846.802	26225–52213	3.25	664	0.58		0.59[2]	0.60				0.59	4.18	5.66
3848.299	21039–47017	2.61	224	−1.23	−1.23						−1.23	2.36	3.84
3849.969	8155–34122	1.01	20		−0.52	−0.44[2]	−0.43	−0.29[1]		−0.59	−0.45	3.14	4.62
3850.819	7986–33947	0.99	22	−1.20	−1.18	−1.24[2]	−1.26				−1.22	2.37	3.85
3852.575	17550–43500	2.18	73	−0.44	−0.47	−0.58[2]	−0.76				−0.57	3.02	4.50
3853.462	23784–49727	2.95	429	−1.18	−0.85		−0.91				−0.98	2.61	4.09
3854.375	25900–51837	3.21	567	−0.47	−0.68	−0.51[1]	−0.37				−0.51	3.08	4.56
3855.329	21999–47930	2.73	283	−1.24	−1.10		−1.56				−1.17	2.42	3.90
3855.846	26140–52067	3.24	567	−0.56	−0.78		−0.59				−0.64	2.95	4.43
3856.373	416–26340	0.05	4		−1.25	−1.13[3]	−1.13	−1.13[3]		−1.13	−1.14	2.45	3.93
3858.474	26140–52050	3.24	565	−0.38	−0.78						−0.58	3.01	4.48
3859.214	19390–45295	2.40	175	0.01	0.09	0.07[2]	0.08				0.06	3.65	5.12
3859.913	0–25900	0.00	4			−0.54[3]	−0.63	−0.56[2]		−0.62	−0.57	3.02	4.49
3861.341	21716–47606	2.69	283	−0.63	−0.35	−0.52[1]	−0.69				−0.55	3.04	4.51
3861.600	26624–52512	3.30	663	−1.25	−0.64		−0.76				−0.70	2.89	4.36
3863.745	21716–47590	2.69	280	−0.64	−0.54	−0.70[1]	−0.73				−0.65	2.94	4.41
3864.307	20875–46745	2.59	221	−1.98							−1.98	1.61	3.08
3865.526	8155–34017	1.01	20			−0.56[3]	−0.60				−0.57	3.02	4.49
3867.218	24336–50187	3.02	488	0.29	0.39	0.12[2]	0.20				0.22	3.81	5.28
3867.925	20875–46721	2.59	221	−1.05	−0.99	−1.21[1]	−1.05				−1.08	2.51	3.98
3868.243	23784–49628	2.95	430	−1.43	−0.93						−1.43	2.16	3.63
3869.561	21999–47835	2.73	284	−0.49	−0.30	−0.52[1]	−0.66				−0.49	3.10	4.57
3871.751	23784–49604	2.95	429	−0.19	0.05	−0.15[1]	−0.21				−0.12	3.47	4.94
3872.503	7986–33802	0.99	20		−0.62	−0.54[3]	−0.54	−0.05[1]		−0.65	−0.57	3.02	4.49
3872.923	21999–47812	2.73	284	−1.03	−0.81		−0.82				−0.89	2.70	4.17
3873.762	19621–45428	2.43	175	−0.04	−0.04	−0.15[2]	−0.02				−0.08	3.51	4.98
3874.053	18378–44184	2.28	120	−1.76			−1.00						
3876.041	8155–33947	1.01	22	−2.32	−2.37	−2.20[1]	−2.34				−2.31	1.28	2.75
3876.670	18378–44166	2.28	121	−2.16			−2.10				−2.13	1.46	2.93
3878.021	7728–33507	0.96	20		−0.65	−0.50[3]	−0.51			−0.64	−0.55	3.04	4.51
3878.574	704–26479	0.09	4			−1.19[3]	−1.18	−1.13[2]		−1.22	−1.18	2.41	3.88
3878.676	19788–45563	2.45	175				−1.45				−1.45	2.14	3.61
3878.740	26406–52181	3.27	664				−0.80				−0.80	2.79	4.26
3883.282	26225–51969	3.25	663	−0.08	0.11	0.02[1]	−0.11				−0.02	3.57	5.04
3884.361	21716–47453	2.69	282	−0.54	−0.32	−0.37[1]	−0.37				−0.40	3.19	4.66
3885.154	24119–49851	2.99	430	−0.78	−0.81		−0.93				−0.84	2.75	4.22
3885.512	19552–45282	2.42	124	−0.41	−0.34	−0.35[2]	−0.46				−0.38	3.21	4.68
3886.284	416–26140	0.05	4		−1.14	−0.90[3]	−0.91	−0.91[2]		−0.93	−0.94	2.65	4.12
3887.050	7377–33096	0.91	20	−0.97	−0.84	−0.72[2]	−0.71			−0.90	−0.81	2.78	4.25
3888.516	12969–38678	1.61	45	−0.11	−0.13	−0.05[2]	−0.01	0.02[1]		−0.13	−0.07	3.52	4.98
3888.825	24336–50043	3.02	488	0.00	0.03		−0.20				−0.06	3.53	4.99
3889.284	21716–47420	2.69	280	−1.66							−1.66	1.93	3.39
3889.931	26340–52040	3.26	564	−1.21			0.37						
3890.390	26140–51837	3.24	567	−1.00	−0.85		−0.87				−0.91	2.68	4.14
3890.844	21999–47693	2.73	280	−0.61	−0.45	−0.62[1]	−0.62				−0.58	3.01	4.47
3891.928	27543–53230	3.41	733	−0.04	0.23	−0.02[1]	−0.05				0.03	3.62	5.08
3892.302	28605–54289	3.55		−1.59							−1.59	2.00	3.46
3892.894	22249–47930	2.76	283	−1.26	−1.07		−1.45				−1.26	2.33	3.79
3892.980	26340–52020	3.26	567	−0.93							−0.93	2.66	4.12
3893.316	22838–48516	2.83	364				−0.76				−0.76	2.83	4.29
3893.393	23784–49461	2.95	430	0.27	0.31	0.20[2]	0.14				0.22	3.81	5.27
3893.914	19621–45295	2.43	175	−0.96			−0.89				−0.92	2.67	4.13
3894.005	26624–52297	3.30	663	−0.20	−0.06		−0.31				−0.19	3.40	4.86
3894.490	25900–51570	3.21	566	−1.83			−0.72						
3895.450	26550–52214	3.29	565				−0.70				−0.70	2.89	4.35
3895.658	888–26550	0.11	4		−1.55	−1.47[3]	−1.50	−1.38[3]		−1.40	−1.44	2.15	3.61
3897.452	23784–49434	2.95	429	−0.51	−0.35		−0.71				−0.52	3.07	4.53

TABLE 3.—*Oscillator Strengths for Ultraviolet Lines of Fe* I—Continued

Wavelength Å	Energy Levels K	Low e.p. Volts	Mult. No.	Arc	Spk	CW(N)	HC	R(N)	KOC	MS	Best	Log gfλ	Log gA/λ
				Log *gf*									
3897.896	21716–47363	2.69	280	0.22	0.03	0.05[1]					0.10	3.69	5.15
3898.011	8155–33802	1.01	20	−1.27	−1.21	−1.52[2]	−1.58				−1.42	2.17	3.63
3899.037	19788–45428	2.45	175	−0.97	−0.96	−0.90[1]	−1.02				−0.96	2.63	4.09
3899.709	704–26340	0.09	4		−1.50	−1.30[3]	−1.37	−1.29[3]		−1.32	−1.32	2.27	3.73
3900.519	26140–51771	3.24	565	−0.30	−0.31	−0.25[1]	−0.29				−0.29	3.30	4.76
3902.948	12561–38175	1.56	45	−0.14	−0.06	0.12[3]	−0.04			−0.05	0.01	3.60	5.06
3903.901	24119–49727	2.99	429	0.03	0.11	−0.04[2]	−0.32				−0.05	3.54	5.00
3906.481	888–26479	0.11	4	−1.91	−1.96	−1.89[2]	−2.06	−1.88[3]		−1.99	−1.92	1.67	3.13
3906.748	26624–52213	3.30	664	−0.30	−0.21		−0.29				−0.27	3.32	4.78
3907.464	22249–47834	2.76	284	−0.98	−0.93		−0.84				−0.92	2.67	4.13
3907.937	22249–47831	2.76	280	−0.35	−0.26	−0.34[1]	−0.29				−0.31	3.28	4.74
3908.691	19757–45334	2.45	153	−2.68	−1.47						−1.47	2.12	3.58
3909.664	26479–52050	3.28	565	−0.48	−0.57		−0.41				−0.49	3.10	4.56
3909.830	22947–48516	2.84	364	−0.49	−0.37	−0.40[1]	−0.57				−0.46	3.13	4.59
3910.846	22249–47812	2.76	284	−0.70	−0.64	−0.56[1]	−0.61				−0.63	2.96	4.42
3911.005	25900–51462	3.21	562	−0.88			−0.95				−0.92	2.67	4.13
3911.699	26624–52181	3.30	664	−1.59			−1.44				−1.52	2.07	3.53
3913.634	18378–43923	2.28	120	−0.88	−0.84	−0.78[1]	−0.85				−0.84	2.75	4.21
3914.273	26479–52020	3.28	567	−0.70	−0.80		−0.73				−0.74	2.85	4.31
3916.733	26106–51630	3.24	606	0.08	0.26	0.14[2]	0.30				0.18	3.77	5.23
3917.183	7986–33507	0.99	20	−1.58	−1.72	−1.61[3]	−1.67				−1.63	1.96	3.42
3918.317	20038–45552	2.48	124	−0.56			−0.57				−0.56	3.03	4.48
3918.418	22947–48460	2.84	364	−0.25			−0.38				−0.32	3.27	4.72
3918.644	24339–49851	3.02	430	0.14	0.24	0.14[2]	−0.02				0.13	3.72	5.17
3919.068	24119–49628	2.99	430	−0.47	−0.23	−0.46[1]	−0.44				−0.40	3.19	4.64
3920.260	978–26479	0.12	4			−1.49[3]	−1.58	−1.44[3]		−1.53	−1.48	2.11	3.56
3920.645	19562–45061	2.42	153				−1.85				−1.85	1.74	3.19
3920.839	26340–51837	3.26	567	−0.91	−0.77		−0.73				−0.80	2.79	4.24
3921.270	20641–46136	2.56	220	−1.78			−1.73				−1.76	1.83	3.28
3922.100	20020–45509	2.48	153	−2.30							−2.30	1.29	2.74
3922.913	416–25900	0.05	4		−1.59	−1.41[3]	−1.51	−1.41[3]		−1.48	−1.44	2.15	3.60
3925.201	26550–52020	3.29	567	−0.74	−0.73		−0.76				−0.74	2.85	4.30
3925.646	22838–48305	2.83	364	−0.22	−0.24		−0.27				−0.24	3.35	4.80
3925.946	23052–48516	2.86	364	−0.10	−0.03	−0.17[1]	−0.30				−0.15	3.44	4.89
3926.001	26140–51604	3.24	562				−0.43				−0.43	3.16	4.61
3927.922	888–26340	0.11	4			−1.29[3]	−1.36	−1.28[3]		−1.34	−1.30	2.29	3.74
3929.114	22249–47693	2.76	280		−1.10		−1.05				−1.08	2.51	3.96
3929.208	26225–51668	3.25	659		−0.32		−0.69				−0.50	3.09	4.54
3930.298	704–26140	0.09	4		−1.49	−1.26[3]	−1.35	−1.29[3]		−1.30	−1.31	2.28	3.73
3931.122	26340–51771	3.26	565	−0.40	−0.42	−0.52[1]	−0.43				−0.44	3.15	4.60
3932.629	26406–51828	3.27	652	−0.03	−0.04	−0.47[1]	−0.46						
3933.606	24772–50187	3.07	488	−0.37	−0.11	−0.42[1]	−0.43				−0.33	3.26	4.71
3935.306	22947–48351	2.84	362	−0.85	−0.85	−1.01[1]	−0.81				−0.88	2.71	4.16
3935.814	22838–48239	2.83	362	−0.11	−0.07	−0.14[2]	−0.16				−0.12	3.48	4.92
3936.772	25900–51294	3.21	564	−1.91							−1.91	1.69	3.13
3937.331	21716–47107	2.69	278	−0.60	−0.58	−0.63[1]	−0.64				−0.61	2.99	4.43
3940.044	27543–52916	3.41	731	−1.27	−0.81		−1.14						
3940.880	7728–33096	0.96	20	−1.99	−2.12	−1.99[2]	−2.08				−2.03	1.57	3.01
3941.283	26340–51705	3.26	562	−0.42	−0.65	−0.52[1]	−0.49				−0.52	3.08	4.52
3942.442	22947–48305	2.84	364	−0.27	−0.15	−0.19[2]	−0.41				−0.24	3.36	4.80
3943.341	17727–43079	2.20	72	−1.40	−1.41	−1.34[1]	−1.29				−1.36	2.24	3.68
3944.748	22947–48290	2.84	361	−1.26			−1.11				−1.18	2.42	3.86
3944.892	24119–49461	2.99	430	−0.61	−0.50	−0.66[1]	−0.69				−0.62	2.98	4.42
3945.119	22249–47590	2.76	280	−0.64	−0.60	−0.80[1]	−0.71				−0.69	2.91	4.35
3947.002	25900–51229	3.21	561	−0.26	−0.36	−0.24[1]	−0.45				−0.33	3.27	4.71
3947.391	19351–44677	2.40	153	−2.30			−1.85						
3947.533	22838–48163	2.83	361	−0.38	−0.24	−0.37[1]	−0.40				−0.35	3.25	4.68
3948.105	26140–51462	3.24	562	0.09	−0.06	0.13[1]	0.00				0.04	3.64	5.07
3948.778	26351–51668	3.27	604	0.38	0.49	0.38[2]	0.29				0.38	3.98	5.41
3949.156	27543–52858	3.41	730	−0.91			−0.78				−0.84	2.76	4.19

TABLE 3.—*Oscillator Strengths for Ultraviolet Lines of Fe* I—Continued

Wavelength Å	Energy Levels K	Low e.p. Volts	Mult. No.	Arc	Spk	CW(N)	HC	R(N)	KOC	MS	Best	Log gfλ	Log gA/λ
				Log *gf*									
3949.956	17550–42860	2.18	72	−0.43	−0.40	−0.50[2]	−0.42				−0.45	3.15	4.58
3951.164	26406–51708	3.27	661	0.26	0.31	0.31[2]	0.25				0.29	3.89	5.32
3951.638	23052–48351	2.86		−1.92							−1.92	1.68	3.11
3952.604	21716–47008	2.69	278	−0.30	−0.24	−0.21[2]	−0.32				−0.26	3.34	4.77
3952.702	22947–48239	2.84	362				−0.57				−0.57	3.03	4.46
3953.155	24339–49628	3.02	430	−0.34	−0.25	−0.38[1]	−0.44				−0.35	3.25	4.68
3953.512	28605–53892	3.55	770	−1.48							−1.48	2.12	3.55
3953.861	22838–48123	2.83	362	−1.17	−1.04	−1.23[1]	−1.06				−1.12	2.48	3.91
3954.715	26351–51630	3.27	606	−1.53	−0.85		−1.21						
3955.352	26479–51755	3.28	562	−0.37	−0.75	−0.41[1]	−0.49				−0.50	3.10	4.53
3955.956	24772–50043	3.07	488	−0.66	−0.56	−0.68[1]	−0.68				−0.64	2.96	4.39
3956.457	26106–51374	3.24	604	0.41	0.49	0.41[1]	0.54				0.46	4.06	5.49
3956.680	21716–46982	2.69	278	0.51	0.41	0.33[1]	0.31				0.39	3.99	5.42
3957.027	26340–51604	3.26	562	−0.08	−0.26		0.00				−0.11	3.49	4.92
3957.620	26479–51740	3.28	564	−1.47	−1.03		−1.27				−1.37	2.23	3.66
3960.284	29357–54600	3.64	913	−0.55	−0.58	−0.61[2]	−0.69				−0.61	2.99	4.42
3961.147	23052–48290	2.86	361	−0.89	−0.90	−1.00[2]	−0.83				−0.92	2.68	4.11
3962.353	26340–51570	3.26	566	−0.99	−1.04	−1.01[1]	−0.89				−0.98	2.62	4.05
3963.108	26479–51705	3.28	562	−0.08	−0.29	−0.09[1]	−0.15				−0.15	3.45	4.88
3963.438	26406–51630	3.27	654	−1.50							−1.50	2.10	3.53
3964.517	22947–48163	2.84	361	−0.71	−0.68	−0.80[1]	−0.65				−0.71	2.89	4.32
3965.511	26140–51351	3.24	565	−0.72	−0.83		−0.78				−0.78	2.82	4.25
3966.064	12969–38175	1.61	45	−1.02	−1.16	−0.99[2]	−1.23				−1.08	2.52	3.95
3966.532	26624–51828	3.30	652				−0.86				−0.86	2.74	4.17
3966.630	25900–51103	3.21	562		0.13	0.34[2]	0.34				0.29	3.89	5.32
3966.824	26624–51826	3.30	659				0.15				0.15	3.75	5.18
3967.423	26628–51826	3.30	604	0.25	0.36	0.34[2]	−0.42				0.32	3.92	5.35
3967.964	26140–51335	3.24	561	−0.23	−0.38	−0.16[1]	−1.03				−0.26	3.34	4.77
3969.260	11976–37163	1.48	43	−0.13	−0.17	0.02[3]	0.08	0.03[1]		0.00	−0.02	3.58	5.01
3969.628	26225–51409	3.25	657		−0.28		−0.31				−0.30	3.30	4.73
3970.391	24772–49951	3.07	488	−0.26		−0.26[1]	−0.28				−0.26	3.34	4.77
3971.325	21716–46889	2.69	277	−0.14		−0.13[2]	−0.14				−0.14	3.46	4.89
3971.820	22249–47420	2.76	281	−1.86			−1.94				−1.90	1.70	3.13
3972.918	28820–53983	3.57	803		−0.87		−1.36						
3973.655	28605–53763	3.55	769	−0.25	−0.29	−0.31[1]	−0.30				−0.29	3.31	4.74
3974.397	26140–51294	3.24	564	−1.11	−1.08		−0.71				−1.10	2.50	3.93
3974.764	17927–43079	2.22	72	−1.95			−1.86				−1.90	1.70	3.13
3975.210	19913–45061	2.47	153	−1.92			−1.92				−1.92	1.68	3.11
3975.842	31307–56452	3.88	977	−0.81	−0.81						−0.81	2.79	4.22
3976.390	24336–49477	3.02	487	−1.30			−1.42				−1.36	2.24	3.67
3976.615	27543–52683	3.41	729	0.06		−0.01[1]	0.00				0.02	3.62	5.05
3976.865	24339–49477	3.02	431	−0.51	−0.58		−0.79				−0.63	2.97	4.40
3977.744	17727–42860	2.20	72	−0.31	−0.35	−0.22[2]	−0.28				−0.28	3.32	4.75
3978.464	22838–47967	2.83	361		−1.20		−1.37				−1.28	2.32	3.74
3979.630	26340–51461	3.26	561	−1.11			−1.01				−1.06	2.54	3.96
3980.650	19562–44677	2.42	153	−2.43			−2.24				−2.34	1.26	2.68
3981.104	19552–44664	2.42	22	−2.06							−2.06	1.54	2.96
3981.774	21999–47107	2.73	278	−0.32	−0.28	−0.24[2]	−0.36				−0.29	3.31	4.73
3983.350	24336–49433	3.02	485		−1.23	−1.47[1]	−1.85				−1.35	2.25	3.67
3983.959	21999–47093	2.73	277	0.05	−0.12	0.06[3]	−0.14				0.00	3.60	5.02
3984.930	26479–51567	3.28	561	−1.44		−1.55[1]					−1.50	2.10	3.52
3985.322	20641–45726	2.56	219			−1.85[1]					−1.85	1.75	3.17
3985.393	26624–51708	3.30	661		−0.36	−0.50[2]	−0.44				−0.45	3.15	4.57
3986.176	26225–51305	3.25	655	−0.13	−0.09	−0.21[2]	−0.09				−0.15	3.45	4.87
3989.006	28820–53882	3.57		−1.12							−1.12	2.48	3.90
3989.859	28605–53661	3.55	768	−0.43		−0.59[2]	−0.53				−0.54	3.06	4.48
3990.377	24575–49628	3.05	527	−0.64		−0.70[2]	−0.72				−0.69	2.91	4.33
3992.395	26628–51668	3.30	604	−1.63		−1.58[1]	−1.51				−1.57	2.03	3.45
3994.117	24575–49604	3.05	526	−0.58	−0.59	−0.71[2]	−0.73				−0.66	2.94	4.36
3995.199	26351–51374	3.27	604	−1.15	−0.89	−1.12[2]	−1.29				−1.11	2.49	3.91

TABLE 3.—*Oscillator Strengths for Ultraviolet Lines of Fe* I—Continued

Wavelength Å	Energy Levels K	Low e.p. Volts	Mult. No.	Arc	Spk	CW(N)	HC	R(N)	KOC	MS	Best	Log gfλ	Log gA/λ
				Log *gf*									
3995.986	21999–47017	2.73	279	−0.58	−0.65	−0.66[2]	−0.78				−0.67	2.93	4.35
3996.261	24119–49135	2.99	561	−1.55		−1.78[1]					−1.78	1.82	3.24
3996.779	33507–58520	4.15	1074	−1.12		−0.61[1]					−0.61	2.99	4.41
3996.968	29799–54811	3.69	945	−0.25	−0.16	−0.22[2]	−0.21				−0.21	3.39	4.81
3997.395	21999–47008	2.73	278	0.45	0.36	0.38[3]	0.32				0.38	3.98	5.40
3998.055	21716–46721	2.69	276	−0.01	−0.12	−0.04[3]	−0.04				−0.05	3.55	4.97
4000.266	26340–51331	3.26	556	−0.83		−0.87[1]	−1.08				−0.98	2.62	4.04
4000.460	24119–49109	2.99	426	−0.66	−0.68	−0.80[2]	−0.78				−0.74	2.86	4.28
4001.663	17550–42533	2.18	72	−1.10	−1.12	−1.09[2]	−1.05				−1.09	2.51	3.93
4002.665	23245–48221	2.88	320	−1.84		−1.67[2]	−1.54				−1.68	1.92	3.34
4003.764	27543–52512	3.41	728	−0.59	−0.48	−0.51[2]	−0.55				−0.53	3.07	4.49
4004.832	26106–51069	3.24	601			−0.47[1]					−0.47	3.13	4.55
4004.976	24336–49298	3.02	486			−0.76[1]	−0.85				−0.80	2.80	4.22
4005.244	12561–37521	1.56	43	−0.11	−0.02	−0.07[3]	−0.10	−0.12[1]		−0.15	−0.09	3.51	4.93
4006.159	26340–51294	3.26	564			−1.56[1]					−1.56	2.04	3.46
4006.314	26351–51305	3.27	603		−0.15	−0.23[1]	−0.17				−0.18	3.42	4.84
4006.631	25092–50043	3.11	488		−0.39	−0.43[1]	−0.58				−0.44	3.16	4.58
4006.768	23270–48221	2.88	320		−0.97	−0.99[1]	−1.22				−1.06	2.54	3.96
4007.274	22249–47197	2.76	277	−0.44	−0.44	−0.45[2]	−0.46				−0.45	3.15	4.57
4009.715	17927–42860	2.22	72	−0.39	−0.42	−0.44[3]	−0.43				−0.43	3.17	4.58
4010.180	29372–54301	3.64	915	−1.42		−1.29[1]	−1.55				−1.42	2.18	3.59
4010.770	23111–48037	2.86	320	−2.03		−1.72[1]	−1.55						
4011.412	20641–45563	2.56	218	−1.40	−1.40	−1.54[1]	−1.50				−1.46	2.14	3.55
4011.710	19757–44677	2.45	153	−1.77		−1.85[1]	−1.91				−1.84	1.76	3.17
4012.160	26106–51023	3.24	601	−1.72		−1.61[1]	−1.59				−1.64	1.96	3.37
4013.641	25900–50808	3.21	557	−0.89	−0.98	−1.02[1]	−0.95				−0.96	2.64	4.05
4013.798	24336–49243	3.02	485			−1.07[1]					−1.07	2.53	3.94
4013.822	24336–49243	3.02	486			−0.71[1]	−0.68				−0.70	2.90	4.31
4014.280	24339–49243	3.02	426	−1.32	−1.14	−1.37[1]	−1.38				−1.30	2.30	3.71
4014.534	28820–53722	3.57	802	0.38	0.52	0.58[3]	0.58				0.54	4.14	5.55
4016.429	26479–51370	3.28	560	−0.66	−0.89	−0.66[2]	−0.75				−0.72	2.88	4.29
4017.093	22249–47136	2.76	279			−1.09[1]					−1.09	2.51	3.92
4017.152	24575–49461	3.05	527		−0.11	−0.17[2]	−0.22				−0.17	3.43	4.84
4018.282	26340–51219	3.26	560		−0.78	−0.63[2]	−0.70				−0.70	2.90	4.31
4019.050	21039–45914	2.61	219	−1.88	−1.59	−1.80[1]	−1.74				−1.75	1.85	3.26
4020.490	29372–54237	3.64	913	−1.13	−0.88	−1.05[1]	−1.17				−1.06	2.54	3.95
4021.622	26140–50999	3.24	557	−1.08		−1.20[1]					−1.14	2.46	3.87
4021.870	22249–47107	2.76	278	0.20	0.08	0.12[3]	0.06				0.12	3.72	5.13
4022.212	22838–47693	2.83		−1.74		−1.66[1]					−1.70	1.90	3.31
4022.450	19390–44244	2.40	173	−2.37		−2.22[1]	−2.21				−2.27	1.33	2.74
4022.744	26479–51331	3.28	556	−1.10		−1.17[1]	−1.33				−1.20	2.40	3.81
4024.109	22249–47093	2.76	277	−1.30	−1.16	−1.35[2]	−1.33				−1.28	2.32	3.73
4024.735	26140–50980	3.24	560	−0.04	−0.33	−0.06[2]	−0.10				−0.12	3.48	4.89
4029.640	26340–51149	3.26	556	−0.29	−0.65	−0.42[2]	−0.47				−0.45	3.16	4.56
4030.186	17727–42533	2.20	72	−1.51	−1.51	−1.47[1]	−1.51				−1.50	2.11	3.51
4030.499	25900–50704	3.21	560	0.05	−0.20	0.08[2]	0.09				0.02	3.63	5.03
4031.243	24336–49135	3.02	486	−1.51		−1.41[1]	−1.58				−1.50	2.11	3.51
4031.727	24339–49135	3.02	427	−1.49		−1.42[1]					−1.44	2.17	3.57
4031.965	26406–51201	3.27	655	−0.21	−0.26	−0.30[2]	−0.33				−0.28	3.33	4.73
4032.469	23245–48037	2.88	320		−1.11	−1.24[1]	−1.46				−1.27	2.34	3.74
4032.629	11976–36767	1.48	44	−1.74	−1.89	−1.74[2]	−1.85				−1.79	1.82	3.22
4033.190	20641–45428	2.56	218	−1.64		−1.72[2]	−1.69				−1.69	1.92	3.32
4036.370	22249–47017	2.76	279	−2.10		−1.95[1]					−2.02	1.59	2.99
4037.725	18378–43138	2.28	118	−2.03	−1.55								
4038.622	26628–51381	3.30	600	−1.52		−0.99[2]					−0.99	2.62	4.02
4039.940	21999–46745	2.73	276	−1.75		−1.54[2]	−1.59				−1.60	2.01	3.40
4040.650	26624–51365	3.30	655	−0.35	−0.35	−0.30[2]	0.04				−0.27	3.34	4.73
4041.288	26628–51365	3.30	603	−0.72	−0.81	−0.74[2]	−0.92				−0.79	2.82	4.21
4041.911	26628–51361	3.30	602			−1.25[1]	−1.25				−1.25	2.36	3.75
4043.901	21999–46721	2.73	276			−0.56[2]	−0.70				−0.61	3.00	4.39

TABLE 3.—*Oscillator Strengths for Ultraviolet Lines of Fe* I—Continued

Wavelength Å	Energy Levels K	Low e.p. Volts	Mult. No.	Arc	Spk	CW(N)	HC	R(N)	KOC	MS	Best	Log gfλ	Log gA/λ
				Log *gf*									
4043.993	26140–50861	3.24	559		−0.37	−0.63[1]					−0.50	3.11	4.50
4044.612	22838–47556	2.83	359	−0.30	0.14	−0.17[2]	−0.33	−0.30[1]			−0.19	3.42	4.81
4045.815	11976–36686	1.48	43			0.68[3]	0.65			0.62	0.66	4.27	5.66
4046.629	24772–49477	3.07	487				−1.18				−1.18	2.43	3.82
4047.315	18378–43079	2.28	117	−1.68		−1.84[1]	−1.88				−1.80	1.81	3.20
4049.331	20875–45563	2.59	218	−1.31	−1.34	−1.35[2]	−1.39				−1.35	2.26	3.65
4051.923	27395–52067	3.40	700	−0.80	−0.91	−0.68[2]	−0.82				−0.78	2.83	4.22
4052.312	27167–51837	3.37	700	−0.93		−0.89[1]	−0.96				−0.93	2.68	4.07
4052.466	26479–51149	3.28	563	−0.83		−1.04[1]	−1.06				−0.98	2.63	4.02
4052.664	24575–49243	3.05	524		−1.05	−1.14[1]	−1.36				−1.18	2.43	3.82
4052.724	26140–50808	3.24	557			−1.16[1]	−1.07				−1.11	2.50	3.89
4053.820	24772–49433	3.07	485	−1.16		−1.47[1]	−1.34				−1.32	2.29	3.68
4054.180	26340–50999	3.26	557	−1.28		−1.17[1]	−1.24				−1.23	2.38	3.77
4054.833	27395–52050	3.40	698			−0.15[1]	−0.42				−0.28	3.33	4.72
4054.883	27560–52214	3.42	698		−0.33	−0.21[1]	−0.40				−0.31	3.30	4.69
4055.038	20641–45295	2.56	218	−0.84	−0.84	−0.86[1]	−0.54				−0.77	2.84	4.23
4055.980	29357–54005	3.64	914	−1.81		−1.60[1]	−1.59				−1.67	1.94	3.33
4056.530	23111–47756	2.86	320	−2.10		−1.82[1]					−1.96	1.65	3.04
4057.346	22249–46889	2.76	277	−1.00		−1.04[2]	−1.09				−1.04	2.57	3.96
4057.654	27543–52181	3.41	729	−2.01		−1.69[1]					−1.85	1.76	3.15
4058.227	25900–50534	3.21	558	−0.37	−0.50	−0.28[2]	0.01				−0.38	3.23	4.62
4058.756	19552–44184	2.42	120	−1.18	−1.31	−1.19[2]	−1.18				−1.21	2.40	3.79
4059.726	28605–53230	3.55	767	−0.50	−0.52	−0.52[2]	−0.52				−0.52	3.09	4.48
4062.444	22947–47556	2.84	359	0.02	0.02	0.05[3]	0.02	0.05[1]			0.04	3.65	5.04
4063.286	27167–51771	3.37	698	−0.06		0.34[1]	0.03				0.10	3.71	5.10
4063.596	12561–37163	1.56	43			0.43[2]	0.56	0.42[2]		0.41	0.44	4.05	5.44
4064.450	12561–37158	1.56	44	−2.27		−2.47[1]	−2.27				−2.34	1.27	2.66
4065.392	27666–52257	3.43	698	−0.50	−0.67	−0.70[2]	−0.62				−0.64	2.97	4.36
4066.590	24119–48703	2.99	424	−0.73	−0.61	−0.51[1]	−0.82				−0.67	2.94	4.33
4066.979	22838–47420	2.83	358	−0.25	−0.20	−0.19[2]	−0.30				−0.23	3.38	4.77
4067.274	20641–45221	2.56	217	−0.52	−0.65	−0.37[1]	−0.53				−0.52	3.09	4.48
4067.984	25900–50475	3.21	559	0.30	0.03	0.29[2]	0.31				0.24	3.85	5.24
4069.080	26479–51048	3.28	557	−1.25		−1.13[2]	−1.10				−1.15	2.46	3.85
4070.766	26140–50699	3.24	558	−0.03	−0.33	0.01[2]					−0.08	3.53	4.91
4071.520	20875–45428	2.59	218			−0.88[1]					−0.88	2.73	4.11
4071.740	12969–37521	1.61	43			0.40[3]	0.44	0.46[2]		0.35	0.42	4.03	5.41
4072.518	27666–52214	3.43	698	−0.45	−0.63	−0.43[1]	−0.56				−0.52	3.09	4.47
4073.760	26340–50880	3.26	558	−0.08	−0.35	−0.14[2]	−0.02				−0.15	3.46	4.84
4074.789	24575–49109	3.05	524	−0.14	−0.17	−0.14[2]	−0.24				−0.17	3.44	4.82
4076.232	24772–49298	3.07	486	−1.13	−1.20	−0.94[1]	−1.10				−1.09	2.52	3.90
4076.498	21039–45563	2.61	218			−0.90[1]	−1.14				−1.02	2.59	3.97
4076.636	25900–50423	3.21	558	0.17	0.06	0.24[2]	0.27				0.18	3.79	5.17
4076.810	26340–50862	3.26	557			−0.48[1]	−0.59				−0.54	3.07	4.45
4076.884	26340–50861	3.26	559			−1.42[1]					−1.42	2.19	3.57
4078.356	21039–45552	2.61	217	−0.59	−0.72	−0.61[2]	−0.58				−0.62	2.99	4.37
4078.822	29372–53882	3.64		−1.88		−1.45[1]							
4079.186	27560–52067	3.42	700	−0.81		−0.85[1]					−0.83	2.78	4.16
4079.841	23052–47556	2.86	359	−0.39	−0.51	−0.52[2]	−0.43	−0.48[1]			−0.48	3.13	4.51
4080.226	26479–50981	3.28	558	−0.33	−0.66	−0.34[1]	−0.43				−0.44	3.17	4.55
4080.886	26550–51048	3.29	557	−0.92		−1.06[2]	−0.98				−1.00	2.61	3.99
4082.125	27560–52050	3.42	698	−0.69		−0.70[1]	−0.81				−0.73	2.88	4.26
4082.432	29320–53808	3.63	906	−0.90		−0.78[1]	−0.88				−0.85	2.76	4.14
4083.554	18378–42860	2.28	117	−1.54		−1.59[1]	−1.60				−1.58	2.03	3.41
4083.780	27560–52040	3.42	697	−0.61		−0.63[1]	−0.80				−0.68	2.93	4.31
4084.498	26875–51351	3.33	698	0.17	−0.06	0.13[2]	0.08				0.09	3.70	5.08
4085.011	22947–47420	2.84	358	−0.39	−0.41	−0.41[1]	−0.51				−0.43	3.18	4.56
4085.312	26140–50611	3.24	559	0.00	−0.34	−0.02[1]	−0.16				−0.13	3.48	4.86
4085.980	33507–57974	4.15	1073	−0.83	−0.80	−0.68[1]					−0.77	2.84	4.22
4087.099	26875–51335	3.33	694	−0.47	−0.76	−0.67[2]	−0.70				−0.65	2.96	4.34
4087.801	29469–53925	3.65	832	−1.84		−1.60[1]					−1.72	1.89	3.27

TABLE 3.—*Oscillator Strengths for Ultraviolet Lines of Fe* I—Continued

Wavelength Å	Energy Levels K	Low e.p. Volts	Mult. No.	Arc	Spk	CW(N)	HC	R(N)	KOC	MS	Best	Log gfλ	Log gA/λ
				Log *gf*									
4088.567	29357–53808	3.64	906	−0.74	−0.56	−0.81[2]	−0.70				−0.72	2.89	4.27
4089.225	23784–48231	2.95	422	−0.96	−0.99	−1.15[2]	−0.94				−1.01	2.60	3.98
4090.077	27395–51837	3.40	700	−0.90	−0.89	−1.09[2]	−1.03				−1.00	2.61	3.99
4090.326	12969–37410	1.61	44	−3.52		−3.55[1]					−3.54	0.07	1.45
4090.984	27167–51604	3.37	695	−0.94		−1.10[2]	−1.05				−1.05	2.56	3.94
4091.557	22838–47272	2.83	357	−1.10	−1.19	−1.28[2]	−1.28	−1.30[1]			−1.24	2.37	3.75
4092.287	29320–53749	3.63		−0.68	−0.78	−0.75[1]					−0.74	2.87	4.25
4092.512	7377–31805	0.91	18	−3.55		−3.74[2]	−3.74				−3.69	−0.08	1.30
4095.274	33802–58213	4.19	1075	−1.35		−1.19[1]					−1.27	2.34	3.72
4095.973	20875–45282	2.59	217		−0.75	−0.60[2]	0.76				−0.68	2.93	4.31
4096.114	29357–53763	3.64	911			−0.70[1]	−0.71				−0.70	2.91	4.29
4096.217	7728–32134	0.96	18			−3.62[1]					−3.62	−0.01	1.37
4097.099	26479–50880	3.28	558		−0.92	−1.00[2]	−1.06				−1.00	2.61	3.99
4098.183	26140–50534	3.24	558	−0.02	−0.42	−0.18[2]	−0.23				−0.20	3.41	4.79
4099.080	26628–51017	3.30	600	−1.39		−1.93[1]	−1.92				−1.92	1.69	3.07
4100.350	34329–58710	4.26	1103	−1.82	−1.74	−1.19[1]							
4100.739	6928–31307	0.86	18	−2.44	−2.72	−2.53[2]	−2.73				−2.59	1.02	2.40
4100.916	19788–44166	2.45	173	−1.91		−2.56[1]							
4101.272	27395–51771	3.40	698	−0.53	−0.72	−0.69[2]	−0.59				−0.64	2.97	4.35
4101.681	20038–44411	2.48	120	−1.65		−1.72[2]	−1.60				−1.67	1.94	3.32
4103.620	26225–50587	3.25	650	−2.06		−1.77[1]					−1.92	1.69	3.06
4104.132	26340–50699	3.26	558	−0.24		−0.61[2]	−0.56				−0.50	3.11	4.48
4104.472	24119–48476	2.99	422	−2.01		−1.93[1]					−1.97	1.64	3.01
4104.970	26875–51229	3.33	694	−1.37		−1.57[2]	−1.27				−1.44	2.17	3.54
4106.265	20875–45221	2.59	217	−1.36		−1.51[1]	−1.44				−1.44	2.17	3.54
4106.437	27395–51740	3.40	697	−0.61	−0.83	−0.78[1]	−0.85				−0.77	2.84	4.21
4107.492	22838–47177	2.83	354	0.17	0.01	0.06[3]	0.07				0.07	3.68	5.05
4108.138	26140–50475	3.24	559	−1.50	−1.28	−1.60[1]					−1.46	2.15	3.52
4109.070	26550–50880	3.29	558	−0.62	−0.95	−0.76[2]	−0.89				−0.80	2.81	4.18
4109.805	22947–47272	2.84	357	−0.14	−0.16	−0.07[3]	−0.18	−0.11[1]			−0.11	3.50	4.87
4111.060	26875–51192	3.33	689				−1.39				−1.39	2.22	3.59
4112.350	27395–51705	3.40	695	−0.87		−1.08[2]	−1.03				−1.01	2.60	3.97
4112.972	33695–58002	4.18	1103	−0.01	−0.37	−0.02[2]	−0.02				−0.09	3.52	4.89
4114.448	22838–47136	2.83	357	−0.35	−0.52	−0.47[2]	−0.33	−0.45[1]			−0.43	3.18	4.55
4114.957	27167–51462	3.37	695	−0.77	−0.90	−0.92[2]	−0.87				−0.88	2.73	4.10
4116.970	26140–50423	3.24	558	−1.63		−1.53[1]					−1.58	2.03	3.40
4117.320	24772–49053	3.07	484			−1.98[1]					−1.98	1.63	3.00
4117.850	27560–51837	3.42	700			−0.98[1]					−0.98	2.63	4.00
4117.870	34547–58825	4.28	1103			−0.78[1]	−1.03				−0.90	2.71	4.08
4118.548	28820–53094	3.57	801	0.90	1.09	0.85[3]	0.87				0.90	4.51	5.88
4118.904	26340–50611	3.26	559	−0.68		−0.96[1]	−1.00				−0.88	2.73	4.10
4120.209	24119–48383	2.99	423	−0.34	−0.40	−0.43[2]	−0.43				−0.41	3.20	4.57
4121.805	22838–47093	2.83	356	−0.41	−0.55	−0.49[2]	−0.49				−0.49	3.13	4.49
4122.522	22947–47197	2.84	356	−0.51	−0.62	−0.65[2]	−0.60				−0.61	3.01	4.37
4123.748	21039–45282	2.61	217	−0.91	−1.04	−1.13[2]	−0.76				−0.99	2.63	3.99
4124.490	29372–53610	3.64		−1.49		−1.53[1]					−1.51	2.11	3.47
4125.622	34040–58272	4.22	1103	−0.21	−0.41	−0.13[1]	−0.16				−0.23	3.39	4.75
4125.883	22947–47177	2.84	354	−1.04	−0.93	−0.97[2]	−1.17				−1.02	2.60	3.96
4126.192	26875–51103	3.33	695	−0.13	−0.56	−0.35[2]	−0.39				−0.36	3.26	4.62
4126.880	22947–47172	2.84	354	−1.93	−1.61	−1.87[1]	−1.96				−1.84	1.78	3.14
4127.611	23052–47272	2.86	357	−0.13	−0.09	−0.11[3]	−0.13	−0.13[1]			−0.12	3.50	4.86
4127.807	26479–50699	3.28	558	−0.29	−0.42	−0.47[1]	−0.33				−0.38	3.24	4.60
4129.220	27560–51771	3.42	698	−1.60		−1.49[2]	−1.78				−1.59	2.03	3.39
4129.474	27395–51604	3.40	695	−1.23		−1.21[1]					−1.22	2.40	3.76
4130.035	12561–36767	1.56	44	−2.68		−2.66[2]	−2.97				−2.74	0.88	2.24
4132.060	12969–37163	1.61	43	−0.26		−0.16[3]	−0.09	−0.16[1]		−0.40	−0.20	3.42	4.78
4132.540	34329–58520	4.26	1103	−0.49							−0.49	3.13	4.49
4132.902	22947–47136	2.84	357	−0.20	−0.18	−0.02[2]	−0.06	−0.08[1]			−0.09	3.53	4.89
4133.869	27167–51351	3.37	698	−0.36	−0.76	−0.48[2]	−0.48				−0.51	3.11	4.46
4134.340	0–24181	0.00	3			−4.23[1]	−4.07				−4.15	−0.53	0.82

TABLE 3.—*Oscillator Strengths for Ultraviolet Lines of Fe* I—Continued

Wavelength Å	Energy Levels K	Low e.p. Volts	Mult. No.	Arc	Spk	CW(N)	HC	R(N)	KOC	MS	Best	Log gfλ	Log gA/λ
				Log *gf*									
4134.433	24336–48516	3.02	482			−0.74[1]					−0.74	2.88	4.23
4134.680	22838–47017	2.83	357	0.32	0.05	0.18[3]	0.13	0.23[1]			0.18	3.80	5.15
4136.512	27167–51335	3.37	694	−0.69		−0.82[2]	−0.96				−0.82	2.80	4.15
4137.002	27543–51708	3.41	726	0.15	0.22	0.12[2]	0.16				0.15	3.77	5.12
4137.417	34547–58710	4.28	1103	−0.89		−0.82[1]					−0.86	2.76	4.11
4137.980	22846–47006	2.83	320	−2.38							−2.38	1.24	2.59
4138.840	18378–42533	2.28	117	−2.74		−2.80[1]	−2.79				−2.78	0.84	2.19
4139.929	7986–32134	0.99	18	−2.80		−2.86[2]	−2.86				−2.84	0.78	2.13
4140.441	27560–51705	3.42	695	−0.81		−1.11[2]	−1.01				−1.01	2.61	3.96
4141.862	24339–48476	3.02	422	−1.03		−1.04[2]	−0.93				−1.01	2.61	3.96
4142.625	34692–58825	4.30	1103	−0.71		−0.33[2]	0.12						
4143.417	24575–48703	3.05	523	0.58	0.62	0.61[2]	0.61				0.61	4.23	5.58
4143.870	12561–36686	1.56	43	−0.33		−0.07[3]	−0.02	−0.04[1]		−0.24	−0.12	3.50	4.85
4145.206	21716–45833	2.69	274	−1.62		−1.71[2]	−1.81				−1.71	1.91	3.26
4146.070	24119–48231	2.99	422	−1.00	−0.80	−0.87[2]	−0.89				−0.89	2.73	4.08
4147.347	26875–50980	3.33	693	−1.23		−1.28[1]					−1.26	2.36	3.71
4147.672	11976–36079	1.48	42	−1.49	−1.52	−1.47[3]	−1.56				−1.50	2.12	3.47
4149.372	26875–50968	3.33	694			−0.22[2]	−0.19				−0.21	3.41	4.76
4149.767	416–24507	0.05	3			−4.81[1]	−4.84				−4.82	−1.20	0.15
4150.258	27666–51755	3.43	695			−0.71[2]	−0.62				−0.68	2.94	4.29

(Paper 70A4–409)

JOURNAL OF RESEARCH of the National Bureau of Standards—A. Physics and Chemistry
Vol. 70A, No. 4, July–August 1966

Publications of the National Bureau of Standards*

Selected Abstracts

Design and statistical procedures for the evaluation of an automatic gamma-ray point-source calibrator, S. B. Garfinkel, W. B. Mann, and W. J. Youden, *J. Res. NBS* **70C2** (*Engr. and Instr.*), *No. 2, 53–63 (Apr.–June 1966).*
A description is given of the mechanical design and operation of an automatic gamma-ray point source calibrator.
The use of statistical design in experiments for evaluating performance factors, such as interchangeability of stations and run differences using the same data obtained in comparisons of the sources, is described in detail.

Reference tables for the Pt-30 percent Rh versus Pt-6 percent Rh thermocouple, G. W. Burns, and J. S. Gallagher, *J. Res. NBS* **70C2** (*Engr. and Instr.*), *No. 2, 89–125 (Apr.–June 1966).*
A new ellipsoidal mirror reflectometer is described, in which radiant flux from an infrared monochromator is focused on a specimen placed at the first focal point of the ellipsoid and a thermopile detector is placed at the second. Errors associated with angular and spatial sensitivity of the detector and with aberrations in the optics were largely eliminated through use of a small averaging sphere placed over the detector. Losses caused by the presence of the entrance hole in the ellipsoidal mirror and from mirror absorption were evaluated both theoretically and experimentally. Corrections for these losses permitted absolute reflectance to be obtained for both diffuse and partially diffuse reflecting specimens. In addition, the unique optic of the ellipsoidal mirror provides more versatility than is available in previous reflectometers. This versatility includes the ability to accurately measure $\rho(\varphi', \theta)$, $\rho(\varphi, \theta, \varphi', \theta')$, ρ(specular), ρ(nonspecular), and ρ(directional annular cone). An analysis of the accuracy of the instrument indicates that an accuracy of better than 1 percent is possible for all engineering materials. The use of the sulfur averaging sphere also allowed the construction of a simple accurate specular reflectometer for calibration of the mirror reference standards used in these measurements.

OMINTAB. A computer program for statistical and numerical analysis, J. Hilsenrath, G. G. Ziegler, C. G. Messina, P. J. Walsh, and R. J. Herbold, *NBS Handb. 101 (Mar. 4, 1966). $3.00.*
This user's manual gives the characteristics and application of a general-purpose interpretive program for the generation of physical and mathematical tables on the digital computer using FORTRAN. The vocabulary and sentence structure permit (with only a few simple rules) the translation of a mathematical statement into text understandable both to the user (not necessarily a programer) and to the machine. The basic vocabulary of slightly over 250 English words is given. These cover the arithmetic and mathematical operations such as ADD, DIVIDE, MULT, SUBTRACT, LOGE, EXP; the elementary and special mathematical functions: SIN, TAN, COSH, TANH, orthogonal polynomials, Bessel functions, elliptic integrals, etc.; and various manipulative operations on columns of numbers and on entire arrays.
Detailed instructions are given also for applying the program to: matrix calculations, statistical analysis of experimental data, least-squares curve fitting, linear and nonlinear interpolation, numerical differentiation and integration, solutions of systems of equations, and location of zeros and maxima and minima of algebraic and transcendental functions.
Numerous examples are given of applications of the program to scientific calculations covering a wide spectrum of problems encountered in a research and development organization. Aside from the comprehensive repertoire of mathematical functions and operations, the important features which are stressed are the flexible format-free input and output provisions and curve plotting facility. March 4, 1966. 256 pages.

Radio meteorology, B. R. Bean and E. J. Dutton, *NBS Mono. 92 (Mar. 1, 1966), $2.75.*
This volume brings together the work done in radio meteorology over the past ten years at the National Bureau of Standards' Central Radio Propagation Laboratory (CRPL). This decade has seen the development, on an international scale, of great emphasis upon the effects of the lower atmosphere on the propagation of radio waves. The CRPL group has concentrated upon the refraction of radio waves as well as the refractive index structure of the lower atmosphere on both synoptic and climatic scales. These are the areas of radio meteorology that are treated in this volume, with additional chapters on radio-meteorological parameters and the absorption of radio waves by the various constituents of the lower atmosphere.

Procedures for precise determination of thermal radiation properties, November 1963 to October 1964, J. C. Richmond, S. T. Dunn, D. P. DeWitt, and W. D. Hayes, Jr., *NBS Tech. Note 267, (Dec. 17, 1965). 45 cents.*
A laser-source integrating sphere reflectometer was designed and built to measure the reflectance of specimens at high temperatures. The sphere was calibrated for linearity of response at 0.632μ by means of a shallow cylindrical cavity with a variable depth-to-radius ratio, having a lining of known reflectance. Preliminary tests showed that the flux emitted by a hot specimen at temperatures up to 2500 °K will not invalidate the reflectance measurement. An ellipsoidal mirror reflectometer was calibrated for all known errors in the 1 to 7.5μ range. A preliminary analysis indicates that the errors in measurement of absolute reflectance with this equipment should not exceed 2 percent. A review of the literature on relation of thermal radiation properties to other properties of materials is presented, together with a summary of the work done in an effort to compute the spectral emmittance of rhodium.

Keypunch controls for string-punching of statistical data, M. J. Brennan, *NBS Tech. Note 282 (Feb. 11, 1966), 25 cents.*
This note describes controls for a keypunch machine used to key statistical data with "string-punching techniques." Since the data are punched into cards that do not contain fixed field sizes, an identification code is punched for each data entry. To avoid a split field (part on one card and the remainder on another), the keypunch machine is programed to provide a justification zone in which an answer identification code or a "delete" code can not be keyed. The cards are automatically serialized for each questionnaire and an arrangement is provided to punch an end-of-questionnaire code in the last card for the questionnaire.

Gas phase radiolysis and vacuum ultraviolet photolysis of 2- and 3-pentanone, A. Scala and P. Ausloos, *J. Phys. Chem.* **70,** *No. 1, 260–269 (Jan. 1966).*
In the photolysis of 3-pentanone and 2-pentanone at 1470 Å and 1236 Å, the major modes of fragmentation of the electronically excited ketones are as follows:

$$C_2H_5COC_2H_5^* \rightarrow C_2H_5 + CO + C_2H_4 + H \quad (1)$$
$$\rightarrow CH_3 + CH_2COC_2H_5 \text{ (or } CH_2CO + C_2H_5) \quad (2)$$
$$CH_3COCH_2CH_2CH_3^* \rightarrow CH_3CO(\text{or } CH_3 + CO) + C_2H_4 + CH_3 \quad (3)$$
$$\rightarrow CH_3CO(\text{or } CH_3 + CO) + C_3H_6 + H \quad (4)$$

On the basis of experiments carried out with $C_2H_5COC_2H_5 - C_2D_5COC_2D_5$ mixtures it can be concluded that "molecular" elimination of methane does also occur to a minor extent. Isotopic analysis of the products formed in the photolysis of $CD_3COCD_2CH_2CH_3$ further indicates that the elimination process

$$CD_3COCD_2CH_2CH_3^* \rightarrow CD_3COCD_2H + C_2H_4 \quad (5)$$

does take place, but to a lesser extent than at 2537 and 3130 Å.

216-375 O - 66 - 7

In the radiolysis neutral excited molecules and ions are produced. When an electrical field is applied during the radiolysis, increased excitation by electron impact occurs. At low field strengths molecules are mainly excited to the first upper singlet and/or triplet state, and decompose in much the same way as reported in the earlier near-ultraviolet photolysis studies. When the field strength is increased the ketone is excited to a higher singlet state and decomposes according to process 1 to 4. Products which are not affected by the application of an electrical field such as C_3H_4 and 1-C_4H_8 can be ascribed to ion molecule reactions. It is proposed that in the radiolysis, transfer of a proton from various fragment ions to the pentanone molecule does occur, and that this is followed by neutralization of the protonated pentanone to yield hydrogen as a product.

New developments in dental materials: A world-wide survey, G. C. Paffenbarger, *Intern. Dental J.* **15,** *No. 3, 311–422 (Sept. 1965).*
General discussion of a symposium prepared by the moderator, G. C. Paffenbarger, chairman, Commission on Dental Materials, Instruments, Equipment and Therapeutics of the Federation Dentaire Internationale.

Total cross section for 14 MeV neutrons using aligned ^{165}Ho nuclei, H. Marshak, A. Richardson, and T. Tamura, *Phys. Rev. Letters* **16,** *No. 5, 194–197 (Jan. 31, 1966).*
The effect of nuclear deformation on the total cross section of ^{165}Ho has been measured using 14 MeV neutrons and an aligned target. The aligned ^{165}Ho target was obtained by cooling a metal single crystal to 0.33 °K using the NBS ^{3}He refrigerator. A finely collimated beam of 14 MeV neutrons was obtained by careful collimation of the alpha particle produced in the reaction ^{3}H(d, T)^{4}He and by detecting it in coincidence with its associated neutron. The NBS 2 MV Van de Graaff was used to provide a 1 μA, 300 keV deuteron beam. The results were successfully explained using an adiabatic coupled-channel calculation and the Optical Model potential. The data do not agree with the predictions of the Black Nucleus Model as we would expect since the wave length of a 14 MeV neutron is only equal to the radius of the holmium nucleus.

A review of zinc oxide-eugenol type filling materials and cements, G. M. Brauer, *Rev. Belge. Med. Dent.-Belg. Tijds. Tandheelk* **20,** *No. 3, 323–364 (1965).*
A review is given of the status of zinc oxide-eugenol type cements as well as modifications of these materials developed in this laboratory and elsewhere. The mechanism of the setting reaction and the physical, histological and clinical properties of these cements are discussed. Zinc oxide-eugenol cement is decidedly superior to other materials in its palliative effect on the pulp and in patient comfort. Whereas, solubility is low and initial adaptation to the cavity walls unusually good, its low strength and lack of resistance to abrasion confine its use to restorations not involving high stress or attrition. Properly formulated, it is the cement of choice for selected restorations.
Recent investigations have explored the possibilities of improving the desirable physical properties. Incorporation of o-ethoxybenzoic acid has led to materials that appear promising as bases and cementing materials for inlays and crowns. Further studies should lead to stronger, more adhesive and more permanent restorative materials that are impermeable to moisture.

Crystal and molecular structure of $C_4B_{20}H_{22}$, *bis* (*o*-dodecacarborane), L. H. Hall, A. Perloff, F. A. Mauer, and S. Block, *J. Chem. Phys.* **43,** *No. 11, 3911–3917 (Dec. 1965).*
The molecular configuration of *bis*-dodecacorborane has been determined in a complete x-ray crystallographic study. The unit cell is monoclinic with $a = 7.014$, $b = 9.862$, $c = 12.360$, and $\beta = 90°51'$. $Z = 4$ and the space group is $p2_1/n$. The two nearly icocahedral halves of the molecule are related by a center of symmetry.

Matrix-isolation infrared spectrum of the free radical CCO, M. E. Jacox, D. E. Milligan, N. G. Moll, and W. E. Thompson, *J. Chem. Phys.* **43,** *No. 10, 3734–3746 (Nov. 1965).*
The photolysis of matrix-isolated cyanogen azide in the presence of carbon monoxide at wavelengths shorter than 2800 A has been found to lead to the appearance of the free radical CCO in concentration sufficient for direct spectroscopic observation. This species has also been produced in low concentration by the photolysis of matrix-isolated carbon suboxide. The three vibrational fundamentals of CCO have been observed in an argon matrix at 381, 1074, and 1977.5 cm^{-1}, and CCO has been found to have a continuum near 5000 A. Isotopic studies are consistent with a linear structure for CCO. Estimates of the force constants and thermodynamic properties of this species are given. CCO has been observed to react with CO with little or no activation energy to form carbon suboxide. Other reactions occurring in the matrix are also discussed.

Matrix-isolation infrared spectrum of the free radical NH_2, D. E. Milligan and M. E. Jacox, *J. Chem. Phys.* **43,** *No. 12, 3487–4493 (Dec. 15, 1965).*
The free radical NH_2 has been produced in concentration sufficient for direct infrared detection by photolysis with a microwave-powered hydrogen discharge of ammonia isolated in argon, nitrogen, and carbon monoxide matrices at 14 °K. Ultraviolet absorptions characteristic of both NH and NH_2 are observed in photolyzed argon and nitrogen matrix samples. In the CO matrix, infrared observations show a high concentration of HCO after photolysis, further demonstrating the production of H atoms by the photolysis of ammonia. Two of the infrared fundamentals of $^{14}NH_2$, at 1499 and 3220 cm^{-1}, and of $^{15}NH_2$, at 1495.5 and 3215 cm^{-1}, one of NHD, at 1321 cm^{-1}, and one of ND_2, at 1110 cm^{-1}, have been observed. Spectra observed in an argon matrix are relatively complex, suggesting that rotation of NH_2 may be possible in this matrix. The force constants and thermodynamic properties of NH_2 are estimated. The photolysis of matrix-isolated ammonia has been found to be relatively inefficient, in contrast to an earlier prediction.

Matrix isolation study of the photolysis of cyanogen azide. The infrared and ultraviolet spectra of the free radical NCN, D. E. Milligan, M. E. Jacox, and A. Bass, *J. Chem. Phys.* **43,** *No. 9, 3149–3160 (Nov. 1, 1965).*
The infrared and ultraviolet absorption spectra of the free radical NCN have been observed following photolysis at wavelengths longer than 2800 A of cyanogen azide isolated in argon, nitrogen, carbon monoxide, and carbon dioxide matrices. The infrared-active vibrational fundamentals of NCN appear at 423 and at 1475 cm^{-1}. Isotopic studies are consistent with this identification. The force constants and thermodynamic properties of NCN have been estimated. Two ultraviolet absorption systems are associated with NCN. The first of these, previously reported, lies near 3290 Å. The second system is comprised of a progression of bands spaced at intervals of approximately 1045 cm^{-1}, lying between 3000 and 2400 Å. The nature of this second transition is discussed. At wavelengths longer than 2800 Å both cyanogen azide and NCN have been found to photolyze with the production of carbon atoms. The nature of the new features observed in the infrared and ultraviolet spectral regions after photolysis with short wavelength radiation is considered.

Photolysis of cyclobutane at photone energies below and above the ionization energy, R. D. Doepker and P. Ausloos, *J. Chem. Phys.* **43,** *No. 11, 3814–3819 (Dec. 1, 1965).*
The photolysis of cyclo-C_4H_8 and of cyclo-C_4H_8-cyclo-C_4D_8 mixtures has been investigated at 1470 and 1236 Å in the absence and presence of NO. In addition, a series of experiments were carried out in which H_2S was used as a free radical interceptor in the photolysis of cyclo-C_4D_8 at 1236 Å. Approximately 90 percent of the observed products can be accounted for by the primary process: $C_4H_8 + h\nu \rightarrow 2\ C_2H_4$. The extent to which the internally exicted ehtylene formed in this process will decompose further, increases with diminishing pressure and wavelength.
The photolysis of cyclobutane has been investigated at energies above the ionization energy (I. E. = 10.3), using the argon resonance lines at 11.54 and 11.72 eV. It is shown that when NO is added to the system, *cis*-2-butene, *trans*-2-butene and 1-butene are major products. These butenes are, however, not produced when NO (I. P. = 9.25 eV) is replaced by O_2 (I. P. = 12.1 eV) and are only formed in trace amounts when no additives are present. It is suggested that the parent ion acquires the olefinic structure and undergoes charge exchange with NO.

The effect of gamma-irradiation on a polyamide, V. J. Kransnansky, M. S. Parker, and R. E. Florin, *J. Phys. Chem.* **70,** *No. 1, 40–46 (Jan. 1966).*
Electron spin resonance and optical spectroscopy were used to study the kinetics of intermediates produced by the irradiation of a polyamide MXD-6. This polymer derived from meta xylylene diamine and adipic acid showed remarkable stability to irradiation in previous studies. It is concluded that the colored intermediate is a radical species, whose molar extinction coefficient is $\sim 10^5$ at 3000 Å.
At temperatures above 85 °C the decay of the active species measured by both methods tends to become second order after an initial rapid decay. This complex decay rate during the initial period was attributed to radicals having a very high decay rate or a diffusion controlled bimolecular reaction of pairs. The derived activation energy for diffusion was 19 to 29 kcal/mole.

The thermal degradation mechanism of polystryene, L. A. Wall, S. Straus, J. H. Flynn, D. McIntyre, and R. Simha, *J. Phys. Chem.* **70,** *No. 1, 53–62 (Jan. 1966).*
New and extensive measurements of—(1) the rates of volatilization and (2) the molecular weights as a function of the extent of pyrolysis are reported for various polystyrene samples, in particular, fractions spanning a broad range of molecular weights. The experimental observations are shown to be described quite well by the results of computer calculations based on the theory of free radical degradation and a mechanism involving four elementary reactions—initiation, depropagation, intermolecular transfer, and termination by disproportionation.

Deposition of energy by neutrons in spherical cavities, R. S. Caswell, *Radiation Res.* **27,** *No. 1, 92–107 (Jan. 1966).*
A theoretical description of the interaction of neutrons with a spherical cavity has been developed in terms of four types of recoil particle interactions with the cavity called for convenience insiders, starters, stoppers, and crossers. Energy loss distributions are calculated for polyethylene-ethylene and tissue cavities and are found to agree with experimental measurements within the probable uncertainty of those measurements. Conditions for optimum use of proportional counter cavity dosimeters and the interpretation of measurements made with these instruments are discussed.

High-frequency elastic moduli of simple fluids, R. Zwanzig and R. D. Mountain, *J. Chem. Phys.* **43,** *No. 12, 4464–4471 (Dec. 15, 1965).*
This article presents a calculation of the infinite frequency elastic moduli of monatomic fluids. When the intermolecular potential has the standard Lennard-Jones form, the elastic moduli are shown to be related to the pressure and internal energy of the fluid. Numerical values of the elastic moduli at various densities and temperatures are presented in tabular and graphical form. An identity is derived relating the shear and bulk moduli of any isotropic material in which particles interact by means of two body central forces; this is a generalization of the familiar Cauchy identity occurring in the theory of elasticity of solids. The approach is based on analysis of the high frequency limit of exact time-correlation function expressions for shear and bulk viscosity.

Nuclear moments of Pm^{147}, J. Reader, *Phys. Rev.* **141,** *No. 3, 1123–1128 (Jan. 1966).*
The nuclear magnetic dipole and electric quadrupole moments of Pm^{147} have been derived from an analysis of the optical hyperfine structure of singly ionized Pm^{147}. The hyperfine constants for the $[4f^5\ {}^6H_{5/2},\ 6s]_2$ ground state are $A=-10.24\pm0.20$ mK; $B=-10.6\pm2.6$ mK. By using the known atomic beams data for the $[4f^6 6s^2\ {}^6H_{7/2}]$ state of neutral Pm to subtract out the contribution of the $[4f^6\ {}^6H_{5/2}]$ core to the observed magnetic splitting factor, the splitting factor of the 6s electron was found to be $a_{6s}=+214.2\pm4.9$ mK. The nuclear moments deduced from the hyperfine constants are $\mu_I(Pm^{147})=+2.58+0.07$ nm and $Q(Pm^{147})=+0.74\pm0.20$ b.

Chemical analysis, G. M. Brauer and G. M. Kline, *Encyclopedia of Polymer and Technology* **3,** *633–665 (John Wiley & Sons, Inc., New York, N.Y., 1965).*
The chemical analysis of polymeric materials is reviewed. Preparation of the sample, physical tests, thermal degradation techniques and chemical procedures such as analysis for functional and end groups and characterization tests are discussed. Instrumental techniques that are employed in the analysis of polymers are described and systematic schemes for the analysis of high molecular weight compounds are outlined.

Viscosity and density of boron trioxide, A. Napolitano, P. B. Macedo, and E. T. Hawkins, *J. Am. Ceramic Soc.* **48,** *No. 12, 613–616 (1965).*
Extensive and accurate viscosity values for molten B_2O_3 are reported over the continuous range from 20 poises (at 1400 °C) to 10^{10} poises (at 318 °C). The measurements were made with a wide range rotating cylinder viscometer. The melts were pretreated by bubbling super dry nitrogen through them to insure that the water content was at a minimum. Densities were also determined between 1400 and 400 °C. Above 800 °C the temperature dependence of the viscosity curve was Arrhenius, below this it had a smooth curvature showing no breaks. At the low temperatures, although its curvature decreased, the viscosity curve was not Arrhenius.

Proposed standard for measuring and reporting physical properties of optical materials, G. W. Cleek, F. J. P. Consitt, and W. D. Lawson, *Infrared Phys.* **5,** *141–160 (Dec. 1965).*
For some time there has been evidence of a lack of data on the properties of optical materials, particularly as a function of temperature. This has been particularly apparent to designers of optical equipment which has to operate in unusual environments e.g., in space vehicles, or which has to withstand severe conditions during critical periods of operation e.g., during rocket launch. For instance refractive indices have in general been measured only around room temperature but optical instruments with complex lens systems may be required to function at either much higher or much lower temperatures.
Another problem arises through different manufacturers of optical materials using different methods and specimens for measuring physical properties and presenting the data differently. This frequently makes it difficult for a user to compare directly optical materials from different sources and in general he does not wish to set up and carry out comparative measurements himself. Thus the development of a joint set of standards on methods of measuring and reporting the properties of optical materials was considered highly desirable.
With the needs of the optical designer in mind the authors have attempted to list specific properties of interest, outline standard methods of measuring these properties, and suggest standard methods of presenting the results. We have used for illustration, in Appendix C, the data on synthetic sapphire listed in the manufacturer's data sheets.

Techniques for detection of high-altitude nuclear explosions, A. G. Jean, C. E. Hornback, R. H. Doherty, J. R. Winkelman, and R. T. Moore, *Proc. IEEE* **53,** *No. 12, 2088–2098 (Dec. 1965).*
The Central Radio Propagation Laboratory (CRPL) is conducting a study for the Advanced Research Projects Agency (ARPA) project VELA of ground based techniques for detecting geophysical effects produced by nuclear explosions at altitudes above about 20 km and in space. This activity is called HANDS for High Altitude Nuclear Detection Studies. A substantial amount of experimental data exists on effects produced by high-altitude explosions and theoretical predictions have been made of effects expected from explosions in space. The ability to record and identify these signatures is limited by knowledge of the natural background. The objective of the HANDS is to acquire data on natural background required in the design of future detection systems. The experimental facility for collecting background data at conventional and more rapid rates from a collection of colocated geophysical sensors is described.

Departures from local thermal equilibrium in a magnetically-driven shock wave, E. L. Eckerle and R. W. P. McWhirter, *Phys. Fluids* **9,** *No. 1, 81–89 (Jan. 1966).*
An experimental study is reported of the time-resolved spectrum of the plasma produced by the magnetically driven shock-wave in a T-tube. It is shown that the population densities of the excited levels of helium ions in the plasma depart from the values they

would have in Local Thermal Equilibrium. On the other hand if LTE is assumed and the electron temperature estimated for the intensity ratio of He II (4686 Å) to He I (5876 Å) then in the conditions of the experiment an error of a factor of two in the electron temperature arises. The reason for the departure from LTE was shown to be the rapid rate of change of the plasma conditions (especially the electron temperature). This is so great that the ionization and recombination rates, being slower, cause the population densities to lag behind the electron density and electron temperature. These rates were found to be consistent with the rates calculated by Bates et al., in their collisional-radiative model for the ionization and recombination of hydrogen-like ions.

Precision of cubic lattice parameter measurements by the Kossel technique, H. Yakowitz, *Trans. Symp. Electron Probe Analysis, Oct. 12–15, 1964 Washington, D.C., pp. 417–438 (John Wiley & Sons, Inc., New York, N.Y., 1966).*

The major factors affecting the precision of cubic lattice parameter measurement by means of the Kossel technique are considered. It is shown that three special cases can be solved rigorously for projection distortion effects and that obtaining these cases is not difficult. The fact that a lens ratio method should be employed to reduce measured lengths on the film to lattice parameter values is emphasized. General formulae for the lattice parameter and the geometric sensitivity are presented. Correction and minimization of errors resulting from refractive index effects and temperature variations is indicated to be possible. An example of the determination of the lattice parameter of LiF is given. The sensitivity of the method, expressed the relative standard error of the mean lattice parameter of LiF, is given by

$$\frac{\Delta a}{a_{LiF}} = 2.5_4 \times 10^{-6}.$$

Radiative corrections. I. High-energy bremsstrahlung and pair production, K. Mork and H. Olsen, *Phys. Rev.* **140,** *No. 6B, B1661–B1674 (Dec. 20, 1965).*

The radiative corrections to the high energy bremsstrahlung and pair production spectra are calculated in the Weizsacker-Williams approximation. Results for the soft-photon radiative correction to the spectra are given and for the case of pair production also the soft plus hard photon radiative correction is obtained. The radiative correction to the total pair production cross section is found to be practically independent of the photon energy and of the atomic number of the target material. Comparison with available experimental data shows essential agreement within the relatively wide experimental limits.

Random-walk calculations of diffusion coefficients, R. E. Howard, *Proc. 5th Intern. Symp. Reactivity of Solids, Munich, Germany, 1964, pp. 250–255 (Elsevier Publ. Co., Amsterdam, The Netherlands, 1965).*

An extension is made of the random-walk technique of calculating correlation factors in diffusion. In particular, closed form expressions for the infinite series that appear in such calculations are obtained under general conditions. Applications are made to simple cases of tracer diffusion by the interstitialcy and by the vacancy mechanism. Results of a calculation on diffusion of tracers by di-vacancies in a NaCl type crystal are presented.

Relative transition probabilities for prominent Ni I and Ni II lines in the near-ultraviolet, G. D. Bell, D. R. Paquette, and W. L. Wiese, *Astrophys. J.* **143,** *No. 2, 559–572 (Feb. 1966).*

Relative transition probabilities of 16 Ni I lines and 53 Ni II lines in the wavelength range from 2000–3600 Å have been measured with a wall-stabilized arc. The arc was operated at 10 amps in argon with a small admixture (.01%) of nickel-carbonyl. The spectrum was photoelectrically observed through the hollow electrodes. The relative intensity calibrations were performed with calibrated tungsten strip lamps or by utilizing the continuous emission of a hydrogen arc operated at known plasma conditions. The axis temperature of the argon nickel-carbonyl arc was determined from intensity measurements of argon lines of known transition probabilities and the application of the arc plasma equations. For the great majority of the relative f-values the experimental and theoretical uncertainties are 8 percent or better, but for a few weak lines the uncertainities go as high as 30 percent. Comparisons with other experimental and theoretical results are undertaken and fair agreement is obtained.

The correction factor for fast neutron reactions on sulfur and oxygen in the manganous-sulfate-bath calibration of neutron sources, W. M. Murphey, *Nucl. Instr. Methods* **37,** *No. 1, 13–21 (1965).*

A Monte Carlo calculation has been made of the correction for neutrons lost to (n,α) and (n,p) reactions with sulfur and oxygen in the manganous-sulfate-bath calibration of neutron sources. The correction factor is given as a function of initial neutron energy for monoenergetic neutrons in an infinite bath and as a function of manganous sulfate concentration. The correction factors for various published source spectra are also given. The uncertainty in the correction for a given source spectrum due to uncertainties in the source spectrum is much larger than those due to the Monte Carlo calculation or the cross sections.

Other NBS Publications

J. Res. NBS 70B2 (Math. and Math. Phys.), No. 2 (Apr.–June 1966), 75 cents.

On a sequence of points of interest for numerical quadrature. S. Haber.

On abstract numerical integrations. J. J. Sopka.

Treatment of outliers in samples of size three. F. J. Anscombe and B. A. Barron.

A note on contaminated samples of size three. T. A. Willke.

Realizing the distance matrix of a graph. A. J. Goldman.

Pairs of nonsingular matrices. K. Goldberg.

Upper bounds for the determinant of a row stochastic matrix. K. Goldberg.

Groups preserving ordering in vectors. K. Goldberg.

J. Res. NBS 70C2 (Engr. and Instr.), No. 2 (Apr.–June 1966), 75 cents.

Design and statistical procedures for the evaluation of an automatic gamma-ray point-source calibrator. S. B. Garfinkel, W. B. Mann, and W. J. Youden. (See above abstracts.)

Testing of lenses with the wave front reversing interferometer. K. Muraoka.

Ellipsoidal mirror reflectometer. S. Thomas Dunn, J. C. Richmond, and J. A. Wiebelt.

Reference tables for the Pt-30 percent Rh versus Pt-6 percent Rh thermocouple. G. W. Burns and J. S. Gallagher. (See above abstracts.)

Coaxial power meter calibration using a waveguide standard. G. F. Engen.

A note on the numerical evaluation of thermal radiation characteristics of diffuse cylindrical and conical cavities. B. A. Peavy.

Quarterly radio noise data September, October, November, 1964, W. Q. Crichlow, R. T. Disney, and M. A. Jenkins, NBS Tech. Note 18–24 (Feb. 10, 1966), 50 cents. (Formerly the Central Radio Propagation Laboratory of the National Bureau of Standards, now Environmental Science Services Administration, Boulder, Colo.)

Earth's field static calibrator for accelerometers, P. S. Lederer and J. S. Hilten, NBS Tech. Note 269 (Feb. 1, 1966). 20 cents.

Radiochemical analysis: Activation analysis, instrumentation, radiation techniques, and radioisotope techniques, July 1964 to June 1965, ed. J. R. DeVoe, NBS Tech. Note 276 (Jan. 7, 1966), $1.00.

An outline for cooperative action on the determination of x-ray mass attenuation coefficients in the wavelength range from 0.5 to 100 Å (25 to 0.12 keV), K. F. J. Heinrich, NBS Tech. Note 284 (Feb. 21, 1966). 15 cents.

Computation of the permeability and permittivity of a relatively small ring sample in a toroidal coil, E. G. Johnson, Jr., NBS Tech. Note 311 (Jan. 25, 1966). 30 cents.

An atlas of solar flare effects in the ionosphere observed with a high-frequency Doppler technique, September 1960–December 1962, D. M. Baker, NBS Tech. Note 326 (Dec. 1, 1965). 60 cents.

(Formerly the Central Radio Propagation Laboratory of the National Bureau of Standards, now Environmental Science Services Administration, Boulder, Colo.)

The seasonal variation of nightglow NaI 5890–96 A, [01] 5577 A and [01] 6300 A in the tropics, L. L. Smith and R. W. Owen, NBS Tech. Note 329 (Jan. 10, 1966). 35 cents. (Formerly the Central Radio Propagation laboratory of the National Bureau of Standards, now Environmental Science Services Administration, Boulder, Colo.)

Computations of the antenna cut-back factor for LF radio waves, D. C. Hyovalti, NBS Tech. Note 330 (Nov. 26, 1965). 30 cents. (Formerly Central Radio Propagation Laboratory of the National Bureau of Standards, now Environmental Science Services Administration, Boulder, Colo.)

A 100 KW 2–25 Mc/s distributed amplifier, designed for use with 10 kw ionospheric sounders, W. B. Harding, M. W. Woodward, and J. C. Carroll, NBS Tech. Note 331 (Feb. 15, 1966). 20 cents. (Formerly Central Radio Propagation Laboratory of the National Bureau of Standards, now Environmental Science Services Administration, Boulder, Colo.)

Quenching of the triplet state of acetone and biacetyl by various unsaturated hydrocarbons, R. E. Rebbert and P. Ausloos, J. Am. Chem. Soc. **87,** No. 24, 5569–5572 (Dec. 20, 1965).

Vacuum-ultraviolet photolysis of ethane at high temperature. II. Collisional deactivation of excited ethylene, R. F. Hampson, Jr., and J. R. McNesby, J. Chem. Phys. **43,** No. 10, 3592–3596 (Nov. 15, 1965).

Foreword, R. G. Scott, Book, Cryogenics, pp. V (Reinhold Publ. Corp., New York, N. Y., 1964).

MAGIC-A machine for automatic graphics interface to a computer, D. E. Rippy and D. C. Humphries, Proc. Fall Joint Computer Conf., Nov. 20-Dec. 2, 1965, Las Vegas, Nevada, pp. 819–830 (Spartan Books, Inc., Wash., D.C. 1965).

The NBS time scale and its relation to other time scales, J. A. Barnes and R. C. Mockler, (Proc. XIV General Assembly of URSI, Tokyo, Japan, 1963), Book, Progress in Radio Science 1960–1963. Vol. **I.** Radio Standards and Measurements, ed. R. W. Beatty, p. 41 (Elsevier Publ. Co., Amsterdam, The Netherlands, 1965).

Annual report of the National Bureau of Standards, C. E. Moore, Astron. J. **70,** No. 9, 637–639 (Nov. 1965).

Oxygen metastable atom production through photodetachment, L. M. Branscomb, S. J. Smith, and G. C. Tisone, J. Chem. Phys. **43,** No. 8, 2906–2907 (Oct. 15, 1965).

The current revision of the solar spectrum table λ2935 Å to λ8770 Å, C. E. Moore, Proc. Utrecht Symp. Solar Spectrum, Utrecht, The Netherlands, Aug. 26–31, 1963, ed. C. DeJager, pp. 89–101 (D. Reidel Publ. Co., Dordrecht, The Netherlands, 1965).

Influence or irregular terrain on propagation, J. W. Herbstreit, (Proc. XIV General Assembly of URSI, Tokyo, Japan, 1963), Book, Progress in Radio Science 1960–1963. Vol. **II.** Radio and Troposphere, ed. F. du Castel, pp. 141–156 (Elsevier Publ. Co., Amsterdam, The Netherlands, 1965).

Application of a high-intensity, multi-slit Raleigh interferometer to sedimentation studies, I. H. Billick and R. J. Bowen, J. Phys. Chem. **69,** 4024–4030 (1965).

Dissociation of ammonium ion in methanol-water solvents, M. Paabo, R. G. Bates, and R. A. Robinson, J. Phys. Chem. **70,** No. 1, 247–251 (1966).

Electrochemistry, W. J. Hamer, Book, Encyclopedia of Physics, pp. 200–203 (Reinhold Publ. Corp., New York, N.Y., 1966).

Kinetics of the hydroxyl radical in aqueous solution, F. Sicilio, R. E. Florin, and L. A. Wall, J. Phys. Chem. **70,** No. 47, 47–52 (Jan. 1966).

Manganese-hydrogen bond distance in $HMn(CO)_5$, T. C. Farrar, W. Ryan, A. Davison, and J. W. Faller, J. Am. Chem. Soc. **88,** 184 (Jan. 5, 1966).

Patterns of thinking in searching patent applications by manual and machine-assisted methods, J. R. Cornog and P. P. Ellis, J. Chem. Doc. **5,** 215–225 (Nov. 1965).

Separation of pyrenediones by column chromatography, A. J. Fatiadi, J. Chromatog. **20,** 319–324 (1965).

Zone refiner with temperature control, F. Ordway, Anal. Chem. **37,** 1178–1180 (Aug. 1965).

A simple method for making stereoscopic drawings, F. Ordway, Am. Mineralogist **50,** 1496–1498 (1965).

A system for accurate direct and alternating voltage measurements, F. L. Hermach, J. E. Griffin, and E. S. Williams, IEEE Trans. Instr. Meas. **IM-14,** No. 4,-215–224 (Dec. 1965).

Effect of surface roughness on emittance of non-metals, J. C. Richmond, J. Opt. Soc. Am. **56,** No. 2, 253–254 (Feb. 1966).

Comparison of uncertainty ellipses calculated from two spectrophotometric colorimetry methods by an automatic-computer program, I. Nimeroff, J. Opt. Soc. Am. **56,** No. 2, 230–237 (Feb. 1966).

An international comparison of current-ratio standards at audio frequencies, B. L. Dunfee and W. J. M. Moore, IEEE Trans. Instr. Meas. **IM-14,** No. 4, 172–177 (Dec. 1965).

The design and performance of multirange current transformer standards for audio frequencies, B. L. Dunfee, IEEE Trans. Instr. Meas. **IM-14,** No. 4, 190–204 (Dec. 1965).

Color, D. B. Judd, Book, Encyclopedia of Physics, pp. 113–116 (Reinhold Publ. Corp., New York, N.Y., 1966).

Initiation of spherulite growth: The case of concurrent homogeneous and heterogeneous nucleation, F. Gornick, J. Appl. Phys. **36,** No. 10, 3012–3014 (Oct. 1965).

Limits on calorimetric residual entropies of glasses, A. B. Bestul and S. S. Chang, J. Chem. Phys. **43,** No. 12, 4532–4533 (Dec. 15, 1965).

Erratum-Nuclear magnetic moment of Pr^{141} from the hyperfine structure of doubly ionized praseodymium, J. Reader and J. Sugar, Phys. Rev. **140,** No. 7AB, AB3 (Dec. 27, 1965).

Photometry, L. E. Barbrow, Book, Encyclopedia of Physics, pp. 516–519 (Reinhold Publ. Corp., New York, N.Y. 1966).

Two-dimensional probability distribution in a turbulent field, F. N. Frenkiel and P. S. Klebanoff, Phys. Fluids **8,** No. 12, 2291–2293 (Dec. 1965).

Relativistic electron precipitation into the mesosphere at subauroral latitudes, D. K. Bailey and M. A. Pomerantz, J. Geophys. Res. **70,** No. 23, 5823–5830 (Dec. 1, 1965).

Absolute-velocity mossbuaer spectrometer, J. J. Spijkerman and F. C. Ruegg, Trans. Am. Nucl. Soc. **8,** No. 2, 344 (1966).

Adhesive bonding of various materials to hard tooth tissues. V. The effect of a surface-active comonomer on adhesion to diverse substrates, R. L. Bowen, J. Dental Res. **44,** No. 6, 1369–1373 (Nov.–Dec. 1965).

A simple device for adjusting dental interferometers, H. J. Caul and J. W. Kumpula, J. Dental Res. **44,** No. 6, 1412 (Nov.–Dec. 1965).

Determination of trace amounts of cadmium and silver by substoichiometric radioisotopic dilution analysis, A. R. Landgrebe, L. T. McClendon, and J. R. DeVoe, Trans. Am. Nucl. Soc. **8,** No. 2, 315–316 (1966).

Dissociation of acetic acid-d_3 in aqueous solution and related isotope effects from 0 to 50°, M. Paabo, R. G. Bates, and R. A. Robinson, J. Phys. Chem. **70,** 540–543 (1966).

Magnesium isotope ratios in natural samples, E. J. Catanzaro and T. J. Murphy, J. Geophys. Res. **71,** No. 4, 1271–1274 (Feb. 15, 1966).

NMR studies of inorganic fluorides. I. High-resolution ^{19}F spectra of Si_2F_6 and $(SiF_3)_2O$, R. B. Johannesen, T. C. Farrar, F. E. Brinckman, and T. D. Coyle, J. Chem. Phys. **44,** No. 3, 962–964 (Feb. 1, 1966).

On the limiting shape of the distribution function of lengths of a single polymer molecule with excluded-volume effects, J. Mazur, J. Chem. Phys. **43,** No. 12, 4354–4356 (Dec. 15, 1965).

Comparison of xenon and carbon arcs as radiation sources for laboratory weathering of asphalts, K. G. Martin, P. G. Campbell, and J. R. Wright, Am. Soc. Testing Mater. Proc. **65,** 809–830 (1965).

Propagation of electromagnetic pulses in terrestrial waveguides, J. R. Wait, IEEE Trans. Ant. Prop. **AP-13,** No. 6, 904–918 (Nov. 1965).

The low temperature removal of small quantities of nitrogen or methane from hydrogen gas by physical adsorption on a synthetic zeolite, A. J. Kidnay and M. J. Hiza, A.I.Ch.E. J. **12,** No. 1, 58–64 (Jan. 1966).

The analysis, synthesis, and description of biological images, L. E. Lipkin, W. C. Watt, and R. A. Kirsch, Ann. N.Y. Acad. Sci. **128,** No. 3, 984–1012 (Jan. 31, 1966).

Effect of normal-fluid motion on third sound in liquid-helium films, G. L. Pollack, Phys. Rev. **143,** No. 1, 103–109 (Mar. 4, 1966).

Mossbauer line broadening in SnO_2, R. H. Herber and J. Spijkerman, J. Chem. Phys. **42,** No. 12, 4312–4314 (June 15, 1966).

Multivibrator provides bidirectional output pulses, F. C. Ruegg, Electronics **38,** No. 17, 87 (Aug. 8, 1965).

Resonances in the elastic and inelastic electron scattering from N_2, H. G. M. Heideman, C. E. Kuyatt, and G. E. Chamberlain, J. Chem. Phys. **44,** No. 1, 355–358 (Jan. 1, 1966).

Status of linear relations among heats of transport, R. E. Howard and A. B. Lidiard, J. Chem. Phys. **43,** No. 11, 4158–4160 (Dec. 1, 1965).

Stress-strain properties of textile yarns subjected to rifle bullet impact, C. A. Fenstermaker and J. C. Smith, J. Appl. Polymer Sci. **1,** 125–146 (1965).

The effect of humidity on ionization measurements with cavity and free-air chambers, T. P. Loftus, B. Petree, and J. T. Weaver, Jr., Radiology **86,** No. 1, 149 (Jan. 1966).

An investigation of concentric ring antennas with low sidelobes, C. O. Stearns and A. C. Stewart, IEEE Trans. Ant. Prop. **AP-13,** No. 6, 856–863 (Nov. 1965).

On radiation of electromagnetic and electroacoustic waves in plasma. Part II, J. R. Wait, Appl. Sci. Res. **12,** Sect. B, 130–138 (1965).

**Publications for which a price is indicated are available by purchase from the Superintendent of Documents, U. S. Government Printing Office, Washington, D.C. 20402 (foreign postage, one-fourth additional). The NBS nonperiodical series are also available from the Clearinghouse for Federal Scientific and Technical Information, Springfield, Va. 22151. Reprints from outside journals and the NBS Journal of Research may often be obtained directly from the authors.*

U.S. GOVERNMENT PRINTING OFFICE : 1966 OL—216-375

JJR-A OCT 46129
UNIVERSITY MICROFILMS INC
SERIALS SECTION
313 NORTH FIRST ST
ANN ARBOR MICH

UN
GOVERNMENT PRINTING OFFICE
DIVISION OF PUBLIC DOCUMENTS
WASHINGTON, D.C. 20402

OFFICIAL BUSINESS

POSTAGE AND FEES PAID
U.S. GOVERNMENT PRINTING OFFICE

JOURNAL OF RESEARCH of the National Bureau of Standards
A. Physics and Chemistry

Vol. 70A, No. 4 July–August 1966

Contents

Page

Elastic constants of synthetic single crystal corundum. Wayne E. Tefft. 277

Phase equilibria as related to crystal structure in the system niobium pentoxide-tungsten trioxide. R. S. Roth and J. L. Waring. 281

Properties of aqueous mixtures of pure salts. Thermodynamics of the ternary system: water-calcium chloride-magnesium chloride at 25 °C. R. A. Robinson and V. E. Bower. 305

Properties of aqueous mixtures of pure salts. Thermodynamics of the ternary system: water-sodium chloride-calcium chloride at 25 °C. R. A. Robinson and V. E. Bower. 313

Use of the consistency check in the vector verification method. Alan D. Mighell, and R. A. Jacobson. 319

Self-reversal in the spectral lines of uranium. Donald D. Laun. 323

Oscillator strengths for ultraviolet lines of Fe I. Charles H. Corliss and Brian Warner. 325

Publications of the National Bureau of Standards. 373

Library of Congress Catalog Card Number: 62–37059

For sale by the Superintendent of Documents, U.S. Government Printing Office, Washington, D.C., 20402. Price $1.00 (single copy). Subscription price: $5 a year; $1.00 additional for foreign mailing.

UNITED STATES GOVERNMENT PRINTING OFFICE, WASHINGTON : 1966